Studies on the ammonia permeability of aquaporins

Dissertation

zur Erlangung des Doktorgrades

der Mathematisch-Naturwissenschaftlichen Fakultät

der Christian-Albrechts-Universität zu Kiel

vorgelegt von

Dawid Krenc

Kiel 2012

Gutachten:	Prof. Dr. Eric Beitz
Zweites Gutachten:	Prof. Dr. Markus Bleich
Tag der mündlichen Prüfung:	06.12.2012
Zum Druck genehmigt:	06.12.2012

Prof. Dr. Wolfgang J. Duschl
(Dekan)

To my parents, and to all those who enjoy science for its own sake

But in 1937 a man named Young did a very interesting one. He had a long corridor with doors all along one side where the rats came in, and doors along the other side where the food was. He wanted to see if he could train the rats to go in at the third door down from wherever he started them off. No. The rats went immediately to the door where the food had been the time before.

…

He finally found that they could tell by the way the floor sounded when they ran over it. And he could only fix that by putting his corridor in sand. So he covered one after another of all possible clues and finally was able to fool the rats so that they had to learn to go in the third door. If he relaxed any of his conditions, the rats could tell.

…

I looked into the subsequent history of this research. The next experiment, and the one after that, never referred to Mr. Young. They never used any of his criteria of putting the corridor on sand, or being very careful. They just went right on running rats in the same old way, and paid no attention to the great discoveries of Mr. Young, and his papers are not referred to, because he didn't discover anything about the rats. In fact, he discovered *all* the things you have to do to discover something about rats.

…

So I have just one wish for you - the good luck to be somewhere where you are free to maintain the kind of integrity I have described, and where you do not feel forced by a need to maintain your position in the organization, or financial support, or so on, to lose your integrity. May you have that freedom.

Richard Feynman in "Surely you're joking, Mr. Feynman!"

Table of contents

Abbreviations

Amp	Ampicillin
Amt	Ammonium transporter
APS	Ammoniumperoxodisulfate
AQP	Aquaporin
AQY	Yeast aquaporin
ar/R constriction	Aromatic/arginine constriction of some aquaporins
AUC	Area under the curve
Bcc	*Burkholderia cenocepacia*
bp	Base pair
BSA	Bovine serum albumin
BTB	Bromothymol blue
cRNA	Capped RNA (or copy RNA)
dNTP	Deoxynucleoside triphosphate
DDM	β-D-dodecylmaltoside
DEPC	Diethylpyrocarbonate
DMSO	Dimethylsulfoxide
DTT	1,4-Dithiothreitol
Ec or *E. coli*	*Escherichia coli*
EDTA	Ethylenediaminetetraacetic acid
Fps1	*S. cerevisiae* glycerol facilitator (*fdp1* suppressor)
GlpF	Glycerol uptake facilitator
gpd	glycerol-3-phosphate dehydrogenase
HA-tag	Human influenza hemagglutinin-tag
hAQP	Human Aquaporin
HEPES	2-(4-(2-hydroxyethyl)-piperazin-1-yl)-ethanesulfonic acid
HRP	Horseradish peroxidase
IC_{50}	Inhibitory concentration for a half-maximal effect
IgG	Immunoglobulin G
kDa	kilodalton (1000 g/mol)
Le	*Lycopersicon esculentum* (tomato)
2-ME	2-mercaptoethanol
MEP	Methylamine permease
MES	2-(N-morpholino)ethanesulfonic acid
MIP	Major intrinsic protein
MOPS	3-(N-morpholino)propanesulfonic acid
M-TBS-T	Milk powder and Tween 20-containing TBS

Na	Sodium (as in “ampicillin Na”)
NCBI	National Center for Biotechnology Information
OD_x	Optical density (apparent absorption) at x nm
PAGE	Polyacrylamide gel electrophoresis
PBS	Phosphate buffered saline
PDB ID	Protein data bank identity number
PES	Polyether sulfone
Pf	*Plasmodium falciparum*
P_f	Osmotic water permeability coefficient
Pfu	*Pyrococcus furiosus*
pH_c	Cytosolic pH
PIP	Plasma membrane intrinsic protein (plant AQPs)
PVDF	Polyvinylidene difluoride
rAQP	Rat Aquaporin
rAQP8*	rAQP8 ΔQ5 S31P
rpm	Rounds per minute
Sc or *S. cerevisiae*	*Saccharomyces cerevisiae*
SD medium	Synthetic defined (or dextrose) medium
SD KHL	SD medium containing lysine, histidine and leucine
SDS	Sodium dodecyl sulfate
TAE	Tris acetate EDTA
τ	Relaxation time of exponential decay
TBE	Tris borate EDTA
TBS	Tris-buffered saline
TE	Tris EDTA
TEA	Tetraethylammonium
TEMED	N,N,N′,N′-Tetramethylethane-1,2-diamine
Tg	*Toxoplasma gondii*
TIP	Tonoplast intrinsic protein (a class of plant aquaporins)
Tris	Tris(hydroxymethyl)aminomethane
wt	Wild-type
X. laevis	*Xenopus laevis*
YNB	Yeast nitrogen base
YPD	Yeast peptone dextrose

1 Introduction

1.1 Aquaporins

The facilitated permeation of human red blood cells by water and glycerol, and their respective inhibition by mercuric and cupric ions, have been known since at least the 1940s (LeFevre, 1948). Similarly, the facilitated uptake of glycerol by the prokaryote *Escherichia coli*, and its inhibition by cupric ions, has been known since at least the 1970s (Sanno *et al.,* 1968, Eze *et al*., 1977). The erythrocyte water channel protein was identified by labelling with a radioactive mercury isotope (Benga *et al.*, 1986). Better equipped, Agre and coworkers were able to characterize the protein and to prove its water channel function: The moment of truth came when a *Xenopus laevis* oocyte producing the channel protein was subjected to a hypoosmotic medium and burst, while its non-producing counterpart was left unscathed (Preston *et al*., 1992). The water channel was named Aquaporin 1 (AQP1). Its discovery paved the way for that of other members, among them AQP3, which turned out to be the glycerol channel of human erythrocytes (Roudier *et al.*, 1998), and GlpF, the glycerol channel of *E. coli* (Maurel *et al.*, 1994).

Aquaporins have since been found in members of bacteria, archaea and eukaryotes (Zardoya, 2005). Apart from water and glycerol, the solutes conducted by aquaporins include small neutral molecules up to the size of adenine (Tsukaguchi *et al.*, 1999) and silicic acid (Ma *et al.*, 2006), and in at least one case anions such as chloride and nitrate (Ikeda *et al.*, 2002).

1.1.1 Aquaporin function

Transcellular water and glycerol movement

AQP1 had been identified as an integral membrane protein anchoring the membrane skeleton of an erythrocyte to its plasma membrane (Denker *et al*., 1988). It had also been found to be abundantly expressed in the apical brush borders of renal proximal tubules, and with the discovery of its water channel activity this made perfect sense: Large amounts of water need to be reabsorbed into the blood stream following glomerular filtration. Biological membranes are all water-permeable to some extent, depending on their lipid and protein composition (Hill and Zeidel, 2000), but as demonstrated by the above-mentioned bursting of AQP1-producing *Xenopus* oocytes, a ten- to hundredfold increase in water permeability can, under certain conditions, make all the difference.

Numerous tissues in the human body require a balanced entry and exit of water, so it was no surprise to detect AQP1 in, for example, the hepatic bile ducts, the capillary endothelia of the lung, the cilliary epithelium of the eye, and the apical membranes of the choroid plexus epithelium in the brain (Nielsen *et al.*, 1993). But its absence in many other tissues, such as the renal collecting-ducts and the salivary glands, was notable and correctly presumed to indicate the existence of other aquaporin isoforms.

In the renal collecting ducts this turned out to be the water channel subsequently named AQP2 (Fushimi *et al.*, 1993, Sasaki *et al.*, 1994). It was found to be essential for the vasopressin-dependent concentration of urine, and it remains one of the most striking examples of the vesicular trafficking of aquaporins. Malfunctioning of its regulated plasma membrane localization leads to nephrogenic diabetes insipidus (Deen *et al.*, 1994).

The erythrocyte glycerol channel AQP3 also turned up in the renal collecting ducts. Unlike AQP2, which is found in the apical membranes in rapidly variable amounts according to the body's needs, AQP3 is localized constitutively in the basolateral membranes of collecting duct principal cells (Ishibashi *et al.*, 1994, 1995, Ecelbarger *et al.*, 1995). Its deletion in mice was found to impair renal water reabsorption and to lead to nephrogenic diabetes insipidus (Ma *et al.*, 2000). Its role as a glycerol channel became evident when it was found that the skin defects of AQP3-deficient mice are essentially due to a reduced glycerol content of the stratum corneum (Hara and Verkman, 2003).

Following the discovery of AQPs 1-3, nine more isoforms were identified in humans. Figure 1.1 shows the relatedness of their amino acid sequences. For comparison, the amino acid sequences of the *E. coli* water channel, AQPZ (Calamita *et al*., 1995), and glycerol channel, GlpF, are included in the analysis.

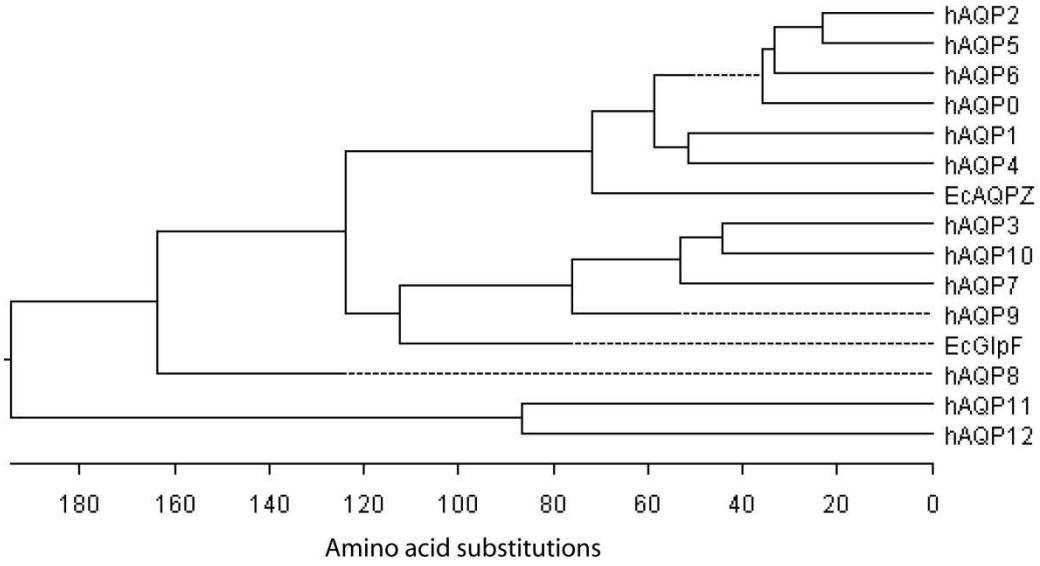

Figure 1.1: Phylogenetic tree based on an amino acid sequence alignment of human and E. coli aquaporins. *Sequences are from the National Center for Biotechnology Information (NCBI), except for that of AQP12 (Itoh et al., 2005). Among the aquaporins shown, E. coli AQPZ is the smallest with 233 amino acids, human AQP7 the largest with 342 amino acids. The alignment and the phylogenetic tree were generated with the programme MegAlign using the ClustalW algorithm.*

Looking at the phylogenetic tree it becomes apparent that nine of the human aquaporins form two groups, one bearing a certain similarity with AQP1 and *E. coli* AQPZ, the other being more similar to AQP3 and *E. coli* GlpF. This may lead one to suggest that the former are water channels, whereas the latter are in addition glycerol-permeable (aquaglyceroporins), and indeed this is the case. Thus, AQP4 mediates water transport through, among others, the basolateral side of the renal collecting duct epithelium, joining forces with AQP3 (Chou *et al.*, 1998, Mobasheri *et al.*, 2007), while defective trafficking of AQP5 within acinar cells of the salivary and the lacrimal glands is associated with the dry mouth and eyes characteristic of Sjögren's syndrome (Steinfeld *et al.*, 2001, Tsubota *et al.*, 2001). AQP7, on the other hand, enables reabsorption of glycerol from the glomerular filtrate that flows through the proximal tubules (Sohara *et al.*, 2005), and glycerol diffusion out of adipocytes into the bloodstream (Ishibashi *et al.*, 1998, Hara-Chikuma *et al.*, 2005), whence it can be taken up by hepatocytes via AQP9 (Tsukaguchi *et al.*, 1999, Rojek *et al.*, 2007). AQP10 is an aquaglyceroporin expressed in the small intestine (Ishibashi *et al.*, 2002). AQP6 has very unusual properties which will be described below. AQP0, so named because it had been studied as an abundant eye lens protein before the discovery of AQP1, shows another unusual property and will be described below.

Three human aquaporins belong to neither group as judged by sequence alignment. In fact, AQP8 is an efficient water channel, but one that is in addition capable of conducting unprotonated ammonia and hydrogen peroxide, but not glycerol (Koyama *et al.*, 1998, Bienert *et al.*, 2007). It will be described in detail in Section 1.2. The functions of AQP11 and AQP12 remain somewhat obscure, although deletion of the former in mice leads to their death by renal failure with cyst formation in the proximal tubules (Morishita *et al.*, 2005), while the latter is specifically expressed in the acinar cells of the pancreas (Itoh *et al.*, 2005). AQP11 appears to be water- but not glycerol permeable (Yakata *et al.*, 2011). The permeability properties of AQP12 have not yet been elucidated.

Brown rats (*Rattus norvegicus*) and house mice (*Mus musculus*) have the same set of thirteen aquaporins that we do, with some unsurprising differences in tissue expression patterns (*e. g.* Tsukaguchi *et al.*, 1999, Liu *et al.*, 2007), which is why their study has been useful in understanding aquaporin function in our body. Most multicellular organisms probably have aquaporins that facilitate water transport between tissues. The nematode *Caenorhabditis elegans* genome encodes eight aquaporins, six of them found to be water- and/or glycerol-permeable in *Xenopus* oocytes, multiple deletions of which did not seriously affect survival under tested conditions (Huang *et al.*, 2007). The zebrafish *Danio rerio* has eighteen aquaporins, which are grouped like the mammalian ones (Fig. 1.1) because of multiple subisoforms that have arisen from a whole-genome duplication (Tingaud-Sequeira *et*

al., 2010). The genome of the plant *Arabidopsis thaliana* contains thirty eight aquaporin-like sequences (Quigley *et al.*, 2002).

Solute transport

Molecules other than water and glycerol have been found to pass through aquaporins, and in some cases this has proven to be beneficial to the organism.

A remarkable example is the uptake of silicic acid ($Si(OH)_4$) by rice plant roots through a member of the aquaporin family, deletion of which reduces silica content, disease resistance and grain yield (Ma *et al.*, 2006).

In the marine bacterium *Salinispora tropica*, an aquaporin arsenate reductase fusion protein has been shown to conduct arsenous acid ($As(OH)_3$), and is proposed to function in arsenate detoxification (Wu *et al.*, 2010). In contrast to this, an aquaglyceroporin of *Leishmania major* serves as the uptake route of antimonous acid ($Sb(OH)_3$), and deletion of a single copy of the gene increases the parasites' resistance to the drug about tenfold (Gourbal *et al.*, 2004). More recently, it was found that non-functionality of an aquaglyceroporin gene in *Trypanosoma brucei* increases its tolerance to the drugs pentamidine and melarsoprol (Baker *et al.*, 2012). The authors' tentative conclusion that these rather large molecules may pass through the Trypanosome aquaglyceroporin is under investigation.

Facilitated urea permeation through a variety of aquaglyceroporins has apparently never been shown to be of physiological significance. The existence of specific urea channels may be a reason for this (Tsukaguchi *et al.*, 1999, Klebl *et al.*, 2003, Smith, 2009, Witte, 2011).

Hydrogen peroxide permeability of specific aquaporins has been reported, and it may be physiologically meaningful since the molecule serves as a signal in both plants and animals (Bienert *et al.*, 2006 and 2007, Niethammer *et al.*, 2009, Miller *et al.*, 2010).

Gas transport

AQP1 is abundantly expressed in red blood cells and in the capillary endothelia of the lung, and its potential role in the facilitated membrane permeation of carbon dioxide has been proposed (Cooper and Boron, 1998). In the tobacco plant *Nicotiana tabacum*, carbon dioxide transport facilitated by NtAQP1 has been shown to be physiologicall meaningful in that reduced or increased expression can lower or raise the rate of photosynthesis (Uehlein *et al.*, 2003). So far, there has been evidence both in favour and against physiologically meaningful aquaporin-mediated plasma membrane permeation by carbon dioxide, and passionate arguments continue over it (Boron *et al.*, 2011, de Groot and Hub, 2011).

Another important gas, nitrogen monoxide, has been shown to permeate plasma membranes more easily in the presence of AQP1, the absence of which has been found to affect endothelium-dependent relaxation of vascular smooth muscles (Herrera and Garvin, 2007).

The aquaporin-facilitated membrane permeation of ammonia will be the subject of Section 1.2.

Ion conduction

AQP6, despite its sequence similarity with AQPs 0, 2 and 5 (Fig. 1.1), has several unusual properties: It conducts anions such as halides and nitrate, in addition to water, glycerol and urea, it is activated by a pH below about 5.5, as well as by the presence of about 0.1 mM mercuric chloride, and it is expressed intracellularly (Yasui *et al.*, 1999, Ikeda *et al.*, 2002, Holm *et al.*, 2004). In acid-secreting alpha-intercalated cells of renal collecting ducts it colocalizes with a proton-ATPase. In the rat brain, AQP6 is found in synaptic vesicles together with a proton-ATPase, where it participates in the vesicular swelling that precedes secretion, although there it may be functioning as a water channel since rat AQP1 takes on a similar role in exocrine pancreatic zymogen granules (Cho *et al.*, 2002, Jeremic *et al.*, 2005, Lee *et al.*, 2010). Mouse and human AQP6 bind calmodulin at their N-termini in a calcium-dependent manner *in vitro*, which potentially affects their cellular localization *in vivo* (Beitz *et al.*, 2006 b, Rabaud *et al.*, 2009). The anion conductance of rat AQP6 can be abolished by a single amino acid substitution (see Section 1.1.2), thereby increasing water permeability, but anion conductivity cannot be reproduced by an analogous mutation in other aquaporins (Liu *et al.*, 2005).

Despite these remarkable properties, the precise function of AQP6 is not clear, and it remains the only definite example of an ion-conducting aquaporin. Experiments with AQP6 knockout mice have not been described.

AQP1 has been reported to conduct monovalent cations when stimulated with cyclic GMP in *Xenopus* oocytes, but not so in human embryonic kidney cells or when reconstituted in planar lipid bilayers (Tsunoda *et al.*, 2004, Yool and Campbell, 2012).

Neural signalling and cell volume sensing

The water-selective AQP4 is expressed in glial cells and its deletion in mice has revealed possible functions in neuronal excitability, as suggested, for example, by decreased seizure susceptibility (Binder *et al.*, 2004, Verkman, 2005).

Another study using AQP4-null mice found the absence of this aquaporin to reduce Ca^{2+}-signalling in astrocytes of isolated brain slices exposed to osmotic shocks (Thrane *et al.*, 2011).

Cellular motility

A remarkable finding is the reduced motility of endothelial cells in AQP1-null mice, which slows the growth of implanted tumours by slowing their vascularization. Cultured non-endo-

thelial cells made to express AQP1 or AQP4 show increased motility (Saadoun *et al.*, 2005). Other examples have been found, such as the reduced motility of AQP3-deficient skin keratinocytes (Papadopoulos *et al.*, 2008), and the phenomenon is being studied in the model organism *Dictyostelium discoideum* (von Bülow *et al.*, 2012). Among the reasons proposed for such an effect are the increased water flow at the leading edges of migrating cells, caused by cytoskeletal rearrangements and ion fluxes (Schwab, 2001), as well as an involvement of aquaporins in cytoskeleton attachment to the plasma membrane, at least in the case of AQP1 (Monzani *et al.*, 2009).

Cellular junction formation by aquaporins

AQP0 is the major plasma membrane protein, or major intrinsic protein (MIP), of the eye lens fibre cells, and as such its function in junction formation was studied well before its water channel activity became known (Bok *et al.*, 1982, Mulders *et al.*, 1995). The full-length 26 kDA isoform is water-permeable but does not participate in junction formation, whereas the opposite is true for the proteolytically cleaved 22 kDa isoform (Gonen *et al.*, 2004). The latter predominates in the lens core, the former in the lens cortex. Mutations or deletions of the AQP0 gene affect lens focussing power and transparency, leading to dominant cataract formation (Berry *et al.*, 2000, Shiels *et al.*, 2001). AQP0 is probably the best-studied aquaporin from a physiological point of view (Chepelinsky, 2009). To this day, aquaporins are said to belong to the major intrinsic protein family.

Another aquaporin capable of junction formation is AQP4. It is expressed as two splicing variants, the shorter one of which forms orthogonal arrays in the plasma membranes of various tissues, *e. g.* glial cells. Compared to AQP0, this property is much less pronounced for AQP4, and it may be physiologically irrelevant (Hiroaki *et al.*, 2006, Zhang and Verkman, 2008).

Overall, cellular junction formation by aquaporins is probably rare.

Aquaporin functions in unicellular organisms

The usefulness of aquaporin-facilitated water and solute transport in multicellular organisms is, in some cases, obvious, but how about their function in unicellular organisms?

Facilitated glycerol transport in *E. coli* has been shown to allow the bacterium to grow faster when provided with glycerol as the sole carbon source (Richey and Lin, 1972). Similarly, the yeast *S. cerevisiae* can grow on glycerol as the sole carbon source (Fast, 1973), although the major function of its aquaglyceroporin Fps1 appears to be in osmoregulation (Tamás *et al.*, 1999).

Facilitated plasma membrane water permeability in unicellular organisms is harder to explain. In fact, many if not most prokaryotes and unicellular eukaryotes appear to live

without any water-selective aquaporins (Tanghe *et al.*, 2006). Among the clear functions found are the enhanced freeze tolerance and spore formation of yeast synthesizing their water-permeable aquaporins AQY1 and/or AQY2 (Tanghe *et al.*, 2002, Sidoux-Walter *et al.*, 2004). In this regard it is of interest that some laboratory *S. cerevisiae* strains have mutated AQY genes which code for non-functional proteins (Bonhivers *et al.*, 1998, Carbrey *et al.*, 2001, Meyrial *et al.*, 2001), whereas loss of the regulatable aquaglyceroporin Fps1 has not been reported.

In *E. coli*, studies of AQPZ expression and of the effects of its deletion have yielded conflicting results, two groups having found maximal expression either during the mid-exponential or the late exponential phase of growth, and either increased sensitivity or increased tolerance to osmotic stress (Calamita *et al.*, 1995, Soupene *et al.*, 2002).

Finally, although not quite a unicellular organism, why does an erythrocyte need water and glycerol channels? Mice lacking AQP1 apparently do not suffer from erythrocyte defects, although the osmotic water permeability coefficient of the latter is reduced about eightfold (Ma *et al.*, 1998). Similarly, the erythrocytes of AQP9-deficient mice show markedly reduced glycerol permeability but no apparent physiological defect (Liu *et al.*, 2007). Erythrocytes of a few human beings who lack functional AQP1 (so-called “Colton-null” individuals), normally present at around 10^5 copies per cell, show mildly reduced lifespan, surface area and deformability, and a six- to sevenfold reduced osmotic water permeability coefficient, but no severe defects (Mathai *et al.*, 1996, Denker *et al.*, 1988). AQP3, present at around 10^4 copies per cell, accounts for some of the remaining water flux and for all of the facilitated glycerol flux through Colton-null erythrocyte membranes (Roudier *et al.*, 1998). Humans lacking it have not been described.

Other functions

The facilitated membrane permeation of water, glycerol, and other, mostly neutral and small solutes is the major function of aquaporins. Cellular junction formation by AQP0 in the vertebrate eye lens is the only other function studied in detail.

At the time of writing, data on 1008 members of the major intrinsic protein family from 340 organisms has been deposited at the MIPMod Database which includes information from completely sequenced genomes only (Gupta *et al.*, 2012). Many of these aquaporins probably have not been studied functionally. With over a million species known, and at least ten times as many thought to exist on the planet, a few surprising features of aquaporin function surely remain to be discovered and can only be imagined at present.

1.1.2 Aquaporin structure and selectivity

In 1994, Jung and colleagues published the so-called hourglass model of the human Aquaporin 1 structure, based on biochemical and low-resolution electron crystallographic data (Jung *et al.*, 1994). The membrane topology of AQP1 according to this model is shown in Figure 1.2.

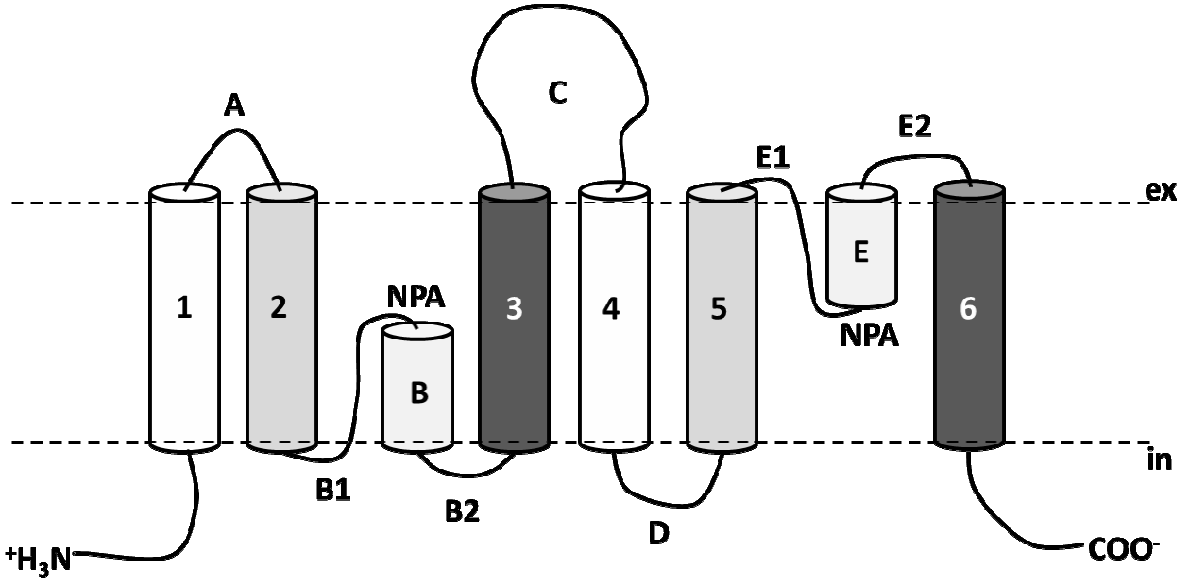

Fig. 1.2: Two-dimensional membrane topology of human AQP1 as deduced from biochemical studies and low-resolution electron crystallographic data. *Dotted lines indicate the extracellular (ex) and intracellular (in) lipid membrane boundaries. N- and C-termini and loops are symbolized by lines, alpha helices by cylinders. Loops are lettered, transmembrane helices are numbered and colour-coded to indicate the internal symmetry. The positions of two conserved asparagine/proline/alanine (NPA) motifs are indicated.*

Aquaporins are typically about 300 amino acids in length. Their peptide chain crosses the membrane six times, forming alpha-helices, and the N- and C-termini are located intracellularly. Two long loops (B and E in Fig. 1.2) fold into the membrane, forming two half-helices. Each half-helix is N-terminally capped by conserved asparagine/proline/alanine (NPA) motifs. The juxtaposition of the NPA motifs within the membrane was correctly predicted, but the formation of alpha-helical structures by loops B and E, as shown in Figure 1.2, had not been expected (Jung *et al.*, 1994).

A remarkable feature of aquaporins is their low but significant internal sequence homology, suggesting an ancient gene duplication event (Wistow *et al.*, 1991, Preston and Agre 1991). Differences in length, ranging from 261 to 342 amino acids among human aquaporins, are mainly due to the lengths of the loops and the N- and C-termini. The intracellular termini and loop D frequently participate in regulation, affecting aquaporin localization and channel gating (Wellner *et al.*, 2005, Törnroth-Horsefield *et al.*, 2005). Extracellular loops may be N- or O-glycosylated (Denker *et al.*, 1988, von Bülow *et al.*, 2012). Smith and Agre (1991) tentatively predicted human AQP1 to form tetramers, consisting of both glycosylated and non-

glycosylated monomers. This was confirmed by low-resolution electron crystallographic data which showed an asymmetry of the monomers necessitating their oligomerization within the membrane (Walz *et al.*, 1994, Jung *et al.*, 1994). Using radiation inactivation studies, van Hoek *et al.* (1991) predicted the functional water channel of renal proximal tubules to have a molecular mass of about 30 kDa, close to that of the AQP1 monomer (28 kDa), and Preston *et al.* (1993) arrived at the same conclusion by coexpression of wild-type and mercuric ion-insensitive AQP1 in *Xenopus* oocytes.

Finally, with the resolution of electron crystallographic data reaching approximately 4 Å, the three-dimensional fold of human AQP1 monomers became known (Fig. 1.3), and the position of amino acids within the structure could be determined with reasonable accuracy (Murata *et al.*, 2000, de Groot *et al.*, 2001).

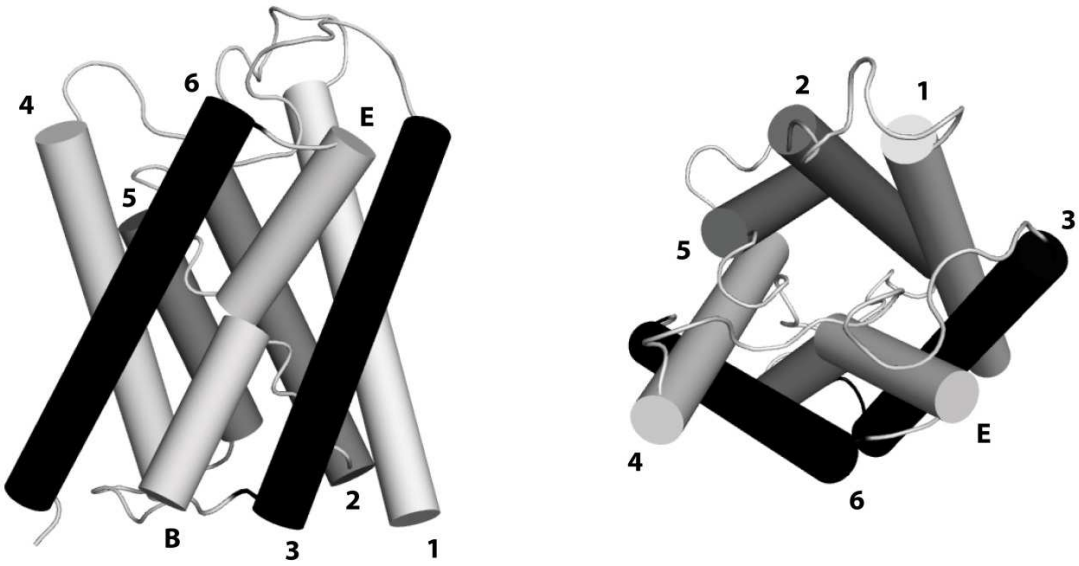

Fig. 1.3: Three-dimensional structure of human AQP1 as deduced from high-resolution electron crystallographic data. *Alpha-helices are coloured and numbered as in Fig. 1.2.* ***Left****: View along the membrane plane.* ***Right****: View from the extracellular side through the channel. The structural data was obtained from the Protein Data Bank (PDB ID: 1H6I). Eight N-terminal and thirty six C-terminal amino acids are missing.*

The six transmembrane helices are somewhat tilted with respect to the membrane, and are arranged in a right-handed bundle. The half-helices meet at the centre, together forming what looks almost like a seventh transmembrane helix.

Interactions stabilizing this arrangement have been meticulously described by Murata *et al.* (2000), among them a salt bridge between Glutamic acid 17 and Histidine 74, conserved among aquaporins, and a number of “glycine/alanine ratchets”, also conserved, which allow local coiled-coil-like interactions between helices (one of these highly conserved glycine residues, situated at the intersection of Helices 2 and 5, is replaced by an asparagine residue in AQP6, mutation of which abolishes anion permeability while increasing water permeability, see Section 1.1.1).

Helices 2 and 5, being the shortest transmembrane helices, are situated at the centre of the aquaporin tetramer, while Helices 4 and 6 and the half-helices face the lipid membrane (Figs. 1.3 and 1.4). Tetramerization gives rise to a hydrophobic central pore which may conduct small hydrophobic molecules such as carbon dioxide (see Section 1.2).

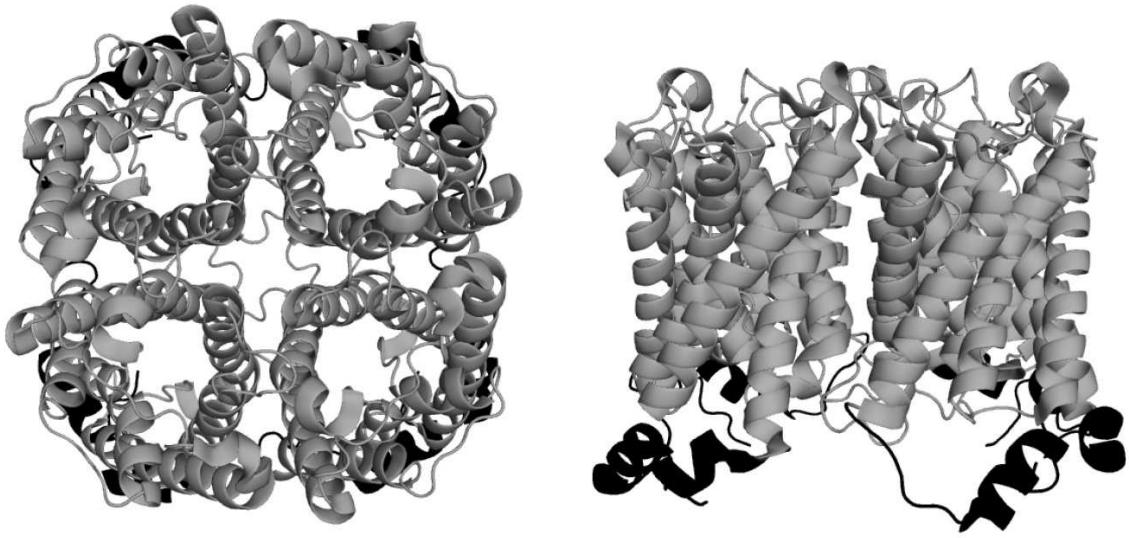

Fig. 1.4: Three-dimensional structure of the human AQP5 tetramer. Left*: View from the extracellular side. Please note the four channels and the central pore. The latter accommodates the C14-alkyl chain of a phosphatidyl serine molecule in this particular crystal structure (not shown).* ***Right****: View from the membrane plane. The N- and C-termini, both containing alpha-helical segments, are coloured black (the longer C-terminus is prominent at the bottom right). AQP5 was chosen because it is deposited as a tetramer in the Protein Data Bank (PDB ID: 3D9S). Twenty C-terminal amino acids are missing.*

At the time of writing, the crystal structures of 15 aquaporins from 11 eukaryotic, archaeal and bacterial species have been solved, and they all show the same basic topology and three-dimensional fold as human AQP1 (Table 1.1).

With a resolution of 1.15 Å, the crystal structure of the water-selective aquaporin of the yeast *Pichia pastoris* (PpAQY1) allows for the localization of individual water molecules, as shown in Figure 1.5 (Fischer *et al.*, 2009). As expected for a selective channel, the permeant molecules pass in a single file, although not necessarily a continuous one. Computational studies reveal that the main water rate-limiting barriers are located at two hydrophobic sections which sandwich the NPA region, and that the average dipole of the water molecules aligns with the half-helix macro-dipoles during passage (de Groot and Grubmüller 2001, Aponte-Santamaria *et al.*, 2010). Osmotic water flow through AQP1 in erythrocytes has been reported to be inwardly rectified, with inward flow about 40 to 50 % greater than outward flow for the same osmotic gradient (Farmer and Macey, 1970).

Table 1.1**: **Aquaporin structures solved by X-ray or electron crystallography up to the year 2011.
Aquaporins are classified according to their permeability for water (w) or glycerol (g), with brackets indicating a lack of published functional testing. Structures for open and closed conformations are available in some cases. AQP4 structures are trimmed ("aa" stands for amino acid). Homo sapiens, Rattus norvegicus, Bos taurus and Ovis aries are mammals, Spinacia oleracea is a flowering plant, Plasmodium falciparum and Pichia pastoris are unicellular eukaryotes, Methanothermobacter marburgensis and Archaeoglobus fulgidus are archaea, and Escherichia coli and Agrobacterium tumefasciens are gram-negative bacteria. The table does not list redundant or mutant structures.

Organism	AQP	permeant	comment	method	resolution (Å)	PDB ID
Homo sapiens	AQP1	w	refined structure	e^-	3.8	1H61
Homo sapiens	AQP4	w	aa 32-254	X	1.8	3GD8
Homo sapiens	AQP5	w		X	2.0	3D9S
Rattus norvegicus	AQP4	w	aa 23-323	e^-	3.2	2D57
Bos taurus	AQP0	w	open	e^-	2.4	2B6P
Bos taurus	AQP1	w		X	2.2	1J4N
Ovis aries	AQP0	w	closed	e^-	1.9	2B6O
Spinacia oleracea	PIP2;1	w	open	X	3.9	2B5F
Spinacia oleracea	PIP2;1	w	closed	X	2.1	1Z98
P. falciparum	AQP	g/w		X	2.1	3C02
Pichia pastoris	AQY1	w	closed, pH 3.5	X	1.2	2W2E
M. marburgensis	AQPM	g/w		X	1.7	2F2B
A. fulgidus	AQP	(g/w)		X	3.0	3NE2
E. coli	GlpF	g/w		X	2.2	1FX8
E. coli	AQPZ	w		X	3.2	2ABM
A. tumefasciens	AQPZ	(w)		X	2.0	3LLQ

An important feature of water and solute channels, the exclusion of protons, was shown by computational studies to be partly due to the electrostatic field generated by the half-helix backbones, the positive ends of which meet at the NPA region (de Groot *et al.* 2003). Experimentally lowering this electrostatic barrier by replacing an asparagine with aspartic acid (presumably deprotonated) in rat AQP1 does not however lead to a marked increase in proton permeation, unless conserved pore-lining arginine and histidine residues (Fig. 1.5) are concomitantly replaced by, respectively, uncharged valine and alanine residues. This triple mutation not only increases proton, but also sodium and potassium ion permeation by approximately one order of magnitude (Wu *et al.*, 2009). The importance of the positively charged arginine residue in proton exclusion had been predicted by early computational studies (de Groot and Grubmüller, 2001).

Replacing either of the highly conserved asparagines by serine does not seem to affect water or glycerol permeability of aquaporins, but may increase sodium permeability. Other mutations at this position, including exchanges by the typically helix-capping amino acid residues threonine and aspartic acid, are mostly deleterious (Wree *et al.*, 2011). Among the 1008 aquaporin sequences listed in the MIPMod Database at the time of writing, exchanges of asparagine to other amino acids are found in 22 pore-helix caps (11 each for the two motifs, or about 1 %), exchanges of proline and alanine in 83 and 191 caps, respectively

(about 4 % and 9 %). Double exchanges such as SPT or CPY occur, triple exchanges apparently do not (Gupta *et al.*, 2012). Guan *et al.* (2010) found the plasma membrane targeting of NPA mutants of rat AQP4 to be affected. Overall, the NPA motifs appear to have a mainly structural role.

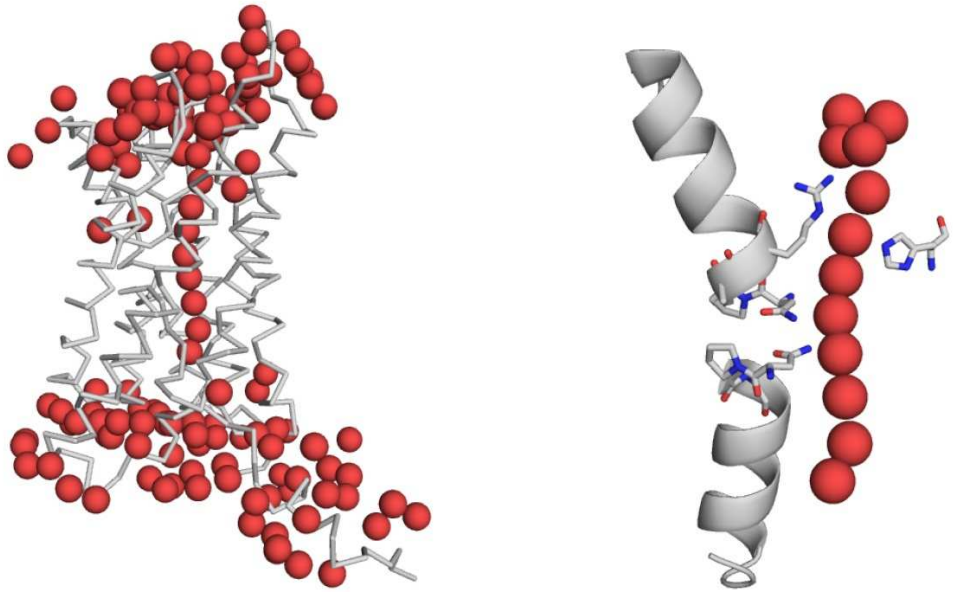

Fig. 1.5: Permeation of water molecules through an aquaporin monomer. Left*: The aquaporin backbone is shown as a ribbon, the water molecules as spheres representing their oxygen atoms. Note the single file of water molecules at the centre of the aquaporin monomer. The gap between the last single-file water molecule and the bulk water molecules is present as such in the crystal structure.* ***Right****: Close-up showing the two half-helices which meet with their asparagine/proline/alanine caps (represented as sticks) at the centre of the channel. The asparagine amide nitrogens point towards the passing water molecules. The arginine and histidine residues, located at the extracellular half of the channel, make up its narrowest constriction where water molecules are singled out. Most other amino acid residues lining the channel are hydrophobic (not shown). The yeast aquaporin Pichia pastoris AQY1 was chosen because its structure has been determined at the highest resolution of any aquaporin to date (1.15 Å, PDB ID: 2W2E).*

The arginine and histidine residues shown in Figure 1.5 are part of the narrowest section of the channel, frequently termed the aromatic/arginine (ar/R) constriction because of an aromatic amino acid residue situated next to the arginine in most aquaporins (82 % of the aquaporins listed in the MIPMod Database). The ar/R constriction of bovine AQP1 is depicted in Figure 1.6.

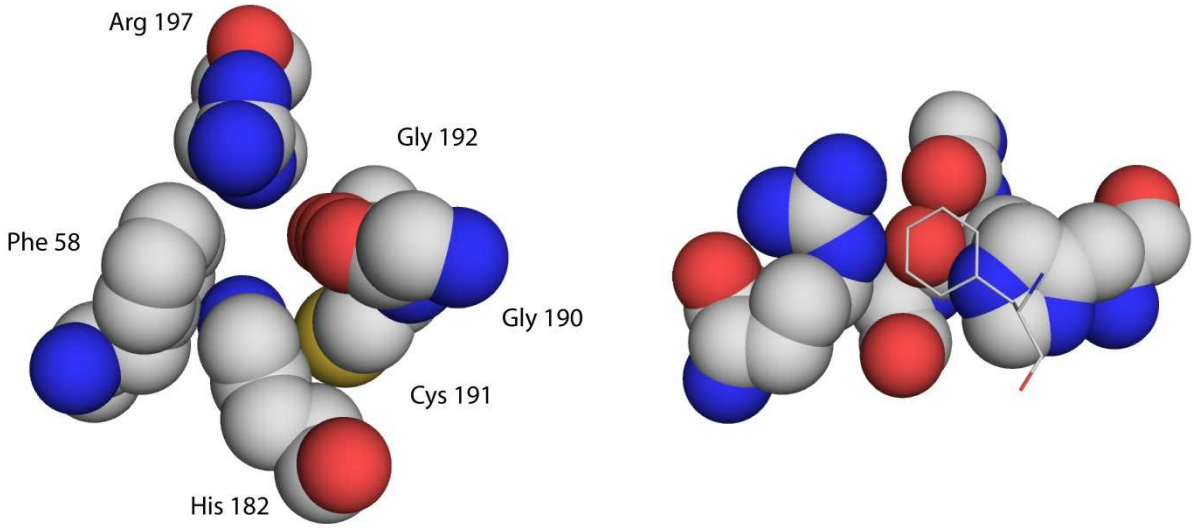

Fig. 1.6: Aromatic/arginine constriction of bovine AQP1 (92 % amino acid sequence identity with human AQP1). Left*: View from the extracellular side through the channel. Phenylalanine 58 is situated in the middle of Helix 2, Histidine 182 close to the C-terminal end of Helix 5, Cystein 191 in Loop E1, and Arginine 197 in Helix E (see Figs. 1.2 and 1.3). Cystein 191 is the channel's mercuric ion-sensitive site.* ***Right****: View along the membrane plane at the string of carbonyl groups belonging to Loop E1. The orientation of the arginine and histidine residues is the same as in Fig. 1.5. Phenylalanine 58 is shown as a wire model. Please note the hydrogen-bonding of the arginine residue with its backbone carbonyl group. (PDB ID: 1J4N).*

A string of backbone carbonyl groups lines one side of the constriction in all aquaporins. It is part of a string of four carbonyl groups and the asparagine amide of Loop E1 (Figs. 1.2 and 1.5) which line the narrow section of the channel, with a corresponding array of hydrophilic groups provided by Loop B1 at the intracellular half of the channel.

The ar/R constrictions of the water-selective AQPZ and the glycerol-permeable GlpF of *E. coli* are compared in Figure 1.7. As expected, the ar/R constriction of the glycerol-permeable channel is wider than that of the water-selective one, with approximate diameters of 3.4 Å and 2.2 Å, respectively - a water molecule has a diameter of approximately 2.8 Å (Fu *et al.*, 2000, Savage *et al.*, 2003 and 2010). In addition, the glycerol channel is wider than the water channel along most of its length of about 20 Å, in particular at the NPA region, where the respective diameters are about 4.6 Å and 3.2 Å (Wang *et al.*, 2005). Mutating the ar/R constriction of AQPZ to resemble that of GlpF accordingly does not produce a glycerol-permeable channel but merely results in a loss of water permeability by an order of magnitude (Savage *et al.*, 2010).

A surprising finding is the low water permeability of GlpF despite its greater width as compared to AQPZ: At 1 % (w/w) protein/lipid ratio, the presence of AQPZ increases water permeability of liposomes by about two orders of magnitude, GlpF by about one, with sucrose as osmolyte (Borgnia *et al.*, 2001, Savage *et al.*, 2010). Similar results are obtained by functional characterization of GlpF expressed in *Xenopus* oocytes and in *S. cerevisiae* protoplasts (Maurel *et al.*, 1994, Song *et al.*, 2012). Computational studies predict similar

water permeability of both channels (Jensen and Mouritsen, 2006) and of GlpF and the water-selective human AQP1 (Hub and de Groot, 2008).

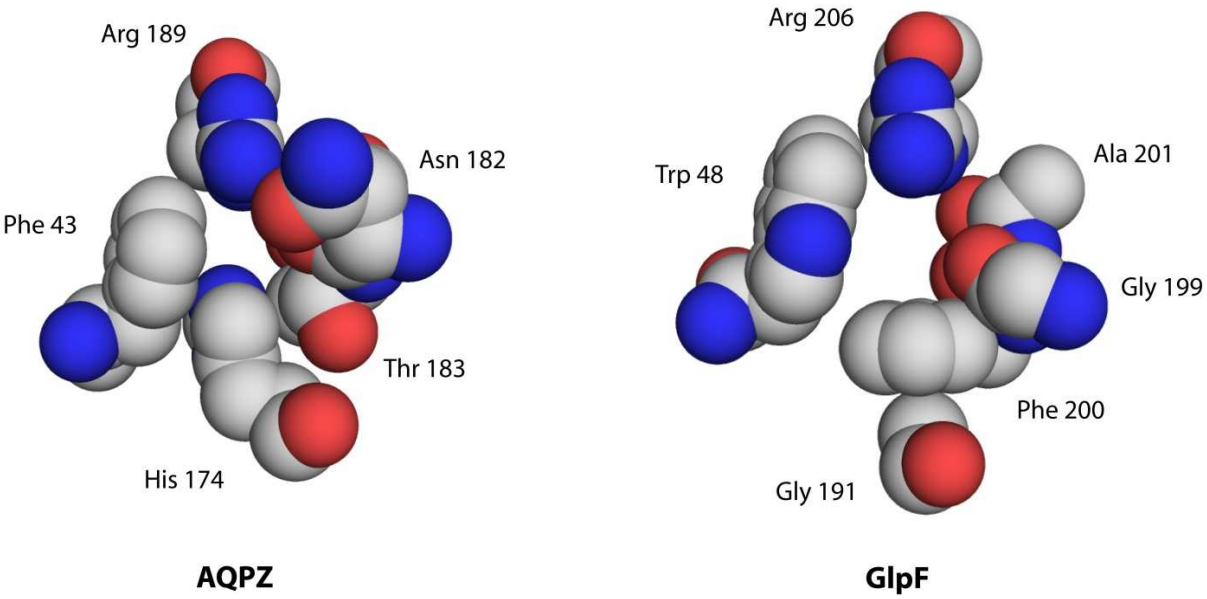

Fig. 1.7: Aromatic/arginine constrictions of a water-selective and a glycerol-permeable aquaporin. Left*: E. coli AQPZ (PDB ID: 2ABM, first monomer of the first tetramer). A histidine is commonly found opposite to the arginine in water-selective aquaporins. In this particular crystal structure, the side chain of Asparagine 182 appears to contribute to the channel-lining carbonyl groups, although in the native protein it may not do so.* ***Right****: E. coli GlpF (PDB ID: 1FX8). A glycine (Gly 191) lies opposite to the constriction arginine, leaving space for a phenylalanine residue equivalent to Thr 183 in AQPZ and Cys 191 in bovine AQP1 (Fig. 1.6). In some aqua-glyceroporins, a tyrosine is found instead of phenylalanine, and phenylalanine in place of tryptophan. The carbon backbone of a passing glycerol molecule slides along the hydrophobic wedge created by the two aromatic residues, its hydroxyl groups interact with the arginine residue.*

Again, experiments have provided a clue as to why glycerol channels may not conduct water as efficiently as water channels: The single aquaglyceroporin of the malarial parasite *Plasmodium falciparum* (PfAQP) has an ar/R constriction identical to that of *E. coli* (Fig. 1.7) and the remainder of the channel is very similar, yet it conducts both glycerol and water when expressed in *Xenopus* oocytes, the latter to a degree comparable to rat AQP1 (Hansen *et al.*, 2002). It turns out that a glutamic acid residue in the long extracellular Loop C (Figs. 1.2 and 1.3), which folds into the extracellular pore mouth, or vestibule, is responsible for this effect. Mutating it to aspartic acid or glutamine does not affect channel function, whereas mutating it to serine abolishes water permeability while not significantly affecting glycerol permeability (Beitz *et al.*, 2004). The solving of the PfAQP crystal structure has shown that this may be due to an increased saturation of hydrogen bond donor sites of its constriction arginine when compared to *E. coli* GlpF (Fig. 1.8, Newby *et al.*, 2008).

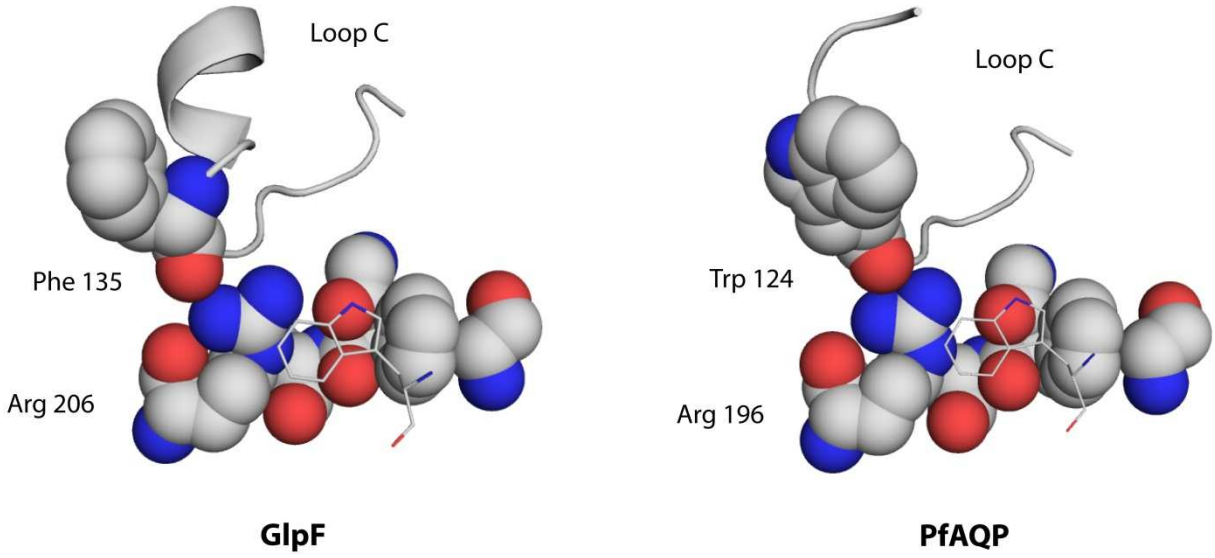

***Fig. 1.8**: **Effect of Loop C on the hydrogen bond saturation of the constriction arginine side chain in E. coli GlpF and P. falciparum AQP.** View along the membrane plane as in Figs. 1.5 and 1.6. E. coli GlpF does not conduct water efficiently under most experimental conditions. In PfAQP, the particular arrangement of the backbone carbonyl group of Tryptophan 124 probably necessitates an adjacent glutamic acid residue (Glu 125, not shown). Mutating Glu 125 to serine abolishes water but not glycerol permeability. (GlpF: 1FX8, PfAQP: 3CO2).*

Of the crystal structures other than GlpF listed in Table 1.1, all but rat AQP4 (PDB ID: 2D57) show a C-loop constriction arginine hydrogen bond comparable to that of PfAQP (the rat AQP4 S180D crystal structure, with a mutation in the intracellular D-loop, and not listed in Table 1.1, shows the standard arrangement, PDB ID: 2ZZ9). The crystal structures of GlpF without glycerol (PDB ID: 1LDA) and the mutant W48F F200T (PDB ID: 1LDF) show the same arrangement as in Figure 1.8. Keeping in mind that the structures of crystallized proteins may differ from their native counterparts, it appears that *E. coli* GlpF rather than PfAQP is exceptional in that it prefers glycerol over water.

The above example shows how important it can be to consider spatially neighbouring amino acid residues of the ar/R constriction. Nevertheless, identification of putative ar/R constriction residues by amino acid sequence alignment allows one to predict whether a given aquaporin is water-selective or whether it may be a solute channel in addition.

1.2 Ammonia permeability of aquaporins

Some chemical properties of ammonia

At room temperature and sea level atmospheric pressure ammonia (NH_3) is a gas which avidly dissolves in water up to a concentration of about 31 mol %, with an initial heat of solvation of around -7.3 kcal/mol. In water it is a weak base of pK_b 4.77 at 20 ℃, so at

neutral pH the majority of it is present as ammonium ions (NH_4^+). Ammonia molecules are similar to water molecules in size and polarity, with respective gas phase dipole moments of 1.47 D and 1.85 D, and hexadecane partition coefficients of -2.66 and -4.38 at 25 °C, but due to their third hydrogen atom they differ in shape and symmetry (Weast, 1977, Walter and Gutknecht, 1986). Ammonia molecules can undergo dipole inversions with characteristic frequencies in the gas phase (Wiberg, 1995). They are good hydrogen bond acceptors, but poor hydrogen bond donors, with a calculated ammonia-water hydrogen bonding energy of approximately 7.8 kcal/mol ($HO\text{-}H\cdots NH_3$), as compared to about 6.0 kcal/mol for a water-water hydrogen bond (Nelson *et al.*, 1987, Zhu and Yang, 1994, Poater *et al.*, 2002). Two hydrates, $NH_3 \cdot H_2O$ (Mp -79.00 °C) and $NH_3 \cdot 2H_2O$ (Mp -78.83 °C), can be isolated (Wiberg, 1995). Ammonia forms stable complexes with several metal ions, among them cupric ones (Hathaway and Tomlinson, 1970). Ammonium ions have properties similar to those of potassium ions in solution, such as nearly identical ionic mobilities in water at 25 °C (Atkins and de Paula, 2006). Ammonium-water hydrogen bonds are strong, at a calculated value of 22.1 kcal/mol and a measured heat of solvation of ammonium ions of -86.8 kcal/mol, yet ammonium ions rotate rapidly in water, with a correlation time of the order of 1 ps (Perrin and Gipe, 1987, Brugé *et al.*, 1999, Poater *et al.*, 2002).

Some biological properties of ammonia

Ammonia is an important nitrogen source for microorganisms and plants. It is made by the reduction of atmospheric nitrogen, catalysed by nitrogenase enzymes in specialized procaryotes, at the cost of hydrolysis of at least 16 ATP molecules per nitrogen molecule. Its main entry points in cellular metabolism are the synthesis of glutamic acid with 2-oxoglutaric acid, necessitating reduction, and the synthesis of glutamine with glutamic acid. Depending on the organism, excess ammonia may be excreted as such, or in the form of uric acid, urea, or other nitrogen-containing molecules such as amino acids (Berg *et al.*, 2002, Hess *et al.*, 2006). Humans are ureotelic, the amount of urea generated in the liver and excreted by the kidneys depending on age, nutrition, pathological states and other factors, with urine concentration generally being situated somewhere between 200 mM and 400 mM. Ammonium is also excreted with the urine, at a concentration of about 30 to 50 mM, comparable to that of potassium (Pocock and Richards, 2004, Deam and Lentner, 1969). Unlike bulk nitrogen excretion by urea, ammonium excretion serves in the long-term regulation of acid-base balance, decreasing in states of acidosis and increasing in states of alkalosis, effectively raising, together with hydrogen phosphate ions, urine pH which could otherwise drop below a value of 3. Ammonium excretion is inversely related to potassium status (Adeva *et al.*, 2012). The blood plasma concentration of ammonium ions is found to be between about 0.005 and 0.02 mM in healthy adults, compared to about 4 to 7 mM urea (Pocock and Richards, 2004,

Deam and Lentner, 1969). The thousandfold increase in ammonium concentration from blood to urine may partly be explained by its generation from glutamine and a few other amino acids in the kidney, especially in the proximal tubule mitochondria (Weiner and Verlander, 2011, Adeva *et al.*, 2012). Some of the ammonium generated by the kidney is released into the blood circulation. Permanently elevated blood levels are indicative of liver disease. Hyperammonemia is believed to be a cause of the encephalopathy associated with hepatic failure, although blood ammonium concentrations do not correlate well with the severity of symptoms (Adeva *et al.*, 2012).

Ammonia permeability of biological membranes

Due to their respective acidity and basicity, the passage of ammonium and ammonia through a membrane is inextricably linked to changes in pH in the adjacent aqueous compartments. Since both are present at physiological pH, the degree of this change will depend on their relative permeability, with no change if the ammonium permeability is higher than the ammonia permeability by a factor of 10^{pKa-pH}, *e. g.* 100 if the initial pH on both sides is 7.25 and the pK_a is 9.25 (Musa-Aziz *et al.*, 2009). For this reason, and for lack of a radioactive nitrogen isotope, most ammonia permeability studies make use of pH measurements or changes in fluorescence of pH-sensitive dyes. The heavy nitrogen isotope ^{15}N allows for nuclear magnetic resonance or mass spectrometric studies, but these are apparently rarely used (Musa-Aziz *et al.*, 2009).

The passage of ammonium ions is subject to membrane potential and needs to be accompanied by transport of other ions if it is to be electroneutral. In the mammalian kidney, several ion transporters and channels contribute to ammonium permeation across epithelial membranes: sodium-proton-exchangers which despite their name also serve as sodium-ammonium-exchangers, barium-sensitive potassium channels, potassium-ammonium-exchangers, a sodium-potassium-chloride symporter, and the sodium-potassium-ATPase (Weiner and Verlander, 2010). The passage of unprotonated ammonia across the apical membrane of proximal tubule cells is facilitated by an uncharacterized transport pathway. In the thick ascending limb of the loop of Henle, ammonia passage is not facilitated. In the collecting duct intercalated cells (A and non-A-non-B) the Rhesus proteins RhCG and RhBG facilitate ammonia passage through both apical and basolateral membranes (Weiner and Verlander, 2010).

Ammonia is a small molecule and, compared to water, a more hydrophobic one which may be expected to diffuse through the lipid portion of membranes at a substantial rate. When considering its facilitated permeation it is thus worth comparing the permeability of a variety of membranes, both artificial and biological. A common measure is the permeability coefficient P (m s^{-1}) which, when multiplied with a concentration gradient (mol m^{-3}), yields the

permeation rate (mol m^{-2} s^{-1}). Table 1.2 lists a number of ammonia and osmotic water permeability coefficients found in the literature.

Table 1.2: Ammonia permeability coefficients of a variety of artificial and biological membranes.
Where available, the corresponding osmotic water permeability coefficient (P_f) is given for comparison. Standard deviations are omitted for clarity and range between 2 and 30 % (52 % in one case). Abbreviations and citations are explained below. Brackets indicate a lack of explicit specification or of the method of calculation. The table does not represent a complete list of ammonia permeability coefficients found in the literature.

Organism/lipids	method	*T* (℃)	P_{NH3} ($\mu m\ s^{-1}$)	P_f ($\mu m\ s^{-1}$)	P_{NH3}/P_f	comment	cit.
egg PC	mem. pot.	25	1300	34	38	planar bilayer	1
POPC	fluor.	25	360	72	5.0	LUV, *D* ≈ 130 nm	2
Sph/Ch 6/4	fluor.	25	24	2.2	11	LUV, *D* ≈ 130 nm	2
POPC	calculated	27	1300	-	-	computer simulation	3
POPE	calculated	27	170	-	-	computer simulation	3
soy PC	$[NH_4^+]$, pH	(RT)	520	-	-	planar bilayer	4
soy PC/Ch 2/1	$[NH_4^+]$, pH	(RT)	160	-	-	planar bilayer	4
Ch/Ec/Sph 3/2/1	$[NH_4^+]$, pH	(RT)	16	11	1.5	planar bilayer	5
PE/Ch/PS/PI	fluor.	25	79	44	1.8	40/37/20/3, liposomes	6
Ch/GSL/Sph/PC	fluor.	25	1.3	2.4	0.5	52/21/18/9, liposomes	6
Ec	fluor.	23	138	55	2.5	LUV, *D* ≈ 110 nm	7
G. max, B. japon.	fluor.	(22)	79	60	1.3	PBM vesicles	8
A. nidulans	chemical	(30)	6.4	-	-	whole cells, pH 9.5-10	9
R. sphaeroides	chemical	(30)	2.6	-	-	whole cells, pH 9.5-10	10
O. cuniculus	pH	37	50	-	-	perfused CCDT	11
S. scrofa	fluor.	RT	44	2.8	16	gastric par. cell AM vesicles	12
(rabbit)	fluor.	RT	15	2.3	6.5	urinary bladder AM vesicles	13
R. norvegicus	fluor.	20	23	9.4	2.4	MTAL AM vesicles, amiloride	14
R. norvegicus	fluor.	20	29	12	2.4	MTAL BM vesicles, amiloride	14
C. lupus	fluor.	18	12	-	-	MDCK monolayer, AM perm.	15
H. sapiens	pH	37	108	-	-	erythrocytes	16
H. sapiens	NMR	21	2100	-	-	erythrocytes	17
H. sapiens	fluor.	15	4.5	-	-	erythrocyte ghosts	18
X. laevis	pH_e	23	(4)	1.9	(2)	oocytes, pH 7.4, spring	19
X. laevis	pH_e	23	(8)	1.9	(4)	oocytes, pH 7.4, autumn	19
X. laevis	pH_e	(RT)	(1.3)	1.4	(1)	oocytes, pH 7.4	20

Abbreviations: *PC (phosphatidyl choline), POPC (palmitoyl oleyl PC), Sph (sphingomyelin), Ch (cholesterol), PE (phosphatidyl ethanolamine), Ec (E. coli lipid extract), PS (phosphatidyl serine), PI (phosphatidyl inositol), GSL (glycosphingolipids), Glycine max (soy plant) infected by Bradyrhizobium japonicum (a nitrogen-fixing bacterium), Anacystis nidulans (a cyanobacterium), Rhodobacter sphaeroides (gram-negative, phototrophic), Oryctolagus cuniculus (New Zealand white rabbit), Sus scrofa (domestic pig), Rattus norvegicus (brown rat), Canis lupus (dog), Xenopus laevis (African clawed frog), mem. pot. (membrane potential), fluor. (fluorimetry), pH_e (extracellular pH), RT (room temperature), LUV (large unilamellar vesicle), D (mean diameter), MDCK (Madin-Darby canine kidney epithelial cell line), PBM (peribacteroid membrane), CCDT (renal cortical collecting duct tubule), par. (parietal), AM (apical membrane), BM (basolateral membrane), MTAL (renal medullary thick ascending limb).*
Citations: *[1] Walter 1986, [2] Lande 1995, [3] Hub 2010, [4] Antonenko 1997, [5] Saparov 2007, [6] Hill 2000, [7] Hwang 2010, [8] Niemietz 2000, [9] Ritchie 1987, [10] Ritchie 1987 b, [11] Hamm 1985, [12] Priver 1993, [13] Chang 1994, [14] Rivers 1998, [15] Golchini 1988, [16] Klocke 1972, [17] Labotka 1995, [18] Ripoche 2004, [19] Holm 2005, [20] Zeuthen 2006.*

Ammonia permeability coefficients in the literature are found to range between about 1 and 10^3 µm/s. Simple artificial membranes such as those made of pure or extracted phosphatidyl choline species tend to have the highest permeability, addition of cholesterol lowers it. The lowest ammonia permeability is found for certain biological membranes, such as those of renal medullary thick ascending limb-derived vesicles, and for artificial membranes mimicking

their lipid composition. Human erythrocytes contain ammonia-permeable Rhesus glycoproteins (Ripoche *et al.*, 2004). In Table 1.2, the erythrocyte ammonia permeability determined by three groups is listed for comparison. The differences are striking, with permeability coefficients of 108, 2100 and 4.5 µm/s reported. They are mainly due to differing treatment of unstirred layer-effects: Klocke *et al.* (1972) dismiss them on the basis of geometric considerations, Labotka *et al.* (1995) take them very seriously, Ripoche *et al.* (2004) point out that Labotka and colleagues obtain a comparable ammonia permeability coefficient if they exclude unstirred-layer effects from their calculations. Determining permeability coefficients for non-electrolytes with high basal membrane permeability is delicate work.

Assuming that the ammonia permeability coefficients listed in Table 1.2 are correct within an order of magnitude, then for biological membranes without ammonia-permeable channels a value of 10^1 µm/s appears to be a reasonable approximation. The corresponding osmotic water permeability coefficient is generally no more than tenfold lower. Some groups also determined activation energies of unfacilitated ammonia passage, and these range from about 15 to 25 kcal/mol, the corresponding value for water being consistently close to 15 kcal/mol (not shown).

Table 1.3 lists ammonia and osmotic water permeability coefficients of artificial or *Xenopus* oocyte membranes in the absence or presence of aquaporins.

Table 1.3: Ammonia permeability coefficients of artificial or biological membranes in the absence or presence of aquaporins. *Osmotic water permeability coefficients (P_f) are listed for comparison. Relative standard deviations of permeability coefficients range between 5 and 25 %. "Density" refers to the number of aquaporin monomers per membrane area. Brackets indicate lack of specification, differing units, or estimates. Abbreviations and citations are given below.*

Organism/lipids	method	*pH*	*T* (°C)	AQP	density (μm^{-2})	P_{NH3} ($\mu m\ s^{-1}$)	P_f ($\mu m\ s^{-1}$)	comment	cit.
Ec	fluor.	6.8	23	-	-	138	55	LUV, $D \approx 110$ nm	1
Ec	fluor.	6.8	23	Nod26	8800	350	95	LUV, $D \approx 110$ nm	1
Ec	fluor.	6.8	(RT)	-	-	120	30	LUV, $D \approx 150$ nm	2
Ec	fluor.	6.8	(RT)	hAQP1	540	120	120	LUV, $D \approx 150$ nm	2
Ch/Ec/Sph 3/2/1	$[NH_4^+]$, pH	6.0	(RT)	-	-	16	11	planar bilayer	3
Ch/Ec/Sph 3/2/1	$[NH_4^+]$, pH	6.0	(RT)	rAQP8	(1/50 p/l)	105	27	planar bilayer	3
X. laevis	pH_e	7.4	23	-	-	(4)	1.9	oocytes	4
X. laevis	pH_e	7.4	23	hAQP1	(10^3)	(4.5)	31	oocytes	4
X. laevis	pH_e	7.4	23	rAQP8	(10^3)	(6)	33	oocytes	4
X. laevis	pH_e	7.4	23	rAQP9	(10^3)	(6)	10	oocytes	4

Abbreviations: *Ec (E. coli lipid extract), Ch (cholesterol), Sph (sphingomyelin), Xenopus laevis (African clawed frog), fluor. (fluorimetry), pH_e (extracellular pH), RT (room temperature), Nod26 (Nodulin26, an aquaglyceroporin of the soybean plant Glycine max), h/rAQP (human/rat AQP), p/l (protein/lipid ratio w/w), LUV (large unilamellar vesicle), D (mean diameter).*

Citations: *[1] Hwang 2010, [2] Zeidel 1994, [3] Saparov 2007, [4] Holm 2005.*

AQP1 does not seem to increase ammonia permeability in liposomes, in *Xenopus* oocytes it does so barely and perhaps not significantly at a similar surface density (~ 10^3 channels per μm^2), whereas water permeability is substantially increased in both cases. Nodulin 26 and AQP9 are aquaglyceroporins with proven glycerol permeability (Rivers *et al.*, 1997, Tsukaguchi *et al.*, 1999), and both increase ammonia permeability significantly. Characteristically, neither increases water permeability as much as human AQP1. AQP8 increases both ammonia and water permeability in an artificial membrane as well as in *Xenopus* oocytes.

Other groups have shown AQP1 to increase the ammonia permeability of *Xenopus* oocytes, without calculating permeability coefficients, by measuring acidification rates close to the extracellular side of the plasma membrane (Nakhoul *et al.*, 2001, Musa-Aziz *et al.*, 2009 b). A possible reason for such a discrepancy is the unspoken principle of channel-mediated membrane permeability measurements pictured in Figure 1.9.

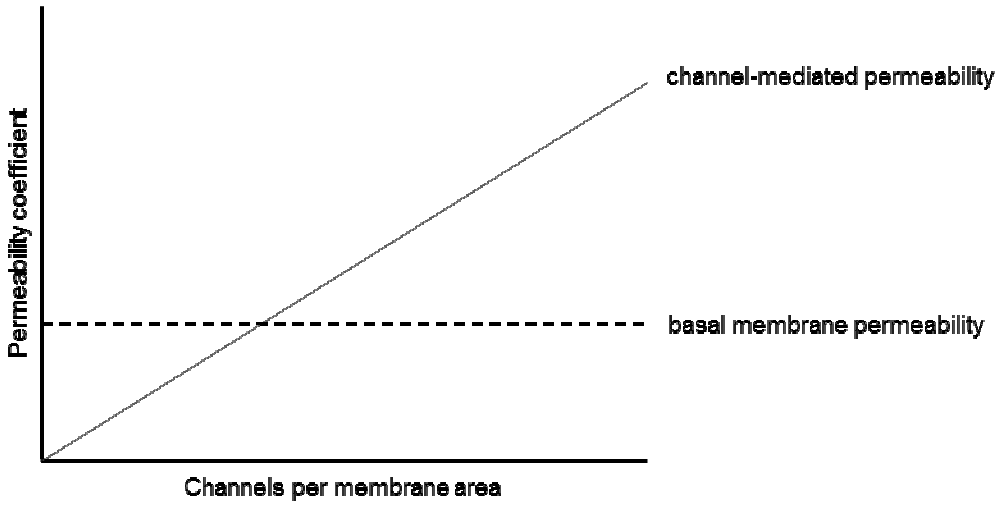

Fig. 1.9: Channel permeability detection threshold. *High basal membrane permeability for a particular solute will mask channel contribution below a certain density. The slope of channel-mediated permeability is proportional to the single channel-permeability and varies with the solute. The density of channels is limited. The detection threshold depends on the precision of the experimental method, and on the number of experiments. Channel-mediated permeability similar to the basal membrane permeability should be detectable in most cases. Basal membrane permeability may be affected by the presence of other channels.*

Unless the channel density of a membrane reaches a certain threshold, contribution of the former to solute permeability will remain undetectable. For ion channels this threshold is probably very low, for small non-electrolytes such as ammonia it may be high. Thus, AQP1 may conduct ammonia, although probably at a single channel-permeability too low to detect at typical densities (*e. g.* ~ 10^3 μm^{-2} in erythrocytes).

Musa-Aziz and coworkers have also studied AQP4- and AQP5-producing *Xenopus* oocytes. Neither protein significantly affects ammonia permeability, whereas water permeability is increased (Musa-Aziz *et al.*, 2009 b).

Molecular determinants of aquaporin ammonia permeability

The literature on ammonia permeability by aquaporins reveals the following findings: The aquaglyceroporins Nod26, rAQP3, rAQP9, PfAQP, *Toxoplasma gondii* AQP and *Trypanosoma brucei* AQP all conduct ammonia (Niemietz and Tyerman, 2000, Hwang *et al.*, 2010, Holm *et al.*, 2005, Zeuthen *et al.*, 2006). The aquaporins hAQP1, rAQP4, hAQP5 and rAQP1 do not conduct ammonia, or poorly so (Zeidel *et al.*, 1994, Nakhoul *et al.*, 2001, Jahn *et al.*, 2004, Holm *et al.*, 2005, Beitz *et al.*, 2006, Musa-Aziz *et al.*, 2009 b). Members of a phylogenetically distinct class of aquaporins, represented by AQP8 in mammals (Fig. 1.1), and by the tonoplast intrinsic proteins (TIP) in plants, conduct ammonia at a rate comparable to that of water permeation (Jahn *et al.*, 2004, Holm *et al.*, 2005, Saparov *et al.*, 2007).

Aquaglyceroporins have a wider pore than aquaporins, in particular at the ar/R constriction (Fig. 1.7), and this may explain their higher ammonia permeability. At the time of writing, no high-resolution structure of a member of the AQP8/TIP class of aquaporins is available, but the conserved structural elements of aquaporins allow for a confident prediction of the amino acids that make up their ar/R constriction by sequence alignment (Fig. 1.10).

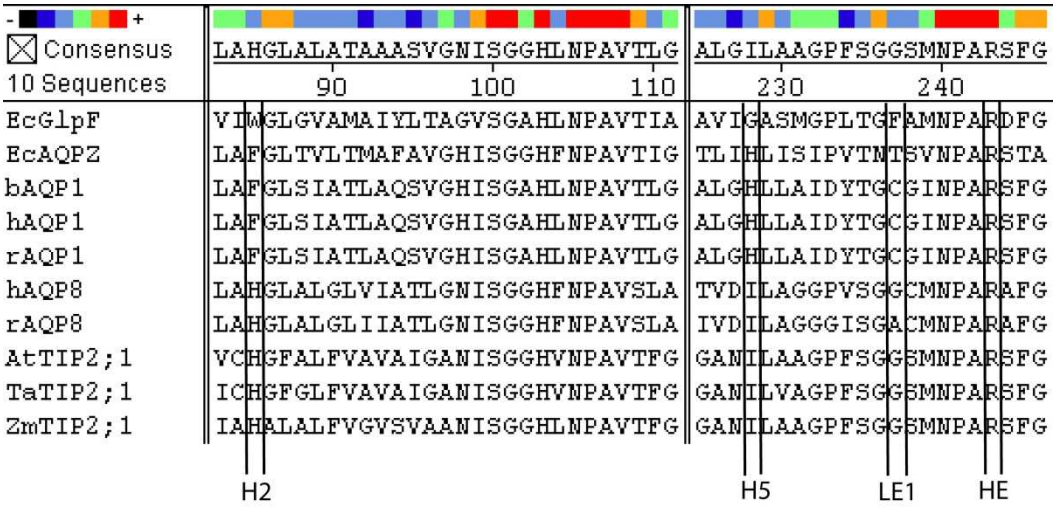

Fig. 1.10: Amino acid sequence alignment of members of water- and water/ammonia-selective aquaporins. *Amino acids that make up the aromatic/arginine constriction are framed. H2, H5, HE, and LE1 denote Helices 2, 5, E and Loop E1 (Figs. 1.2 and 1.3). E. coli GlpF and AQPZ (Fig. 1.7) are included for comparison with bovine, human, and rat aquaporins and plant tonoplast intrinsic proteins (TIP) from Arabidopsis thaliana (At), Triticum aestivum (Ta, wheat) and Zea mays (Zm, corn). Amino acids up- and downstream of both NPA motifs are included. Sequences are from the NCBI. The alignment was generated with the programme MegAlign using the ClustalW algorithm.*

Compared to the water-selective aquaporins AQP1 and AQPZ, AQP8 and TIPs have a histidine in place of a phenylalanine, and an isoleucine in place of a histidine. Arginine is found in both, with the exception of valine in a subclass of TIPs not shown. The AQP8 constriction contains a cysteine a single position downstream compared to the AQP1 constriction. Figure 1.11 shows a model of the ar/R constriction of rat AQP8.

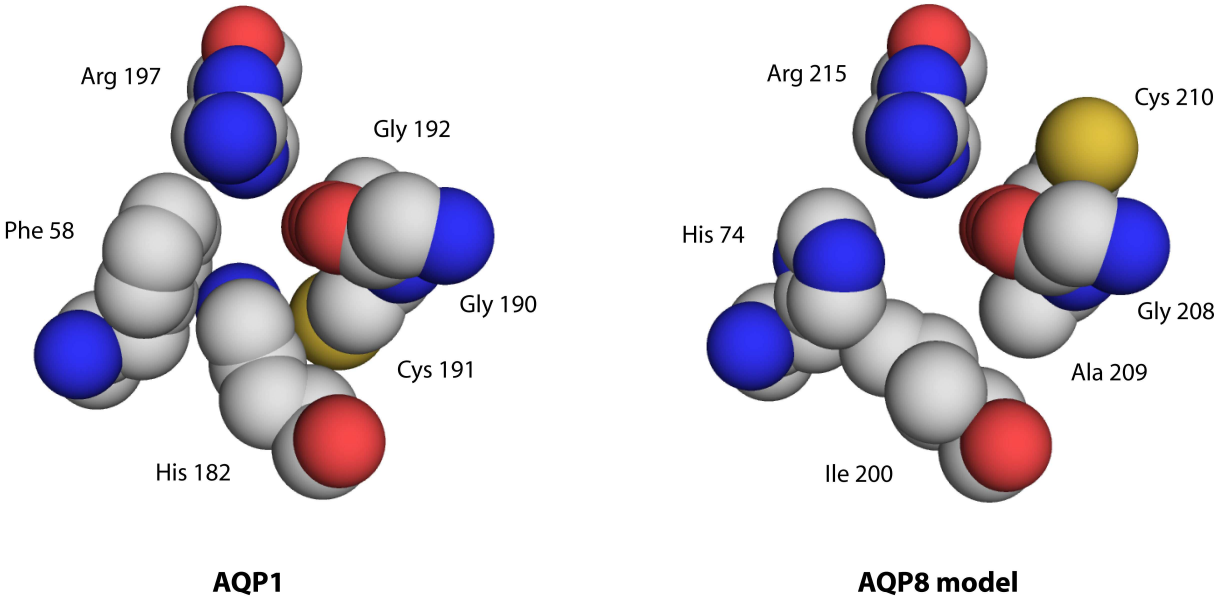

Fig. 1.11: Aromatic/arginine constrictions of a water-selective and an ammonia-permeable aquaporin. *The structure of the constriction of rat AQP8 is based on the amino acid sequence alignment shown in Fig. 1.10, and on the known structure of bovine AQP1. A histidine in place of a phenylalanine, and an isoleucine in place of a histidine are characteristic for animal AQP8 and plant tonoplast intrinsic proteins, some members of which have been shown to conduct ammonia and urea in addition to water.*

If the relative positions of constriction amino acid backbone atoms in AQP8/TIPs are similar to those of AQP1, then the resulting constriction is wider and, due to the isoleucine residue, more hydrophobic.

In the wheat aquaporin TaTIP2;1 (Fig. 1.10), mutation of the constriction histidine to phenylalanine reduces the ammonia permeability as judged by growth on limited ammonium nitrogen of an ammonium transporter-deficient yeast strain heterologously producing the aquaporin. Mutating isoleucine to histidine has a similar effect, mutating glycine to cysteine has none (Jahn *et al.*, 2004). Expression of TaTIP2;1 in *Xenopus* oocytes increases water permeability and the extracellular acidification rate upon addition of ammonium chloride (presumably due to passage of unprotonated ammonia into the cell). The double mutant TaTIP2;1 I184H G193C does not increase ammonium-induced acidification, whereas water permeability is the same as for wild-type TaTIP2;1-producing oocytes (Holm *et al.*, 2005).

Mutating the ar/R constriction of the water-selective *Arabidopsis thaliana* plasma membrane intrinsic protein 2;1 (AtPIP2;1) to resemble those of a variety of *Arabidopsis* TIPs (requiring triple mutations), does not increase ammonia permeability in yeast complementation assays. TaPIP2;1 with an ar/R constriction resembling that of some *Arabidopsis* nodulin-like intrinsic proteins (NIP), does increase ammonia permeability. The major difference compared to TIPs is a tryptophan or an alanine in place of the histidine (Histidine 72 in hAQP8, Fig 1.11, Dynowski *et al.*, 2008).

In rat AQP1, with an ar/R constriction identical to that of bovine AQP1 (Figs. 1.10 and 1.11), mutating histidine to alanine or arginine to valine increases ammonia and methylamine

permeability as judged by yeast complementation assays and ammonium-induced extracellular acidification in *Xenopus* oocytes (Beitz *et al.*, 2006). The authors suggest that an increased hydrophobicity, as well as a widening of the ar/R constriction, is required for passage of the ammonia molecule which is slightly larger and more hydrophobic than water. Jahn *et al.* (2004) suggest the same.

A computational study on solute passage through *E. coli* GlpF, human AQP1 and its double mutant H180A R195V supports this assumption, pointing out that a major barrier of AQP1 to small solute-passage is a loss of water-protein hydrogen bonds (Hub and de Groot, 2008). Incidentally, this study reveals that ammonia permeation of human AQP1 is comparably favourable to that of a palmitoyl oleyl phosphatidyl ethanolamine membrane as judged by free energy barriers (~ 4.5 kcal/mol), *i. e.* ammonia can pass through a "water-selective" aquaporin (Fig. 1.9).

Dynowski *et al.* (2008) point out that this view may be too simple, since water-selective TaPIP2;1 could not be made to conduct ammonia by mutating ar/R constriction residues. They refer to a study by Bertl and Kaldenhoff (2007) which shows that ammonia may pass through the central pore of TaTIP2;2 (Fig. 1.4) when expressed in yeast. This conclusion is based on differential inhibition by mercuric chloride of water and ammonia permeability through TaTIP2;2. The high affinity of ammonia to mercuric ions and the possible precipitation of mercuric amidochloride (Wiberg, 1995) are not mentioned. Site-directed mutagenesis of central pore-lining amino acids has not been reported.

In summary, the ar/R constriction is probably responsible for an ammonia permeability of AQP1 too low to detect in some cases. Mutating its ar/R constriction to resemble that of human AQP8 was the starting point of the work presented here.

Localization and function of AQP8 and tonoplast intrinsic proteins

Of the 1008 aquaporins listed in the MIPMod Database (Gupta *et al.*, 2012), 12 % are predicted to have a histidine as the aromatic amino acid in their constriction, compared to 48 % with a phenylalanine. An isoleucine opposite to the constriction arginine (or valine in some cases) is predicted for 10.8 % of these aquaporins, both histidine and isoleucine for 10.6 %. In other words, the couple histidine/isoleucine appears to be conserved as a partial ar/R constriction motif, comparable to the phenylalanine/histidine couple in water-selective aquaporins. Among MIPMod Database-listed organisms, it is mostly found in plant and animal aquaporins (83 % and 15 % of aquaporins containing the motif), but also in the aquaporins of the unicellular marine choanoflagellate *Monosiga brevicollis,* a eukaryote believed to be among the closest unicellular relatives of animals (King *et al.*, 2008), and the endosymbiotic prokaryote *Candidatus Protochlamydia amoebophila*, isolated from a soil-

inhabiting *Acanthamoeba* species, which despite its name apparently contributed genes to plants about a billion years ago (Collingro *et al.*, 2005, *Moustafa et al.*, 2008).

As suggested by their name, tonoplast intrinsic proteins are mainly found in tonoplasts, the vacuolar membranes of plants, but plasma membrane localization has also been reported (Gattolin *et al.*, 2011).

Studies on AQP8 have mostly been carried out in mice and rats, where it is found in the airways, gastrointestinal tract, pancreas, liver, spleen, kidneys, male and female reproductive organs, and, in mice at least, the heart, gall bladder, brain and spinal cord (Ishibashi *et al.*, 1997, Ma *et al.*, 1997, Koyama *et al.*, 1997, 1999, Wellner *et al.*, 2000, Calamita *et al.*, 2001, 2001 b, 2005 b, Tani *et al.*, 2001, Elkjaer *et al.*, 2001, McConnell *et al.*, 2002, Oshio *et al.*, 2004, Laforenza *et al.*, 2005). Reports on mRNA and protein distribution are occasionally conflicting, and studies have not been as thorough in humans, but the following organs definitely contain AQP8 mRNA and/or protein in man, rat and mouse: liver, pancreas, kidneys, colon, and testes (Koyama *et al.*, 1998, Lehmann *et al.*, 2008, Yeung, 2010, Molinas *et al.*, 2012). In the zebra fish, at least one of three AQP8 isoforms is present in the corresponding organs as well (Tingaud-Sequeira *et al.*, 2010).

AQP8 has repeatedly been found in intracellular compartments. Its glucagon-, cAMP-, and microtubule-dependent shuttling between hepatocyte bile canalicular membranes and intracellular vesicles, reminiscent of AQP2-trafficking in the kidney principal collecting duct cells, has been studied thoroughly (Lehmann *et al.*, 2008). Most remarkably perhaps, it is found in the inner membrane of mitochondria, including those of hepatocytes and renal proximal tubule cells, where it appears to facilitate ammonia and hydrogen peroxide permeation (Lee *et al.*, 2005, Calamita *et al.*, 2005, Molinas *et al.*, 2012, Marchissio *et al.*, 2012). Whether this is physiologically meaningful remains controversial (Yang *et al.*, 2006, 2006 b).

AQP8 gene knockout in mice produces a surprisingly mild phenotype, with a peculiar increase in testicular weight or in the number of mature ovarian follicles (Yang *et al.*, 2005, Su *et al.*, 2010). Knockout of AtTIP1;1 and AtTIP1;2 produces a similarly mild phenotype in *Arabidopsis thaliana*, with a minor increase in anthocyanin content and a decrease in catalase activity of whole plant rosette extracts (Schüssler *et al.*, 2008).

Ammonium transporters and Rhesus proteins

When considering the ammonia permeability of aquaporins, it is worth comparing them to the ammonium transporter/Rhesus protein family. The latter are also found in bacteria, archaea and eukaryotes. Depending on the organism, their primary role is in ammonium scavenging or cellular transit (Khademi and Stroud, 2006).

Their structure resembles aquaporins in that there is an internal twofold symmetry. Unlike aquaporins, they have eleven or twelve transmembrane helices, and no membrane loops or

partial helices which meet end-to-end. They form trimers in the membrane. Their vestibules, in particular those of the ammonium-scavenging Amt family, are built to attract and stabilize ammonium ions by hydrogen bonds and electrostatic interactions (including cation-Π–interactions). Two stacked phenylalanine residues are found at the extracellular opening, the channel-proximal one being essential for functioning. Their channels are entirely hydrophobic except for a conserved couple of coplanar histidines arranged in series on one side of the channel and hydrogen-bonded between their δ-nitrogens. The conduction of ammonia, or of ammonia and a proton, is possible depending on the specific protein. The latter mode of transport is not entirely understood. Passage of protons and cations, including potassium, is energetically unfavourable and has accordingly not been found by experimental studies. Water molecules most likely occupy the channel, yet Amt/RhCG proteins do not conduct water. Some ammonium transporters bind glutamine synthetase (Khademi and Stroud 2006, Gruswitz *et al.*, 2010, Lamoureux *et al.*, 2010).

1.3 Aquaporin inhibitors

Mercurous chloride (Hg_2Cl_2) had been used as a diuretic since at least the days of Paracelsus in the 16th century, before it was replaced in the 20th century by less toxic organic derivatives. The mercurial diuretics represented by mercaptomerin (Fig. 1.12) were for a time the most effective diuretics available, and their use continued even after safer and similarly potent ones had been discovered (Doerge *et al.*, 1971).

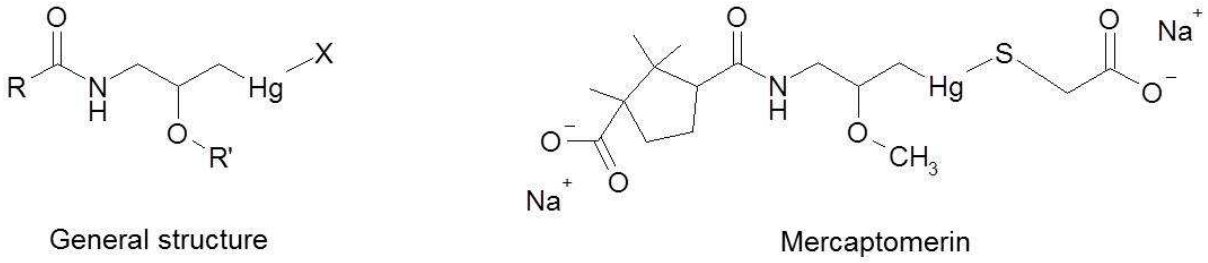

Fig. 1.12: Mercurial diuretics. *The general structure is shown on the left, the structure of mercaptomerin as an example on the right. At least three methylene groups are required between the mercury and nitrogen atoms, shorter bridges leading to a loss of diuretic activity. "R" represents a variety of hydrophilic residues important for function, "R'" depends on the solvent used for mercuriation, "X" determines pharmacokinetic properties more than activity. A likely target of this class of mercurial diuretics is Cysteine 189 of AQP1 (equivalent to Cysteine 191 in bovine AQP1, Fig. 1.6).*

The site of action of mercurial diuretics was studied in the 1950s and found to be located in the proximal tubules of the kidney, where it appeared to inhibit the passive permeability to sodium and water (Vander *et al.*, 1958). One report mentions the possibility of active water

transport, noting that the specific transport processes for common ions were not affected by thiomerin (identical to mercaptomerin, Robinson, 1986). In retrospect, these findings may be explained by inhibition of AQP1, abundant in proximal tubules, but apparently this has not been proven. If true, the mercurial diuretics remain the only clinically useful aquaporin inhibitors, although inhibition of vasopressin receptors in the kidney collecting ducts by a class of drugs named vaptans produces aquaresis by indirect inhibition of AQP2-mediated water reabsorption (Yamamura *et al.*, 1998, Verbalis, 2006).

Copper (Cu^{2+}), silver (Ag^{+}), gold (Au^{3+}), zinc (Zn^{2+}) and mercury (Hg^{2+}) ions have been shown to inhibit a variety of aquaporins by binding to cysteine or histidine residues, with maximal inhibition increased by bulky organic residues attached to them (Preston *et al.*, 1993, Roudier *et al.*, 1998, Niemietz and Tyerman, 2002, Yukutake *et al.*, 2009). The mercurial diuretics had been comparatively safe, yet nowadays they are considered too toxic, so drugs containing other metal ions are unlikely to be suitable.

A number of organic molecules have been found to inhibit aquaporins more or less specifically, among them the naturally occurring flavonoid phloretin which also blocks urea channels and glucose tranporters (LeFevre, 1959, Macey and Farmer, 1970, Roudier *et al.*, 1998). Occasionally, there are conflicting reports on aquaporin inhibition, as in the case of tetraethylammonium ions or acetazolamide, which apparently inhibit the human AQP1-mediated swelling of *Xenopus* oocytes, but not the shrinkage of erythrocytes (Ma *et al.*, 2004, Detmers *et al.*, 2006, Yang *et al.*, 2006 c).

Recently, selective inhibition of AQP9 has been shown to significantly reduce glucose output of perfused mouse livers with glycerol as the sole gluconeogenic substrate. The inhibitory compound had been found by computational high-throughput screening with a homology model of AQP9, followed by testing the most promising candidates with murine aquaporin-synthesizing Chinese hamster ovary cells in a fluorescence-based swelling assay. The aquaglyceroporins AQP3 and AQP7 are unaffected by the test compound, as is AQP8 (Jelen *et al.*, 2011).

The usefulness of aquaporin inhibition has been demonstrated by the mercurial diuretics and also by the indirectly acting vasopressin receptor antagonists. Regarding glycerol and solute transport, inhibition of human aquaglyceroporins such as AQP9 may be valuable for the treatment of glycerol-related metabolic disorders, whereas inhibition of parasite aquaglycero-porins, such as that of *Plasmodium falciparum*, could serve as an adjunct therapy of life-threatening cases (Zeuthen *et al.*, 2006 b, Liu *et al.*, 2007).

1.4 Thesis outline

The primary objective of the presented work is to understand how water-selective aquaporins can exclude ammonia, a molecule similar in size and polarity to water.
To this end, single as well as multiple mutations are to be introduced in the aromatic/arginine constriction of water-selective rat AQP1, to mimick the corresponding region of the water- and ammonia-permeable human AQP8. Analogous mutations are to be introduced in AQP8. Testing of ammonia and methylamine permeability will be by phenotypic yeast assays, and, if possible, by electrophysiological measurements in *X. laevis* oocytes. Water permeability measurements using yeast protoplasts or *X. laevis* oocytes will serve to assess the integrity of the channel mutants. Depending on the outcome, additional AQP1 and AQP8 mutants may be generated and tested.
Another objective is to assess the suitability of yeast growth assays in the study of aquaporin inhibition, with a view to high-throughput screening.

2 Materials

2.1 Equipment and consumables

Adolf Wolf SANOclav, Bad Überkingen-Hausen

Autoclave “Sanoclav“

Bandelin, Berlin

Bath sonicator “Sonorex RK 514”

Beckman Coulter, Krefeld

DNA Sequencer “CEQ 8000 Genetic Analysis System”

Ultracentrifuge “Optima XL-80 K”, Ultracentrifuge rotor “50.2 Ti”, Polycarbonate ultracentrifuge bottles (25 mm x 89 mm, 26 ml), Polyallomer microfuge tubes (9.5 mm x 38 mm, 1.5 ml)

Beranek Laborgeräte, Weinheim

Ultracentrifuge adaptors for Beckman polyallomer microfuge tubes

BioLogic, Claix, France

Stopped-flow module “SFM-300”, Motor power supply “MPS-60”,
Modular optical system “MOS-200”, Monochromator “BH-10-61UV”,
Cuvette “FC-08”, Lamp power source “ALX 250”, Photomultiplier “PMS-250”,
Software “Bio-Kine 32 V4.46”

Bio-Rad Laboratories, München

Electrophoresis power supply “Power Pac 200”

Blotting apparatus “Trans-Blot SD semidry transfer cell”

Cawo Photochemisches Werk, Schrobenhausen

Autoradiography case “ABS-Cassette”

Photographic processing apparatus “Cawomat 2000 IR“

Clemens, Waldbüttelbronn

PCR machines “Dualblock Primus advanced HT2X” and “Primus 25”

Software “HT Manager”

Dometic WAECO, Emsdetten

Wine fridge “MF-6W“ (for oocyte incubation)

Edmund Bühler, Hechingen

Tilt shaker “WS-10”

Dual-action shaker “KL2”

Engelbrecht, Edermünde

Microscope slides (26 mm x 76 mm)

Eppendorf, Hamburg

Adjustable-volume pipette “Eppendorf Research” (0.1 - 2.5 µl)

“BioPhotometer 6131”

“Centrifuge 5415R”

GE Healthcare (Amersham Biosciences), Little Chalfont, UK

PVDF blotting membrane “Hybond-P” (0.45 µm pore size)

Autoradiography film “Hyperfilm ECL”

Gerhard Menzel Glasbearbeitungswerk, Braunschweig

Microscope cover slips (24 mm x 46 mm)

Gesellschaft für Labortechnik, Burgwedel

Shaking water bath “GFL 1083”

Gonotec, Berlin

Osmometer “Osmomat 030-D”

Grant Instruments, Shepreth, UK

Block heater “QBT” for 1.5 and 2 ml centrifuge tubes

Greiner bio-one, Frickenhausen

96-well plates and other consumables

Hamamatsu Photonics, Iwata City, Japan

Mercury-xenon lamp “L2482” (150 W) for stopped-flow apparatus

Heidolph, Schwabach

Magnetic stirrer “MR mini“

Hellma, Müllheim

Precision cell (Quartz cuvette) “105.202-QS”

Henke Sass Wiolf, Tuttlingen

Injection needles “Fine-ject“ (0.8 mm x 40 mm)

Hewlett-Packart, Böblingen

Scanner “Scanjet G4050”

H + P Labortechnik, Oberschleißheim

Magnetic stirrer “Variomag Mono“

IKA-Werke, Staufen

Magnetic stirrer “IKAMAG RET-GS”

Infors, Bottmingen, Switzerland

Incubation shaker “Infors HT Minitron”

Julabo Labortechnik, Seelbach

Refrigerated/heating circulator “F12-ED”

(for stopped-flow apparatus, from 21.04.2011 on)

Kavalierglass (Simax), Sázava, Czech Republic

Glass beakers and bottles

Kern & Sohn, Balingen

Electronic balance “ABS 120-4” (1 mg, 120 g)

Kisker Biotech, Steinfurt

Thin 1 ml pipette tips

Leica Microsystems, Wetzlar

Dissecting microscope “MZ 6”

LI-COR Biosciences, Bad Homburg

“DNA Sequencer 4200”

Liebherr, Bulle, Switzerland

Freezer “GN 1056-20” (-20 ℃)

Metrohm, Zofingen, Switzerland

“pH-meter 605” (used with glass electrode “Schott BlueLine 16”)

Mettler-Toledo, Gießen

Electronic balance “PB3002-S DeltaRange” (0.1 g, 3.1 kg)

MWG-Biotech, Ebersberg

LI-COR DNA-sequencer evaluation software “BaseImagIR V. 4.2.”

New Brunswick Scientific, Wesseling-Berzdorf

Freezer “Innova U535” (-80 ℃)

Roller drum “TC-7” (used inside Heraeus incubator “Kelvitron t”)

Olympus, Hamburg

Microscope “CK2/ULWCD 0.30” (one for observing yeast, another one for oocyte assays)

Osram, Augsburg

Halogen lamp “64607 EFM”, 8 V 50 W, for “Bioscreen” (ordered via iLF bioserve, Germany, from Oy Growth Curves, Finland)

Oy Growth Curves, Helsinki, Finland

Combined incubation shaker and turbidometer “Bioscreen C microbiology reader”

100-well plates “Honeycomb 2”

Software “EZExperiment”

Panasonic

CCTV camera “WV-CD20”

Microwave oven “NN-E245W”

Pechiney Plastic Packaging Company, Chicago, USA

“Parafilm”

Peqlab Biotechnologie, Erlangen

Vertical double gel electrophoresis system “PerfectBlue Twin S”

Block heater “HX-2” for 1.5 - 2 ml centrifuge tubes

Pharmacia Biotech, Dübendorf, Switzerland

Electrophoresis power supply ”EPS 300”

Polygen, Langen

10-column DNA-Synthesizer

DNA-Synthesizer frits

Rainin, Oakland, Canada

Adjustable-volume pipettes “Rainin Classic” (0.2 - 2 µl, 2 - 20 µl, 20 - 200 µl, 200 - 1000 µl)

Raytest, Straubenhardt

UV-transilluminator “IDA UVT-20 S/M” for agarose gel fluorescence imaging, Video printer “Mitsubishi P91”

Roche, Mannheim

Digital fluorescence and chemiluminescence imager “Lumi-Imager F1“

Savant Instruments, Farmingdale, USA

Vacuum centrifuge “DNA SpeedVac DNA110”

Sarstedt, Nümbrecht

Pipette tips, centrifuge tubes and other consumables

Petri dishes with cams (92 mm x 16 mm)

Polystyrene cuvettes (10 mm x 4 mm x 45 mm)

Syringe filters “Filtropur S” (PVDF 0.22 µm, PES 0.20 µm, PES 0.45 µm)

Schleicher & Schuell, Dassel

Blotting paper “Whatman 3 MM Chr”

Schott, Mainz

Erlenmeyer flasks

Glass electrodes “BlueLine 14” and “BlueLine 16”

pH-meter “Lab 850” (used with glass electrode “BlueLine 14”)

Scientific Industries, Bohemia, USA

“Vortex Genie 2“

Siemens (SG Water), Hamburg

Water purification system “SG Ultraclear 2003”

Sigma-Aldrich, Steinheim

Glass beads, unwashed, 425 - 600 µm

Süd-Laborbedarf, Gauting

Centrifuge tubes and other consumables

Thermo Fisher Scientific (Haake), Waltham, USA

Refrigerated/heating circulator “D8 GH”

(for stopped-flow apparatus, until 08.04.2011)

Thermo Fisher Scientific (Heraeus), Waltham, USA

Centrifuge “Biofuge pico”

Centrifuge “Multifuge 1S-R”

Clean bench “HERAguard”

Drying oven “function line”

Incubator “Kelvitron t” (used exclusively for incubation at 37 °C)

World Precision Instruments, Berlin

Microsyringe pump “Nanoliter 2000 Injector 240V“

Glass capillaries “4878” for the above (8.9 cm)

WTB Binder Labortechnik, Tuttlingen

Hot air sterilizer (1.2 kW, single door, ~ 50 L)

WTW Wissenschaftlich-Technische Werkstätten, Weilheim

“Microprocessor Conductivity Meter LF537”

Conductometer electrode assembly “TetraCon 96“

Zeitz-Instrumente, München

Glass capillary puller “DMZ-Universal Puller”

Departmental workshop (Pharmacy Department Kiel)

Chambers for agarose gel electrophoresis (platinum wires separated by ~ 15 cm)

2.2 Chemicals

Purities are given as stated on packaging. All chemicals were stored at room temperature (~ 20 - 30 °C) unless mentioned otherwise.

Acros Organics, Geel, Belgium

Xylene cyanol FF (“pure“)

AppliChem, Darmstadt

Glycine (≥ 99.5 %), 2-Propanol (≥ 99.7 %), SDS (≥ 97 %)

Avantor Performance Materials (J. T. Baker), Griesheim

Acetic acid (99 - 100 %), Ethanol (≥ 99.9 %), HCl 25 %

Fluka Biochemika, Basel, Switzerland

L-alanine (≥ 99.0 %), NH_4HCO_3 (≥ 99 %), Methylamine 41 % (for oligonucleotide synthesis, 4 °C), L-serine (≥ 99.0 %), TEA Cl (≥ 98 %)

Genaxxon Bioscience, Ulm

Ampicillin Na (≥ 99 %), SDS (≥ 97 %), TEMED (≥ 99.0 %, 4 °C)

Merck, Darmstadt

$(NH_4)_2CO_3$, Bromothymol blue, DMSO (≥ 99.9 %), Glycerol 85 %, HCl 1 mol/l "Titrisol", Methanol, $MgCl_2 \cdot 6H_2O$ (99 - 102 %), KCl (99.0 - 100.5 %), $NaNO_2$ (≥ 97 %)

Riedel-de-Haën, Seelze

NaOH 0.2 mol/l, $NaNO_3$ (≥ 99.5 %)

Roth, Karlsruhe

Ammonia 32 % (for oligonucleotide synthesis, 4 ℃), NH_4CH_3COO (≥ 97 %), NH_4Cl (≥ 99.5 %), $(NH_4)_2SO_4$ (≥ 99.5 %), $(NH_4)_2S_2O_8$ (≥ 98 %), L-arginine (≥ 98.5 %, NH_4^+ ≤ 0.02 %, "USP, for biochemistry"), $B(OH)_3$ (≥ 99.5 %), Bromophenol blue Na, $CaCl_2 \cdot 2H_2O$ (≥ 99 %), $Na_2HPO_4 \cdot 2H_2O$ (≥ 99.5 %), DTT (≥ 99 %, 4 ℃), Formaldehyde 37 % ("Rotipuran"), Formamide (≥ 99.5 %, "deionized"), α-D(+)-glucose$\cdot H_2O$ ("for microbiology"), Glycerol ≥ 86 %, EDTA (≥ 99 %), EDTA 2Na (≥ 99 %), HEPES (≥ 99.5 %), L-leucine (≥ 99 %, "cell culture quality"), $LiCH_3COO$ (≥ 99 %), MES (≥ 99 %), MOPS (≥ 99 %), 2-Mercaptoethanol (≥ 99 %), KOH (≥ 85 %), KH_2PO_4 (≥ 99 %), L-proline (≥ 98.5 %, "USP, for biochemistry"), $NaCH_3COO$ (≥ 99 %), NaCl (≥ 99.5 %), NaOH (≥ 99 %), D-sorbitol (≥ 98 %), D(+)-sucrose (≥ 99.5 %), Tetracyclin HCl (≥ 95 %), Tris (≥ 99.9 %, "Pufferan"), Urea (≥ 99.5 %)

Sigma-Aldrich, München

L-asparagine$\cdot H_2O$ (≥ 98.0 %, "cell culture tested"), L-aspartic acid Na$\cdot H_2O$ (≥ 98 %), L-glutamic acid Na$\cdot H_2O$ (≥ 99.8 %), L-glutamine (≥ 99 %, free ammonia < 0.2 %, glutamic acid ~ 0.5 %), L-histidine HCl$\cdot H_2O$ (≥ 98 %, "reagent grade"), L-isoleucine ("cell culture tested"), $LiCH_3COO \cdot 2H_2O$, L-lysine HCl (≥ 98 %, "reagent grade"), CH_3NH_4Cl, Polyethylene glycol 3350, Succinic acid ("cell culture tested"), L-threonine (≥ 99.5 %), L-valine (≥ 99.5 %)

Unknown origin

Orange G (aliquot brought from another laboratory in a minimally labelled glass bottle)

2.3 Water

Water used for all experiments was deionized and filtered ("SG Ultraclear 2003", Siemens SG Water). For DNA manipulation and the washing of *S. cerevisiae* cells, it was autoclaved in borosilicate glass bottles (~ 120 ℃, + 1 bar, ~ 20 min). For RNA manipulation, it was DEPC-treated (3.1.13).

2.4 Antibodies, enzymes, kits and reagents

Stored according to label instructions.

Agfa-Gevaert, Mortsel, Belgium

Photographic processing solutions “G153 developer” and “G354 fixer”

Ambion, Austin, USA

“mMESSAGE mMACHINE RNA transcription kit“

AppliChem, Darmstadt

Tween 20 (“molecular biology grade”)

Beckman Coulter, Krefeld

“Genome Lab Dye Terminator Cycle Sequencing Quick Start Kit”

Bio-Rad Laboratories, München

Liquid wax “Chill-Out“

“Bio-Rad Protein Assay”

Fermentas, St. Leon-Rot

λ-DNA (0.3 µg/µl), dNTPs (100 mM), Restriction endonucleases (10 U/µl) BamHI, DpnI, HindIII, NotI, PstI, XbaI, XhoI, and appropriate buffer concentrates, “RiboRuler High Range RNA Ladder”, “2x RNA Loading Dye Solution”, T4 DNA Ligase (5 U/µl) and appropriate buffer concentrate

GE Healthcare (Amersham Biosciences), Little Chalfont, UK

“Thermo Sequenase Primer Cycle Sequencing Kit”

“ECL Plus Western Blotting Detection System”

Genaxxon Bioscience, Ulm

“Albumin fraction V” (pH 7.0, bovine)

“GenAgarose LE” (for DNA electrophoresis)

dNTPs (100 mM)

Gonotec, Berlin

NaCl/H_2O 300 mOsmol/kg calibration standard

Jackson Immuno Research Europe, Suffolk, UK

HRP-conjugated goat anti-mouse IgG

Macherey-Nagel, Düren

“Nucleotrap” silica-matrix based kit for gel extraction without columns

Merck, Darmstadt

”CertiPUR“ buffer solutions pH 4.01, pH 7.00, pH 9.00 at 25 ℃

MP Biomedicals, Illkirch, France

Ethidium bromide tablets 100 mg

“Zymolyase-20T“ (20,000 U/g, from Arthrobacter luteus)

National Diagnostics, Atlanta, USA

Sequencing gel reagents “SequaGel XR Monomer Solution” and “SequaGel Complete Buffer”

New England Biolabs, Frankfurt am Main

Restriction endonucleases, T4-DNA ligase buffer concentrate

Peqlab Biotechnologie, Erlangen

Protein markers “peqGOLD I” (not prestained) and “peqGOLD III” (prestained)

Promega, Madison, USA

DNA purification kit “Wizard Plus SV Minipreps”

Roche, Mannheim

“Collagenase A from *Clostridium histolyticum*”

Mouse monoclonal IgG “Anti-HA (12CA5)” (lyophilized, 200 µg)

“Rapid DNA Ligation Kit”

“Complete EDTA-free protease inhibitor cocktail tablets”

Roth, Karlsruhe

“Albumin fraction V” (≥ 98 %, “pulv.”, bovine), Acrylamide solution “Rotiphorese Gel 40”, Coomassie staining solutions “Roti-Blue” and “Rotiphorese Blue R”, “DMT removal reagent” for oligonucleotide synthesis

SAFC (Proligo Reagents), Hamburg

All Proligo reagents were used for the synthesis of oligodeoxynucleotides.
Acetonitrile, “Activator 42” (0.25 mol/l), Capping reagents “Cap A” and “Cap B”,
CPG dA(bz) (500 Å / 1000 Å, 1 g, 30 µmol/g), CPG dC(ac) (500 Å / 1000 Å, 1 g, 37 µmol/g), CPG dG(ib) (500 Å / 1000 Å, 1 g, 38 µmol/g), CPG dT (500 Å / 1000 Å, 1 g, 31 µmol/g), DMT-dA(bz)-β-CEPA, DMT-dC(ac)-β-CEPA, DMT-dG(ib)-β-CEPA, DMT-dT-β-CEPA, “Oxidizer” (0.02 mol/l)

Santa Cruz Biotechnology, Heidelberg

Mouse monoclonal IgG against AQP1 “sc-25287” (200 µg/ml)

Sigma-Aldrich, München

DNA sodium salt from salmon testes “Type III”

Mineral oil (“molecular biology tested”)

RibonucleaseA from bovine pancreas “Type II-A” (88 Kunitz units/mg, “chromatographically purified, essentially salt free”)

Stratagene, La Jolla, USA

“Pfu Turbo DNA Polymerase AD” (2.5 U/µl) and appropriate buffer concentrate

2.5 Plasmids and genes

All plasmids and genes were from our laboratory unless mentioned otherwise. The plasmid names are followed by a list of encoded proteins and their mutations, excluding proteins that confer antibiotic resistance or auxotrophy.
Plasmid solutions were stored at 4 ℃ or at -20 ℃.

pRS426-MET25 (Mumberg *et al.*, 1994)
rAQP1 wt, F56H, H180I, C189G, H180A, R195V, R195S, H180A/R195V, H180A/R195S
hAQP1-HA wt, H180A
hAQP2-HA wt, H172A
hAQP4-2HA wt, H201A
hAQP5-HA wt, H173A
hAQP3-HA
hAQP9-HA
EcGlpF
LeAMT1;1

pRS416-MET25 (Sikorski and Hieter, 1989)
Fps1

pDR196 (Wipf *et al*., 2003)
hAQP9-HA
hAQP10-HA
BccGlpF
EcGlpF
LeAMT1;1
PfAQP

pOG1 (Hansen *et al.*, 2002)
rAQP1

pXβG-ev1
rAQP8 ΔQ5 S31P (T. Zeuthen, Copenhagen)

pYES topo
hAQP8 (T. Jahn, Copenhagen)

2.6 Primers

Primers were ordered commercially (MWG Biotech, Ebersberg) or synthesized at the laboratory, dissolved in water, and stored at -20 °C.

Sequencing primers

Primers used for sequencing with the "LI-COR DNA-sequencer" were labelled with a fluorescent dye at their 5'-ends ("IRDye 800"). Those used with the "CEQ8000" Sequencer did not have to be labelled (3.1.9).
pRS426-MET25 is abbreviated pRS426. "s/as" stand for "sense/antisense".

met25	5'-AGTAAAGCGTCTGTTAGAAAGG-3'	(pRS426 s)
cyc1	5'-ATAGGGACCTAGACTTCAG-3'	(pRS426 as, pYES2 as)
T3	5'-AATTAACCCTCACTAAAGGG-3'	(pOG1 as)
T7	5'-TAATACGACTCACTATAGGG-3'	(pOG1 s, pYES2 s)

On two occasions, mutagenesis primers (7 and 29, see below) served as sequencing primers.

Cloning primers

"for/re" stand for "forward/reverse". Restriction sites are marked in bold. rAQP8 ΔQ5 S31P is abbreviated rAQP8.

rAQP8_BamHI_for	5'-GAGAGA**GGATCC**ATGTCTGGGGAGACGCCG-3'
rAQP8_HindIII_re	5'-GAGAGA**AAGCTT**TCACCTCGACTTTAGAAT-3'
hAQP8_BamHI_for	5'-GAGAGA**GGATCC**ATGTCAGGAGAGATAGCC-3'
hAQP8_HindIII_re	5'-GAGAGA**AAGCTT**TCACCGAGCCTTCAGGAT-3'

Mutagenesis primers

"u/d" stand for "up/down" and are equivalent to "sense/antisense". "X" denotes a random amino acid. The mutating codons are marked in bold. rAQP8 ΔQ5 S31P is abbreviated rAQP8. Numbers in brackets serve as codes for later reference.

rAQP1_H180F_u	5’-TTGTCTGTGGCTCTTGGA**TTC**CTGCTGGCCATTGAC-3’	(1)
rAQP1_H180I_u	5’-TCTGTGGCTCTTGGA**ATC**CTGCTGGCCATTGAC-3’	(2)
rAQP1_H180L_u	5’-TTGTCTGTGGCTCTTGGA**CTC**CTGCTGGCCATTGAC-3’	(3)
rAQP1_H180M_u	5’-GTCTGTGGCTCTTGGA**ATG**CTGCTGGCCATTGACTA-3’	(4)
rAQP1_H180N_u	5’-TTGTCTGTGGCTCTTGGA**AAC**CTGCTGGCCATTGAC-3’	(5)
rAQP1_H180Q_u	5’-TTGTCTGTGGCTCTTGGA**CAA**CTGCTGGCCATTGAC-3’	(6)
rAQP1_H180I_d	5’-GTCAATGGCCAGCAG**GAT**TCCAAGAGCCACAGA-3’	(7)
rAQP1_H180X_d	5’-TCCAAGAGCCACAGACAAGCCAATGGCAAGTGGG-3’	(8)
rAQP1_C189G_u	5’-ATTGACTACACTGGC**GGT**GGGATCAACCCTGCC-3’	(9)
rAQP1_C189G_d	5’-GGCAGGGTTGATCCC**ACC**GCCAGTGTAGTCAAT-3’	(10)
rAQP1_C189A_u	5’-ATTGACTACACTGGC**GCT**GGGATCAACCCTGCC-3’	(11)
rAQP1_C189A_d	5’-GGCAGGGTTGATCCC**AGC**GCCAGTGTAGTCAAT-3’	(12)
rAQP8_H74F_u	5’-GCAGCCTGCCCTGGCT**TTT**GGGCTGGCCTTGGG-3’	(13)
rAQP8_H74F_d	5’-CCCAAGGCCAGCCC**AAA**AGCCAGGGCAGGCTGC-3’	(14)
rAQP8_I200H_u	5’-CTCTGTCATTGTGGAT**CAC**CTGGCAGGTGGTGG-3’	(15)
rAQP8_I200H_d	5’-CCACCACCTGCCAG**GTG**ATCCACAATGACAGAG-3’	(16)
hAQP8_C53A_u	5’-CTCTTCATATTCATCGGG**GCC**CTGTCGGTCATTGAG-3’	(17)
hAQP8_C53S_u	5’-CTCTTCATATTCATCGGG**TCC**CTGTCGGTCATTGAG-3’	(18)
hAQP8_C53X_d	5’-CCCGATGAATATGAAGAGAGCAGAGCCCAGCAG-3’	(19)
hAQP8_H72F_u	5’-CTGCAGCCGGCCCTGGCC**TTC**GGGCTGGCCTTGGGG-3’	(20)
hAQP8_H72X_d	5’-GGCCAGGGCCGGCTGCAGCAGCCCAGTGTCCGTC-3’	(21)
hAQP8_F145A_u	5’-AATGCATCTGGGGCGGCC**GCT**GTGACAGTCCAGGAG-3’	(22)
hAQP8_F145X_d	5’-GGCCGCCCCAGATGCATTCCAGAACCTCTCCTCA-3’	(23)
hAQP8_I198H_u	5’-TTTGCCGTCACCGTGGAT**CAC**CTGGCTGGGGGCCCT-3’	(24)
hAQP8_I198X_d	5’-ATCCACGGTGACGGCAAAGCCGATGGAGAACGGG-3’	(25)
hAQP8_C208A_u	5’-GGCCCTGTGTCTGGAGGC**GCC**ATGAATCCCGCCCG-3’	(26)
hAQP8_C208S_u	5’-GGCCCTGTGTCTGGAGGC**TCC**ATGAATCCCGCCCG-3’	(27)
hAQP8_C208X_d	5’-GCCTCCAGACACAGGGCCCCCAGCCAGGATATCC-3’	(28)
rAQP1_F56H_u	5’- AAGGTGTCACTGGCC**CAT**GGTCTGAGCATCGCT-3’	(29)

2.7 Organisms

Stratagene, Waldbronn

Escherichia coli XL1-blue MRF’

University of Kiel, Department of Physiology

Xenopus laevis oocytes

Own laboratory

Saccharomyces cerevisiae 31019b Δfps1

(*MAT*a *ura3*Δ *mep1*Δ *mep2*::*LEU2 mep3*::*kanMX2 yll043w*Δ*0*)

31019b (Marini *et al.*, 1997) was from another laboratory.

Saccharomyces cerevisiae BY4742 Δfps1

(*MAT*α *his3*Δ*1 leu2*Δ*0 lys2*Δ*0 ura3*Δ*0 yll043w*::*kanMX*)

Saccharomyces cerevisiae BY4742 Δfps1 Δgpd1/2

(*MAT*α *lys2*Δ*0 ura3*Δ*0 fps1*Δ0 *gpd1*::*LEU2 gpd2*::*HIS3*)

BY4742 (Brachmann *et al.*, 1998) was from Euroscarf, Frankfurt.

2.8 Growth media

The following are the raw materials other than the chemicals used in the preparation of growth media for *Escherichia coli* and *Saccharomyces cerevisiae*.

AppliChem, Darmstadt

LB medium powder (Lennox), LB agar (Lennox)

Becton Dickinson, Heidelberg

“Bacto Agar”, “Bacto Peptone”, “Bacto Tryptone”, “Bacto Yeast Extract”, “Difco Yeast Nitrogen Base w/o Amino Acids and Ammonium” (YNB)

Oxoid, Basingstoke, UK

“Agar Bacteriological” (despite the name this was used exclusively for yeast)

Roth, Karlsruhe

LB medium powder (Lennox), LB agar (Lennox)

All solid media and most liquid media were autoclaved (~ 120 °C, + 1 bar, ~ 20 min).

Liquid media that were filtered (PES or PVDF Ø 0.2 µm) are indicated. Liquid media were filtered into sterile plastic containers, heat-sterilized (~ 170 °C, 4 h) Erlenmeyer flasks, or autoclaved borosilicate glass bottles, under laminar flow.

All solid media were stored at 4 °C, liquid media were stored at room temperature unless indicated otherwise.

Percentages are given in weight per volume (% w/V) if not specified.

E. coli growth media

1000 x Ampicillin
(ampicillin Na 10 %, -20 °C)

1000 x Tetracyclin
(tetracyclin 1.5 %, -20 °C)

LB medium (Lennox)
(tryptone 1 %, yeast extract 0.5 %, NaCl 0.5 %, or prepared from LB-medium-powder 2 %)

LB agar (Lennox)
(tryptone 1 %, yeast extract 0.5 %, NaCl 0.5 %, “Bacto Agar” 1.5 %, or prepared from LB-agar-powder 3.5 %)

Antibiotic-containing LB media
(ampicillin 100 µg/ml or tetracycline 15 µg/ml, added after autoclaving)

S. cerevisiae growth media

1000 x Histidine
(L-histidine HCl·1H_2O 2 %, 4 °C)

200 x Leucine
(L-leucine 2 %)

1000 x Lysine
(L-lysine HCl 2 %, 4 °C)

50 x Proline
(L-proline 5 %)

YPD
(yeast extract 1 %, peptone 2 %, D-glucose 2 %)

SD KHL
(YNB 0.17 %, $(NH_4)_2SO_4$ 0.5 %, D-glucose·H_2O 2 %, NaOH → pH 5.6, L-lysine HCl 20 mg/l, L-histidine HCl·1H_2O 20 mg/l, L-leucine 100 mg/l)
Amino acids were added after autoclaving.
SD KHL medium used for subsequent yeast protoplast preparation or yeast growth assays was not autoclaved but filtered (Ø 0.2 µm PES), and pH was set after addition of amino acids.

YPD and SD KHL agar
("Oxoid Agar" 2 % in the respective media)

***S. cerevisiae* growth assays**

Succinic acid 0.5 M, Tartaric acid 1 M, MES 1 M, MOPS 1M, HEPES 1 M, $(NH_4)_2SO_4$ 1 M, CH_3NH_3Cl 1 M, L-lysine HCl 2 %, L-histidine HCl·H_2O 2 %, L-leucine 2 %, L-proline 5 %, YNB 0.85 %, D-glucose·H_2O 15 %, all filtered sterile or autoclaved, L-lysine and L-histidine solutions stored at 4 ℃, NaOH 5 or 10 M

Assay media are described in the methods section.

2.9 Solutions

Storage conditions are specified where relevant. Percentages are given in weight per volume (% w/V) if not specified.

Plasmid extraction from *E. coli* (non-kit)

Ribonuclease A 10 µg/µl (4 ℃, -20 ℃ for stocks)

P1 buffer
(Tris/HCl 25 mM, EDTA 10 mM, pH 8.0)

P2 buffer
(NaOH 0.2 M, SDS 1 %)

P3 buffer
(KCH_3COO 3 M, pH 5.5)

Ethanol 70 % V/V

Agarose gel electrophoresis

50 x TAE buffer
(Tris/acetate 2 M, EDTA 0.05 M, pH 8.0)

Ethidium bromide solution 1 %
(stored at 4 ℃ in a 15 ml plastic tube wrapped in aluminium foil)

10 x Loading dye “blue/purple”
(bromophenol blue 0.25 %, xylene cyanol 0.25 %, glycerol 30 %, EDTA 0.1 M, 4 ℃)

10 x Loading dye “orange”
(Orange G 0.4 %, glycerol 30 %, EDTA 0.1 M, 4 ℃)

λ-marker
(PstI- or EcoRI/HindIII-digested λ-DNA 50 µg/ml, 10 x Loading dye “orange“ 10 %, 4 ℃ , -20 ℃ for laboratory stock)

DNA sequencing (“LI-COR”)

APS solution 10 % (-20 ℃)

10 x TBE buffer
(Tris 0.89 M, boric acid 0.89 M, Na_2EDTA 0.02 M, resulting pH ~ 8.3)

DNA sequencing ("Beckman Coulter")

Ethanol 95 % V/V and 70 % V/V

$NaCH_3COO$ 3 M, pH 5.2

Na_2EDTA 0.1 M, pH 8.0

Site-directed mutagenesis

dNTP solution
(dATP 2.5 mM, dCTP 2.5 mM, dGTP 2.5 mM, dTTP 2.5 mM, 4 ℃, -20 ℃ for long-term storage)

***E. coli* transformation**

$CaCl_2$ 0.1 M, autoclaved, 4 ℃

Glycerol 20 %, autoclaved, 4 ℃

10 x CM solution
($CaCl_2$ 0.1 M, $MgCl_2$ 0.1 M, autoclaved, 4 ℃)

1.5 X LB medium
(Tryptone 1.5 %, yeast extract 0.75 %, NaCl 1.5 %, PIPES/NaOH 10 mM, pH 6.5, autoclaved)

Transformation and storage solution (TSS)
(1.5 x LB medium 75 % V/V, PEG 3350 10 %, $MgCl_2$ 20 mM, DMSO 5 % V/V, autoclaved except for DMSO, 4 ℃)

***S. cerevisiae* transformation**

$LiCH_3COO$ 1 M, autoclaved

PEG 3350 50 %, autoclaved

TE buffer
(Tris/HCl 10 mM, EDTA 1 mM, pH 8.0)

Single stranded carrier DNA solution (SSC DNA)
(DNA sodium salt from salmon testes “Type III” 0.2 % in TE Buffer, -20 ℃)
Before use, SSC DNA solution was boiled for ~ 5 min in a 1.5 ml tube on a heating block or floating on boiling water.

Yeast transformation buffer
(per 326 µl: $LiCH_3COO$ 1 M 36 µl, PEG 3350 50 % 240 µl, boiled SSC DNA 50 µl, on ice)

E. coli and _S. cerevisiae_ glycerol stocks

Glycerol 60 % or 80 %, autoclaved

cRNA synthesis

DEPC-treated water
(DEPC 0.1 %, autoclaved after overnight incubation)

$NaCH_3COO$ 3 M, pH 5.2

10 x MOPS buffer
(MOPS/NaOH 200 mM, $NaCH_3COO$ 50 mM, EDTA 10 mM, pH 7.0, 10 ml aliquots stored at -20 ℃)

X. laevis oocyte buffers

ND96
(NaCl 96 mM, KCl 2 mM, $CaCl_2$ 1.8 mM, $MgCl_2$ 1 mM, HEPES/NaOH 5 mM, pH 7.4)

OR2
(NaCl 82.5 mM, KCl 2 mM, $MgCl_2$ 1 mM, HEPES/NaOH 5 mM, pH 7.4)

Hypotonic phosphate buffer
(NaH_2PO_4/Na_2HPO_4 7.5 mM, pH 7.5)

S. cerevisiae microsome isolation

Protease inhibitor stock solution
(Roche "Complete EDTA-free protease inhibitor cocktail tablets", 1 tablet dissolved in 1 ml H_2O, 4 °C)

Extraction buffer
(Tris/HCl 20 mM, Na_2EDTA 1 mM, DTT 1 mM, $MgCl_2$ 10 mM, glycerol 5 %, pH 8.0)

Extraction buffer "simplified"
(Tris/HCl 25 mM, Na_2EDTA 5 mM, pH 7.5)

Buffer M
(NaH_2PO_4/Na_2HPO_4 100 mM, NaCl 50 mM, pH 8.0)

10 x DDM solution
(DDM 25 % in buffer M)

Storage buffer
(Tris/HCl 20 mM, EDTA 0.1 mM, KCl 100 mM, DTT 1 mM, glycerol 10 %, pH 7.5)

SDS-PAGE

4 x Stacking gel buffer
(Tris/HCl 1.5 M, SDS 0.4 %, pH 8.8)

4 x Resolving gel buffer
(Tris/HCl 0.5 M, SDS 0.4 %, pH 6.8)

10 x Cathode buffer
(Tris base 0.25 M, glycine 1.92 M, SDS 1 %, pH not set)

4 x Sample loading buffer
(Tris/HCl 0.25 M, DTT 0.4 M, SDS 8 %, bromophenol blue 0.02 %, glycerol 40 % V/V, pH 6.8, -20 ℃)

“Rotiphorese Blue R” staining solution
(“Rotiphorese Blue R” 50 % V/V)

“Roti-Blue” staining solution
(“Roti-Blue” 20 % V/V, methanol 20 % V/V)

Destaining solution
(acetic acid 10 % V/V, ethanol 30 % V/V)

Western blotting

5 x Transfer buffer
(Tris/HCl 25 mM, glycine 192 mM, 0.0375 % SDS, pH 8.3)

Transfer buffer
(5 x Transfer buffer 20 % V/V, methanol 20 % V/V)

10 x TBS
(Tris/HCl 0.2 M, NaCl 1.35 M, pH 7.6)

TBS-T
(10 x TBS 10 % V/V, Tween 20 ~ 0.1 % V/V)

M-TBS-T
(3 % milk powder in TBS-T, 4 ℃)

Antibody stock solutions

Mouse monoclonal IgG against AQP1
(0.2 mg/ml PBS, from supplier, 4 ℃)

Mouse monoclonal IgG against HA-tag
(0.4 mg/ml PBS, -20 ℃)

HRP-conjugated goat anti-mouse IgG
(0.4 mg/ml, NaH_2PO_4/Na_2PO_4 5 mM, NaCl 125 mM, BSA 7,5 mg/ml, glycerol 50 % V/V, -20 ℃)

2.10 Test compounds

Test compounds were received as weighed dry substances or as DMSO solutions in 2 ml glass bottles or in 2 ml plastic vials and stored at 4 ℃ or at -20 ℃.
They were designed by S. Wacker and B. de Groot (Göttingen), K. Simmons and P. Johnson (Leeds), or by R. Haddoub, R. Castangia and S. Flitsch (Manchester), and synthesized by the latter two groups, or ordered from ChemBridge (San Diego, USA), Maybridge (Thermo Fisher Scientific, Waltham, USA), or Enamine (Riga, Latvia).
Mercuric chloride and phloretin were a kind gift from P. Gena and G. Calamita (Bari). They were stored in 1.5 ml centrifuge tubes wrapped in aluminium foil. Phloretin was stored at 4 ℃.

3 Methods

Many of the methods described were varied to some degree, and several, especially among the "non-standard" ones, evolved with increasing experience. The summaries should be viewed as "consensus" or "best". Details considered important are given.

3.1 Nucleic acid manipulation

3.1.1 Plasmid extraction from *E. coli*

***E. coli* cultures**

To 5 ml LB medium inside a glass tube was added 5 µl ampicillin stock solution. The medium was inoculated with a fresh (< 7 days old) *E. coli* colony from an agar plate or with a scraping from an *E. coli* glycerol stock (3.1.12), and incubated overnight at 37 ℃ on a roller drum. Incubation time did not exceed 20 hours. To harvest the cells, the vortexed culture was poured into 1.5 ml centrifuge tubes and centrifuged at 10,000 x g for 2 min, discarding the supernatant. This step was repeated once or twice if the kit was to be used.

"Wizard" kit plasmid extraction

Plasmid extraction using the "Wizard"-kit was done according to instructions, without the use of alkaline protease solution. Autoclaved water was used instead of the provided nuclease-free water, allowing it 2 min to dissolve the column-bound plasmid DNA before the final centrifugation step.

The resulting solution was stored at 4 ℃ or at -20 ℃.

Non-kit plasmid extraction

The bacterial pellet was resuspended in 150 µl P1 buffer after adding 2 µl Ribonuclease A solution, and the tube was kept on ice. 200 µl P2 buffer was added and the sample mixed gently by inverting the tube twice. Within 5 min, 200 µl of cold 4 ℃ P3 buffer was added, again inverting the tube twice, and the sample was then kept on ice for 10 min. Two centrifugations (4 ℃, 10,000 x g, 5 min) followed, each time transferring the supernatant to a new tube. An equal amount of isopropanol (~ 500 µl) was added, and the sample mixed by inverting it several times. After 10 min at room temperature, it was centrifuged (4 ℃, 16,000 x g, 30 min). The supernatant was discarded by pouring carefully, and the tube left open and upside-down on tissue paper. 1 ml ethanol 70 % V/V was added, and the sample

carefully mixed and centrifuged (16,000 x g, 5 min). The supernatant was removed by thorough pipetting, and the sample left to dry on a block heater at 50 °C for 2 min.
The plasmid DNA was dissolved in 40 µl water (allowing at least 10 min for rehydration before pipette-mixing) and stored at 4 °C or at -20 °C.

3.1.2 Agarose gel electrophoresis

A suspension of 0.5 g agarose in 50 ml TAE buffer was heated inside a microwave oven (800 W, 2 min). Evaporated water was replaced. 1 µl ethidium bromide solution (1 %) was added, and after gentle mixing the liquid was poured into the gel mould, immediately moving bubbles to the edges with a pipette tip. The liquid was allowed to solidify for ~ 30 min, and the resulting gel was transferred to the electrophoresis chamber containing TAE buffer. Combs were removed at this point.
DNA samples were mixed with 10 x loading dye and pipetted into the gel pockets. PstI- or EcoRI/HindIII-digested λ-DNA (5 µl, corresponding to 250 ng total DNA) was used for later size and concentration determination.
Electrophoresis was performed at 100 V (6.7 V/cm) for 15 - 45 min, depending on the desired resolution.

3.1.3 Concentration and purity determination

Following agarose gel electrophoresis

Agarose gel electrophoresis allowed the subsequent visualization of nucleic acid impurities, as well as concentration estimates by comparison with PstI- or EcoRI/HindIII-digested λ-DNA bands under UV light at 366 nm. Plasmid DNA was linearized by restriction digestion prior to gel electrophoresis.

UV photometry

The sample was diluted and its UV absorption at 230 nm, 260 nm, 280 nm, and 320 nm measured in a quartz cuvette of 1 cm path length, against water as blank. An A_{260} of 0.2 - 0.8 was considered adequate. For double-stranded DNA, ε_{260} = 20 $l \cdot g^{-1} \cdot cm^{-1}$ (50 ng/µl for A_{260} = 1 and l = 1 cm) was used to calculate the concentration, and $A_{260}/A_{280} \geq 1.8$ was considered sufficient with regard to protein impurities. A_{260}/A_{230} was recorded for the sake of curiosity, but never served to reject a sample. A_{320} was always 0.

3.1.4 Restriction digestion

Components were pipetted into a 200 µl PCR tube in the following order:
Water, appropriate buffer concentrate, DNA solution (~ 0.1 - 10 µg DNA), restriction enzymes (0.05 U/µl reaction mixture). Total volume was generally 10 µl, sometimes up to 50 µl. The sample was pipette-mixed and incubated at 37 °C for at least 30 min (control digestion) or 2 h (subsequent ligation).
Parent DNA digestion following site-directed mutagenesis, or plasmid linearization for subsequent cRNA synthesis, are described in the respective sections.

3.1.5 Polymerase chain reaction

The PCR was used for cloning purposes, site-directed mutagenesis, and DNA sequencing. Components and conditions for each are described in the respective sections.

3.1.6 Extraction from agarose gels

A piece of gel containing the desired DNA fragments was excised with a scalpel and weighed inside a 1.5 ml centrifuge tube. The DNA was then extracted by using the “Nucleo Trap” kit (Macherey-Nagel) according to instructions, eluting with 25 µl water. The resulting solution was either used directly or stored at -20 °C. Gel pieces were also stored at -20 °C in case of postponed extraction.

3.1.7 Ligation

Components were pipetted into a 200 µl PCR tube in the following order, to a total volume of 10 µl: Plasmid DNA solution (~ 100 ng), insert DNA solution (molar ratio plasmid/insert ~ 1:3), appropriate buffer concentrate, T4-DNA ligase (5 U). Components other than the ligase were mixed thoroughly, whereas addition of ligase was followed by gentle stirring. The sample was incubated at room temperature for 15 - 60 min and subsequently used to transform competent *E. coli*.

For some experiments, the “Roche Rapid Ligation Kit” was used according to instructions, with the amount of plasmid DNA and plasmid/insert ratio the same as described above.
All ligations were “sticky-end” ligations. Plasmid/insert ratios other than 1:3 were usually tried in parallel.

3.1.8 Site-directed mutagenesis

Changes in nucleotide sequence were made according to the instructions provided by the “QuikChange Site-Directed Mutagenesis Kit” (Stratagene), without using the actual kit.
The template was always pRS426-MET25 containing the gene of interest (~ 7000 bp altogether). The mutagenesis primers are described in the materials section. Choice of GC-content was limited by the template DNA sequence.
Components were pipetted into a 200 µl PCR tube in the following order, to a total volume of 50 µl: Water, 10 x Pfu buffer, dNTP solution (10 nmol each), u/d primer solution (38 pmol each), template DNA (50 - 500 ng), Pfu Turbo DNA Polymerase (2 U). In one instance, a second pair of primers was used simultaneously, without changing the amount of dNTPs.
One of the following PCR programmes was used, neither proving superior:

95 °C 30 s, 16 · (95 °C 30 s, 55 °C 1 min, 68 °C 16 min), 68°C 20 m in, 8 °C
95 °C 30 s, 12 · (95 °C 30 s, 55 °C 1 min, 68 °C 16 min), 68°C 20 m in, 8 °C

10 µl of the reaction mixture was removed for later comparison by agarose gel electrophoresis. DpnI (8 U) was added to the remaining solution, to digest methylated parent DNA (37 °C, ≥ 5 h). 10 µl of DpnI-digested PCR product was used to transform competent *E. coli*, the remainder being frozen (-20 °C). Success of mutagenesis was ascertained by DNA sequencing.

3.1.9 Sequencing

DNA was sequenced by using the standard dideoxy chain-termination method. Two different manufacturers’ equipment and reagents were employed and are described separately. Sequences were viewed with the “DNASTAR” software package, or, in the case of Method 1, also directly on the recorded gel image.

Method 1

A template/primer mix was prepared by combining plasmid solution (~ 0.8 µg DNA, instructions stating “50 - 100 ng/kb”), fluorescently labelled primer solution (2 pmol) and water to a volume of 13 µl. 3 µl each was then pipetted to the bottoms of four 200 µl PCR tubes. 1 - 2 µl of dNTP/ddNTP/polymerase mix (“Thermo Sequenase Primer Cycle Sequencing Kit”, GE Healthcare) was pipetted to the sides of those tubes and flushed down with drops of ~ 10 - 50 µl liquid wax or mineral oil.
One of the following PCR programmes was used, neither proving superior:

95 °C 2 min, 30 · (95 °C 20 s, 52 °C 20 s, 72 °C 20 s), 4 °C
95 °C 2 min, 30 · (95 °C 30 s, 55 °C 30 s, 72 °C 60 s), 4 °C

5 µl formamide-containing loading dye (provided by the kit) was added and 0.8 - 1 µl of each sample loaded onto a polyacrylamide gel made from the following components:
“SequaGel XR 7.5 %” 30 ml, “SequaGel Complete buffer reagent” 7.5 ml, DMSO 0.4 ml, APS 10 % 0.3 ml, filtered (Ø 0.45 µm PES). The gel had an acrylamide content of 6 %, and a thickness of 250 µm.
Electrophoresis was performed with the “LI-COR DNA Sequencer 4200”, with TBE buffer as electrolyte, at ~ 1.5 kV (~ 30 V/cm) and 45 °C. “BaseImagIR V.4.2” software was used to evaluate the recorded fluorescence signals.

Method 2

3’-labelled DNA fragments were generated by PCR using the “Genome Lab Dye Terminator Cycle Sequencing Quick Start Kit” (Beckman Coulter) according to instructions, with the exception of halving all given volumes (PCR reaction 10 µl instead of 20 µl).
Electrophoresis was performed with the “CEQ 8000 DNA Sequencer”, with provided electrolyte, under the “LFR-1” or “LFR-a” settings of the programme “GenomeLab GeXP V.10.2”. Capillary length was the standard 33 cm.

Two-dideoxynucleotide-sequencing

Following sire-directed mutagenesis, many samples had to be sequenced to identify successful mutants. To save reagents and space on the gel, Method 1 was frequently employed with only two ddNTP mixtures instead of four, choosing them according to expected codon change, and with regard to balancing the consumption of reagents. Evaluation was by viewing the recorded fluorescence signals directly.

3.1.10 Competent *E. coli*

E. coli (strain "XL1-blue") competent for transformation were prepared by one of two methods.

$CaCl_2$ method

This method is based loosely on that described by Cohen *et al*., in 1972.

E. coli from a glycerol stock were spread on tetracycline-containing LB agar and grown overnight at 37 °C. A single colony was used to inoculate 5 ml tetracycline-containing LB medium inside a 100 ml Erlenmeyer flask, and grown at 37 °C and 180 rpm for ~ 9 h. The culture was then transferred to 100 ml tetracycline-containing LB medium inside a 500 ml Erlenmeyer flask and grown at 20 °C and 180 rpm overnight, to an OD_{600} of 0.4 - 0.6. The resulting culture was collected in two 50 ml tubes, kept on ice for 10 min, and centrifuged (4 °C, 2,000 x g, 10 min). Each supernatant was replaced by 15 ml $CaCl_2$-solution (0.1 M, 4 °C). After 10 min on ice the cells were resuspended by gentle shaking (this could take more than 10 min), and centrifuged (4 °C, 2,000 x g , 10 min). This step was repeated with 10 ml $CaCl_2$-solution, and the cells were finally resuspended in 5 ml $CaCl_2$-solution containing 20 % glycerol. Both suspensions were then unified and kept on ice for at least 4 h, with occasional shaking. 100 µl aliquots inside pre-cooled (-20 °C) 1.5 ml tubes were stored at -80 °C.

PEG-Mg^{2+}-DMSO method

This method is based on that described by Chung *et al*. in 1989.

E. coli from a glycerol stock were spread on tetracycline-containing LB agar and grown overnight at 37 °C. A single colony was used to inoculate 5 ml of tetracycline-containing LB medium inside a glass tube and grown on a roller drum at 37 °C overnight. 1 ml of this culture was then added to 100 ml tetracycline-containing LB medium inside a 500 ml Erlenmeyer flask and grown at 37 °C and 200 rpm to an OD_{600} of 0.3 - 0.4. The resulting culture was collected in two 50 ml tubes, kept on ice for 10 min, and centrifuged (4 °C, 1,000 x g, 10 min). Each supernatant was replaced by 10 ml TSS (4 °C) and the cells were resuspended by gentle shaking and pipette-mixing. Centrifugation and resuspension in 10 ml TSS were repeated, followed by 10 min incubation on ice. 100 µl aliquots inside pre-cooled (-20 °C) 1.5 ml tubes were stored at -80 °C.

3.1.11 Transformation of *E. coli*

One of two transformation methods was used, depending on the way the competent cells had been prepared. For intact plasmid DNA (i. e. not nicked or freshly ligated), a simplified "quick transformation" procedure was applied. Selection was by plasmid-conferred ampicillin resistance.

$CaCl_2$ method

10 µl DNA solution and 10 µl 10 x CM solution were mixed with 80 µl water inside a 1.5 ml tube and kept on ice. A frozen 100 µl aliquot of competent *E. coli* was allowed to thaw on ice, and the above solution was added. After 30 min on ice the sample was subjected to a heat pulse (42 °C, 45 s) on a block heater, followed by cooling on ice for 2 min. 0.8 ml LB medium was then added, and the sample incubated at 37 °C on a roller drum for 45 - 60 min.
The cells were pelleted and resuspended again after removing 0.9 ml of the supernatant. The resulting suspension was plated on pre-warmed ampicillin-containing LB agar under laminar flow or next to a Bunsen flame, and incubated at 37 °C overnight.

PEG-Mg^{2+}-DMSO method

The DNA solution (10 µl) was added to a suspension of competent *E. coli* just beginning to thaw, followed by the procedure described for the $CaCl_2$ method.

Quick transformation

1 µl of DNA solution was added to a suspension of competent *E. coli* just beginning to thaw, followed by 15 min incubation on ice and plating on ampicillin-containing LB agar as described for the $CaCl_2$ method.

3.1.12 *E. coli* glycerol stocks

0.8 ml of the ampicillin-containing overnight culture of *E. coli* was mixed with 0.4 ml autoclaved glycerol 85 % inside a 1.5 ml tube and frozen at -80 °C.
E. coli glycerol stocks were prepared under non-sterile conditions.

3.1.13 cRNA synthesis

DEPC-treatment

Water, centrifuge tubes and pipette tips used for cRNA synthesis were DEPC-treated (2.9). Water containing 0.1 % V/V DEPC was autoclaved after overnight incubation. The same procedure was applied for the plasticware by immersion in DEPC-containing water inside Erlenmeyer flasks or glass bottles, with autoclaving followed by slow (lid on) drying at 50 °C.

DNA template preparation

pOG1 containing the gene of interest was linearized by digestion with NotI. Components were pipetted into a 1.5 ml tube in the following order, to a final volume of 50 µl:
Plasmid DNA solution (~ 4 µg DNA), water, appropriate buffer concentrate, NotI (10 U). The sample was pipette-mixed and incubated at 37 °C overnight. 2 µl was removed to verify complete digestion by agarose gel electrophoresis. The sample was then transferred to a new 1.5 ml tube, mixed with 1/10 volume of $NaCH_3COO$ 3 M pH 5.2 and 2.5 volumes of ethanol (-20 °C), and kept at -20 °C for 1 h. The resulting suspension was centrifuged (4 °C, 16,000 x g, 15 min), the supernatant removed, water and ethanol (-20 °C) added to give ~ 70 % ethanol, and the subsequent centrifugation (4 °C, 16,000 x g, 15 min) and supernatant removal was followed by drying in a vacuum centrifuge ("DNA SpeedVac DNA110", "medium" setting, 5 min).

cRNA synthesis

The NotI-digested DNA template served to synthesize cRNA according to the instructions provided by the "mMESSAGE mMACHINE RNA transcription kit" (Ambion). Purification was by precipitating with lithium chloride (LiCl solution provided). Ethanol was removed by drying in a vacuum centrifuge ("DNA SpeedVac DNA110", "medium" setting, 5 min). The cRNA was redissolved in 25 µl water. Quantification was by UV photometry, assuming

$\varepsilon_{260} = 25\ l \cdot g^{-1} \cdot cm^{-1}$ (40 ng/µl for $A_{260} = 1$ and $l = 1$ cm).

Verification of transcript length was by denaturing aga-rose gel electrophoresis as described below. The solution was diluted to a concentration of ~ 100 ng/µl, and 5 µl aliquots in 1.5 ml tubes were stored at -80 °C.

Denaturing agarose gel electrophoresis

A suspension of 0.66 % agarose in 50 ml water was heated inside a microwave oven (800 W, 2 min). When the flask could be held without much discomfort, 10 ml 10 x MOPS

buffer, 1.5 ml formaldehyde 37 %, and water were added to reach the original weight of ~ 50 g. The gel was poured into the same kind of gel mould used for standard agarose gels, and bubbles were immediately moved to the sides with a pipette tip.
2 µl of diluted (100 ng/µl) cRNA sample was mixed with 2 µl loading buffer ("2 x RNA Loading Dye Solution", Fermentas), and incubated at 70 °C for 10 min on a block heater, followed by 5 min incubation on ice. The same was done with a RNA marker solution ("RiboRuler High Range RNA Ladder", Fermentas).
Electrophoresis was performed at 80 V (~ 5.3 V/cm) for ~ 90 min. The ethidium bromide-stained RNA was visualized by illumination at 366 nm.

3.2 Cloning and mutagenesis constructs

Subcloning of raqp8 and haqp8

DNA fragments coding for rAQP8 ΔQ5 S31P and hAQP8 were first sequenced and then amplified from pXβG-ev1 rAQP8 ΔQ5 S31P and pYES topo hAQP8 (2.5) by PCR, using the primers described in the materials section (2.6), the same components as for the mutagenesis PCR (3.1.8, 20 pmol of each primer), and the following programme:

95 °C 5 min, 28 · (95 °C 30 s, 55 °C 45 s, 72 °C 4 min), 72 °C 10 mi n, 4 °C

Annealing temperatures of the primers were calculated by using the formula:

$T_a \approx (60 + 0.41 \cdot G - 600 / n)$ °C

With G the GC-content (%) and n the number of nucleotides. Of the two primers' calculated annealing temperatures, the lower one was chosen. The programme is based on a standard PCR protocol. It was modified according to the experience of a senior laboratory member (B. Wu), taking the low catalytic rate of the Pfu polymerase (compared to Taq polymerase) into account.
PCR products were purified by agarose gel electrophoresis and subsequent extraction (3.1.6). They were inserted into the multiple cloning site of pRS426-MET25 by ligation of the respective BamHI/HindIII-digests (3.1.7). Resulting constructs were sequenced using standard primers (2.6).

Mutagenesis constructs

Site-directed mutagenesis was performed as described (3.1.8). Primer codes refer to those given in the materials section (2.6). All mutations were verified by sequencing. Completely sequenced constructs are indicated. The plasmid was pRS426-MET25.

Aquaporin	Mutation	Template	Primers	Complete seq.
rAQP1	F56H/H180I	F56H	2, 7, 9, 10	yes
	F56H/C189G			yes
	F56H/H180I/C189G			yes
	C189A	C189G	11, 12	no
	F56H/C189A	F56H/C189G	11, 12	yes
	F56H/H180I/C189A	F56H/H180I/C189G	11, 12	no
	H180I/C189A	H180I	11, 12	no
	H180L	H180I	3, 8	yes
	H180M	H180I	4, 8	yes
	H180F	H180I	1, 8	yes
	H180N	wt	5, 8	yes
	H180Q	wt	6, 8	yes
	F56H/H180L	F56H	3, 8	no
	F56H/H180M	F56H	4, 8	no
	F56H/H180F	F56H	1, 8	no
rAQP8	ΔQ5 S31P H74F	ΔQ5 S31P	13, 14	yes
	ΔQ5 S31P I200H	ΔQ5 S31P	15, 16	yes
hAQP8-HA	C53A	wt	17, 19	yes
	C53S	wt	18, 19	no
	F145A	wt	22, 23	yes
	I198H	wt	24, 25	yes

Constructs made by restriction digestion and ligation

The following DNA fragments, coding for generated AQP mutants, were transferred from pRS426-MET25 to pOG1 by digestion (3.1.4) with BamHI/HindIII, and subsequent ligation (3.1.7):

rAQP1 F56H, H180I, F56H/H180I, H180L, H180M, H180F, H180N, H180Q

rAQP8 ΔQ5 S31P wt, I200H

The resulting constructs were not sequenced, but verified by BamHI/HindIII digestion and agarose gel electrophoresis.

3.3 Protein manipulation

All procedures intended for protein analysis were carried out at ~ 0 - 4 ℃, unless mentioned otherwise. Water was autoclaved.

3.3.1 Isolation of the microsomal fraction from *S. cerevisiae*

This procedure was performed twice during the course of this work, separated by two years during which the laboratory's standard method was modified.

Method 1

Yeast were grown in 100 ml SDKHL medium inside 500 ml Erlenmeyer flasks at 29 ℃ and 180 rpm to an OD_{600} of ~ 1. They were collected in two 50 ml tubes (1,268 x g, 10 min), and washed with 25 ml water and 10 ml extraction buffer ("simplified", see 2.9). The unified pellet was frozen at -20 ℃.

On the day of microsome isolation, the pellet was thawed on ice, and resuspended in 0.5 ml extraction buffer after addition of 15 µl protease inhibitor stock solution and ~ 0.5 g acid-washed glass beads (Ø ~ 0.5 mm). It was vortexed 10 x 30 s at maximum setting, with cooling periods during which other samples were vortexed, then centrifuged (2,500 x g, 10 min) and the supernatant was transferred to an ultracentrifuge tube. This step was repeated after addition of 0.5 ml extraction buffer. The ultracentrifuge tube was then filled to the rim with extraction buffer, without the addition of protease inhibitor stock solution because

of the large volume (~ 25 ml per tube). Ultracentrifuge tubes were weighed, and extraction buffer added or removed to ensure equilibrium of pairs within +/- 3 mg. Ultracentrifugation was at ~ 100,000 x g for 45 min including acceleration. The supernatant was carefully removed, and the microsomal pellet resuspended in 0.2 ml buffer M. The suspension was transferred to a 1.5 ml tube and frozen at -20 ℃. After determination of protein concentration (3.3.3), 10 x DDM solution was added for solubilization.

Method 2

Essentially the same as Method 1, with the following differences:
50 ml SDKHL, extraction buffer not “simplified”, no washing with extraction buffer, yeast resuspended in 2 µl extraction buffer for 1 mg wet pellet, weight of glass beads added was similar to that of the suspension, cell disruption inside 1.5 ml tubes instead of 50 ml tubes, use of 1.5 ml ultracentrifuge tubes, resuspension in storage buffer, no solubilization with DDM after Bradford assay, addition of protease inhibitor stock solution for storage (15 µl per 200 µl).

Simplified method

Yeast protoplasts (3.5) were pelleted, resuspended in water, vortexed a few seconds at maximum setting and centrifuged (7,500 x g, 10 min). The supernatant was transferred to a new 1.5 ml tube, centrifuged (16,000 x g, ~ 30 min), and the pellet resuspended in storage buffer with added protease inhibitor stock solution (15 µl per 200 µl).
7,500 x g was chosen because a large fraction of mitochondria is removed at this acceleration (at least for rat hepatocyte mitochondria, see Calamita *et al.*, 2005), and because the centrifuge operated at this speed in the “fast cool” setting (“Centrifuge 5415R”, Eppendorf).

Acid-washed glass beads

Glass beads (Ø ~ 0.5 mm) were washed with ~ 1 volume HCl 5.8 M inside a glass bottle for ~ 3 h, rinsed 10 times with ~ 5 volumes of water, then autoclaved and dried at 50 ℃.

3.3.2 Collection of membrane fractions from *X. laevis* oocytes

X. laevis oocytes stored inside 1.5 ml tubes at -80 ℃ (3.6) were thawed on ice. For every oocyte, 100 µl hypotonic phosphate buffer was added, and the resulting suspension pipette-mixed. The suspension was centrifuged (500 x g or 100 x g, 5 min), as was the supernatant (16,000 x g, 30 min). Care was taken to remove any debris floating on the surface before

removing the supernatant. The pellet was suspended in 4 x SDS-PAGE sample loading buffer (10 µl per oocyte equivalent) and incubated at 37 °C for 30 min. The resulting sample was frozen at -20 °C, or immediately analyzed by SD S-PAGE (3.3.4).

3.3.3 Concentration measurement

The approximate protein concentration of yeast microsome fractions (3.3.1) was measured according to the method described by Bradford in 1976, using the "Bio-Rad Protein Assay" reagent.

2 - 10 µl yeast microsome suspension was mixed with 390 µl water and 100 µl reagent inside a 1.5 ml tube by vortexing. After ~ 5 min, the sample was poured into a polystyrene cuvette and its A_{595} measured, accepting a range of 0.15 - 1.5 for practical reasons. A calibration curve had been prepared by a colleague with BSA ("Fraction V", 1 - 15 µg/ml).

The reagent supplier's manual states that "the sample cannot be a suspension or an unfiltered homogenate". Yet this was the case, so measured concentrations could only be considered relative.

3.3.4 SDS-Polyacrylamide gel electrophoresis

Gel preparation

Running and stacking gel solutions were prepared inside 25 ml glass beakers, from the components and in the order given in the following table:

	Running gel		**Stacking gel**
Acrylamide	**13.2 %**	**16.5 %**	**6 %**
Water	5 ml	4 ml	2.4 ml
4 x Resolving gel buffer	3 ml	3 ml	-
4 x Stacking gel buffer	-	-	1.0 ml
Bis-/acrylamide solution	4 ml	5 ml	0.6 ml
TEMED	10 µl	10 µl	6 µl
APS 10 %	80 µl	80 µl	25 µl

The given amounts were enough for two gels, including a generous surplus. Stacking and running gels had a length of about 1.5 cm and 6 cm, respectively, excluding pockets, and a thickness of ~ 0.8 mm. The total concentration of the bis-/acrylamide solution was 40 % ("Rotiphorese Gel 40", Roth), the ratio was 1:37.5. The intended bis-/acrylamide con-

centrations of the resolving gel were 10 % and 12.5 %, and that of the stacking gel was 5 %. However, the laboratory's standard protocol implicitly referred to 30 % total bis-/acrylamide concentration ("Rotiphorese Gel 30"), and was used erroneously. TEMED and APS concentrations had been optimised by a fellow laboratory member (N. Fricke). A layer of isopropanol served to smooth the upper rim of the resolving gel. Gels (contained between glass and ceramic plate) were frequently prepared in advance and stored at 4 ℃, wrapped in wet paper towels inside plastic bags.

Electrophoresis

Gels were mounted vertically ("PerfectBlue Twin S", Peqlab) and cathode buffer was used for both the cathode and the anode chamber. Samples were mixed with 4 x loading buffer and incubated at 37 ℃ for ~ 30 min. For yeast (3.3.1), the equivalent of ~ 10 µg BSA (3.3.3) was pipetted into each pocket. For *X. laevis* oocytes (3.3.2), the membrane fraction of one oocyte was taken. Protein markers "peqGOLD I" or "peqGOLD III" (Peqlab) were used, the latter more frequently because it is prestained.
Electrophoresis was at 150 - 200 V (~ 25 - 33 V/cm) for 80 - 110 min, usually until the dye bands disappeared into the anode-bathing buffer. The temperature was not regulated.

Staining

Following electrophoresis, the stacking gel was discarded and the resolving gel subjected to blotting (3.3.5). After blotting, it was stained with Coomassie Brilliant Blue G250 solution ("Rotiphorese Blue R") for 1 h, and washed in destaining solution overnight. For later experiments, colloidal staining solution ("Roti-Blue") was used, staining overnight and destaining with several aliquots of water within less than 1 h. All de-/staining procedures took place at room temperature and under constant tilt-shaking. Stained gels were scanned.

3.3.5 Western blotting

Blotting

Proteins were blotted onto a PVDF membrane, with transfer buffer-soaked Whatman paper for electrode contact. The membrane was first "activated" by immersion in methanol and in transfer buffer. From anode to cathode, a triple layer of paper was followed by the membrane, the gel, and another triple layer of paper. Membrane and paper closely matched the resolving gel in dimensions (~ 54 mm x 85 mm), the bottom section of the gel usually having to be sliced off. Trapped bubbles were freed by carefully rolling a Pasteur pipette over

the final stack. Electrophoresis was generally at 10 V for 60 - 80 min, with current density ranging from ~ 1 - 3 mA/cm^2.

Antibody incubation

After blotting, the membrane was nicked at one of its corners, for later identification of the protein side, and saturated with milk protein by incubating it in M-TBS-T for 1 h at room temperature. It was then incubated overnight in M-TBS-T containing an appropriate amount of primary antibody (see below). This was followed by 4 - 6 rinsings in TBS-T at room temperature, each lasting ~ 5 - 20 min. Incubation with an appropriate dilution of the secondary antibody in M-TBS-T (see below) took place for ~ 1 h, and was followed by thorough rinsing with TBS-T as described above. All incubations and rinsings were under constant rotary or tilt-shaking inside square or circular Petri dishes.

Antibody dilutions (for the stock solutions, see 2.9):

Mouse monoclonal IgG against AQP1	1:1000
Mouse monoclonal IgG against HA-tag	1:3000
HRP-conjugated goat anti-mouse IgG	1:2000 - 1:10000

Detection

The membrane was positioned protein-side up on a Petri dish, and covered with 1 ml of reagent mixture (“ECL Plus Western Blotting Detection System”, GE Healthcare). After ~ 5 min, excess reagent was allowed to drip off, and the membrane was wrapped in plastic foil before enclosing it in a radiography case (“ABS-Cassette”, Cawo). In a dark room, the chemiluminescence was recorded by 30 s to 30 min exposure of radiography film (“Hyperfilm ECL”, GE Healthcare). The film was developed immediately (“Cawomat 2000 IR“, Cawo), and scanned later.

On the two final occasions, the chemiluminescence was recorded digitally (“Lumi-Imager F1“, Roche).

3.4 *S. cerevisiae* growth assays

Two strains of *S. cerevisiae* were used for growth assays: 31019b Δfps1 for ammonia assays, and BY4742 Δfps1 for methylamine assays (2.7). Manipulation of yeast and yeast media was always under laminar flow, and all containers and pipette tips were sterilized,

either by autoclaving (~ 120 °C, + 1 bar, ~ 20 min) , heat sterilization (~ 170 °C, 4 h), or by the supplier. Pasteur pipettes used for spreading yeast suspensions on solid media were sterilized by immersion in ethanol (~ 70 % V/V) and subsequent flaming.

3.4.1 Transformation of *S. cerevisiae*

The following procedure is based on that described by Gietz *et al.* in 1995. Selection was by plasmid-conferred uracil auxotrophy (2.5).

S. cerevisiae from a glycerol stock were spread on YPD agar and grown at 29 °C for 3 - 5 days. The culture was then kept at 4 °C and used for up to 3 months.

A piece of a single colony was picked and transferred to 5 ml YPD medium inside a 50 ml or a 100 ml Erlenmeyer flask, and grown overnight at 29 °C and 180 rpm. 0.5 ml of the overnight culture was transferred to 50 ml YPD medium inside a 250 ml Erlenmeyer flask and grown at 29 °C and 180 rpm to $OD_{600} \approx 0.6$. The culture was collected in a 50 ml tube and centrifuged (2,500 x g, 5 min). The cells were washed with 25 ml water, resuspended in 1 ml water and transferred to a 1.5 ml tube. They were then pelleted and resuspended in water to a final volume of 1 ml. 60 - 100 µl aliquots were distributed among 1.5 ml tubes, one for each transformation. These were centrifuged (10,000 x g, ~ 10 s), and enough water removed by pipetting to leave ~ 30 µl on top of each pellet. To each was added ~ 0.4 µl plasmid solution (~ 50 - 500 ng DNA), followed by ~ 326 µl of freshly prepared yeast transformation buffer. Cells were resuspended by repeated quick but gentle sliding of the tubes' bottoms along a wire test tube basket, followed by vortexing. Samples were then incubated for 45 - 60 min at 42 °C on a block heater, during which time SDKHL agar plates were prepared by allowing them to dry and to reach room temperature under laminar flow. Samples were centrifuged (16,000 x g, ~ 10 s), supernatants removed by careful pipetting, and 1 ml of water added to each. Cells were resuspended by pipette-mixing, and 50 - 200 µl suspension was spread on SDKHL agar. Petri dishes were sealed with parafilm and incubated at 29 °C for up to a week, to allow transformed cells to grow and form colonies with a diameter of at least ~ 0.5 mm.

Transformation efficiency (number of colonies per amount of DNA) was consistently found to be about two or more orders of magnitude higher for BY4742 Δfps1 as compared to 31019b Δfps1.

Glycerol stocks

0.4 ml of an overnight culture of *S. cerevisiae* in SDKHL was mixed with 0.8 ml glycerol 60 % inside a 1.5 ml tube and frozen at -80 °C.

Alternatively, ~ 1.3 ml of an overnight culture was centrifuged (10,000 x g, ~ 10 s) and the cells resuspended in 0.9 ml or 0.45 ml fresh SDKHL medium. 0.3 ml glycerol 80 % or 0.7 ml glycerol 40 % was then added, and the suspensions were frozen at -80 ℃.

3.4.2 Yeast preparation

A yeast transformant colony or a scraping from a glycerol stock (3.4.1) were picked and suspended in 1.6 ml SDKHL inside a glass tube. The culture was grown on an orbital shaker overnight or until turbid (29 ℃, 180 - 200 rpm). I t was then poured into a 1.5 ml tube, washed twice or thrice with water (1 ml, 16,000 x g, ~ 3 s), and resuspended in water to a final volume of 0.5 ml. The OD_{600} of a dilution, usually a hundredfold, was measured, accepting values of about 0.1 - 0.7. Suspensions of the desired OD_{600} were then prepared in other 1.5 ml tubes and used for growth assays.

3.4.3 Ammonia assay

Principle

S. cerevisiae strain 31019b Δfps1 lacks the three ammonium transporters Mep1-3, as well as the ammonia-permeable glyceroporin Fps1. In theory, it thus cannot take up ammonia except by diffusion through the lipid bilayer of the plasma membrane. This slows growth on medium containing low concentrations of an ammonium salt as the only nitrogen source. The heterologous expression of an ammonium/ammonia-permeable membrane protein-encoding gene may improve growth. Varying the pH allows to deduce whether ammonium ions or ammonia are transported.

Medium composition

Media for ammonia assays had the following standard composition:

Buffer 20 mM, $(NH_4)_2SO_4$ 2 mM, D-glucose·H_2O 3 %, YNB 0.17 %, NaOH → pH, (agar 2.1 % for solid media).

The concentrations of all components, except the agar, were varied extensively and are specified if they deviate from the standard composition. Succinic acid (pK_{a1} ~ 4.2, pK_{a2} ~ 5.6), MES (pK_a ~ 6.2), MOPS (pK_a ~ 7.2) and HEPES (pK_a ~ 7.6) served as buffers for the appropriate pH ranges. The use of 3 % anhydrous glucose may have been intended, but it was standard laboratory practise to substitute with the monohydrate without adjusting the percentage.

Standard plates

Water, $(NH_4)_2SO_4$ and buffer stock solutions were mixed inside a glass bottle, and the pH was carefully set with NaOH solution. Agar was added, and the suspension was autoclaved (~ 120 ℃, + 1 bar, ~ 20 min). In the meantime, glu cose and YNB stock solutions were mixed inside 100 ml Erlenmeyer flasks and kept in a shaking water bath at 55 ℃. Components were unified inside the bottle, mixed gently by inversion, and ~ 25 ml was poured into each Petri dish (92 mm x 16 mm). Plates were left open-lidded under laminar flow for ~ 5 - 15 min. Total volume was usually 90 ml, sometimes 120 ml, enough for 3 or 4 plates. Water lost during autoclaving was not replaced, so actual concentrations were somewhat higher than nominal ones.

pH gradient plates

pH gradient plates (Maresova and Sychrova, 2005) were made by successive pouring of two gels inside a single square Petri dish (~ 12 cm x 12 cm x 1.5 cm), as shown in the following schematic:

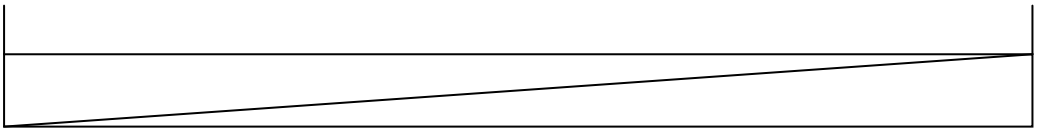

Fig. 3.1: Gradient plate schematic, side view.

Bottom and top gels had the following compositions:

	Bottom gel	**Top gel**
HEPES	40 mM	-
NaOH	pH 8.0	-
Agar	2.0 %	2.0 %
Nitrogen source	10 mM	10 mM
YNB	0.17 %	0.17 %
D-glucose	2.7 %	2.7 %
BTB	25 ppm	25 ppm
Tartaric acid	-	pH 4

Components were added in the given order, to a final volume of 40 ml each. The addition of agar was followed by autoclaving as described for standard gels. Nitrogen sources were $(NH_4)_2SO_4$ (5 mM) or L-glutamine (10 mM), with one ammonium ion considered equivalent to one molecule of L-glutamine. Bromothymol blue (BTB) was intended as a pH indicator. The necessary amount of tartaric acid was estimated in a mock experiment, with all components

included but without the autoclaving. Its final concentration turned out to be ~ 1 mM. The choice of bottom gel was based on the observation that solidification is considerably faster at alkaline pH. To create the necessary tilt, the lid of a standard Petri dish ($h \approx 8$ mm) was found to be an adequate support. After pouring, the sol had to be spread by gentle lifting and lowering of the plate. Each sol was allowed to cool and solidify for ~ 10 min under laminar flow. The resulting gradient gel was left to dry for ~ 30 min with the lid partially removed. Plates were used within 24 h.

Plate assays

Drops of 5 µl yeast suspension (3.4.2) were pipetted onto the gel in the desired pattern. A grid drawn on paper and placed below the plate allowed accurate positioning of the drops. Plates were left to dry for ~ 10 - 15 min. They were sealed with parafilm and incubated at 29 ℃ until the yeast had grown sufficiently.

Liquid cultures

All components were mixed, the pH carefully set with NaOH solution, water added to reach the final volume (graduated centrifuge tube or cylinder), and the resulting solution filtered (PES or PVDF Ø 0.2 µm) into 50 ml centrifuge tubes or autoclaved borosilicate glass bottles. Liquid media were usually prepared the day before the assay.

Liquid cultures allowed the recording of growth curves. This was either done by taking samples from Erlenmeyer cultures, or by automated measurements with the “Bioscreen C microbiology reader” (Oy Growth Curves, Finland).

Bioscreen

100-well plates (Fig. 3.2) are used for the “Bioscreen C MBR”, each well having a total volume of ~ 600 µl ($d \approx 7$ mm, $h \approx 15$ mm). Two plates can be used per experiment.

290 µl medium was pipetted into each well, followed by the addition of 10 µl yeast suspension (3.4.2). The starting OD_{600} was intended to be ~ 0.1 or 0.2, and so yeast suspensions of $OD_{600} \approx 3$ or 6 were prepared, forgetting to take the smaller path length (~ 7.5 mm for 300 µl medium) into account. Substance dilution series (e. g. NH_4^+ 40 mM, 20 mM, 10 mM…) were prepared directly inside consecutive wells, pipette-mixing ten times each. Using the provided software, “EZExperiment”, the standard instrument settings were as follows:

29 ℃, 420 - 580 nm, 30 min measurement interval, 10 s “medium intensity” shaking before each measurement (see 4.3.3 and 5.2.1).

The wideband filter (420 - 580 nm) was chosen as recommended by the manual, since measurements are thus less influenced by possible colour changes during growth. Data were

visualized and evaluated using a spreadsheet (“Excel”, Microsoft). Areas under the curves (AUC) were calculated by adding rectangle areas obtained with the following formula:

$$0.5 \cdot (OD_i + OD_{i+1}) \cdot (t_{i+1} - t_i)$$

The starting *OD* (*t* = 0 h) was subtracted from each value.
Growth rates were calculated by the following formula:

$$(OD_{i+1} - OD_i) / (t_{i+1} - t_i)$$

Floating averages (5 points, corresponding to a period of 2 h) were calculated, and the maximum values were determined.

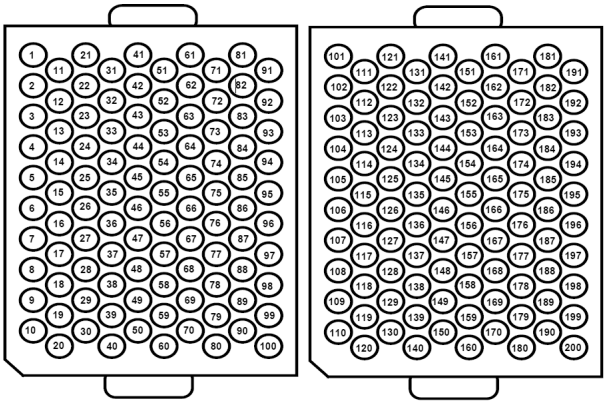

Fig. 3.2: ”Bioscreen” assay plate schematic. *Two plates fit inside the incubator, in the relative position shown here.*

Erlenmeyer cultures

To measure pH and conductivity changes, yeast were grown in 20 - 50 ml assay medium inside Erlenmeyer flasks (29 °C, 200 rpm). The starting OD_{600} was 0.1 or 0.15. Samples (1.0 ml) were taken at least daily for 1 week, followed by less regular intervals for up to 3 weeks. The OD_{600} of each sample was measured, and 0.9 ml was transferred from the cuvette (narrow 1 ml pipette tips, Kisker) to a 1.5 ml tube. Yeast were removed by two centrifugations (16,000 x g, 5 min), each time leaving behind 0.1 ml supernatant to minimise contamination. Conductivity was measured (“LF537” and “TetraCon 96”, WTW) after diluting 0.2 ml supernatant a hundredfold with water inside a 50 ml tube. The remaining 0.5 ml served to measure the pH (“pH-meter 605”, Metrohm, and “BlueLine 16”, Schott).
Flasks were weighed before and after sample-taking to estimate evaporative loss.

3.4.4 Methylamine assay

Principle

S. cerevisiae strain BY4742 Δfps1 lacks the methylamine-permeable glyceroporin Fps1. Methylammonium ions are taken up by the methylamine permeases Mep1-3. At high concentrations they are toxic and prevent growth. The heterologous expression of a methylamine-permeable membrane protein-encoding gene enables uncharged methylamine to leave the cell if the external pH is lower than the intracellular pH. The assay was described in more detail by Beitz *et al.*, in 2006.

Medium composition

Media for methylamine assays had the following standard composition:

Buffer 20 mM, CHCl 50 mM, L-proline 0.1 %, L-lysine HCl 20 ppm, L-histidine HCl·H_2O 20 ppm, L-leucine 100 ppm, D-glucose·H_2O 3 %, YNB 0.17 %, NaOH → pH, (agar 2.1 % for solid media).

MES (pK_a ~ 6.2) and MOPS (pK_a ~ 7.2) served as buffers for the appropriate pH ranges. Succinic acid (pK_{a1} ~ 4.2, pK_{a2} ~ 5.6) was used for one assay, as indicated. As for the ammonia assay, the percentage of glucose monohydrate was not adjusted.

Standard plates

Assay plates were prepared as described for the ammonia assay (3.4.3), with the notable difference of adding the methylammonium solution after autoclaving.

Assay

Only standard plate assays and “Bioscreen” assays were performed, as described for the ammonia assay (3.4.3).

3.5 Osmotic assays with *S. cerevisiae* protoplasts

Yeast have a cell wall which limits their swelling or shrinking in response to changes in external osmotic pressure. Osmotic assays are more easily performed if the cell wall is digested. The following buffers and procedures are based on ones described by Bertl and Kaldenhoff in 2007.

Buffers

A set of four buffers was used for the preparation of yeast protoplasts, and for the osmotic assays. Their general compositions were as follows:

Buffer	**I**	**II**	**III**	**IV**
Osmolyte	-	1.8 M	1.2 M	1.2 M
Solute	-	-	0.3 M	-
NaCl	-	-	50 mM	50 mM
$CaCl_2$	-	-	5 mM	5 mM
MOPS	-	-	10 mM	10 mM
KH_2PO_4	50 mM	50 mM	-	-
NaOH	-	-	pH 7.2	pH 7.2
KOH	pH 7.2	pH 7.2	-	-
2-ME	0.2 % V/V	0.2 % V/V	-	-

Osmolytes were D-sorbitol or D-sucrose. Solutes were glycerol or formamide. For water permeability measurements, additional osmolyte was added instead of solute. The solutions were filtered (PES Ø 0.45 µm) into autoclaved glass bottles. 2-Mercaptoethanol was added after filtering. Unless mentioned otherwise, the osmolyte was D-sorbitol.

The protocol of an experienced laboratory (A. Bertl, R. Kaldenhoff) was followed initially, and so for early experiments the buffer was Tris/HCl pH 7.0 (rather than pH 8.0 as in the above-mentioned publication).

Protoplast preparation

Yeast were prepared as described (3.4.2), except for resuspending them in 0.5 ml SDKHL, and without washing. They were then grown in 20 - 150 ml SDKHL (29 ℃, 180 - 200 rpm) to an OD_{600} of ~ 0.6 - 3 (aiming at $OD_{600} \approx 1$), and harvested in 50 ml tubes (2,500 x g, 5 min). The supernatant was removed carefully before measuring the wet pellet weight. The pellet was resuspended in Buffer I (~ 3 ml/40 mg wet pellet) and incubated (29 ℃, 100 rpm in a tilted position, ~ 15 min). This was followed by the addition of BSA (~ 100 mg/40 mg wet pellet), Buffer II (~ 6 ml/40 mg wet pellet), and zymolyase-20T (~ 0.5 mg/40 mg wet pellet, dissolved in a 1:2 mixture of Buffers I and II), and by gentle but thorough mixing before further incubation (s. a., 60 min). Digested yeast were washed twice in 1 - 2 ml Buffer IV (4 ℃, 2000 x g for sorbitol, 4000 x g for sucrose, 5 min), and finally resuspended in 2 - 4 ml Buffer IV. The OD_{600} was measured, and the suspension stored at 4 ℃ in the same 50 ml tube until use.

A mock experiment with no yeast showed that mixing 50 µl Buffers I/II and 2 ml Buffer IV gives rise to a fine-grained precipitate, possibly made of calcium and phosphate ions.

The ratio of wet pellet weight to OD units (OD_{600} multiplied by the culture volume in ml) was consistently found to be ~ 1 - 2 mg/ml.

Osmotic assays

Osmotic assays with yeast protoplast suspensions were performed using a stopped-flow apparatus ("BioLogic", see materials section).

The protoplast suspension was diluted with cold (4 °C) buffer IV to an OD_{600} of ~ 2 inside a 10 ml glass beaker, usually to a total volume of 2 ml. It was taken up as bubble-free as possible in a 6 ml plastic syringe which was then mounted on the stopped-flow module. The same was done with the hyper- and isoosmotic buffers, or with water. Each sample was driven into and out of its reservoir several times, until no bubbles appeared (even in the turbid protoplast suspension rising bubbles were quite visible). Sample volumes were set, after which at least 5 min (usually 10 min or more) were allowed to pass before the first measurement, for temperature equilibration.

Measurements were performed by mixing the protoplast suspension with an equal volume of buffer and recording the light scattering (90°). The following settings and conditions were applied:

Temperature:	20 °C or as specified
Total volume per shot:	150 µl
Total flow rate:	6.5 ml/s
Lamp power:	100.0 W or 150.0 W ± 0.1 W
Wavelength:	546 nm or 436 nm
Detector voltage:	350 - 500 V (usually 450 V)
Output filter:	0.3 ms
Data points:	8,000 (maximum)
Acquisition time:	as appropriate

For evaluation, average curves were normalized and time constants determined as described in the results section (4.3.2).

3.6 Osmotic assays with *X. laevis* oocytes

Oocyte preparation

Oocytes from *X. laevis* frogs were collected by a fellow laboratory member (J. von Bülow). The tissue containing them was washed 3 times with OR2 buffer, cut to small pieces with a forceps, and digested by incubation in Collagenase A solution (0.5 mg/ml OR2 buffer) for 30 min at 37 °C and gentle orbital shaking. The digested tissue was washed 3 - 5 times with ND96 buffer, and Stage V and VI oocytes were selected under a dissecting microscope. Due to inexperience, some Stage IV oocytes were also selected for early experiments. Harvested oocytes were stored in ND96 buffer at 4 °C for up to 1 day before injection. A Pasteur pipette with a broadened and flame-smoothed tip was used for all oocyte transfers.

cRNA injection

Oocyte injections were done with the help of a microsyringe assembly consisting of a nanoliter injector and a dissecting microscope. The microsyringes were made from glass capillaries with a capillary puller, using a programme chosen by the host laboratory (M. Bleich). cRNA solution (50 nl, ~ 0.1 ng/nl) was injected into the pigmented pole. DEPC-treated water or ND96 buffer were injected as controls. After injection, oocytes were incubated in fresh ND96 buffer inside 96-well plates, 1 - 2 oocytes per well, for 2 - 4 days at ~ 15 °C.

Osmotic assay

Before the first measurement, oocytes were transferred to fresh ND96 buffer, and ND96 buffer was diluted threefold with water and filled into a small Petri dish (35 mm x 10 mm) that was then placed on a microscope. A single oocyte was carefully dropped into the diluted buffer, and pictures of its silhouette were taken every 15 s for 60 s with a CCTV camera mounted on the microscope. Between dropping the oocyte, adjusting the position of the Petri dish, and taking the first picture, ~ 10 - 20 s would pass. After the last picture, the oocyte was placed back into undiluted ND96 buffer to recover. Burst oocytes were discarded immediately. A few oocytes were transferred to 1.5 ml tubes and frozen at -80 °C for later protein analysis (3.3.2).

Measurements were performed at room temperature (~ 20 - 25 °C, depending on the season and on the time of day).

Evaluation

Recorded silhouettes were used to calculate changes in relative volume, assuming perfectly spherical oocytes. This was done with a macro created with the programme “ImageJ” by E.

Beitz. Relative volume changes of several oocytes were averaged. The osmotic water permeability coefficient P_f was then calculated with the following equation:

$$P_f = \frac{V_0 \cdot \frac{\Delta(V/V_0)}{\Delta t}}{S_0 \cdot V_w \cdot \Delta c}$$

V_0 and S_0 are the resting volume and surface area of an oocyte, assuming a radius of 600 µm. V_w is the molar volume of water (~ 18 ml/mol), and Δc is the osmotic gradient (~ 140 mosmol/l). The relative volume change between 0 s and 15 s (first and second images) was chosen for calculations. For osmotic assays with *X. laevis* oocytes, P_f is usually expressed in units of µm/s.

3.7 Osmotic assays with human blood cells

Buffers

A buffer described by Carlsen and Wieth in 1976 was used for experiments with blood cells. Its composition was as follows:

NaCl 154 mM, KH_2PO_4 0.25 mM, Na_2HPO_4 0.25 mM, D-glucose 5 mM, KOH → pH 7.4

It was prepared as a 10 x concentrated solution ($\rho \approx 1.06$ g/cm^3) and diluted. Glycerol or formamide were added upon dilution (60 mM) to make hyperosmotic buffers for assays. The pH had to be set again after dilution. Diluted buffers were filtered (PES Ø 0.2 µm) into 50 ml tubes. Carlsen buffers were stored at 4 ℃.

Blood cell preparation

The skin of a fingertip was wiped with 70 % ethanol and pricked with a sterile injection needle (Ø 0.8 mm). Drops of blood were encouraged to form by gentle squeezing. They were taken up with a pipette, ~ 5 µl at a time, and directly transferred into ice cold Carlsen buffer inside a 1.5 ml tube (~ 40 - 80 µl blood per 950 µl buffer). For practical reasons, the suspension was distributed among two tubes. It was pipette-mixed and centrifuged (4 ℃, 2,000 x g, 10 min), and the supernatant was removed. The cells were washed twice more in this way, and unified in 0.5 ml Carlsen buffer. The suspension was used immediately or kept at 4 ℃ for up to 3 days. Even after several weeks, erythrocyte suspensions had not lysed much, although freezing and thawing led to complete lysis. It was found that a nominal OD_{600} of ~ 140

corresponded to a hematocrit of ~ 6.5 %. Microscopy (300 x magnification) revealed mostly spherical and more or less spiky erythrocytes, some of them aggregated, despite a measured osmolality of 300 mosmol/kg. Larger, smooth and spindle-shaped cells may have been leukocytes, the little specks were probably thrombocytes.

Osmotic assays

Osmotic assays with blood cells were performed as described for yeast protoplasts (3.5), with the following settings:

Temperature:	26 ℃
Total volume per shot:	150 µl
Total flow rate:	6.5 ml/s
Lamp power:	100.0 W ± 0.1 W
Wavelength:	600 nm
Detector voltage:	450 V
Output filter:	0.3 ms
Data points:	8,000 (maximum)
Acquisition time:	8 s, 40 s, 160 s

Temperature and wavelength were chosen according to Roudier *et al.* (1998). For evaluation, average curves were normalized and time constants determined as described for the yeast protoplast assays (4.3.2).

3.8 Inhibitor assays

Potential aquaporin inhibitors (2.10) were tested with the osmotic assays and growth assays described above (3.4, 3.5, 3.7). Growth assays were limited to yeast synthesizing ammonia-permeable aquaporins. For osmotic assays, test compounds had to be fully dissolved, and so their approximate solubilities were determined as described below.

Stock solutions

Test compounds were dissolved in DMSO to a final concentration of 10 mM, 20 mM, 50 mM, or 100 mM, or as their solubility allowed. It was found that the resulting volume of the solution in relation to the size of the container is an important consideration (the containers usually held no more than 2 ml of fluid). Some compounds were salts and had to be dissolved in

water. Storage at 4 ℃ occasionally led to precipit ation, but warming up by hand was usually enough for resolubilization.

Some of the compounds were received as DMSO solutions inside individual plastic vials (~ 7 mm x 38 mm) covered by a single 96-vial lid. The lid appeared too difficult to remove without causing loss and cross-contamination. Instead, it was pierced above each vial with an injection needle (Ø 0.8 mm), and ~ 100 µl of solution was taken out with a pipette (mixing three times) and transferred to a 96-well plate which later served as the working repository. Some of the compounds were not fully dissolved, and the reach of the pipette tip was limited, so precise concentrations for these compounds were not known.

Solubility determination

Test compound solubilities in assay media were determined turbidimetrically using the "Bioscreen" (3.4.3). The stock solution was diluted, usually a hundredfold, inside the medium of interest. A fourfold dilution series was then prepared directly inside consecutive wells, without adjusting the DMSO concentration, and the apparent absorption was measured at 405 nm and at 600 nm, usually at 20 ℃. The minimum solubility was then estimated by comparison with the blank values.

Experience led to a modification of this method: fourfold dilution series were prepared in DMSO, and the resulting solutions were all diluted inside assay medium a hundredfold. This had the advantage of greater precision, since diluting the suspensions (test compound precipitated inside the medium) is probably somewhat inaccurate. In addition, the DMSO concentration was thus constant, and the solutions could directly be used for assays.

Osmotic assays

The test compound stock solution was diluted together with the yeast or blood cell suspension as described above (3.5 and 3.7). Care was taken to dilute the compound before adding the cells, to avoid high local concentrations. The reservoir of the stopped-flow apparatus was rinsed twice with ~ 1 ml of the appropriate buffer containing the test compound before loading it with the cell suspension containing that compound.

The incubation time was equal to the time needed for cell dilution and subsequent temperature equilibration inside the stopped-flow apparatus, i. e. ~ 10 - 20 min for the first measurement. On some occasions, the time needed for the temperature equilibration of a sample inside the stopped-flow apparatus was used to prepare the next sample. In that case, incubation time was ~ 0.5 - 1.5 h (inside a glass beaker on ice), equal to the time needed for measurements of the previous sample. On two occasions, yeast cells were premixed with test compound-containing buffer inside the stopped-flow apparatus, making use of its three

reservoirs and two mixing chambers. Incubation time was then of the order of the acquisition time, i. e. ~ 1 min for the experiment concerned.
Ideally, the test compound is added to both the cell suspension and the hyperosmotic buffer. Not doing so leads to a halving of its concentration upon mixing, except for quasi-irreversibly binding substances like $HgCl_2$. However, since the aim was to see whether a given compound shows any effect at all, test compounds usually were not added to the hyperosmotic buffer in order to save time. DMSO concentrations of the yeast protoplast suspension and the mixing-buffers were usually the same, to avoid unwanted osmotic effects.

Yeast growth assays

A tenfold predilution of the test compound prepared inside a 1.5 ml tube was further diluted inside a “Bioscreen” plate well, to a final DMSO concentration of 0.1 or 1 % V/V. The assay was then performed as described above (3.4.3).
Precipitation inside wells was considered acceptable, assuming that the resulting turbidity remains constant throughout the duration of the assay.

4 Results

4.1 Permeability characterization of the generated aquaporin mutants

The initial focus of the presented work was the characterization of the ammonia permeability of two aquaporins, AQP1 and AQP8, with regard to their ar/R-constriction regions. In addition, water permeabilities were measured, as they are a useful indicator of channel integrity. Two types of assay were used: yeast growth assays for ammonia permeability characterization, and osmotic assays for water permeability measurements.

4.1.1 Mutating the rat Aquaporin 1 constriction to mimick the human Aquaporin 8 constriction

The first experiments consisted in creating double and triple mutants of rAQP1, with an ar/R-constriction mimicking that of rAQP8. The single mutants rAQP1 F56H, H180I and C189G had previously been prepared by colleagues (H. Long and J. Song).

Growth assays

The first functional assay performed was a methylamine assay with transformants of the yeast strain BY4742 Δfps1. Its results are presented in Figure 4.1.

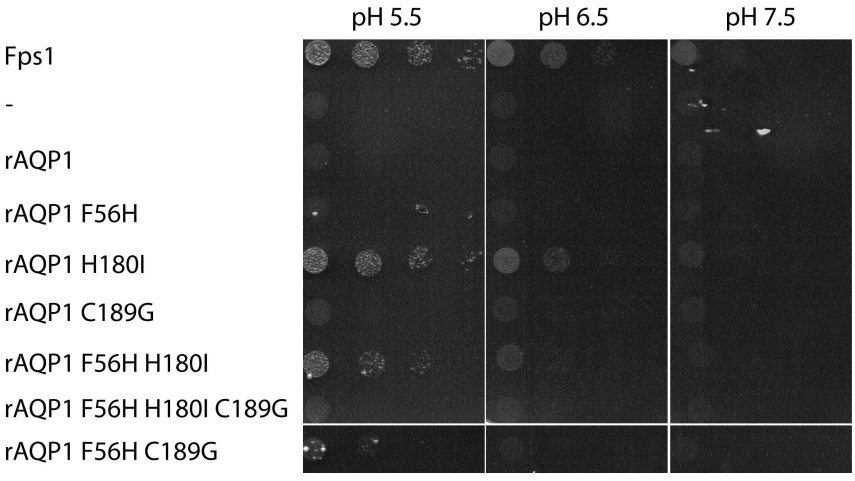

Fig. 4.1: Methylamine assay. *Yeast transformants (BY4742 Δfps1, pRS426 or pRS416 for Fps1) were spotted in tenfold dilution series starting with an OD_{600} of 1, and grown at 29 ℃ for 6 days. The methylamm onium concentration was 50 mM. Yeast synthesizing rAQP1 F56H/C189G were spotted the same day on plates belonging to the same lot.*

Yeast transformants producing Fps1 grew better than those producing no aquaporin. rAQP1 H180I and F56H/H180I led to appreciable growth. The pattern can be seen most clearly for pH 5.5, whence it fades with increasing pH, as expected for a decreasing intra- and extracellular pH gradient. In addition, it appears that the single mutant H180I improved growth more than the double mutant F56H/H180I.

This result had been anticipated. Following transformation, yeast colonies on SDKHL agar grew larger if they expressed Fps1, rAQP1 H180I, F56H/H180I, or F56H/H180I/C189G. This would later be seen numerous times for transformations of the yeast strain BY4742 Δfps1.

For the above experiment, no SDKHL control plate was used. Later assays, including ones with liquid medium, showed no growth difference in SDKHL medium. Why such a difference could be seen on selection plates after transformation is not clear.

Attempts to repeat this experiment were unsuccessful due to a seemingly poor quality of the yeast at the time (grey appearance and poor growth), which led to a near absence of growth on methylammonium-containing agar, irrespective of the expressed protein. It was this difficulty that led to the use of the ammonia assay, with the yeast strain 31019b Δfps1. The results of the first ammonia assay are shown in Figure 4.2.

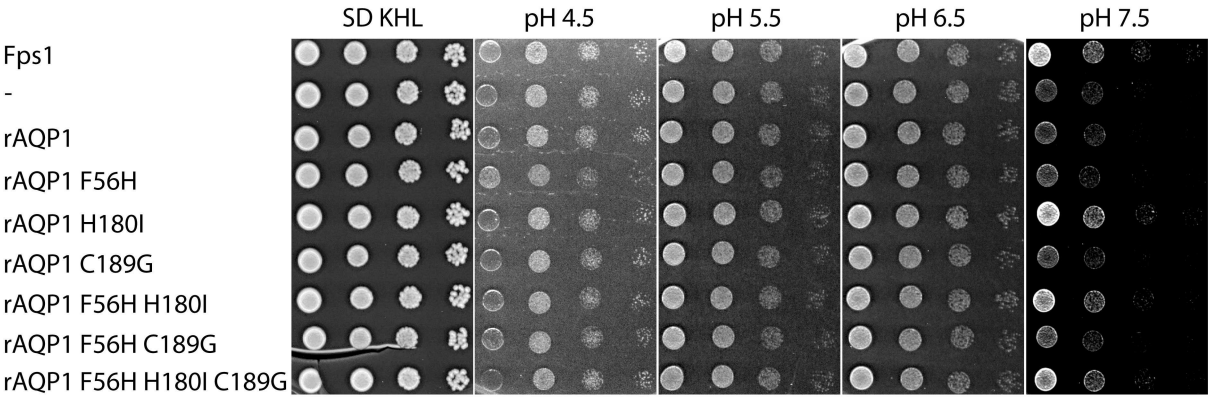

Fig. 4.2: Ammonia assay. *Yeast transformants (31019b Δfps1, pRS426 or pRS416 for Fps1) were spotted in tenfold dilution series starting with an OD_{600} of 1, and grown at 29 ℃ for 4 days. The ammonium concentration was 2 mM. Please note that the scanned image of the pH 7.5-plate is more contrast-adjusted than those of the other plates.*

Growth on the SDKHL plate was uniform, as was the case for the assay plates of pH 4.5, 5.5 and 6.5. A pattern did appear at pH 7.5, and it matched the one found with the methylamine assay (Fig. 4.1), with one exception: growth of yeast synthesizing the rAQP1 triple mutant F56H/H180I/C189G was also improved. This may be due to ammonia being a smaller molecule than methylamine. In any case, the ammonia assay seemed more informative than the methylamine assay, and it was used preferentially thereafter. As will be seen, the contrast in yeast transformant growth could be increased by adjusting the pH and the ammonium concentration.

Protein synthesis in the yeast strain 31019b Δfps1 was verified by Western blotting as shown in Figure 4.3.

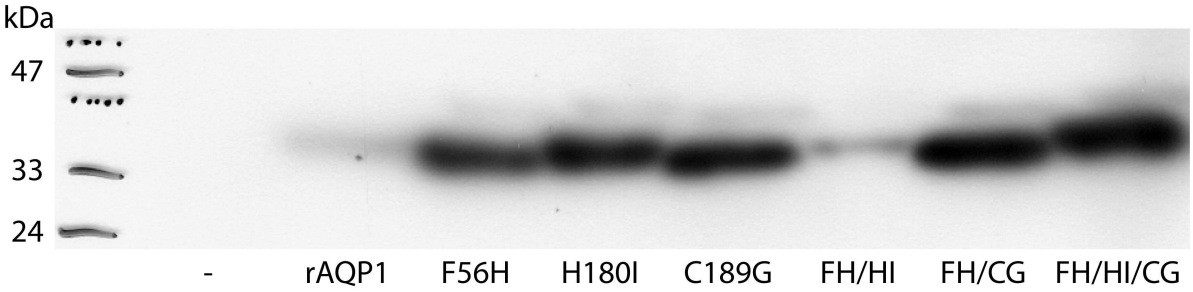

Fig. 4.3: Presence of rAQP1 and mutants of rAQP1 in the microsome fraction of the yeast strain 31019b Δfps1 (pRS426). *The equivalent of 4 - 6 µg BSA per sample was subjected to SDS-PAGE and Western blotting. Detection was with a rAQP1-directed antibody. The shadow-like traces above the thick bands are an artefact caused by moving the photographic film during exposure.*

Wild-type rAQP1 and its mutants were all expressed by this yeast strain. No band was visible for the non-aquaporin-producing yeast, as expected. Production of wild-type rAQP1 and of the mutant F56H/H180I may have been lower than that of the other mutants, but this may have also been due to sample preparation. The calculated molecular weight of rAQP1 is approximately 29 kDa, and so the bands' position above 35 kDa was surprising. It may have been due to an incorrect attribution of protein marker bands. Looking at the section shown in the figure, it is tempting to move the numbers up by one mark each, but the complete image (not shown) suggested that the given attribution is the most likely.

Osmotic assays

To find out whether the rAQP1 mutants conduct water, osmotic assays with yeast protoplasts and with *X. laevis* oocytes were performed.

For the yeast protoplasts this was done only once, with the strain 31019b Δfps1, using a stopped-flow apparatus (3.5). The results are shown in Figure 4.4.

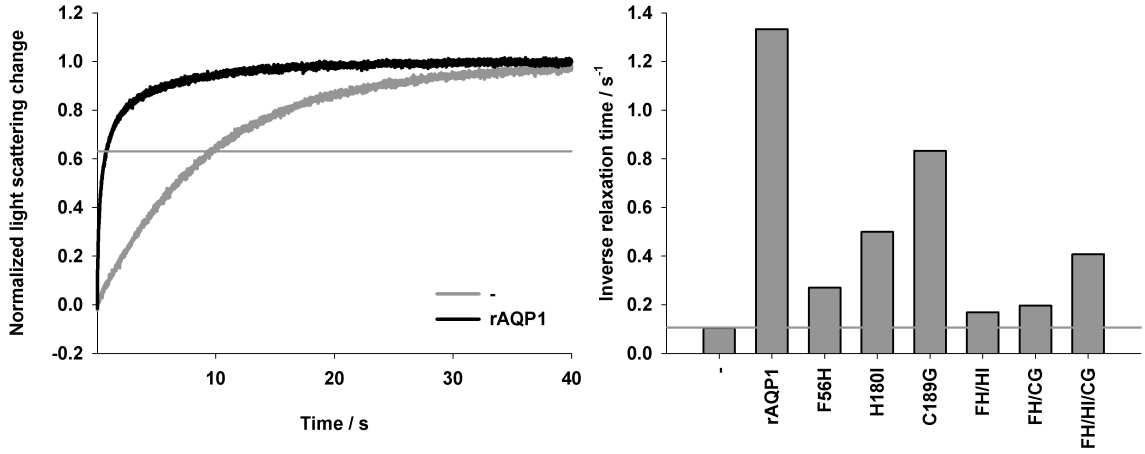

Fig. 4.4: Osmotic assay with yeast protoplasts (31019b Δfps1, pRS426) producing no AQP, wild-type rAQP1 or a mutant of rAQP1. *Inward-directed hypertonic sorbitol gradient 0.15 osmol/l (tonicity ~ 1.11), 20 ℃.* ***Left:*** *Examples of normalized average curves (n = 8 - 9). The horizontal line marks the ordinate value at which the nominal relaxation time was read (y = 1 - 1/e).* ***Right:*** *Inverse relaxation times. The horizontal line marks the control value (no AQP).*

Keeping in mind that whole-cell shrinkage rates do not necessarily reflect single-channel water permeabilities, several tentative observations may be made: C189G was the least disruptive mutation, F56H was the most disruptive one. Both double mutants barely increased the rate of protoplast shrinkage, whereas the triple mutant did so definitely.

The osmotic water permeability coefficient (P_f) of the aquaporin-deficient protoplasts was of the order of 1 µm/s, as will be shown in Section 4.3.2. The relative standard deviation of relaxation times determined from single curves for each sample is not shown, but was typically below 10 % (an example will be seen in Figure 4.27).

Please note that protoplasts producing rAQP1 or no aquaporin were neither prepared nor subjected to measurements on the same day as those producing the rAQP1 mutants. Also, measurements with the former were made one day after preparation, measurements with the latter three days after preparation. However, care was taken to prepare protoplasts in as uniform a manner as possible, and studies by a colleague have shown that time constants determined over the course of 7 days do not vary markedly (D. Wree, thesis 2010).

Two of the rAQP1 mutants were also expressed in *X. laevis* oocytes to study their water permeability in swelling assays. The results are shown in Figure 4.5.

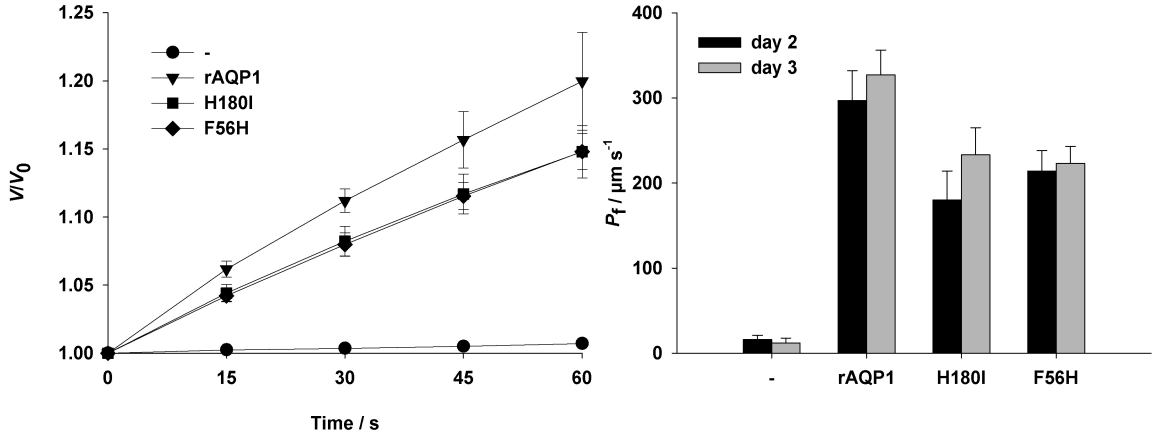

Fig. 4.5: Osmotic assays with X. laevis oocytes producing no AQP, wild-type rAQP1 or a mutant of rAQP1, performed 2 or 3 days after cRNA injection. *Outward-directed hypotonic NaCl gradient 0.14 osmol/l (tonicity 0.33), room temperature (~ 20 - 25 °C).* ***Left:*** *Averaged swelling curves, measured 3 days after cRNA injection. t = 0 s denotes the time at which the first image was taken, not the beginning of swelling.* ***Right:*** *Osmotic water permeability coefficients (P_f). Error bars show the standard deviations (n = 7 - 11, n = 4 for the H_2O-injected oocytes).*

Both rAQP1 F56H and H180I conducted water, with osmotic water permeability coefficients (P_f) of 220 µm/s ± 20 µm/s and 230 µm/s ± 32 µm/s, as compared to 330 µm/s ± 29 µm/s for wild-type rAQP1-producing oocytes and 12 µm/s ± 8 µm/s for water-injected oocytes, three days after injection. Unlike for the yeast protoplast assay (Fig. 4.4), neither mutation proved to be particularly disruptive.

Their synthesis was verified by Western blotting, as shown in Figure 4.6.

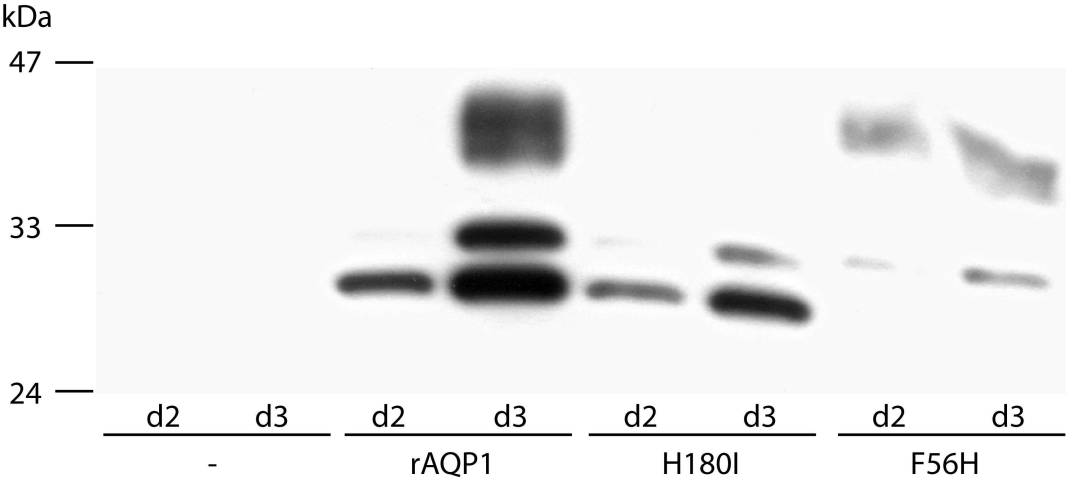

Fig. 4.6: Presence of rAQP1 and two mutants in the membrane fraction of X. laevis oocytes, 2 or 3 days ("d2" or "d3") after cRNA injection. *The equivalent of one oocyte each was subjected to SDS-PAGE and Western blotting. Detection was with a rAQP1-directed antibody.*

The lowest bands marked non-glycosylated proteins (~ 29 kDa). The middle and the top bands marked glycosylated proteins (~ 31 kDa and ~ 35 - 45 kDa) (Preston *et al*., 1992, 1994). Production seemed strongest for wild-type rAQP1, especially 3 days after cRNA injection when the high molecular weight band appeared. This may have been due to a

different concentration of the cRNA solution coding for rAQP1 (prepared by a colleague). The occurence of rAQP1 H180I resembled that of the wild-type protein, except for a lower level and the absence of a high molecular weight isoform. The synthesis of rAQP1 F56H was remarkable in that it showed no trace of non-glycosylated protein, as well as a pronounced share of the high molecular weight isoform both 2 and 3 days after cRNA injection.
The lower production of the mutant aquaporins may explain the lower osmotic water permeability coefficients. For a more accurate comparison, the plasma membrane localization would have to be quantified.

4.1.2 Mutating Cysteine 189 to alanine instead of glycine in rat Aquaporin 1

At the time of writing, nine amino acid sequences of human AQP8 (NCBI) show a glycine at the position corresponding to Cysteine 189 in rAQP1. However, AQP8 sequences from nine other animal species show an alanine at this position, one shows a serine, another one a threonine, none a glycine. Considering alanine rather than glycine as the "default" amino acid, this led to the subsequent generation of the corresponding C189A mutants. The opportunity was seized to also generate rAQP1 H180I/C189A-coding DNA.
Figure 4.7 shows the result of an ammonia assay intended to test these rAQP1 mutants.

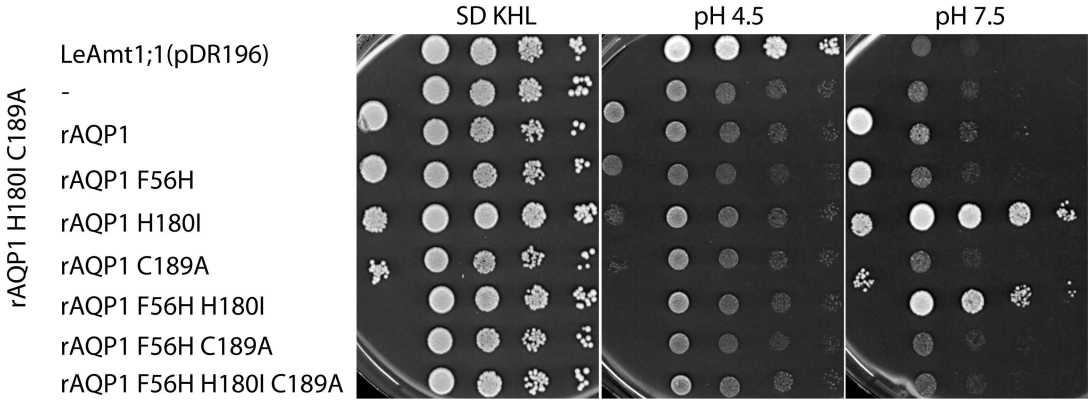

Fig. 4.7: Ammonia assay. *Yeast transformants (31019b Δfps1, pRS426) were spotted in tenfold dilution series starting with an OD_{600} of 1, and grown at 29 ℃ for 3 days. The ammonium concentration was 10 mM. Plates were scanned after 3 more days at 4 ℃. Please note that LeAmt1;1 was encoded by a different plasmid (pDR196).*

As expected, rAQP1 C189A and rAQP1 F56H/C189A did not improve growth at pH 7.5, whereas rAQP1 H180I/C189A did. On the other hand, rAQP1 F56H/H180I/C189A did not lead to any apparent improvement in growth, unlike its C189G-counterpart. This result was found consistently, an example being shown in Table 4.1. However, it must be kept in mind that the DNA encoding it has not been fully sequenced (3.2), and may thus contain an unwanted mutation nullifying the presumed ammonia permeability of the triple mutant.

Growth on SD KHL medium was not perfectly uniform, with rAQP1 H180I-producing yeast doing best, as on the assay medium at pH 7.5. This was also seen at pH 5.5 and 6.5 (not shown). Apart from a general improvement of growth, frequently seen during preparation of yeast protoplasts (3.7), another possible reason was a difference in the dilution of the yeast suspensions used for plating.
Yeast synthesizing the tomato ammonium transporter LeAmt1;1 were occasionally chosen as the positive control in assays covering the pH range from 4.5 to 7.5. For assays conducted solely at pH 7.5 or higher they were of no use, as can be seen in Figure 4.7.
The result of a single methylamine assay including yeast producing the rAQP1 C189A-mutants will be shown in Section 4.1.7. Osmotic assays were not performed. Protein production was not verified.

4.1.3 Mutating Histidine 180 in rat Aquaporin 1

So far, the results of ammonia and methylamine assays had shown the mutation of Histidine 180 to isoleucine in rAQP1 to be a prerequisite for improved yeast growth, and presumably of ammonia- and methylamine permeability. Earlier research had shown the mutation of Histidine 180 to alanine to have the same effect, and this was confirmed by electrophysiological measurements with *X. laevis* oocytes (Beitz *et al*., 2006).
It thus seemed natural to think of a series of mutations extending the length of the isoleucine residue and changing its polarity, and to test these mutations with regard to ammonia permeability. A table of the genetic code served as the initial guide, with the column BUB (base, uracil, base) hosting a nearly complete set of hydrophobic amino acids from valine to phenylalanine. Valine was considered superfluous since its residue's length lies between those of alanine and isoleucine. In addition, asparagine and glutamine were chosen as polar representatives. The asparagine residue is similar in size and shape to the leucine residue, and the glutamine residue is similar in length to the histidine residue.
DNA encoding these rAQP1 mutants as well as three F56H double mutants was prepared, and the proteins were expressed in yeast and in *X. laevis* oocytes for characterization of their ammonia and water permeabilities.

Growth assays

The first assay performed was an ammonia assay. It yielded the following result (Fig. 4.8):

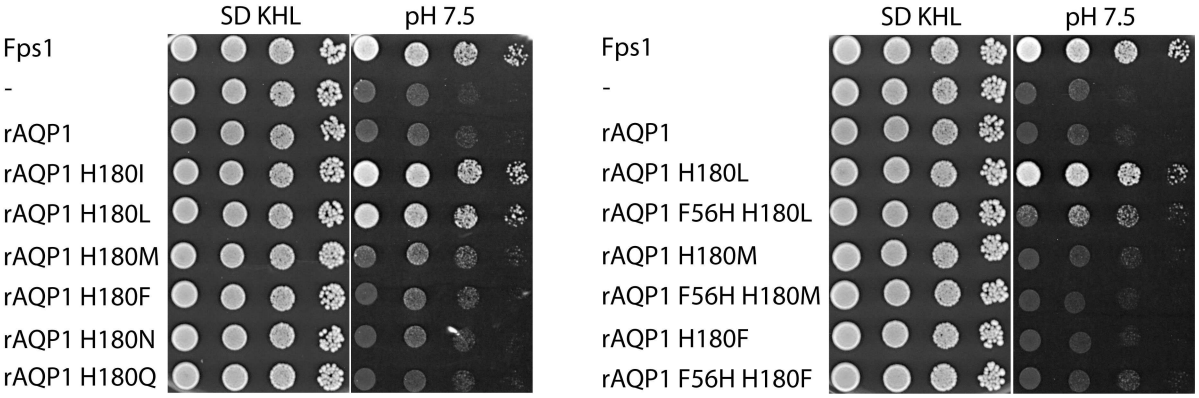

Fig. 4.8: Ammonia assays. *Yeast transformants (31019b Δfps1, pRS426 or pRS416 for Fps1) were spotted in tenfold dilution series starting with an OD_{600} of 1, and grown at 29 ℃ for 3 days. The ammonium concentration was 4 mM. Plates were scanned after 7 more days at 4 ℃. Plates for both assays belonged to the same lot s.*

Yeast producing rAQP1 H180I were included for comparison. Among the single mutants, only rAQP1 H180L led to improved growth on ammonia assay medium at pH 7.5. The double mutant rAQP1 F56H/H180L may have improved growth slightly, but this was not investigated further.

A methylamine assay gave the following result (Fig. 4.9).

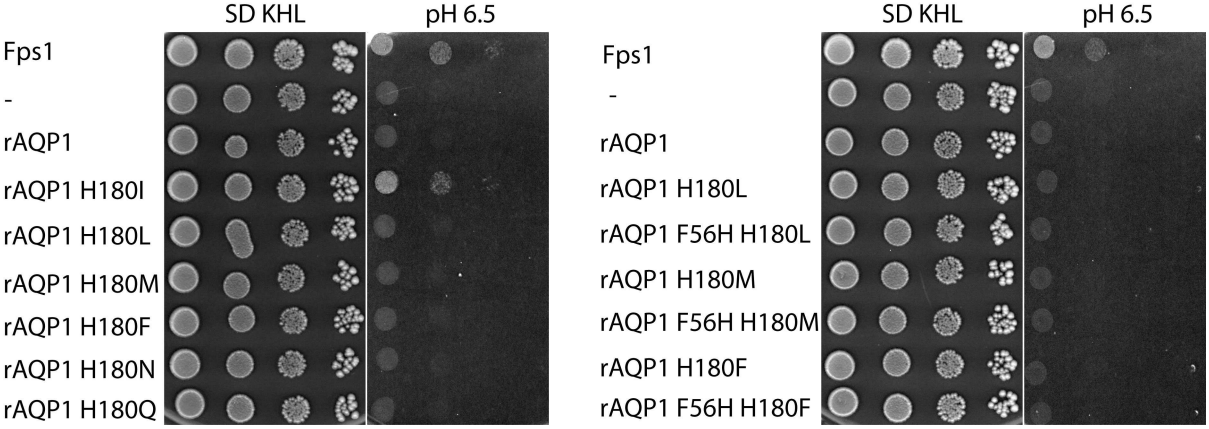

Fig. 4.9: Methylamine assays. *Yeast transformants (BY4742 Δfps1, pRS426 or pRS416 for Fps1) were spotted in tenfold dilution series starting with an OD_{600} of 1, and grown at 29 ℃ for 5 days followed by 2 days at room temperature. The methylammonium concentration was 50 mM. SD KHL plates belonged to the same lot, methylamine plates did not.*

For the single mutants, images of the pH 5.5 and the pH 7.5 plates are unavailable, that is why the pH 6.5 plate is shown. For the double mutants, the pattern at pH 5.5 looked the same as at pH 6.5. At pH 7.5 growth was nearly absent. Compared to the corresponding ammonia assays' results (Fig. 4.8), the major difference was the lack of growth of the rAQP1 H180L-producing yeast.

Protein synthesis in the yeast strain 31019b Δfps1 was verified for the single mutants as shown in Figure 4.10.

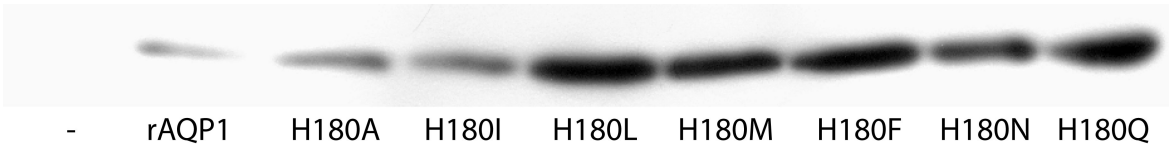

Fig. 4.10: Presence of rAQP1 as well as mutants of rAQP1 in the microsome fraction of the yeast strain 31019b Δfps1 (pRS426). *The equivalent of 2 - 3 µg BSA per sample was subjected to SDS-PAGE and Western blotting. Detection was with a rAQP1-directed antibody. Protein marker bands were too poorly visible in this experiment.*

Please note that the preparations of yeast producing no AQP, rAQP1 and rAQP1 H180I were not the same as those shown in Figure 4.3. This means that for two independent preparations, the production of wild-type rAQP1 appeared lower than for the mutants.
The results of ammonia and methylamine assays including rAQP1 H180A-producing yeast will be shown in Section 4.1.7.

Osmotic assays

The results of a single osmotic assay with yeast protoplasts are shown in Figure 4.11.

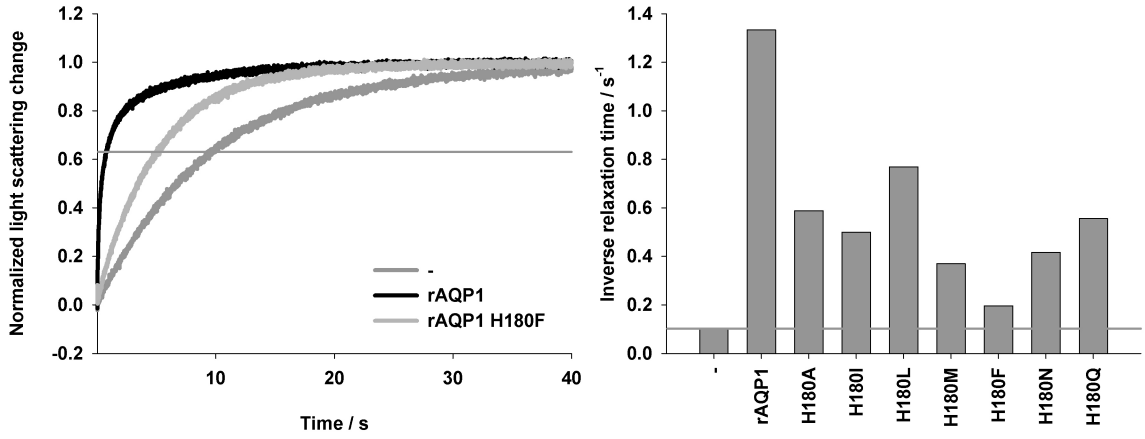

Fig. 4.11: Osmotic assay with yeast protoplasts (31019b Δfps1, pRS426) producing no AQP, wild-type rAQP1 or a mutant of rAQP1. *Inward-directed hypertonic sorbitol gradient 0.15 osmol/l (tonicity ~ 1.11), 20 ℃.* ***Left:*** *Examples of normalized average curves (n = 8 - 9). The horizontal line marks the ordinate value at which the nominal relaxation time was read (y = 1 - 1/e).* ***Right:*** *Inverse relaxation times. The horizontal line marks the control value (no AQP). Data for no AQP, rAQP1 and rAQP1 H180I are the same as in Fig. 4.4.*

All rAQP1 mutants seemed to conduct water, even rAQP1 H180F. Again, keeping in mind the single determination and the differing whole-cell production levels (Fig. 4.10), one may notice a trend towards lower water permeability with increasing pore obstruction by the hydrophobic amino acid residues. Presence of rAQP1 H180N and H180Q increased water-permeability to an extent comparable with that caused by rAQP1 H180I.
For aquaporin-deficient and rAQP1 H180Q-producing yeast protoplasts, measurements were performed at two or three different temperatures, in order to estimate Arrhenius activation energies. The values obtained were approximately 12 kcal/mol ($\tau_{12\,℃}$ = 14.8 s, $\tau_{20\,℃}$ = 8.2 s) and 7 kcal/mol ($\tau_{12\,℃}$ = 2.5 s, $\tau_{16\,℃}$ = 2.3 s, $\tau_{20\,℃}$ = 1.8 s), respectively. They are comparable

to activation energies determined for aquaporin-deficient and ScAQY1-overproducing *S. cerevisiae* cells (not protoplasts) subjected to similar conditions (Soveral *et al.,* 2008).

Water permeation through rAQP1 is inhibited by mercuric chloride which probably binds to the thiol moiety of Cysteine 189 and blocks the ar/R-constriction, as in human AQP1 (Preston *et al.*, 1993). Mercuric chloride can thus be used to probe the constriction region of rAQP1 mutants. This was done for three of the generated rAQP1 mutants, as shown in Figure 4.12.

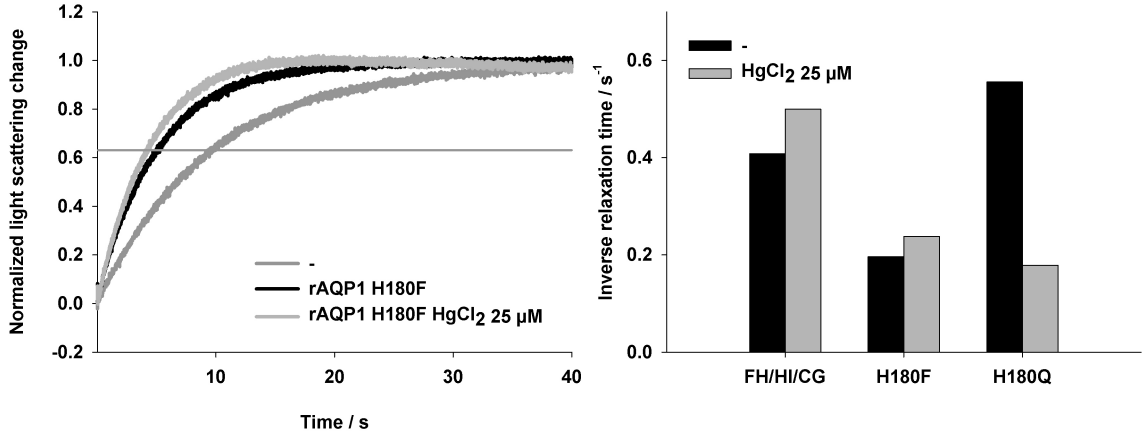

Fig. 4.12: Osmotic assays with yeast protoplasts (31019b Δfps1, pRS426) producing a mutant of rAQP1. *Inward-directed hypertonic sorbitol gradient 0.15 osmol/l (tonicity ~ 1.11), 20 ℃. Incubation with 25 µM mercuric chloride 15 - 20 min prior to measurements.* ***Left:*** *Examples of normalized average curves (n = 7 - 8). The horizontal line marks the ordinate value at which the nominal relaxation time was read (y = 1 - 1/e). The control curves (no AQP and rAQP1 H180F) are identical to those shown in Fig. 4.11.* ***Right:*** *Inverse relaxation times. Measurements for rAQP1 F56H/H180I/C189G were made on two consecutive days.*

Mercuric chloride inhibited rAQP1 H180Q, but not rAQP1 F56H/H180I/C189G which lacks the reactive cysteine residue. rAQP1 H180F was seemingly unaffected, although the shape of the corresponding light scattering curve was unusual in having a maximum. The effect of mercuric chloride on the osmotic shrinkage of aquaporin-deficient yeast protoplasts was not tested. Please note that 25 µM is a rather low concentration of mercuric chloride, with 300 µM common for aquaporin-inhibition studies found in the literature. Inhibition was thus unlikely to be complete (Preston *et al*., 1992).

The water permeabilities of rAQP1 H180F and H180N were also tested with *X. laevis* oocytes, as shown in Figure 4.13.

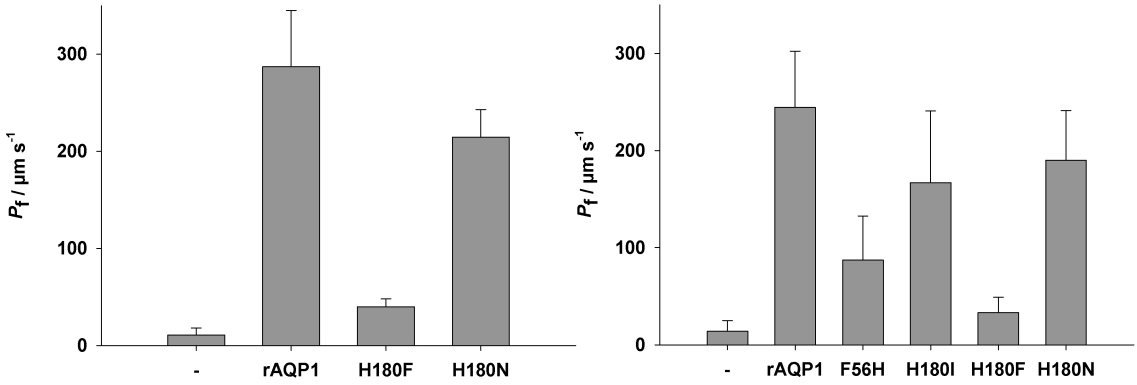

Fig. 4.13: Osmotic assays with X. laevis oocytes producing no AQP, wild-type or mutant rAQP1, 3 days after cRNA injection. *Outward-directed hypotonic NaCl gradient 0.14 osmol/l (tonicity 0.33), room temperature (20 - 25 °C). Osmotic water permeability coefficien ts (P_f) from two experiments. Error bars represent the standard deviations.* ***Left:*** *Experiment one (n = 8 - 13). Total cRNA injected: 5 ng (rAQP1) or 2.5 ng (rAQP1 mutants).* ***Right:*** *Experiment three (n = 12 - 21). Total cRNA injected: ~ 1.3 ng (rAQP1) or 2.5 ng (rAQP1 mutants). The quality of the oocytes may have been somewhat poor in this experiment.*

Synthesis of rAQP1 H180F or H180N increased water permeability of the *X. laevis* oocytes, with osmotic water permeability coefficients of approximately 40 µm/s ± 8 µm/s and 214 µm/s ± 28 µm/s versus 11 µm/s ± 7 µm/s for uninjected oocytes. In a second experiment, which included oocytes producing rAQP1 F56H and H180I for comparison (Fig. 4.13, right), the corresponding P_f values were approximately 33 µm/s ± 16 µm/s and 190 µm/s ± 52 µm/s versus 14 µm/s ± 11 µm/s.

Please note that the cRNA encoding rAQP1 H180F and rAQP1 H180N was not pure (Fig. 4.14 A). Two bands were visible on an RNA gel, one of the expected size of about 1100 nucleotides, the other too small at about 700 nucleotides. The aquaporin-encoding portion is 810 nucleotides in length, the 5' and 3' regulatory and stabilizing regions make up the remaining share of approximately 300 nucleotides, so a possible translation of the 700-nucleotide-cRNA is unlikely to have led to a functional channel. Its share of the total cRNA content was estimated as half. A low yield of the rAQP1 H180N-encoding cRNA required its dilution to a total concentration of about 50 ng/µl, *i. e.* half the usual concentration of 100 ng/µl, and about a quarter with regard to the functional 1100-nucleotide-cRNA (~ 25 ng/µl). For comparability, the rAQP1 H180F-encoding cRNA was diluted to the same final concentration. Western blotting confirmed the synthesis of rAQP1 H180F and rAQP1 H180N (Fig. 4.14 B).

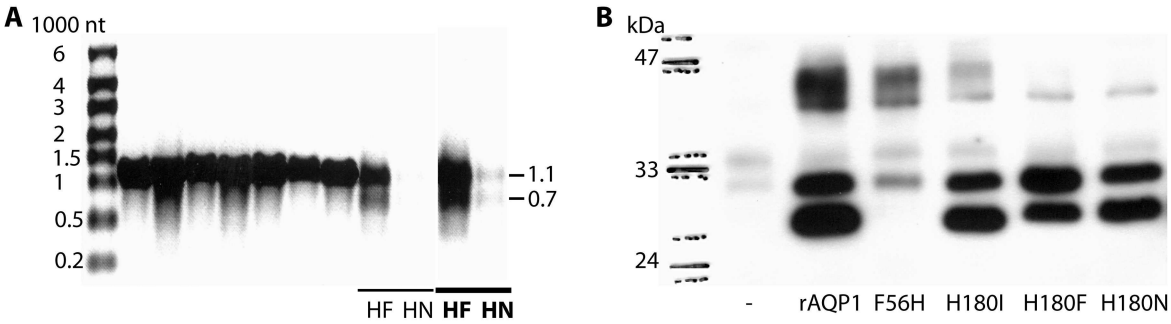

Fig. 4.14: (A) *RNA gel. HX stands for rAQP1 H180X-encoding cRNA. The two rightmost lanes were recorded at longer illumination. Unlabelled lanes contained unrelated samples.* ***(B)*** *Presence of rAQP1 and four mutants in the membrane fraction of X. laevis oocytes 3 days after cRNA injection, from the experiment shown on the right in Fig. 4.13. The equivalent of one oocyte each was subjected to SDS-PAGE and Western blotting. Detection was with a rAQP1-directed antibody. Illumination of the photographic film (32 min) was about ten times the usual duration.*

The Western blot band patterns of wild-type rAQP1 and of its Histidine 180-mutants resembled each other, although there was a marked shift in relative intensity for the H180F mutant, indicating increased glycosylation (Preston *et al*., 1994). The band pattern of rAQP1 F56H was characteristically different, as seen before (Fig. 4.6).The high molecular weight band appeared to consist of two bands of about 39 and 42 kDa. In the control lane two weak bands appeared. They were visible in all other lanes and may be considered unspecific, although one of them overlapped with the glycosylated-AQP-band at about 30 kDa.
The dependence of osmotic water permeability of oocytes on the amount of injected cRNA was tested, and the results are shown in Section 4.3.1.

4.1.4 Mutating the constriction histidine to alanine in other aquaporins

Exchanging Histidine 180 of rAQP1 for an amino acid with a shorter residue such as leucine, isoleucine or alanine, increased this aquaporin's presumed ammonia permeability. A welcome opportunity to test the general validity of this observation presented itself when a colleague generated the corresponding mutations of histidine to alanine in N-terminally HA-tagged human Aquaporins 1, 2, 4, and 5 (hAQPx-HA). It turned out that only hAQP1-HA H180A improved growth of yeast on methylamine-containing medium, but the effect was rather small (H. Long, diploma thesis 2009). Two ammonia assays showed no such effect, an example is given in Figure 4.15.

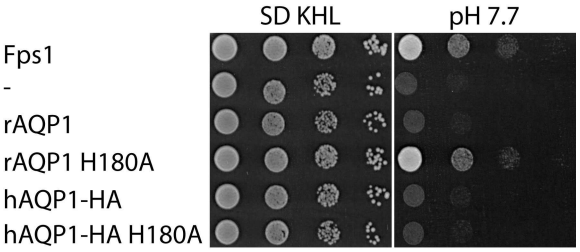

Fig. 4.15: Ammonia assay. *Yeast transformants (31019b Δfps1, pRS426 or pRS416 for Fps1) were spotted in tenfold dilution series starting with an OD_{600} of 1, and grown at 29 ℃ for 3 days. The ammonium concentration was 10 mM, the MOPS concentration was 40 mM.*

Protein synthesis in the yeast strain BY4742 Δfps1 was verified for both hAQP1-HA and hAQP1-HA H180A, but the results were not entirely clear for human Aquaporins 2, 4 and 5 (H. Long, diploma thesis 2009). Nevertheless, yeast protoplasts (31019b Δfps1) transformed with the plasmids coding for each of these aquaporins, were subjected to an osmotic assay. Only hAQP1-HA-producing yeast showed a definite increase in water permeability. For this reason, only hAQP1-HA- and hAQP1-HA H180A-producing yeast were subjected to an osmotic assay in which formamide served to generate the gradient. The corresponding experiment with rAQP1- and rAQP1 H180A-producing yeast was done independently and serves here as a comparison (Fig. 4.16).

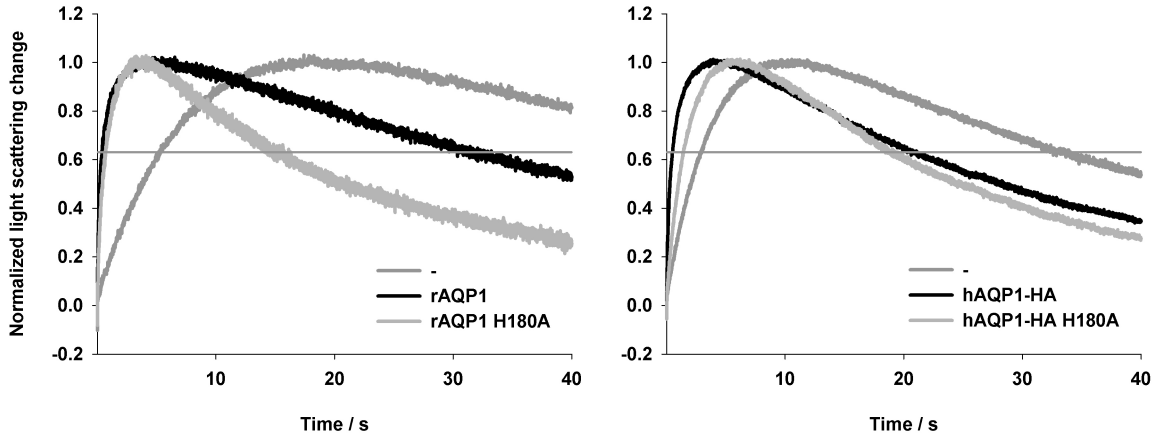

Fig. 4.16: Osmotic assays with yeast protoplasts (31019b Δfps1, pRS426) producing wild-type and mutant rAQP1 or hAQP1-HA. *Normalized average curves.* ***Left:*** *rAQP1. Inward-directed hypertonic formamide gradient 0.15 osmol/l, MOPS/NaOH 10 mM, pH 7.2, 20 ℃ (n = 6 - 9).* ***Right:*** *hAQP1-HA. Inward-directed hypertonic formamide gradient 0.30 osmol/l, Tris/HCl 10 mM, pH ~ 7, 21 ℃ (n = 7 - 8).*

Initial shrinking of the yeast was followed by their reswelling due to an influx of formamide and water. This gave rise to the characteristically shaped light scattering curves. The higher signal-to-noise ratio in the left graph was due to a lower osmotic gradient and a lower lamp power setting. Aquaporin-deficient yeast had high basal formamide permeability. Synthesis of rat or human AQP1 and their mutants increased the shrinkage rate, indicating water permeability. The reswelling rate appeared somewhat increased for the mutant-producing yeast, clearly for rAQP1 H180A, barely for hAQP1-HA H180A. Time constants for the swelling phase were determined by single-exponential curve fitting and found to be

approximately 0.012 s^{-1}, 0.019 s^{-1}, 0.032 s^{-1} (no AQP, rAQP1, rAQP1 H180A) and 0.031 s^{-1}, 0.033 s^{-1}, 0.041 s^{-1} (no AQP, hAQP1-HA, hAQP1-HA H180A), by a method described in Section 4.3.2 (only data following twice the estimated inflection time was used). It must be mentioned that most other rAQP1 mutants investigated in previous sections led to such an apparent increase in the swelling rate when compared to wild-type rAQP1.

The striking difference in shrinking and swelling rates between control yeast in both experiments was possibly due to the experiments being performed ten months apart, to the use of yeast glycerol stocks for inoculation, to an inherent variability of time constants obtained with protoplasts of the yeast strain 31019b Δfps1, or otherwise.

Despite the limited use of such formamide gradient assays, they have shown in this case that hAQP1-HA H180A is functional in the yeast strain used for the ammonia assay, and that it may confer somewhat different permeability properties than wild-type hAQP1-HA, even though this was not apparent in ammonia assays (Fig. 4.15).

4.1.5 Mutating the constriction region in rat Aquaporin 8

A counterpart to the rAQP1-constriction experiments was the mutagenesis of corresponding amino acids in rAQP8. In particular, the aromatic and basic histidine, as well as the isoleucine opposite to the conserved arginine, was of interest.

The available cDNA coded for rAQP8 ΔQ5 S31P, as compared to two *Rattus norvegicus* AQP8 amino acid sequences found at the time of writing (NCBI). A third *R. norvegicus* reference sequence lacked the glutamine (Q5), as did nine *Homo sapiens* AQP8 reference sequences. Serine instead of proline was found in all rat and human AQP8 sequences available at the time. Among AQP8 sequences of nine other animal species, a proline at the corresponding position was found in *Danio rerio* AQP8. Both potential mutations were located in the N-terminal sequence preceeding the first transmembrane helix, as determined by comparison with the amino acid sequence of *Bos taurus* AQP1, the crystal structure of which is known (Sui *et. al.*, 2001). Incidentally, both serine and proline tend to be situated at the N-terminal end of alpha-helices (Richardson and Richardson, 1988). Since the N-terminal amino acids in AQP8 are poorly conserved, the two mutations were unlikely to be of importance. Nevertheless, they will be indicated by an asterisk (rAQP8*) here.

For functional characterization, ammonia assays and osmotic assays were performed. The result of the first ammonia assay is shown in Figure 4.17.

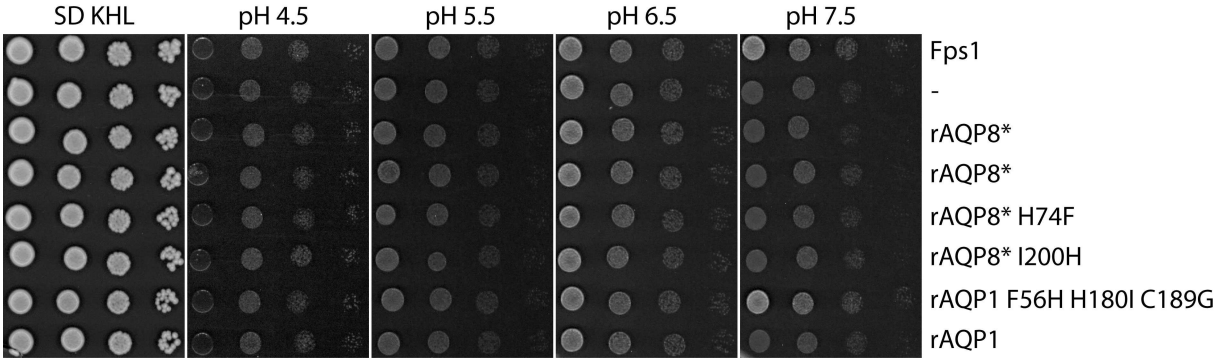

Fig. 4.17: Ammonia assay. *Yeast transformants (31019b Δfps1, pRS426 or pRS416 for Fps1) were spotted in tenfold dilution series starting with an OD_{600} of 1, and grown at 29 ℃ for 4 days. The ammonium concentration was 2 mM. rAQP8* stands for rAQP8 ΔQ5 S31P. rAQP8*-producing yeast from two different transformations were included. The assay was performed on the same day and with the same lot of plates as the one shown in Fig. 4.2.*

None of the rAQP8* wild-type or mutant-synthesizing yeast grew better than the AQP-deficient control, irrespective of the pH. The experiment was repeated once, with the same result. For lack of a specific antibody, synthesis was not verified.

Osmotic assays with yeast protoplasts gave the following results (Fig. 4.18).

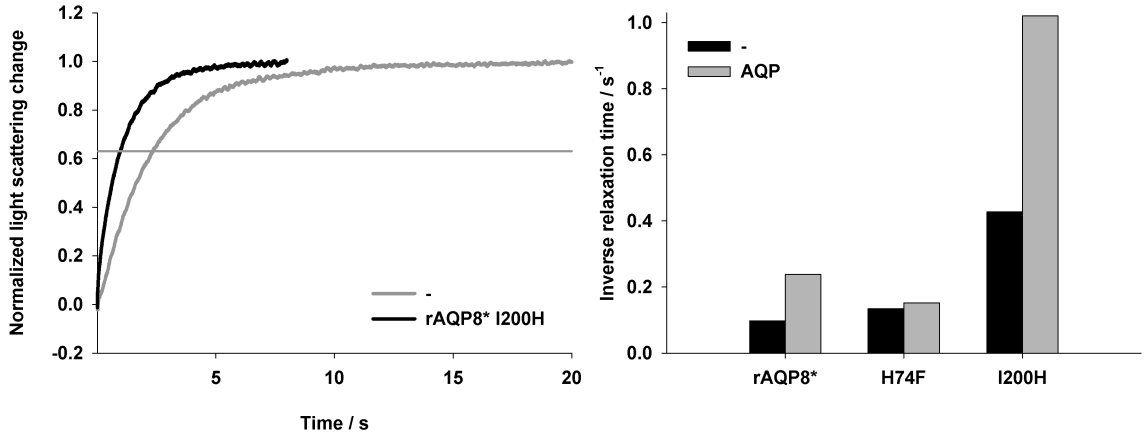

Fig. 4.18: Osmotic assays with yeast protoplasts (31019b Δfps1, pRS426) producing no AQP or a mutant of rAQP8. *rAQP8* stands for rAQP8 ΔQ5 S31P. Inward-directed hypertonic sorbitol gradient 0.3 osmol/l or 0.15 osmol/l (rAQP8* H74F), 20 ℃ or 4 ℃ (rAQP8*), Tri s/HCl 10 mM pH ~ 7 or MOPS/NaOH 10 mM pH 7.2 (rAQP8* H74F).* ***Left:*** *Examples of normalized average curves (n = 6 - 7). The horizontal line marks the ordinate value at which the nominal relaxation time was read (y = 1 - 1/e).* ***Right:*** *Inverse relaxation times (n = 6 - 9). Experiments were performed on different days over the course of two years.*

rAQP8*- and rAQP8* I200H-synthesis improved water permeability, although the effect was small. rAQP8* H74F was not expressed, not located at the plasma membrane, not functional, or otherwise. Please note that the measurements were performed at different times, temperatures and osmotic gradients. The differing basal water permeability (no aquaporin) was in one case (rAQP8*) due to a lower temperature, and in another case (H74F) possibly due to a selection process brought about by the repeated thawing and freezing of yeast transformant glycerol stocks as discussed in Section 5.1.

Water permeability of rAQP8* I200H was also determined in a *X. laevis* oocyte swelling assay, as shown in Figure 4.19.

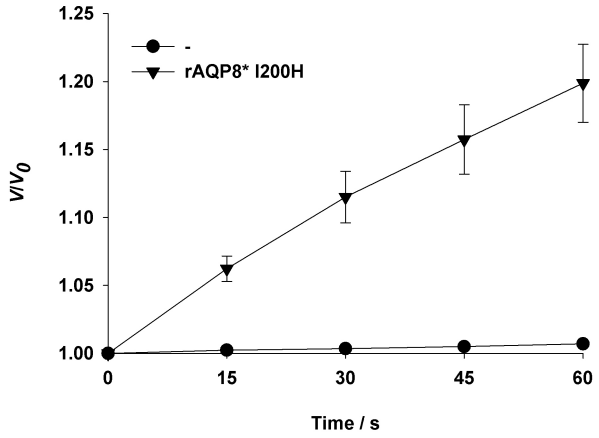

Fig. 4.19: Osmotic assay with X. laevis oocytes producing no AQP or the rAQP8 mutant I200H, performed 3 days after cRNA injection. *rAQP8* stands for rAQP8 ΔQ5 S31P. Outward-directed hypotonic NaCl gradient 0.14 osmol/l (tonicity 0.33), room temperature (~ 20 - 25 °C). Averaged swelling curves, error bars show the standard deviations (n = 4 for the H_2O-injected oocytes, n = 8 for the AQP-producing oocytes). t = 0 s denotes the time at which the first image was taken, not the beginning of swelling. The experiment was performed on the same day as the one shown in Fig. 4.5.*

rAQP8* I200H conducted water. The osmotic water permeability coefficient in this single experiment was found to be 329 µm/s ± 46 µm/s, nearly identical to that found for rAQP1-producing oocytes (Fig. 4.5, the experiments were conducted on the same day). Protein synthesis was not verified.

4.1.6 Mutating the constriction region in human Aquaporin 8

The complete lack of an effect of rAQP8 ΔQ5 S31P-synthesis in yeast on growth under ammonia assay conditions came as a surprise. Rather than repeating the experiment more carefully, the immediate reaction was to ask for cDNA encoding human AQP8 (2.5) and to generate the corresponding mutants, because the experiments of Jahn *et al.* (2004) had been performed with wild-type hAQP8. For detectability of the protein, the cDNA was inserted into a HA-tag-coding plasmid (see 9.2 for the HA-tag sequence). In addition to the mutants hAQP8-HA H72F and I198H, an attempt was made at generating the mutants C53A/S, F145A, and C208A/S. The three amino acid residues are probably located near the arginine residue of the constriction region, and may thus interact with it. They are conserved in AQP8-sequences from ten other animal species, with the exception of Cysteine 149, instead of phenylalanine, in *X. laevis* AQP8. The underlying assumption was that ammonium ions may be repelled by the positively charged arginine residue, and that this may be prevented by cysteine-catalyzed deimination to an uncharged citrulline residue, as found for L-arginine

deiminase (Li *et al.*, 2008). Phenylalanine 145 could conceivably stabilize the presence of an ammonium ion through a cation-π-interaction. However improbable, it was given a try, and the mutants hAQP8-HA C53A/S and F145A were successfully generated. hAQP8-HA H72F was not obtained in three attempts using the same set of primers (2.6).

Only hAQP8, hAQP8-HA, hAQP8-HA C53S, F145A and I198H were tested in yeast. The results of two ammonia assays are shown in Figure 4.20.

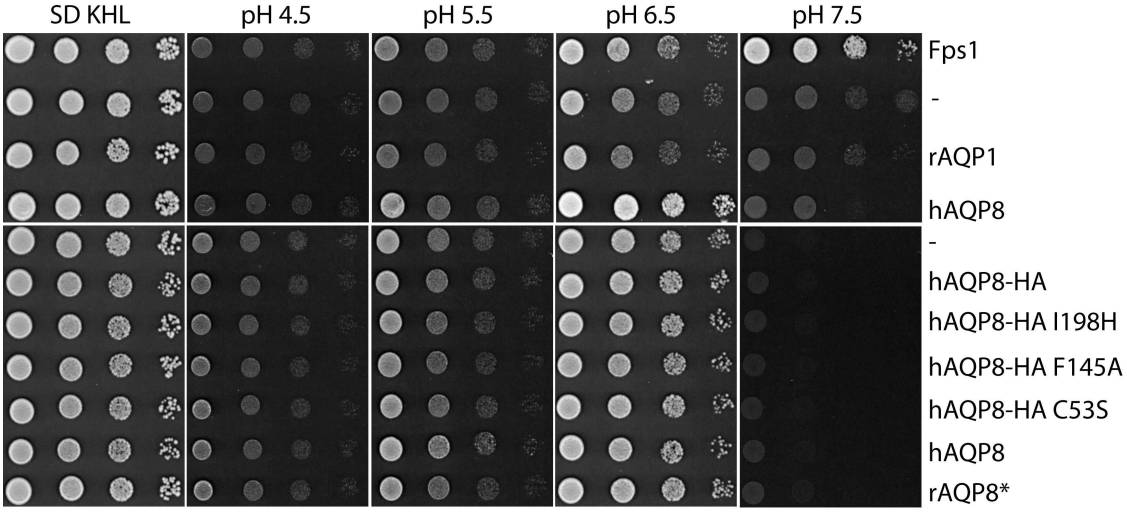

Fig. 4.20: Ammonia assays. *Yeast transformants (31019b Δfps1, pRS426 or pRS416 for Fps1) were spotted in tenfold dilution series starting with an OD_{600} of 1. Top row: 29 ℃ for 2 days, 4 ℃ for 12 days. The ammonium concentration was 4 mM, the buffer concentration was 20 mM. Bottom row: 29 ℃ for 3 days. The ammonium concentration was 4 mM, the buffer concentration was 40 mM. rAQP8* stands for rAQP8 ΔQ5 S31P.*

Untagged hAQP8 may have led to improved growth at pH 6.5 and pH 5.5, but this effect was seen only once. As with rAQP8* and mutants, hAQP8-HA and mutants did not appear to improve growth of yeast transformants under ammonia assay conditions. Please note that the buffer concentration was increased from 20 mM to 40 mM during the period those two experiments were performed. For a buffer concentration of 40 mM the pH range between 6.5 and 7.5 seemed interesting, and so a set of ammonia assay plates covering it was prepared and the assay repeated, with the following result (Fig. 4.21).

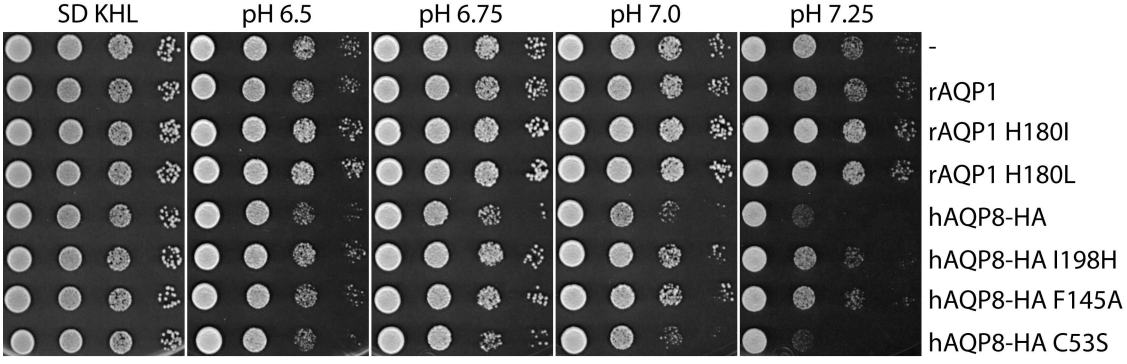

Fig. 4.21: Ammonia assay. *Yeast transformants (31019b Δfps1, pRS426) were spotted in tenfold dilution series starting with an OD_{600} of 1, and grown at 29 ℃ for 3 days. The ammonium concentration was 4 mM, the buffer concentration was 40 mM (MES for pH 6.5, MOPS for the other three).*

hAQP8-HA synthesis led to decreased growth as compared to the absence of an aqua-porin, most clearly visible at a nominal pH of 7.25. The same effect was seen for the mutant hAQP8-HA C53S. For F145A and I198H it was less pronounced. As this may have been due to a reduced synthesis of the latter two proteins, SDS PAGE and immunoblotting were performed, with the result shown in Figure 4.22.

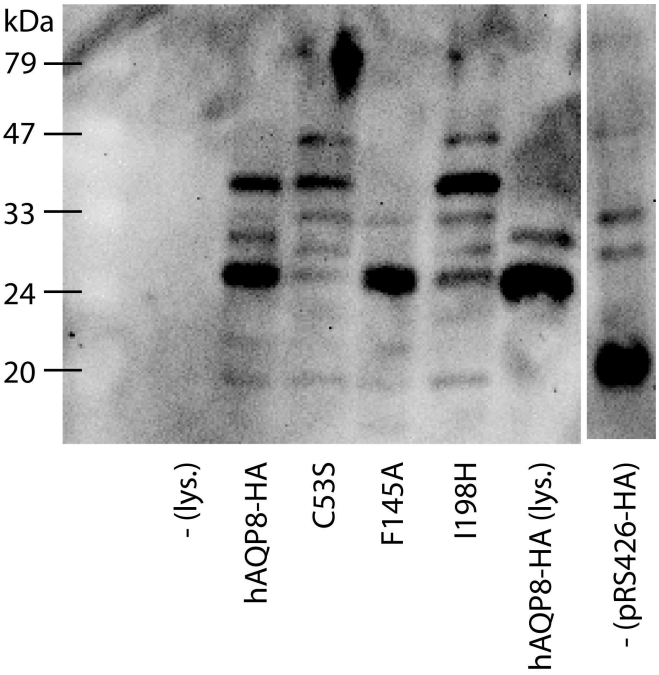

Fig. 4.22: Presence of hAQP8-HA and mutants of it in the microsome fraction of the yeast strain 31019b Δfps1 (pRS426). *The equivalent of 10 µg BSA per sample was subjected to SDS-PAGE and Western blotting. Detection was with a HA-tag-directed antibody. "lys." stands for "lysed protoplasts". The rightmost lane belonged to a second gel processed simultaneously.*

Despite the poor quality of the preparation, synthesis of hAQP8-HA and its mutant F145A could be confirmed, with a major band of approximately 26 kDa detected, close to the expected molecular weight of 29 kDa. The mutants hAQP8-HA C53S and I198H were probably expressed, with weak but specific bands of about 26 kDa as well. A second major band of about 35 kDa was found for all but hAQP8-HA F145A. Wild-type hAQP8-HA gave a third specific signal of about 29 kDa. Lysed yeast protoplasts were prepared as described (3.3.1, "simplified procedure").

It thus seems that hAQP8-HA C53S has retained the properties of wild-type hAQP8-HA, whereas mutating Phe 145 to alanine has caused some loss of function. hAQP8-HA I198H has probably lost some permeability characteristic as well. A single osmotic assay with yeast protoplasts confirmed these observations (Fig. 4.23).

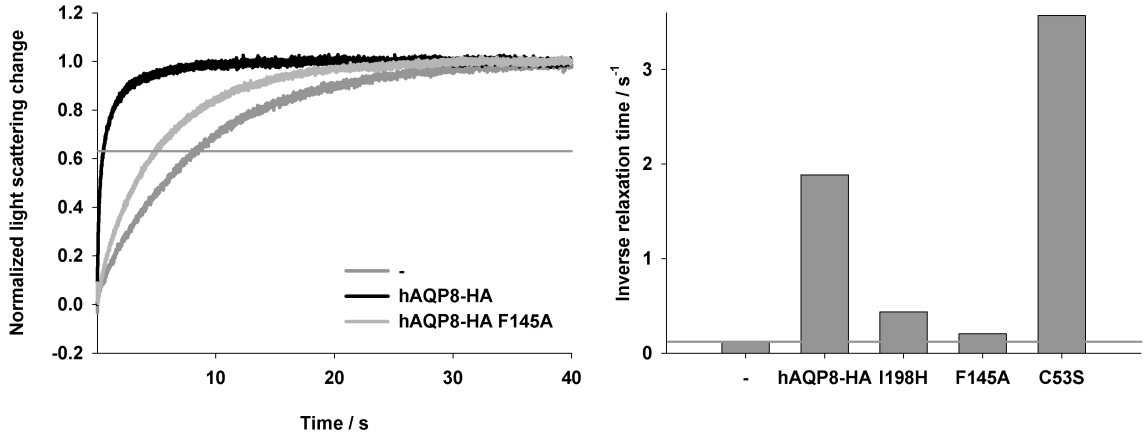

Fig. 4.23: Osmotic assay with yeast protoplasts (31019b Δfps1, pRS426) producing no AQP, wild-type hAQP8-HA or a mutant of hAQP8-HA. *Inward-directed hypertonic sorbitol gradient 0.15 osmol/l (tonicity ~ 1.11), 20 ℃.* ***Left:*** *Examples of normalized average curves (n = 6 - 9). The horizontal line marks the ordinate value at which the nominal relaxation time was read (y = 1 - 1/e).* ***Right:*** *Inverse relaxation times. The horizontal line marks the control value (no AQP).*

Presence of hAQP8-HA increased the yeast protoplast shrinkage rate more than tenfold. The mutation C53S did not diminish water permeability, while I198H and F145A probably led to a decrease in water permeability. The result for hAQP8-HA F145A would have to be confirmed.

A possible effect of the N-terminal HA-tag on the water permeability of hAQP8 was investigated in one other experiment with yeast protoplasts. It was found that both tagged and untagged hAQP8 conduct water, leading to comparable yeast protoplast shrinkage rates ($\tau_{hAQP8} \approx 0.08$ s, $\tau_{hAQP8\text{-}HA} \approx 0.20$ s, both at 4 ℃, the former being the lowest seen over the course of two and a half years of measurements).

4.1.7 Liquid medium ammonia and methylamine assays

So far, ammonia and methylamine assays had been used on limited sets of aquaporin mutant-producing yeast. Although most results were obtained repeatedly, it seemed a good idea to test the whole range of aquaporin mutants simultaneously. The focus was on the rAQP1-mutants. Two ammonia assays and one methylamine assay were performed, both in liquid and on solid medium. Sample growth curves recorded with the “Bioscreen microbiology reader” are shown in Figure 4.24.

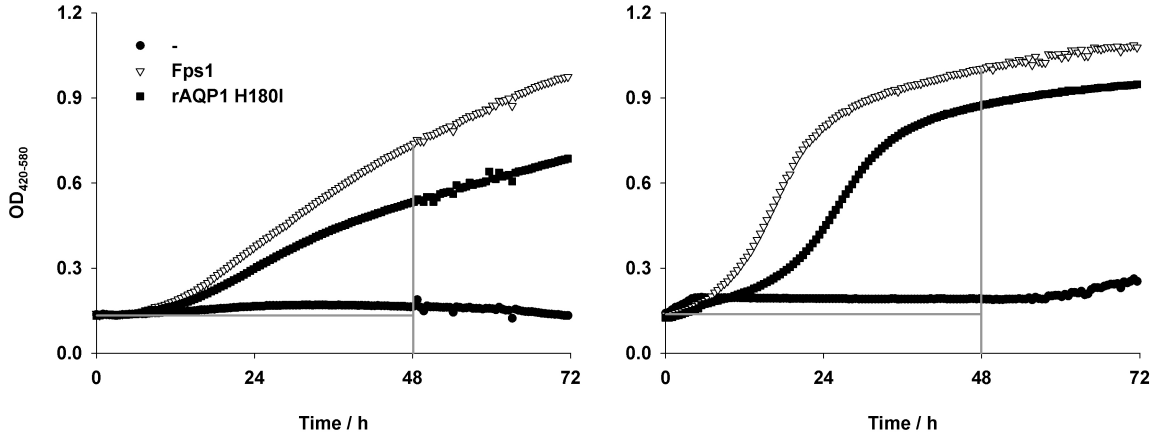

Fig. 4.24: Yeast transformant growth in liquid media at 29 °C, detected turbidimetrically (OD $_{420-580}$). Left: *Ammonia assay (31019b Δfps1, pRS426, pRS416 Fps1). Ammonium 40 mM, MOPS 40 mM, pH 6.9.* ***Right:*** *Methylamine assay (BY4742 Δfps1, pRS426, pRS416 for Fps1). Methylammonium 10 mM, MES 20 mM, pH 5.5. The horizontal and vertical lines mark the boundaries used to calculate the areas under the curves. The choice of 48 h is unrelated to the occurrence of OD measurement fluctuations in those two experiments.*

The areas under the growth curves up to 48 hours (AUC 48 h) were chosen to score yeast growth, and the values obtained are shown in Table. 4.1.

L-glutamine was chosen as an aquaporin-independent nitrogen source for the ammonia assay, and the absence of methylammmonium served as the control in the methylamine assay. Five additional rAQP1-mutants were tested: H180A, R195V/S and the corresponding H180A double mutants, investigated previously by colleagues (Beitz *et al.* 2006, Li *et al.* 2011). N-terminally HA-tagged human AQP9 was included as a heterologous aquaglyceroporin with low selectivity (Tsukaguchi *et al.* 1999). hAQP8-HA was the only representative of the AQP8-family. The results described in previous sections were essentially confirmed. Presence of rAQP1 R195V/S led to slightly improved growth, as seen in other experiments not shown. hAQP8-HA-production proved to be deleterious rather than growth-enhancing, as seen also in Figure 4.21.

Table 4.1: Ammonia and methylamine assays in liquid medium using the "Bioscreen" turbidometer. *Conditions as described in Fig. 4.24. AUC 48 h averages derived from turbidity measurements (n = 3 - 4). Relative standard deviations were mostly below 10 %, except for yeast transformants growing poorly. Mutations refer to rAQP1. Media were prepared no more than 3 days before each assay. Ammonia assays (Experiments 1a and b): "Gln" stands for medium containing L-glutamine instead of ammonium ions. Yeast used in Experiment 1a were from a single transformation, those used in Experiment 1b were grown from glycerol stocks prepared 2 years earlier. Please note that the media used were equal in composition but not identical. Methylamine assay (Experiment 2): "MA" stands for methylammmonium. Yeast were obtained from three transformations over the course of three weeks.*

	Experiment 1a (freshly transformed)		Experiment 1b (glycerol stocks)		Experiment 2	
	Gln	NH_4^+	Gln	NH_4^+	no MA	MA
Aquaporin	AUC 48 h / h					
Fps1	22	18	18	12	31	26
-	29	11	13	1	25	2
rAQP1	21	4	11	1	25	3
F56H	14	2	15	2	22	2
H180I	24	17	18	8	31	16
C189G	16	3	9	1	23	4
FH/HI	15	5	15	3	26	3
FH/CG	14	3	12	1	21	2
FH/HI/CG	25	11	18	3	29	4
C189A	29	12	10	1	22	3
FH/CA	19	3	10	1	22	2
HI/CA	20	16	18	12	34	24
FH/HI/CA	31	26	15	1	32	11
H180A	27	21	18	8	33	22
H180L	30	11	16	4	25	3
H180M	21	5	15	1	23	3
H180F	21	4	14	2	22	3
H180N	18	4	13	1	25	3
H180Q	17	3	17	2	21	3
R195V	28	10	14	2	29	13
R195S	23	8	11	2	26	7
HA/RV	28	22	19	8	31	24
HA/RS	24	15	19	7	32	15
hAQP8-HA	13	3	15	1	21	3
hAQP9-HA	34	32	25	24	34	29

The same yeast transformant suspensions were also placed on solid SD KHL medium, leading to uniform growth, and on solid ammonia and methylamine assay media, showing essentially the same growth pattern as seen in Table 4.1. One important difference was the pronounced growth contrast seen when comparing glutamine- and ammonium-containing assay plates (Fig. 4.25).

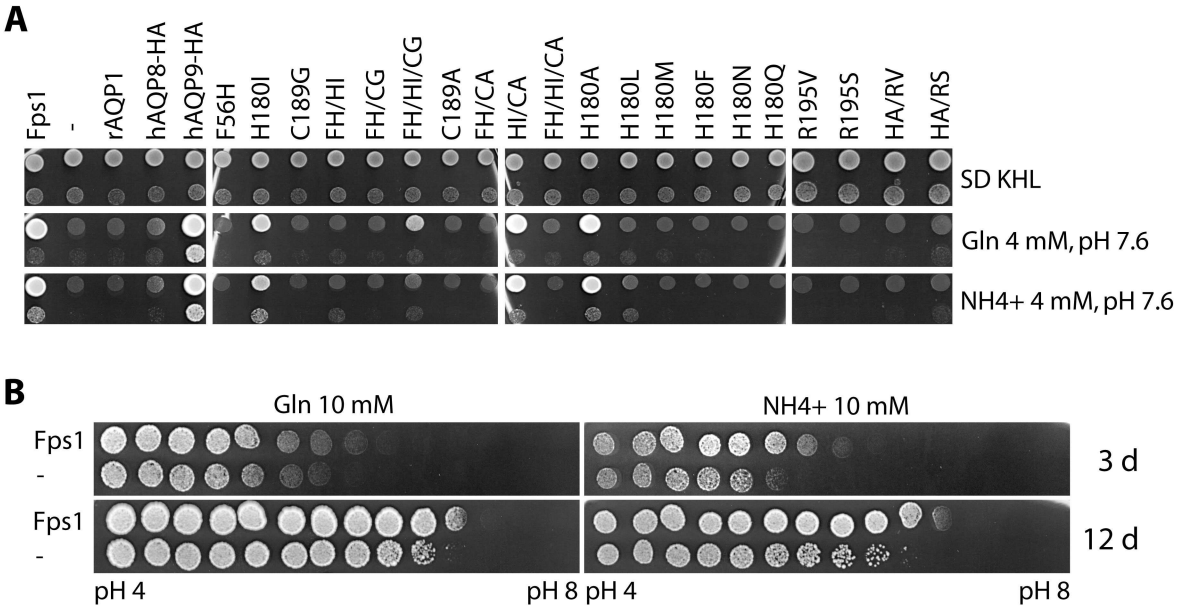

Fig. 4.25: Ammonia assay nitrogen source replacement. (A) *Yeast transformant (31019b Δfps1, pRS426 or pRS416 for Fps1) suspensions of OD_{600} ≈ 6 and 0.03 were spotted onto solid media and grown at 29 ℃ for 3 days (SD KHL) or 10 days (assay plates). The MOPS concentration of the assay plates was 40 mM. "Gln" stands for L-glutamine. Both nitrogen sources were added after autoclaving. Images within each row belonged to a single plate. Mutations refer to rAQP1.* ***(B)*** *The same Fps1- or non-producing yeast transformant suspensions (OD_{600} ≈ 6) were placed on pH gradient agar containing either L-glutamine or ammonium sulfate, with the nominal pH ranging from 4 to 8. Buffering was by HEPES 40 mM and tartaric acid 1 mM. Inoculation was approximately 26 h, i. e. a full day, after gradient agar preparation. The plates were scanned 3 and 12 days after inoculation.*

The similarity between the patterns appearing on the ammonium- and the glutamine-plates was striking (Fig. 4.25 A). It may have had to do with the pH of 7.6 (rather than 6.9). On pH gradient plates, with the nominal pH ranging from about 4 to about 8, the difference between Fps1- and non-producing yeast transformants also showed, although it was less pronounced for glutamine as compared to ammonium sulfate (Fig 4.25 B). Growth of the remaining yeast transformants on the pH gradient plates was analogous to that seen on the standard plates (not shown), except that rAQP1 H180L-producing yeast clearly grew better than rAQP1-producing ones.

The assay seemed to indicate alkaline stress tolerance of the yeast transformants, rather than ammonia uptake by them. It was one of several such clues as will be seen in Sections 4.3.4 and 4.3.5.

4.2 Testing potential aquaporin inhibitors

4.2.1 Choice of aquaporins

The choice of aquaporins for the testing of potential inhibitors was based on three criteria: their availability and functionality within the laboratory, the availability of their crystal structure for collaborators to find potential inhibitors by virtual high-throughput screening, as well as their pharmacological relevance. Table 4.2 gives an overview.

Table 4.2: Aquaporins available for the testing of potential inhibitors. *Availability refers to the time the experiments were to be conducted. Testability refers to functional presence in Saccharomyces cerevisiae as determined by growth assays and osmotic assays. Structure refers to the three-dimensional structure as determined by crystallography.*

Aquaporin	available	testable	structure
hAQP1	+	+	+
hAQP2	+	-	-
hAQP3	+	-	-
hAQP4	+	-	+
hAQP5	+	+	+
hAQP6	-	-	-
hAQP7	-	-	-
hAQP8	+	+	-
hAQP9	+	+	-
hAQP10	+	-	-
hAQP11	-	-	-
hAQP12	-	-	-
rAQP1	+	+	-
rAQP8	+	+	-
PfAQP	+	+	+
TgAQP	+	+	-
BccGlpF	+	+	-
EcGlpF	+	+	+

The following aquaporins fulfilled all three criteria: hAQP1, hAQP5, PfAQP, and EcGlpF. hAQP5-HA-synthesis had led to a small increase in yeast shrinkage rates in a single osmotic assay. EcGlpF was not considered pharmacologically relevant. Only human AQP1 and *Plasmodium falciparum* AQP were deemed testable. As will be seen, an exception was made for human Aquaporin 9.

4.2.2 Human Aquaporin 1

Known inhibitors of human Aquaporin1

Three possible inhibitors of hAQP1 were tested by osmotic assays with yeast transformant protoplasts: mercuric chloride ($HgCl_2$), tetraethylammonium ions (TEA^+) and acetazolamide. Representative results are shown in Figure 4.26. TEA^+ and acetazolamide were tested only once.

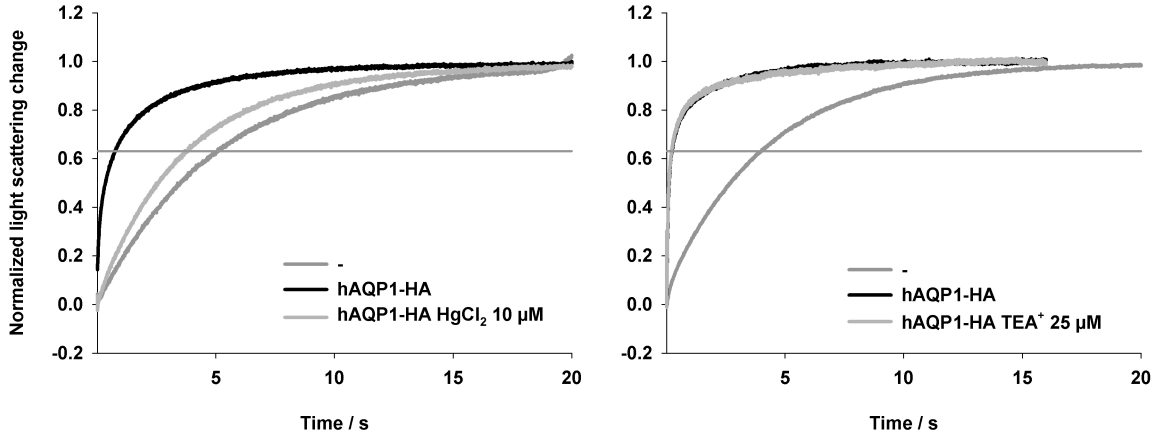

Fig. 4.26: Osmotic assays with yeast protoplasts (31019b Δfps1, pRS426) producing no AQP or hAQP1-HA. *Inward-directed hypertonic sorbitol gradient 0.30 mol/l (tonicity ~ 1.23), Tris/HCl 10 mM, pH ~ 7, 21 ℃. Normalized average curves (n = 4 - 9). The horizontal line marks the ordinate value at which the nominal relaxation time was read (y = 1 - 1/e).* ***Left:*** *Prior incubation with 10 µM mercuric chloride for about 1 h (5 µM nominal concentration after mixing) at room temperature.* ***Right:*** *Prior incubation with 50 µM TEACl (1 - 2 min, 25 µM after mixing).*

Inhibition of hAQP1 by mercuric chloride was confirmed. TEA^+-ions were found to have no effect at 25 µM, whereas a concentration of 4 µM had shown maximum inhibition in experiments with hAQP1-producing *X. laevis* oocytes (Detmers *et al.*, 2006). Acetazolamide was tested at 100 µM final concentration and was found to have no effect. However, the substance was 23 years old, and the result obtained with it may not be valid.

Test compounds

The first set of potential hAQP1-inhibitors consisted of nine compounds. They were found by K. Simmons who performed the virtual high-throughput screening. Some properties are listed in Table 4.3.

Table 4.3: Potential inhibitors of human Aquaporin 1. *The code is not the original one. "cLgP" stands for the calculated octanol/water partition coefficient, expressed as its decadic logarithm. Stock solution concentrations in DMSO, and approximate minimum solubilities (s) in assay buffer (sorbitol 1.2 M, Tris/HCl 10 mM, pH ~ 7) at 20 ℃ are given.*

code	*M* (g/mol)	cLgP	c_{stock} (mM)	s_{buffer} (µM)
h1-KS-1	340.83	2.14	100	1
h1-KS-2	385.89	1.47	100	25
h1-KS-3	326.35	0.44	100	25
h1-KS-4	268.36	2.67	100	5
h1-KS-5	330.41	4.13	100	1
h1-KS-6	259.24	2.00	8	8
h1-KS-7	242.23	2.48	0.8	1
h1-KS-8	335.21	3.28	50	1
h1-KS-9	286.38	3.51	50	1

Each compound was tested three times by osmotic assays with hAQP1-HA-producing yeast protoplasts. Representative results are shown in Figure 4.27.

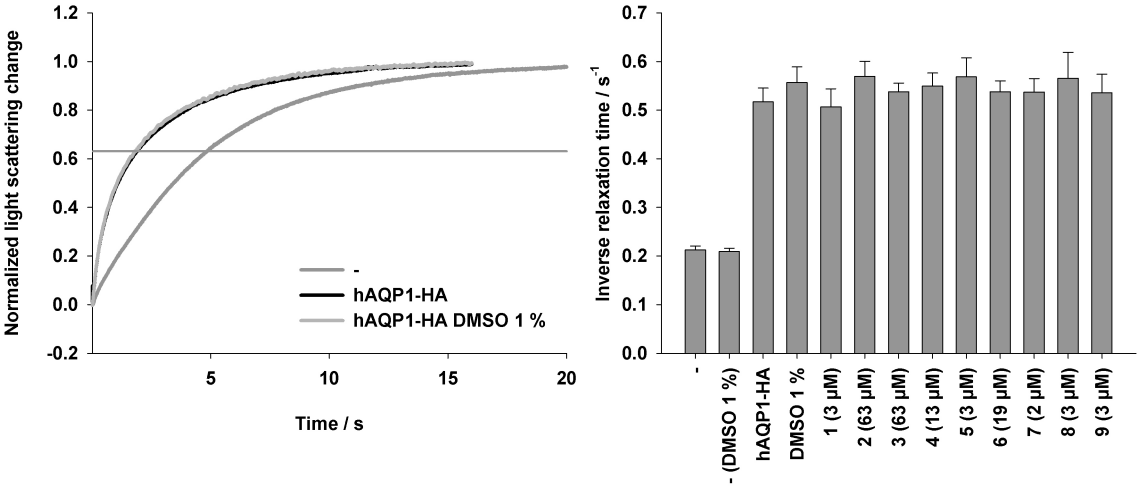

Fig. 4.27: Osmotic assays with yeast protoplasts (31019b Δfps1, pRS426) producing no AQP or hAQP1-HA. *Inward-directed hypertonic sorbitol gradient 0.30 osmol/l (tonicity ~ 1.23), Tris/HCl 10 mM, pH ~ 7, 21 ℃. Prior incubation with indicated test compounds for about 1 - 2 min. The DMSO concentration was constant, it is given in % V/V. The test compound concentration was decreased fourfold over two mixing steps within the stopped-flow apparatus.* ***Left:*** *Examples of normalized average curves (n = 8 - 9). The horizontal line marks the ordinate value at which the nominal relaxation time was read (y = 1 - 1/e).* ***Right:*** *Averages of inverse relaxation times derived from single normalized curves (n = 7 - 9). Error bars show standard deviations. Test compound numbers refer to set h1-KS (Table 4.3). Final concentrations after two mixing steps are given.*

None of the test compounds had an effect on the shrinkage rates of hAQP1-producing yeast protoplasts. Longer incubation times of about 0.5 - 1.5 hours in another experiment did not make a difference. Mercuric chloride was not available at the time the experiments shown in Figure 4.26 were carried out, or it would have been included to make sure that an incubation time of 1 - 2 minutes is sufficient. Please note that the approximate minimum solubilities given in Table 4.3 include a generous safety margin. That is why ten times higher concentrations in assay buffer could be used in the experiment without leading to precipitation visible by the eye or in the light scattering curves.

Three more sets of potential hAQP1-inhibitors, found by R. Haddoub, R. Castangia, and B. de Groot, were tested in groups of three to seven in a single experiment with yeast protoplasts (Table. 4.4). The incubation time was approximately one hour.

Table 4.4: Potential inhibitors of human Aquaporin 1. *The code is not the original one. Stock solution concentrations in DMSO or in water (*), approximate minimum solubilities (s) in assay buffer (sorbitol 1.2 M, MOPS/NaOH 10 mM, pH 7.2) at 22 °C, and the assay concentrations are given. The "test group" shows which compounds were combined for incubation with yeast protoplasts. The total DMSO concentration for each assay was adjusted to 1 % V/V. Please note that test compound concentrations were halved upon mixing in the stopped-flow apparatus.*

code	*M* (g/mol)	c_{stock} (mM)	s_{buffer} (µM)	c_{test} (µM)	test group
h1-RH-2	207.27	50	250	100	5
h1-RH-14	208.30	50	250	100	5
h1-RH-16	259.39	50	20	20	5
h1-RH-19	285.36	50	20	20	5
h1-RH-20	310.39	50	20	20	5
h1-RH-21	280.37	50	250	100	5
h1-RH-22	336.47	50	10	10	5
h1-RC-1	218	20	200	67	4
h1-RC-2	252	20	200	67	4
h1-RC-5	287	20	200	67	4
h1-RC-3	278	20	15	15	3
h1-RC-4	282	20	15	15	3
h1-RC-6	294	20	3	3	3
h1-RC-7	296	20	3	3	3
h1-RC-8	304	2	1	1	3
h1-RC-10	344	20	3	3	3
h1-BG-3	?	20	1	1	3
h1-RC-9	327	20 *	20000	40	2
h1-BG-6	?	20 *	20000	40	2
h1-BG-7	?	20 *	20000	40	2
h1-BG-8	?	20 *	20000	40	2
h1-BG-9	?	20 *	20000	40	2
h1-BG-1	?	20 *	20000	40	1
h1-BG-2	?	20 *	20000	40	1
h1-BG-4	?	20 *	20000	40	1
h1-BG-5	?	20 *	20000	40	1

None of the test compound groups showed any effect on yeast protoplast shrinkage rates, with the overlapping stopped-flow light scattering curves resembling those shown in Figure 4.27.

Compounds h1-RC-1/9/10 were of particular interest because they had been found by collaborators to inhibit, under particular conditions, hAQP1-mediated water permeability of *X. laevis* oocyte membranes. For this reason they were tested again, on human blood cells, the erythrocyte fraction of which is known to express AQP1 (Preston and Agre, 1991) and AQP3 (Roudier *et al.*, 1998). Results of control experiments with blood cells are shown in Figure 4.28.

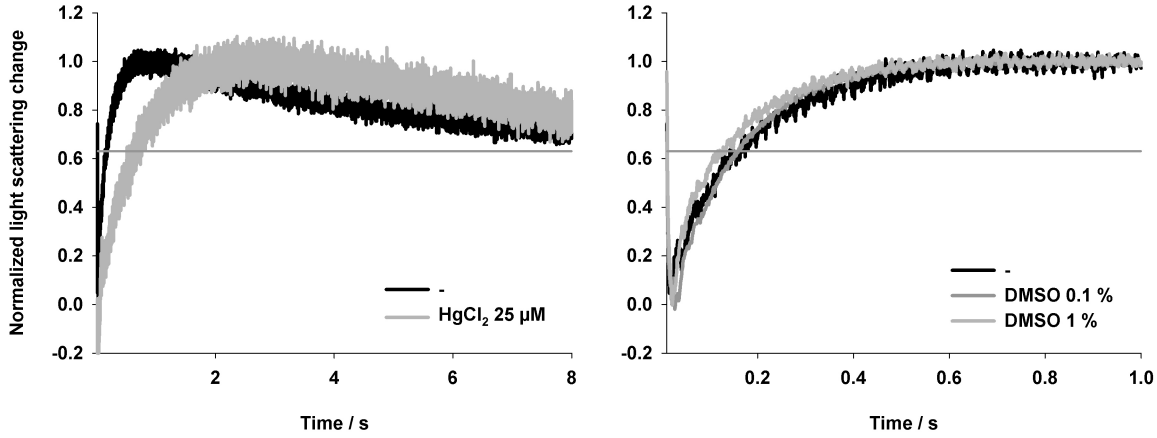

Fig. 4.28: Osmotic assays with human blood cells. *Inward-directed hypertonic glycerol gradient 30 mosmol/l (tonicity ~ 1.10), 26 ℃. Normalized average curves (n = 9). The horizontal line marks the ordinate value at which the nominal relaxation time was read (y = 1 - 1/e).* ***Left:*** *Prior incubation with 25 µM mercuric chloride for about 15 min (12.5 µM nominal concentration after mixing) at 0 ℃.* ***Right:*** *Effect of DMSO. Its concentration is given in % V/V. The experiments were performed on three different days with three different blood cell preparations. For 1 % DMSO the tonicity changes to 1.07 rather than to 1.10. The control curves (-) in both graphs are identical. Differing signal-to-noise ratios are due to differing optical densities of the blood cell suspensions (OD_{600} of 2, 4 or 8), and, in the case of $HgCl_2$-inhibition, to a smaller absolute signal amplitude (~ 1/3 of the control).*

Test compound concentrations were 20 µM or 200 µM for h1-RC-1 or 9, and 4 µM for h1-RC-10. There was no effect on erythrocyte shrinkage rates, with light scattering curves overlapping like those shown on the right in Figure 4.28.

h1-RC-1 did have a marked effect on glycerol influx at 200 µM, but this was probably due to a lowering of the pH from 7.4 to about 6 (h1-RC-1 is a dicarboxylic acid), which decreases hAQP3-mediated glycerol permeability (Zeuthen and Klaerke, 1999). The buffering capacity of the Carlsen buffer (3.7) may be too low.

TEA Cl and acetazolamide were both tested at 200 µM (DMSO 1 % V/V) after about 15 minutes incubation, and were found to have no effect. Together with the lack of an effect of DMSO, this confirms several of the results reported by Yang and colleagues (Yang *et al.*, 2006 c).

Please note that for all blood cell experiments except mercuric chloride inhibition, the test compounds were present in both storage and hyperosmotic buffers at the same concentration, *i. e.* the latter did not change after mixing in the stopped-flow apparatus.

4.2.3 *Plasmodium falciparum* Aquaporin

Known inhibitors of *Plasmodium falciparum* aquaporin

At the time the experiments were to be carried out, no inhibitor of PfAQP had been described in the literature.

DMSO tolerance of yeast

Inhibition of PfAQP was to be tested mainly by yeast growth assays. Since the standard solvent for test compounds was DMSO, its effect on yeast growth had to be determined first. The results of a single assay are shown in Figure 4.29. For technical reasons, AUCs could not be determined for a period exceeding 12 h. Instead, final optical densities recorded after 72 h of growth are shown.

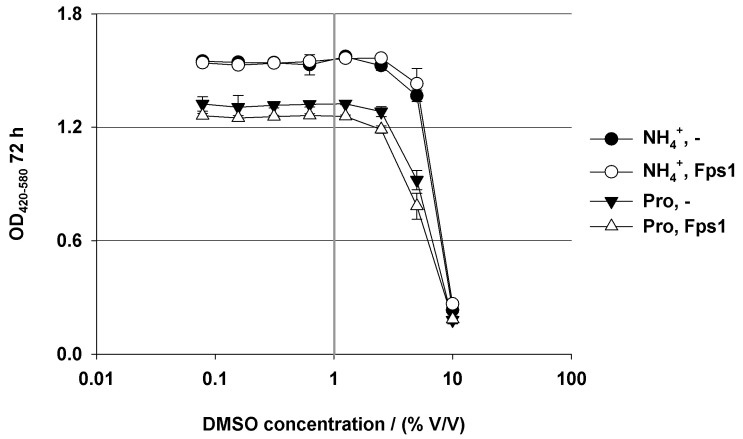

Fig. 4.29: Ammonia assay. *Yeast transformants (31019b Δfps1, pRS426 or pRS416 Fps1) were grown at 29 ℃ for 3 days in liquid media containing 10 mM ammonium (NH_4^+) or L-proline (Pro), as well as varying concentrations of DMSO. The pH was 7.2, the MOPS concentration was 40 mM. Averages of $OD_{420-580}$ measurements of 5 wells each. Error bars represent standard deviations. The starting ODs ranged from about 0.12 to 0.15. Final ODs in the absence of DMSO were, within error, identical to those for the lowest DMSO-concentration shown.*

Under the given conditions, yeast growth was unperturbed by DMSO concentrations of up to about 2 % V/V. Even at 10 % V/V there was some growth. Based on these results, a maximum DMSO concentration of 1 % V/V (~ 140 mM) was decided upon for this type of ammonia assay and the yeast strain 31019b Δfps1. For all growth assays intended to test potential aquaporin inhibitors, test compound concentrations were determined by the stock concentration and thus by the chosen DMSO concentration, irrespective of their solubilities.
Please note that in the above experiment aquaporin-deficient yeast transformants had grown just as much as Fps1-producing ones after 72 hours in ammonium-containing medium. This happened in several ammonia assays and probably depended on the particular transformant colony chosen.

Test compounds

The first set of potential PfAQP-inhibitors was found by K. Simmons. Some of their properties are listed in Table 4.5.

Table 4.5: Potential inhibitors of Plasmodium falciparum aquaporin. *The code is not the original one. Stock solution concentrations in DMSO and approximate minimum solubilities (s) in assay buffer (sorbitol 1.2M, MOPS/NaOH 10 mM, pH 7.2) at 20 °C are given. "n. d." stands for "not determined".*

code	*M* (g/mol)	c_{stock} (mM)	s_{buffer} (µM)
Pf-KS-1	331.39	50	n. d.
Pf-KS-2	345.42	100	n. d.
Pf-KS-3	297.38	50	n. d.
Pf-KS-4	304.39	100	n. d.
Pf-KS-5	336.41	100	n. d.
Pf-KS-6	319.38	100	6
Pf-KS-7	333.41	100	25
Pf-KS-8	347.44	100	n. d.
Pf-KS-9	260.32	100	n. d.
Pf-KS-10	304.33	100	n. d.

Four ammonia assays were performed, with one example given in Figure 4.30.

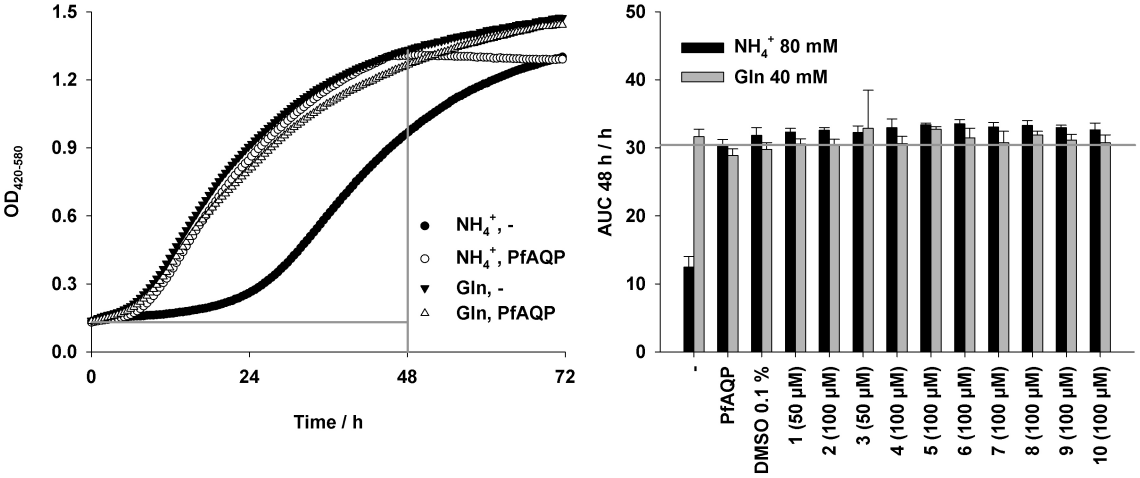

Fig. 4.30: Ammonia assay. *Yeast transformants (31019b Δfps1, pDR196) producing no AQP or PfAQP were grown at 29 °C for 3 days in liquid media containin g 80 mM ammonium (NH_4^+) or 40 mM L-glutamine (Gln), as well as the given concentrations of test compounds. With the compounds, and where indicated, 0.1 % V/V DMSO was present. The pH was 6.9, the MOPS concentration was 40 mM.* ***Left:*** *Examples of growth curves. The horizontal and vertical lines mark the boundaries used to calculate the areas under the curves.* ***Right:*** *Averages of AUC 48 h values derived from OD measurements of 5 wells each. Error bars show standard deviations. Test compound numbers refer to set Pf-KS (Table 4.5). The horizontal line marks the control value (PfAQP, NH_4^+, no DMSO, no compound).*

For AQP-deficient yeast transformants, growth in the presence of ammonium ions or L-glutamine differed sufficiently for the assay to be informative. PfAQP-producing yeast grew equally well in both media. DMSO did not interfere. None of the test compounds showed an effect.

Of the three other assays performed with this set of compounds, two were not informative because of equal growth of AQP-deficient and PfAQP-producing yeast. The other was, and it showed a possible effect of compound Pf-KS-8. Upon closer investigation, using control medium (L-proline) and several concentrations of the compound, the effect could not be substantiated.

In a proteoliposome-based assay (Brändén *et al.*, 2010), Pf-KS-6 had been found to inhibit PfAQP-facilitated sorbitol permeation by about 80 % at a concentration of 10 µM (G. Fischer, conference report). For this reason, it was tested in a glycerol permeability assay with yeast protoplasts, with the result shown in Figure 4.31.

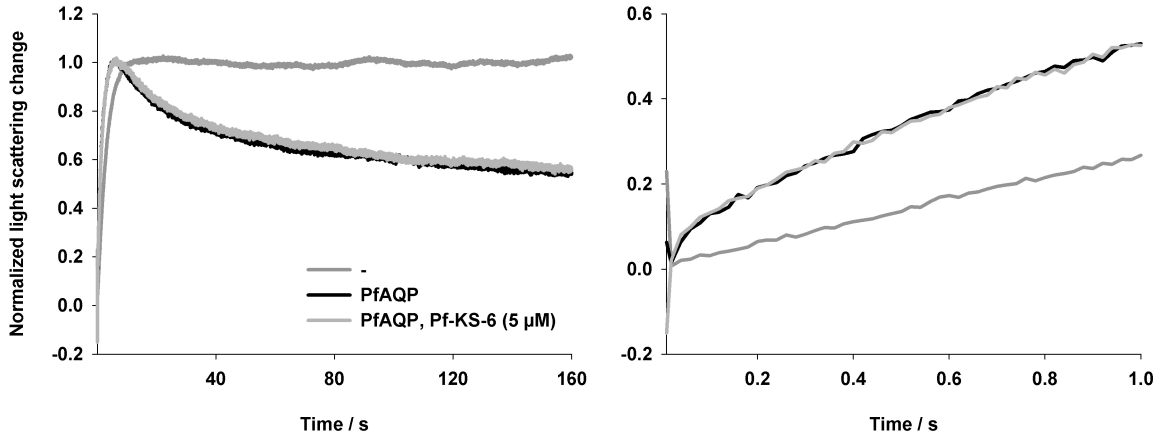

Fig. 4.31: Glycerol permeability assay with yeast protoplasts (BY4742 Δfps1 Δgpd1/2, pDR196) producing no AQP or PfAQP. *Inward-directed hypertonic glycerol gradient 0.30 osmol/l, Tris/HCl 10 mM, pH ~ 7, 21 ℃. The base osmolyte was sucrose (1.2 M). Prior incubation with 10 µM test compound Pf-KS-6 for about 1 h at room temperature (5 µM after mixing). With the test compound, DMSO was present at 0.1 % V/V (0.05 % after mixing). Normalized average curves (n = 5 - 7).* ***Left:*** *Full measurement time.* ***Right:*** *First second. Please note the different ordinate scales.*

Pf-KS-6 seemed to have no effect on PfAQP-mediated glycerol or water permeability. According to K. Simmons, this compound is expected to bind on the intracellular side of the channel.

Another set of potential PfAQP-inhibitors was found by Sören Wacker. They were tested by yeast growth assays and by yeast protoplast glycerol permeability assays, once each. For the glycerol permeability assay, the compounds were split into three groups of four, as shown in Table 4.6. Incubation time was approximately one hour.

Table 4.6: Potential inhibitors of Plasmodium falciparum aquaporin. *The code is not the original one. Stock solution concentrations in DMSO, approximate minimum solubilities (s) in assay buffer (sucrose 1.2 M, glycerol 0.15 M, MOPS/NaOH 10 mM, pH 7.2, DMSO 1 % V/V) at 20 °C, and the assay concentrations are given. The "test group" shows which compounds were combined for incubation with yeast protoplasts. The total DMSO concentration for each assay was adjusted to 1 % V/V. Please note that test compound concentrations were halved upon mixing in the stopped-flow apparatus, while the DMSO concentration was constant.*

code	*M* (g/mol)	c_{stock} (mM)	s_{buffer} (µM)	c_{test} (µM)	test group
Pf-SW-1	470.55	10	6	6	1
Pf-SW-4	238.27	10	100	25	1
Pf-SW-8	413.48	10	100	25	1
Pf-SW-10	461.52	10	1.6	1.6	1
Pf-SW-2	466.42	10	25	6	2
Pf-SW-5	242.66	10	100	25	2
Pf-SW-7	454.55	10	6	1.6	2
Pf-SW-11	484.34	10	1.6	0.4	2
Pf-SW-3	496.55	10	25	6	3
Pf-SW-6	326.40	10	100	25	3
Pf-SW-9	474.97	10	6	1.6	3
Pf-SW-12	402.48	10	1.6	0.4	3

No effect was seen for any of the test groups. The choice of lower concentrations in Groups 2 and 3 was due to an unfounded worry about possible precipitation seen while testing Group 1.

A growth assay did not indicate PfAQP-inhibition either (Fig. 4.32).

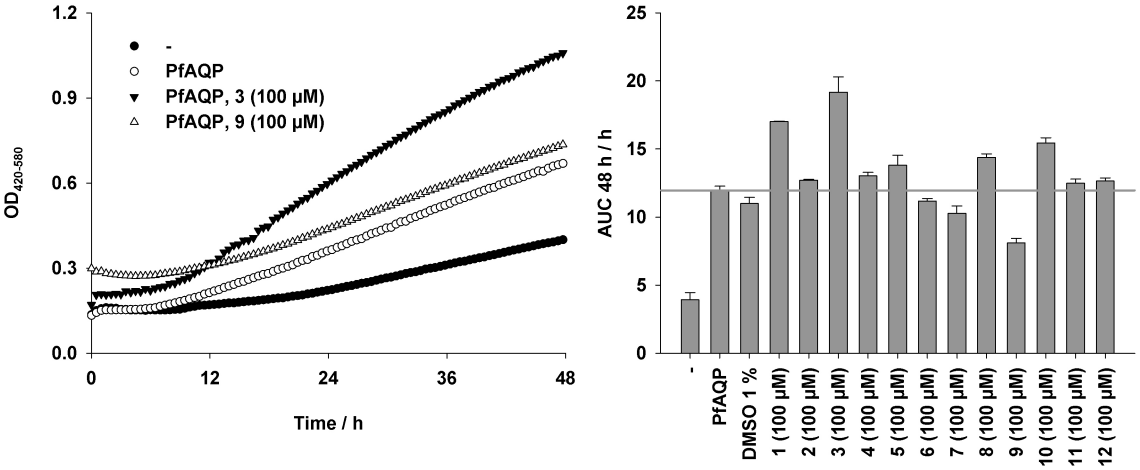

Fig. 4.32: Ammonia assay. *Yeast transformants (31019b Δfps1, pDR196) producing no AQP or PfAQP were grown at 29 °C for 2 days in liquid media containing 40 mM ammonium, as well as the given concentrations of test compounds and 1 % V/V DMSO where indicated. The pH was 6.9, the MOPS concentration was 40 mM.* ***Left:*** *Examples of growth curves (DMSO 1 %). Starting optical densities above about 0.15 are due to precipitated test compound. Test compound numbers refer to set Pf-SW (Table 4.6).* ***Right:*** *Averages of AUC 48 h values derived from OD measurements of 4 wells each. Error bars show standard deviations. The horizontal line marks a control value (PfAQP, no DMSO, no compound).*

At first sight, the AUCs seemed to indicate marked growth inhibition by Pf-SW-9, and growth stimulation by Pf-SW-3. A look at the corresponding growth curves revealed that the former may have been due to gradual dissolution of precipitated compound, whereas the latter may have been due to increasing precipitation. Since turbidimetric measurements do not distinguish between yeast growth and precipitate formation, the resulting curves are not

amenable to simple analysis. Thus, for yeast growth assays, test compound solubilities have to be taken into account. The initial assumption of constant precipitate turbidity was wrong. The medium pH change during ammonia assays was investigated, as will be seen in Section 4.3.4.

4.2.4 Human Aquaporin 9

A colleague's work on human Aquaporins 3 and 9 showed remarkable growth-enhancing properties of the latter in yeast under ammonia and methylamine assay conditions (A. Almasalmeh, diploma thesis), as seen in Figure 4.25 and in Table 4.1. This testability, as well as the collaborators' will to try virtual high-throughput screening on a homology model of a membrane protein, led to the search for and the testing of potential inhibitors of hAQP9.

Known inhibitors of human Aquaporin 9

Phloretin and mercuric chloride have been shown to inhibit hAQP9-mediated solute permeability in *X. laevis* oocytes at 0.1 mM and 0.3 mM, respectively (Tsukaguchi *et al.*, 1999). Glycerol permeability assays with hAQP9-HA-producing yeast protoplasts gave the following results (Fig. 4.33).

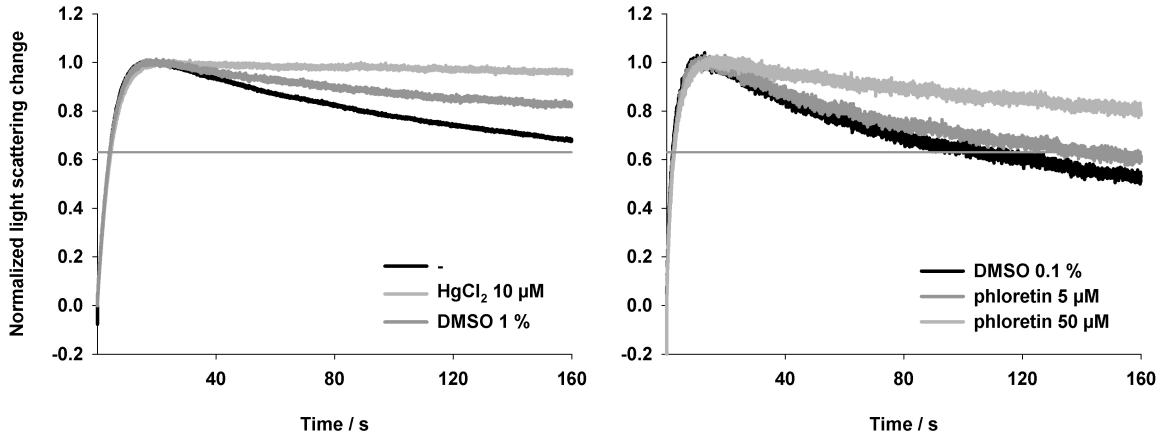

Fig. 4.33: Glycerol permeability assays with yeast protoplasts (BY4742 Δfps1) producing hAQP9-HA. *Prior incubation with the indicated substance for about 1 h at room temperature. The base osmolyte was sucrose (1.2 M). Normalized average curves. There was no appreciable glycerol influx in the absence of the aquaporin.* ***Left:*** *Inhibition by 10 µM mercuric chloride (5 µM nominal concentration after mixing) or 1 % V/V DMSO (0.5 % after mixing). Inward-directed hypertonic glycerol gradient 0.30 osmol/l, Tris/HCl 10 mM, pH ~ 7, 21 ℃ (n = 5 - 8). The coding plasmid was pRS426.* ***Right:*** *Inhibition by 5 µM and 50 µM phloretin (twice that before mixing). The DMSO concentration was constant at 0.1 % V/V. Inward-directed hypertonic glycerol gradient 0.15 osmol/l, MOPS/NaOH 10 mM, pH 7.2, 20 ℃ (n = 8 - 9). The coding plasmi d was pDR196.*

Inhibition by both phloretin and mercuric chloride was confirmed. In an experiment not shown, phloretin failed to inhibit PfAQP at a nominal concentration of 145 µM. It was thus somewhat selective for hAQP9. In addition, DMSO interfered with hAQP9-HA-mediated

glycerol permeability, unlike for PfAQP (not shown). In another experiment done with a different preparation of hAQP9-HA-producing yeast protoplasts, a constant concentration of 1 % V/V DMSO completely inhibited glycerol influx. At constant 0.1 % DMSO, glycerol influx was partly inhibited, but the effect was small enough to be acceptable for inhibitor studies.

The availability of two inhibitors of hAQP9 was a welcome opportunity to find out whether the ammonia assay is suitable for testing potential inhibitors of growth-promoting aquaporins. Two such assays were performed (Fig. 4.34).

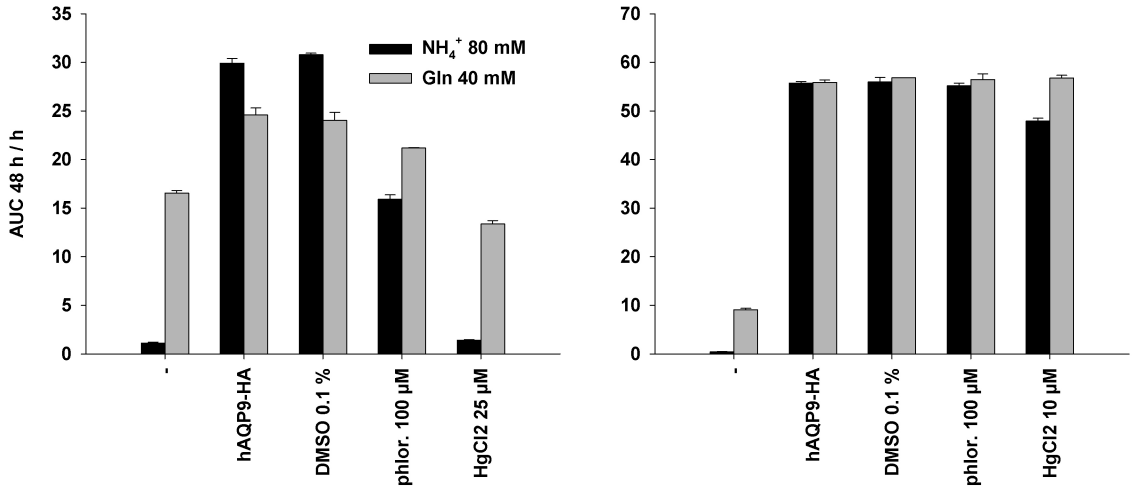

Fig. 4.34: Ammonia assay. *Yeast transformants (31019b Δfps1, pRS426) producing no AQP (-) or hAQP9-HA (all other columns) were grown at 29 ℃ for 2 days in liquid media containing 80 mM ammonium (NH_4^+) or 40 mM L-glutamine (Gln), as well as the given concentrations of test compounds ("phlor." stands for phloretin). There was no DMSO present with the mercuric chloride. The pH was 6.9, the MOPS concentration was 40 mM. Averages of AUC 48 h values derived from OD measurements of 4 wells each. Error bars show standard deviations. Please note the different ordinate scales and mercuric chloride concentrations.* ***Left:*** *Experiment one.* ***Right:*** *Experiment two, performed six days after the first. The same glutamine medium but two different preparations of ammonia medium (of the same composition) were used for the experiments. Yeast transformants were from the same glycerol stocks, but grown longer for experiment one (four days instead of one).*

The first assay showed a promising pattern of nitrogen source-dependent growth inhibition of hAQP9-HA-producing yeast by 100 µM phloretin or 25 µM mercuric chloride. The second assay showed no such pattern, with hAQP9-HA-transformant growth in ammonium medium exceptionally robust.

Since the osmotic assays had been performed with yeast strain BY4742 Δfps1 (Fig. 4.33), the strain used for methylamine assays, the effect of phloretin was also tested on hAQP9-HA-transformants in a methylamine assay, as shown in Figure 4.35.

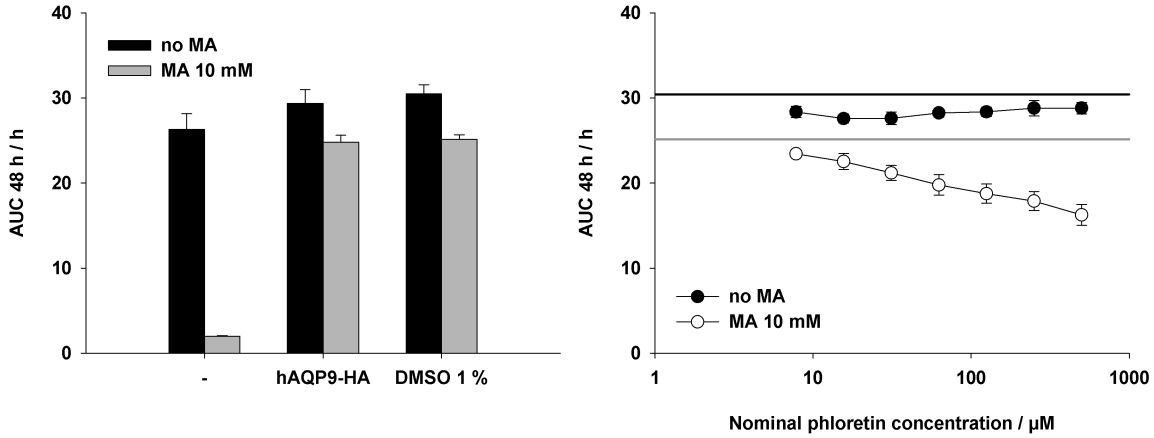

Fig. 4.35: Methylamine assay. *Yeast transformants (BY4742 Δfps1, pDR196) producing no AQP or hAQP9-HA were grown at 29 ℃ for 4 days in liquid media cont aining none or 10 mM methylammonium, as well as the given concentrations of phloretin. The pH was 5.5. Averages of AUC 48 h values derived from OD measurements of 3 - 4 wells each (2 wells for MA 10 mM, phloretin 8 µM). Error bars show standard deviations.* ***Left:*** *Yeast transformants producing no AQP (-) or hAQP9-HA (all other columns) grown in the absence of phloretin.* ***Right:*** *Concentration dependence of phloretin inhibition. The DMSO concentration ranged from 1 % (no phloretin) to 0.5 % V/V (phloretin 0.5 mM). The horizontal lines mark the corresponding values for the absence of phloretin (black: no MA, grey: MA 10 mM). Please note that the phloretin concentrations are nominal (see text).*

The assay media were thirteen months old, but their pH was still 5.5, and there was no visible contamination. Due to a pipetting error, the DMSO concentrations were 1, 0.99, 0.98, 0.97, 0.94, 0.88, 0.75, 0.5 % V/V from wells containing no phloretin to those containing the maximum phloretin concentration, but this probably did not affect the outcome. More importantly, the true phloretin concentrations were lower, since some precipitation was seen and removed by centrifugation prior to loading the wells. An experimental determination of its solubility in methylamine (pH 5.5) and ammonia (pH 6.9) assay buffers, as well as in a stopped-flow assay buffer (pH 7.2), yielded an approximate value of 100 µM for each of these. Thus, the concentrations indicated in Figure 4.35 should be divided by about five.

Regardless of the above considerations, the methylamine assay showed a decrease in yeast transformant growth possibly due to a specific and dose-dependent inhibition of hAQP9 by phloretin. The linearity of the dose dependence seen in the semilogarithmic plot seems to be unusual, however. It may have to do with the presence of 1 % rather than 0.1 % DMSO. The effect was small, possibly due to the low concentrations of phloretin. At the time of writing, this was the most recent experiment, which is why its findings were not applied when testing potential hAQP9-inhibitors.

Test compounds

Two sets of potential hAQP9-inhibitors were tested, with eleven compounds from K. Simmons and seventy six from S. Wacker. The latter were found by screening 9,497,542 molecules from the “Clean Drug-Like”-set of the ZINC database (Irwin and Shoichet, 2005) for possible binding to a homology model of hAQP9 based on the crystal structure of *E. coli*

Glpf (PDB: 1FX8, 32.4 % sequence identity). Some of their properties are listed in Table 4.7. A few of them were not soluble in DMSO at 10 mM, and because they had been received as suspensions little could be done about this (3.8). This is fine, however, as long as one keeps in mind that the assay buffer solubilities determined (column four) may thus be over-estimated. On the other hand, DMSO evaporation in the working repositories (standard 96-well plates, the DMSO condensating on the lids) led to an increase in stock concentrations, and thus to a slight underestimation of the minimum solubilities in the assay buffer.

The compounds were tested once in groups of three to five by glycerol permeability measurements with two preparations of hAQP9-HA-producing yeast protoplasts.

Only Group 1 (h9-KS-1/2/3/4) showed a small effect, as seen in Figure 4.36. The effect may have been similar in magnitude to that of 5 µM phloretin (Fig. 4.33), but no control measurements were made on the same day. The compounds were added at the low concentration of 0.2 µM each, due to exaggerated initial concerns about their solubility. Whether their effect was significant can only be found out by testing each separately at higher and constant concentrations (2 µM in both storage and mixing buffers). Concerns about variations in DMSO concentration due to the pipetting of small volumes of test compound solutions (the smallest volume was 0.2 µl) were dispelled by control measurements with DMSO added in five equal portions to the final concentration of 0.1 %.

Compounds of set h9-KS were tested twice at 100 µM and 1 % DMSO in ammonia assays, of which one gave a sufficient contrast between positive and negative control. h9-KS-8 showed inhibition of yeast growth in both cases, as well as of hAQP9-HA-mediated glycerol permeability in a single yeast protoplast assay (100 µM, DMSO 1 %, both halved upon mixing in the stopped-flow apparatus), as depicted in Figure 4.37.

Compounds of set h9-SW were received as three subsets and tested in ammonia assays at 100 µM and 1 % DMSO. For each compound, one to three useful results were obtained. Only subset one (h9-SW-1 to 22) was tested with L-glutamine medium, once, and in this assay the aquaporin-deficient yeast grew only marginally better than in ammonium medium. Several compounds led to apparent growth boosting, although, as with set Pf-SW-x, this was probably due to changing precipitation (Fig. 4.32). Apparent inhibition of hAQP9-HA-transformant growth under ammonia assay conditions was seen for compounds h9-SW-16 (three times), h9-SW-50 (once) and h9-SW-65 (twice), although again this may have been due to changes in precipitation. Compound h9-SW-16 was tested in a yeast protoplast glycerol permeability assay once, as was h9-KS-8 (Fig. 4.37).

Table 4.7: Potential inhibitors of human Aquaporin 9. *The code is not the original one. Stock solution concentrations in DMSO, approximate minimum solubilities (s) in assay buffer (sucrose 1.2 M, glycerol 0.15 M, MOPS/NaOH 10 mM, pH 7.2, DMSO 1 % V/V) at 20 °C, and the assay concentrations are given. Asterisks indicate which compounds were not soluble in DMSO at 10 mM. The test group shows which compounds were combined for incubation with yeast protoplasts. The total DMSO concentration for each assay was 0.1 % V/V. Please note that test compound concentrations were halved upon mixing in the stopped-flow apparatus, while the DMSO concentration was constant.*

code	*M* (g/mol)	c_{stock} (mM)	s_{buffer} (µM)	c_{test} (µM)	test group
h9-KS-1	351.45	10	1.6	0.16	1
h9-KS-2	388.45	10	1.6	0.16	1
h9-KS-3	411.46	10	1.6	0.16	1
h9-KS-4	473.53	10	1.6	0.16	1
h9-KS-5	476.45	10	< 1.6	0.63	2
h9-KS-6	415.50	10	1.6	0.63	2
h9-KS-10	471.51	10	1.6	0.63	2
h9-KS-11	375.51	10	1.6	0.63	2
h9-KS-7	416.52	10	6	2.5	3
h9-KS-8	368.47	10	25	5	3
h9-KS-9	366.48	10	6	2.5	3
h9-SW-1	284.28	10	100	2	4
h9-SW-2	187.22	10	100	2	4
h9-SW-5	154.15	10	100	2	4
h9-SW-6	236.25	10*	100	2	4
h9-SW-7	256.26	10	100	2	4
h9-SW-8	204.23	10	100	2	5
h9-SW-9	221.09	10	100	2	5
h9-SW-10	262.29	10*	100	2	5
h9-SW-11	304.33	10*	100	2	5
h9-SW-12	273.25	10	100	2	5
h9-SW-13	249.27	10	100	2	6
h9-SW-15	281.28	10*	100	2	6
h9-SW-17	495.62	10	100	2	6
h9-SW-18	252.28	10	100	2	6
h9-SW-19	419.42	10	100	2	6
h9-SW-20	423.38	10	100	2	7
h9-SW-21	297.32	10	100	2	7
h9-SW-22	282.30	10	100	2	7
h9-SW-23	498.78	10	100	2	7
h9-SW-25	447.88	10	100	2	7
h9-SW-26	465.87	10	100	2	8
h9-SW-27	322.33	10	100	2	8
h9-SW-28	352.36	10	100	2	8
h9-SW-29	482.52	10	100	2	8
h9-SW-30	482.32	10	100	2	8
h9-SW-31	487.92	10	100	2	9
h9-SW-32	429.89	10	100	2	9
h9-SW-33	471.47	10	100	2	9
h9-SW-36	431.42	10	100	2	9
h9-SW-37	485.49	10	100	2	9
h9-SW-38	445.45	10	100	2	10
h9-SW-39	471.47	10	100	2	10
h9-SW-40	465.87	10	100	2	10
h9-SW-41	378.39	10	100	2	10
h9-SW-42	331.31	10	100	2	10

Table 4.7: Potential inhibitors of human Aquaporin 9 (continued).

code	*M* (g/mol)	c_{stock} (mM)	s_{buffer} (µM)	c_{test} (µM)	test group
h9-SW-45	315.31	10	100	2	11
h9-SW-46	301.28	10	100	2	11
h9-SW-47	483.50	10	100	2	11
h9-SW-48	457.48	10	100	2	11
h9-SW-49	461.90	10	100	2	11
h9-SW-52	455.47	10	100	2	12
h9-SW-53	297.29	10*	100	2	12
h9-SW-56	451.50	10	100	2	12
h9-SW-57	365.39	10	100	2	12
h9-SW-58	420.40	10	100	2	12
h9-SW-59	492.33	10	100	2	13
h9-SW-60	416.44	10	100	2	13
h9-SW-61	317.73	10	100	2	13
h9-SW-62	347.76	10	100	2	13
h9-SW-63	413.43	10	100	2	13
h9-SW-64	485.49	10	100	2	14
h9-SW-66	436.86	10	100	2	14
h9-SW-67	326.13	10	100	2	14
h9-SW-68	447.51	10	100	2	14
h9-SW-73	471.92	10	25	2	14
h9-SW-4	332.34	10*	25	2	15
h9-SW-34	441.48	10	6	2	15
h9-SW-43	487.92	10	6	2	15
h9-SW-44	327.77	10*	6	2	15
h9-SW-50	331.74	10	6	2	15
h9-SW-16	471.49	10	1.6	2	16
h9-SW-69	499.55	10	6	2	16
h9-SW-70	228.66	10	6	2	16
h9-SW-72	473.94	10	6	2	16
h9-SW-76	363.39	10	6	2	16
h9-SW-24	397.82	10	1.6	2	17
h9-SW-35	281.68	10	1.6	2	17
h9-SW-51	452.52	10	1.6	2	17
h9-SW-54	497.51	10	1.6	2	17
h9-SW-55	298.13	10	1.6	2	17
h9-SW-3	270.25	10	6	0.25	18
h9-SW-14	248.26	10*	1.6	0.25	18
h9-SW-65	363.81	10*	1.6	0.25	18
h9-SW-71	429.89	10	1.6	0.25	18
h9-SW-74	439.47	10	1.6	0.25	18
h9-SW-75	473.94	10	1.6	0.25	18

The approximate minimum solubility of h9-SW-16 according to Table 4.7 is 1.6 µM, so the lack of difficulty when testing it at 100 µM in the stopped flow apparatus was something of a mystery. In any case, it seemed to have no effect on yeast protoplast reswelling, unlike h9-KS-8. Concerning this particular ammonia assay, h9-KS-8 led to a marked decrease in AUC 48 h not because of reduced yeast growth, but because it made the yeast stick to the edges of the assay plate wells after about 24 hours, a phenomenon described in Section 4.3.3. In

another ammonia assay it led to a definite slowing in growth from the beginning. Such irregular growth assay results were common.

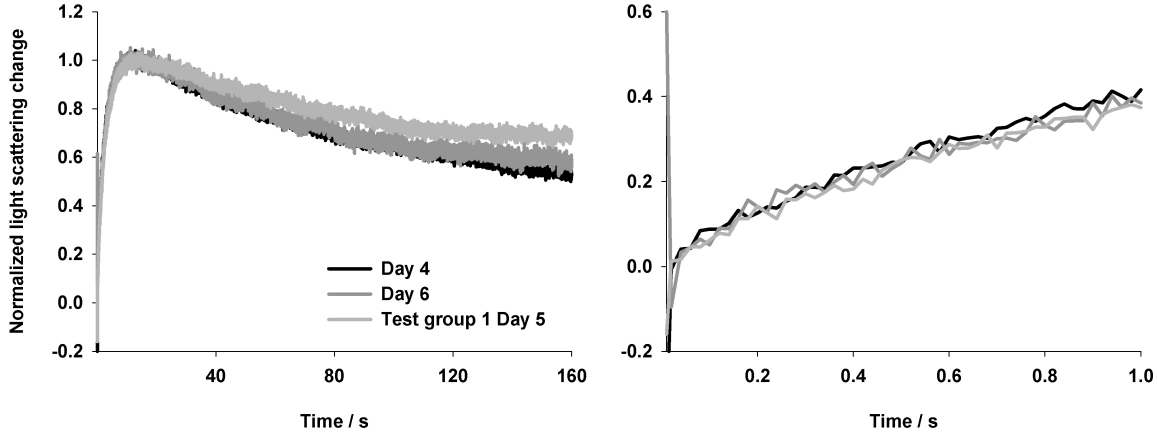

Fig. 4.36: Glycerol permeability assay with yeast protoplasts (BY4742 Δfps1, pDR196) producing hAQP9-HA. *Inward-directed hypertonic glycerol gradient 0.15 osmol/l, MOPS/NaOH 10 mM, pH 7.2, 20 ℃. The base osmolyte was sucrose (1.2 M). The DMSO concentration was constant at 0.1 % V/V. Prior incubation with test group 1 (see Table 4.7) for about 1 h at room temperature. Normalized average curves (n = 9). There was no appreciable glycerol influx in the absence of the aquaporin.* ***Left:*** *Full measurement time. Protoplasts were prepared on Day 1. No control measurements (DMSO 0.1 %) were made on Day 5.* ***Right:*** *First second. Please note the different ordinate scales.*

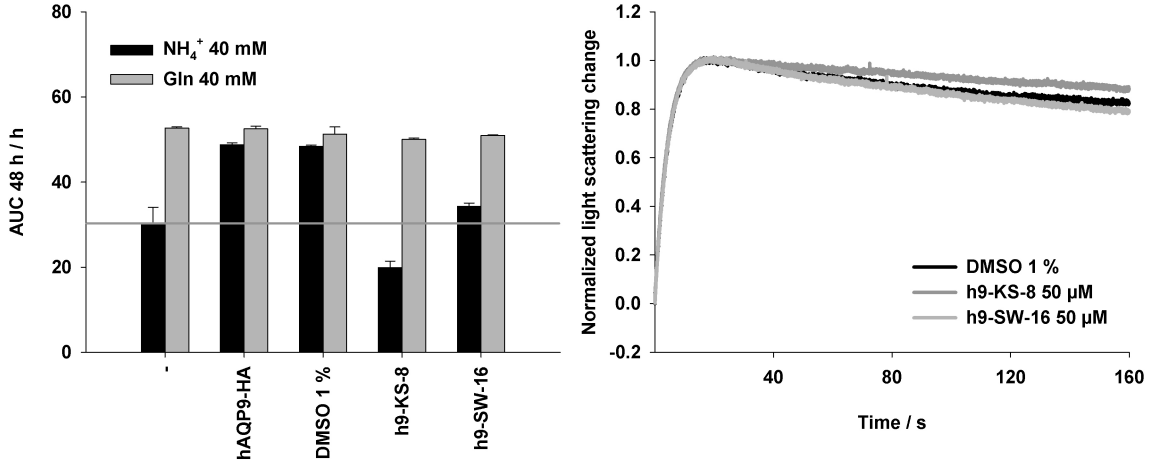

Fig. 4.37: Testing potential inhibitors of human Aquaporin 9. Left: *Ammonia assay. Yeast transformants (31019b Δfps1, pRS426) producing no AQP (-) or hAQP9-HA (all other columns) were grown at 29 ℃ for 2 days in liquid media containing 40 mM ammonium (NH_4^+) or 40 mM L-glutamine (Gln), and, where indicated, 1 % V/V DMSO and 100 µM test compound. The pH was 6.9, the MOPS concentration was 40 mM. Averages of AUC 48 h values derived from OD measurements of 4 wells each. Error bars show standard deviations. The horizontal line marks a control value (no AQP, no DMSO, no compound).* ***Right:*** *Glycerol permeability assay with yeast protoplasts (BY4742 Δfps1, pRS426) producing hAQP9-HA. Inward-directed hypertonic glycerol gradient 0.30 osmol/l, Tris/HCl 10 mM, pH ~ 7, 21 ℃. The base osmolyte was sucrose (1.2 M). Prior incubation with 100 µM of the indicated substance for about 1 h at room temperature. The DMSO concentration was 1 % V/V (0.5 % after mixing). Normalized average curves (n = 6 - 8). There was no appreciable glycerol influx in the absence of the aquaporin. The control curve (DMSO 1 %) is identical to the one shown in Fig. 4.33.*

In summary, the quality of the assays performed does not allow a firm conclusion regarding the hAQP9-inhibiting properties of any of the compounds shown in Table 4.7. No methyl-amine assays were performed to test them.

4.3 Notes on the assays

Many interesting phenomena were observed when performing the osmotic and the yeast growth assays. Some of them were studied in more detail, both for curiosity and for their potential usefulness. In the following sections, the most remarkable findings are presented.

4.3.1 Osmotic assays with *X. laevis oocytes*

The limited concentration of an important cRNA sample (4.1.3, Fig. 4.14) led to an interest in the dependence of *X. laevis* oocyte swelling rates on the amount of injected aquaporin-encoding cRNA.

A solution of approximately 0.8 µg/µl rAQP1-coding cRNA was subjected to a series of fourfold dilutions, down to a concentration of about 0.8 ng/µl. Each dilution was used to inject fourteen to eighteen oocytes (3.6). Three days after injection, the following results were obtained (Fig. 4.38 A).

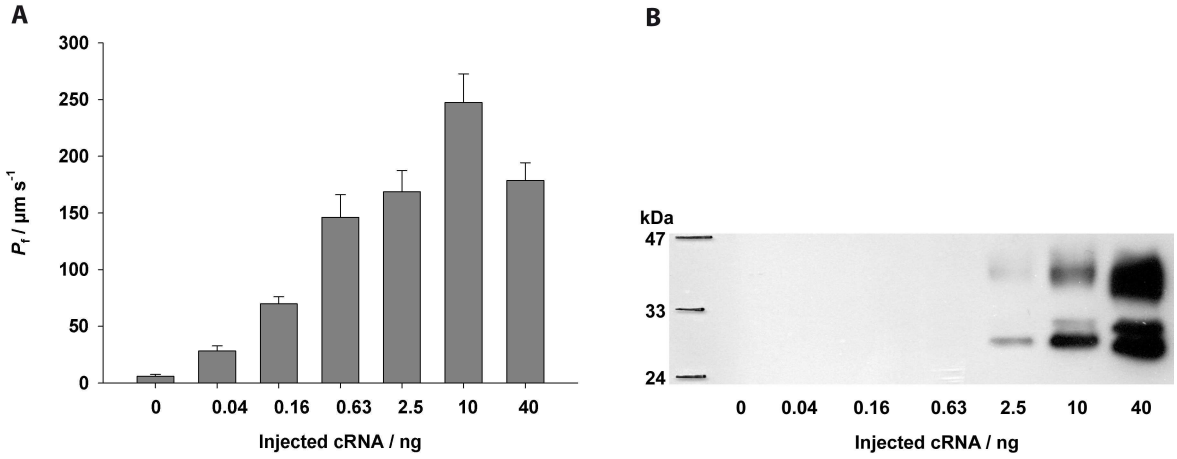

Fig. 4.38: Dependence of the oocyte swelling rate and aquaporin production level on the amount of injected cRNA. (A) *Osmotic assays with X. laevis oocytes producing rAQP1, 3 days after injection of the indicated amounts of cRNA. Outward-directed hypotonic NaCl gradient 0.14 osmol/l (tonicity 0.33), room temperature (~ 20 - 25 °C). Average osmotic water permeability coefficients (P_f). Error bars represent the standard errors of the means (n = 11 - 16).* ***(B)*** *Corresponding synthesis of rAQP1 in the membrane fractions of the oocytes. Five oocytes per set were collected and processed, and the equivalent of one oocyte each subjected to SDS-PAGE and Western blotting. Detection was with a rAQP1-directed antibody.*

The measurements were made in the order of injections, so that production times were very similar at about 70 h, with the exception of the 40 ng-oocytes which were tested about 74 h after injection.

The dependence of P_f-values on the amount of injected cRNA in the semilogarithmic plot appears to be sigmoidal. For clarity, standard errors of the means rather than the three- to fourfold higher standard deviations are shown. The osmotic water permeability coefficient of

250 µm/s ± 100 µm/s (standard deviation) for 10 ng cRNA may look like an outlier, but none of the corresponding single oocyte swelling rates were considered unacceptable upon closer inspection. Remarkably, a thousandfold increase in the amount of injected cRNA (from 0.04 ng to 40 ng) increased the P_f approximately sixfold (from 28 to 180 µm/s), whereas the corresponding total protein synthesis increased much more as judged by Western blotting (Fig. 4.38 B). Thus, injection of about 1 ng rather than 5 ng aquaporin-encoding cRNA (Figs. 4.13 and 4.14) would certainly not result in a corresponding fivefold reduction of the oocyte swelling rate.

4.3.2 Osmotic assays with *S. cerevisiae* protoplasts

Yeast protoplast swelling or shrinking assays are less well established than the corresponding *X. laevis* oocyte assays. Unlike for the latter, protocols vary substantially and two yeast species, *S. cerevisiae* and *Pichia pastoris,* have been used (Bertl and Kaldenhoff, 2007, Fischer *et al.*, 2009, Pettersson *et al.*, 2006). In addition, it is not even necessary to destabilize the cell wall of *S. cerevisiae* for osmotic water permeability measurements (Soveral *et al.*, 2007).

No systematic study of water permeability assays with yeast cells was conducted, and the protocol established by a colleague was followed for uniformity. Nevertheless, a few explorative measurements were made regarding the choice of osmotic gradient and the use of zymolyase, and the evaluation of light scattering data was looked at more carefully.

Light scattering curves

Evaluation of yeast shrinkage or swelling assays was usually restricted to the determination of rate constants. As shown in the following figure, another useful quantity can be obtained from the light scattering curves if the baseline detector voltage is measured (Fig. 4.39).

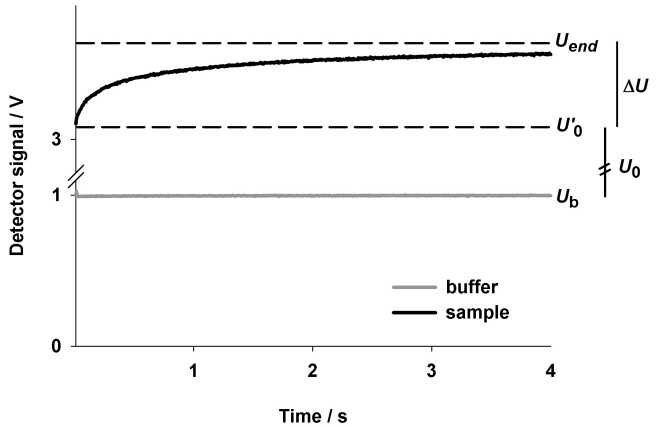

Fig. 4.39: Averaged buffer and sample light scattering curves from a stopped-flow experiment with yeast protoplasts. *U_b = baseline voltage, U'_0 = starting voltage, U_{end} = ending voltage, U_0 = net starting voltage, ΔU = voltage amplitude.*

Dividing the voltage amplitude (ΔU) by the net starting voltage (U_0) yields the relative signal amplitude ($\Delta U/U_0$), a quantity which may correlate with the volume change of the yeast protoplasts.

In the absence of baseline voltage measurements, only the gross starting voltage (U'_0 in Fig. 4.39) is known, and the calculated relative signal amplitude will be too small ($\Delta U/U'_0 < \Delta U/U_0$). For experiments conducted on seventeen days over the course of two months, the baseline voltage was found to be about one third of the starting voltage ($U_b \approx U'_0/3$).

Time constants and relaxation times

Nominal relaxation times (τ) are easy to determine, and for single exponential functions ($A \cdot e^{-kt}$) they are equal to the reciprocal time constant (k). For double exponential functions of the type $A_1 \cdot e^{-k1t} + A_2 \cdot e^{-k2t}$ the relation $\tau^{-1} = (A_1 \cdot k_1 + A_2 \cdot k_2) / (A_1 + A_2)$ may hold (Quigley *et al.*, 2000).

As an example, Table 4.8 lists the nominal relaxation times, time constants and amplitudes determined for the experiments presented in Figs. 4.4 and 4.11. The curve fitting was done with the programme “Biokine” which requires the choice of three time points. Previously, the choice of the first and the last time point had been found to affect the resulting time constants and amplitudes. For uniformity, they were chosen in this case to be 0.05τ, τ, and 5τ. Some curves yielded only a single time constant and amplitude, in which case the former matched the nominal inverse relaxation time, as expected. Please note that the actual equation used for fitting was $y = at + b + A_1 \cdot e^{-k1t} + A_2 \cdot e^{-k2t}$, and that the term “a” was set to zero since there was no baseline drift (Fig. 4.39).

Table 4.8: Osmotic assay with yeast transformant protoplasts as described in Figs. 4.4 and 4.11. *Relative amplitudes and time constants derived from normalized average curves (n = 8 - 9). k and A stand for the time constants and the amplitudes obtained by fitting the curves to an equation of the type $A_1 \cdot e^{-k1t} + A_2 \cdot e^{-k2t}$. The relative light scattering signal amplitudes ($\Delta U/U_0$) were derived from the corresponding average curves. Please note that the data for wild-type rAQP1 is not the same as the one shown in above-mentioned figures, with another subset of curves (80-second-recordings) used to obtain the constants shown here.*

rAQP1	$\Delta U/U_0$	τ^{-1} (s^{-1})	k_1 (s^{-1})	A_1	k_2 (s^{-1})	A_2
-	0.11	0.10	0.10	-0.93	-	-
wt	0.12	1.20	0.72	-0.43	5.78	-0.29
F56H	0.11	0.27	0.22	-0.80	0.85	-0.13
H180I	0.12	0.50	0.34	-0.67	1.89	-0.19
C189G	0.12	0.83	0.52	-0.62	3.82	-0.24
FH/HI	0.11	0.17	0.16	-0.93	-	-
FH/CG	0.11	0.20	0.19	-0.92	-	-
FH/HI/CG	0.12	0.41	0.28	-0.66	0.95	-0.23
H180A	0.14	0.59	0.38	-0.62	1.77	-0.23
H180L	0.09	0.77	0.51	-0.62	3.75	-0.24
H180M	0.12	0.37	0.29	-0.77	1.44	-0.13
H180F	0.09	0.20	0.20	-0.92	-	-
H180N	0.10	0.42	0.26	-0.63	1.64	-0.23
H180Q	0.12	0.56	0.41	-0.67	2.08	-0.21

The obtained time constants could be compared to the nominal inverse relaxation times by plotting them against each other (Fig. 4.40).

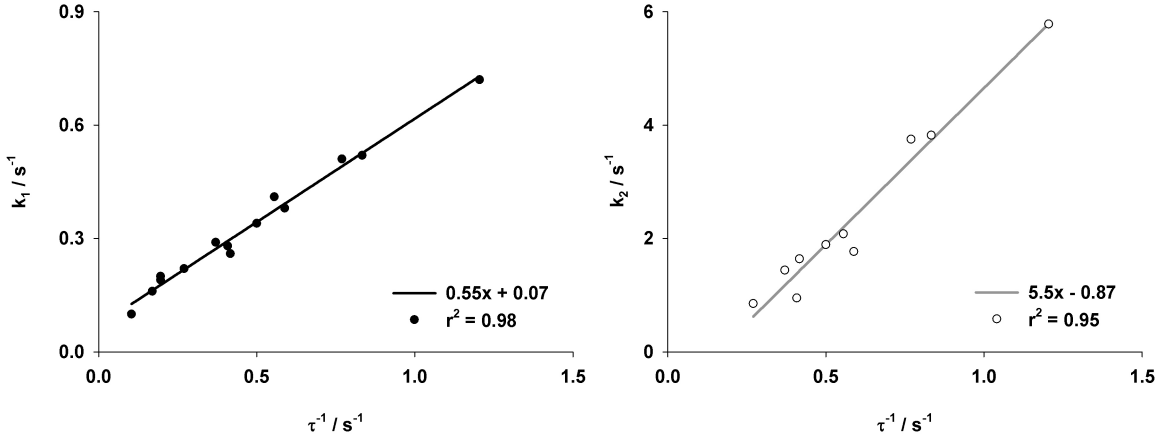

Fig. 4.40: Plots of nominal inverse relaxation times (τ^{-1}) against either of the time constants (k_1 or k_2) listed in Table 4.8. *Equations and correlation coefficients of the linear fits are given.*

The resulting correlation between τ^{-1} and k_1 was remarkable ($r^2 \approx 0.98$), for k_2 it was less pronounced ($r^2 \approx 0.95$). Calculating the mean inverse relaxation times from the amplitudes and time constants by the formula $\tau^{-1} = (A_1 \cdot k_1 + A_2 \cdot k_2) / (A_1 + A_2)$ yielded values about one and a half times as high as the determined ones.

Nominal relaxation times are a suitable means of representing light scattering data of yeast protoplast shrinkage assays. The principal difficulty consists in determining starting voltages for high rates (AQP-producing yeast) and ending voltages, or “plateaus”, for low rates (aquaporin-deficient yeast) of change. An example of the former is illustrated in Figure 4.41. An example of the latter will be seen in Figure 4.42.

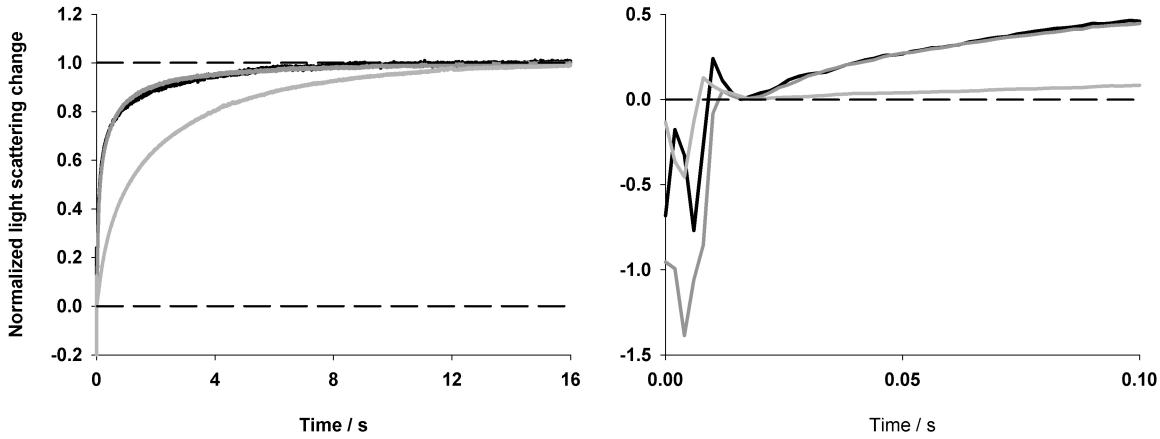

Fig. 4.41: Osmotic assays with yeast protoplasts (31019b Δfps1, pRS426) producing hAQP1-HA. *Inward-directed hypertonic sorbitol gradient 0.30 mol/l (tonicity ~ 1.23), Tris/HCl 10 mM, pH ~ 7, 21 ℃. Normalized average curves (n = 8 - 9) derived from three experiments performed on different days over the course of two weeks. Dashed lines mark normalization borders.* ***Left:*** *Full measurement time.* ***Right:*** *First 100 ms. The dead-time was about 20 ms.*

The time close-up in the righthand graph of Figure 4.41 reveals the assumptions which had to be made due to the sample mixing deadtime. Estimating the true starting point by extrapolation was tried but did not give comparable results. Instead, choosing distinctive features such as “hooks” marking the beginning of a regular light scattering signal change allowed very comparable normalization, especially for measurements made on the same day. A reliable method would be the mixing of samples with the same (isosmotic) buffer: The resulting horizontal light scattering curve would indicate the correct starting voltage.

Osmotic gradient

Initially, the yeast protoplast shrinkage assays were performed at a hypertonic sorbitol or sucrose gradient of 0.3 osmol/l, resulting in a tonicity change of more than 20 % (from 1.33 osmol/l to1.63 osmol/l), and thus in a negative volume change of up to 20 %.

In 1970, Macey and Farmer published the results of osmotic assays with red blood cells, for which they had made sure that volume changes were restricted to ±10 %. Reading this article led to an experiment in which the osmotic gradient was varied from 75 mosmol/l to 300 mosmol/l by premixing Buffers IV and III (3.5) within the stopped-flow apparatus. Its results are shown in Figure 4.42.

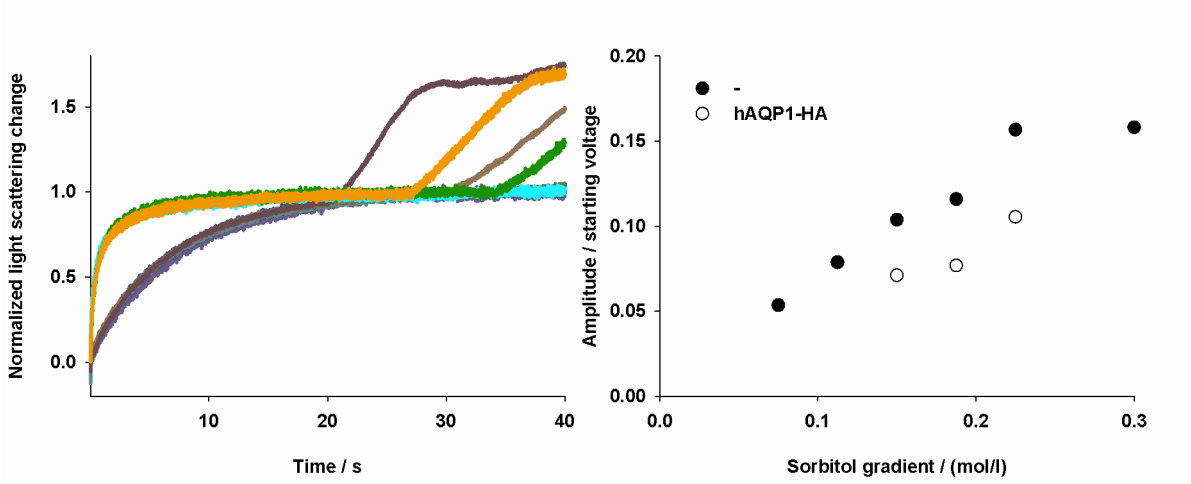

Fig. 4.42: Osmotic assay with yeast protoplasts (BY4742 Δfps1, pRS426) producing no AQP or hAQP1-HA. *Inward-directed hypertonic sorbitol gradients ranging from 0.075 to 0.3 osmol/l (tonicity ~ 1.06 - 1.23), at 21 ℃.* ***Left:*** *Normalized average curves (n = 4 - 6). Nine curves are shown, overlapping in two groups which correspond to the two yeast transformants.* ***Right:*** *Corresponding detector voltage amplitudes divided by the starting voltages ($\Delta U/U'_0$), plotted against the sorbitol gradient.*

The shape of the normalized light scattering curves was independent of the osmotic gradient. The relative signal amplitude ($\Delta U/U'_0$) was approximately proportional to the sorbitol gradient. The shift between amplitudes obtained with aquaporin-deficient and hAQP1-HA-producing yeast may have been due to the deadtime-obstructed localization of the starting voltage for the aquaporin-producing yeast, as shown in Figure 4.41. In the absence of an osmotic gradient, there was an increase in light scattering intensity of about 0.3 % ($\Delta U/U'_0$ = 0.003). The baseline voltage was not determined in this experiment.

The upward deviation seen in four out of the nine light scattering curves in Figure 4.42 was typical for yeast protoplast shrinkage assays performed with sorbitol or sucrose gradients. It was found that the higher the osmotic gradient, the earlier their onset. Since they make it difficult to estimate ending voltages (plateaus) and thus signal amplitudes needed for normalization, a smaller gradient of 0.15 osmol/l was chosen for all subsequent assays. Remarkably, no such upward deviations were seen for hypertonic glycerol gradients with sucrose as the base osmolyte (see Fig 4.31, left, no AQP). Microscopy (300-fold magnification) revealed that they are probably not due to the lysis of yeast protoplasts.

Osmotic water permeability coefficients

The equation used to calculate osmotic water permeability coefficients of *X. laevis* oocytes (3.6) can also be used for *S. cerevisiae* protoplasts. One difficulty lies in knowing the extent of the osmotically induced volume change.

For the experiments summarized in Table 4.8, baseline detector voltages were measured and relative light scattering amplitudes could be calculated more or less accurately. An average of 0.11 ± 0.012 (n = 14) was found. The nominal tonicity after mixing was 1.11 (1.48 osmol/l divided by 1.33 osmol/l), and the tonicity change was thus 0.11, a value

identical to the relative light scattering amplitude. The real volume change of the yeast cells was not known, but a clue came from the results published by Soveral *et al.* in 2008: under similar conditions (initial sorbitol concentration of 1.4 mol/l) a tonicity change of +10 % led to a volume change of approximately -5 % as estimated from a fitted curve (Fig. 1 b in the cited publication). The results are based on microscopic measurements of the diameters of intact yeast cells before and after osmotic shocks of varying tonicities. Assuming that protoplasts behave similarly, the osmotic water permeability coefficient of the aquaporin-deficient yeast protoplasts described in Table 4.8 can be calculated as follows (see 3.6 for a description of the symbols):

$P_f = (V_0 \cdot \Delta(V/V_0)/\Delta t) / (S_0 \cdot V_w \cdot \Delta c)$

$\approx (14\ \mu m^3 \cdot 0.005\ s^{-1}) / (28\ \mu m^2 \cdot 0.018\ l/mol \cdot 0.15\ mol/l)$

$\approx 0.9\ \mu m/s$

The volume and the surface area of yeast protoplasts were calculated assuming a spherical shape and an average radius of 1.5 µm. For an external sorbitol concentration of 1.4 mol/l Soveral *et al.* found an average cell volume of about 10 to 15 μm^3, although with a different yeast strain (10560-6B).

The rate of relative volume change was obtained the following way:

By definition, the total relative voltage change was 1. The initial rate of relative voltage change was 0.10 s^{-1} (Table 4.8). The total relative volume change was estimated to be -5 % or -0.05, as explained above. Multiplying the latter with the initial rate gives -0.005 s^{-1}. For formal reasons, the positive value of 0.005 s^{-1} was used. Please note that the initial rate was also estimated directly by measuring the initial slope of the normalized curve which was found to be 0.20/2.0 s or 0.10 s^{-1}, identical to τ^{-1} and to k.

The true osmotic gradient was not known. Instead, the nominal gradient of 0.15 mol/l was used in the calculation, assuming that yeast cells precisely adjust their intracellular osmolarity to the external one.

Thus, for protoplasts of the aquaporin-deficient *S. cerevisiae* strain 31019b Δfps1, the osmotic water permeability coefficient at 20 °C was of the order of 1 µm/s. Using their microscopy data and a more elaborate calculation, Soveral *et al.* found a corresponding value of 2 µm/s for the aquaporin-deficient *S. cerevisiae* strain 10560-6B Δaqy1/2.

Sorbitol versus sucrose

For all glycerol permeability measurements performed with yeast protoplasts, the base osmolyte was sucrose rather than sorbitol. The reason for this choice was an apparent in-

hibition of glycerol flux through *Plasmodium falciparum* AQP by sorbitol as seen in Figure 4.43.

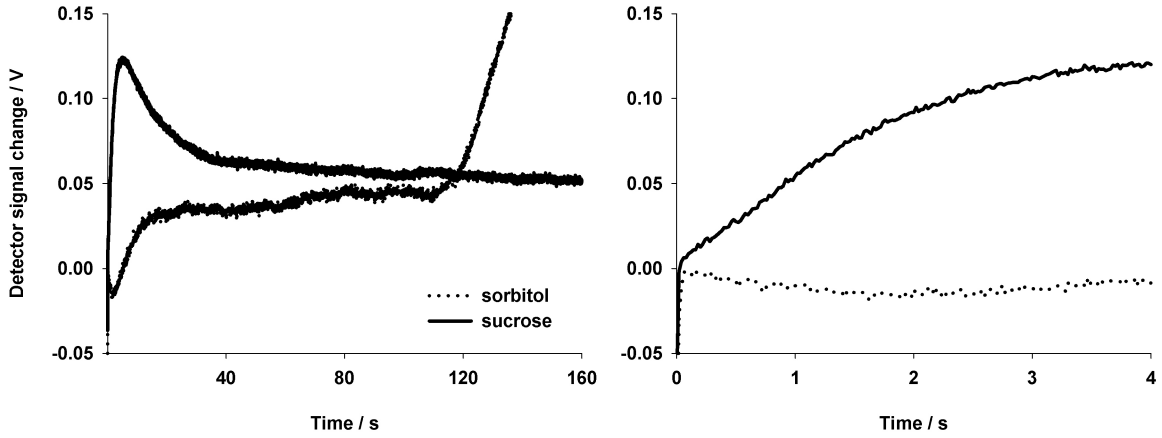

Fig. 4.43: Glycerol permeability assay with yeast protoplasts (BY4742 Δfps1 Δgpd1/2, pDR196) producing PfAQP. *Inward-directed hypertonic glycerol gradient 0.30 osmol/l, Tris/HCl 10 mM, pH ~ 7, 21 ℃. The base osmolyte was either sorbitol or sucrose (both 1.2 M), as indicated. Average curves (n = 6 or 8).* ***Left:*** *Full measurement time.* ***Right:*** *First four seconds.*

It was reasoned that sorbitol might have this effect because of its polyol structure allowing it access to the pore of PfAQP. Sucrose did not cause any such inhibition, possibly due to its different size and shape. The phenomenon was studied more closely by colleagues (Song *et al.*, 2012).

Zymolyase

Fischer *et al.* (2009) did not use zymolyase or any other lytic enzyme for the preparation of *Pichia pastoris* protoplasts. One of the authors confirmed this upon request, explaining that 2-mercaptoethanol appeared sufficient for protoplast preparation, and that it was difficult to obtain reproducible results when using zymolyase.

Two experiments were performed to see what effect the leaving out of zymolyase during yeast protoplast preparation would have on osmotic assays. Their results are shown in Figure 4.44. In Experiment 1, relaxation times were almost identical for hAQP1-HA-producing yeast protoplasts prepared with or without zymolyase (0.25 s and 0.24 s). An oscillation was seen for the latter. This oscillation of about 4 Hz was unrelated to the signal-to-noise ratio which was comparable for both curves. It began after about 0.3 s. In Experiment 2, the corresponding relaxation times were markedly different (1.9 s and 0.8 s), but both were well below that obtained with the aquaporin-deficient protoplasts (4.9 s). No oscillation was observed. For the protoplasts prepared without zymolyase, the relative light scattering amplitude ($\Delta U/U'_0$) was about one third of those of the other two samples. In Experiment 1, there had been no such difference.

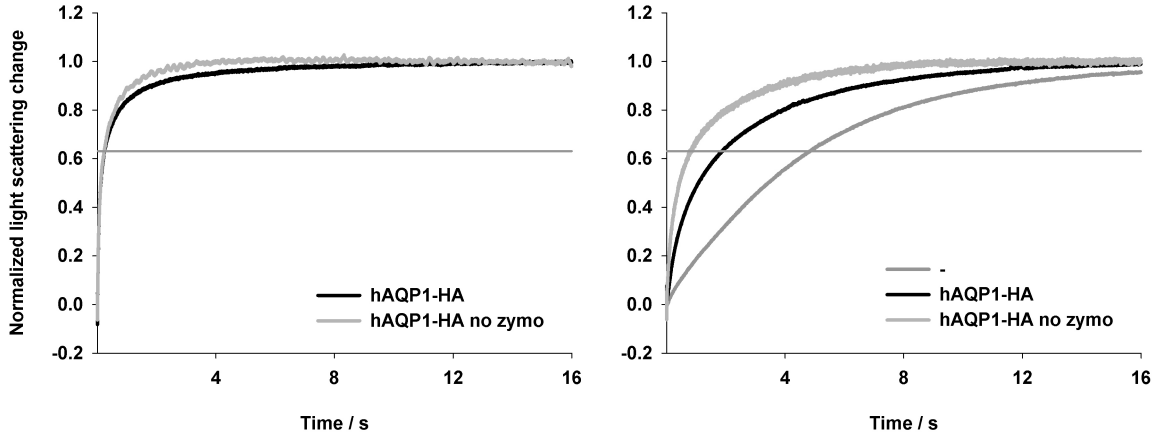

Fig. 4.44: Osmotic assays with yeast protoplasts (31019b Δfps1, pRS426) producing no AQP or hAQP1-HA, prepared with or without zymolyase. *Inward-directed hypertonic sorbitol gradient 0.30 osmol/l (tonicity ~ 1.23), Tris/HCl 10 mM, pH ~ 7, 21 ℃. Normalized average curves. The horizontal line marks the ordinate value at which the nominal relaxation time was read (y = 1 - 1/e). "Zymo" stands for zymolyase.* ***Left:*** *Experiment 1 (n = 8). The control curve is identical to the one shown in Fig. 4.26 (right).* ***Right:*** *Experiment 2 (n = 8 - 9). Control curves are identical to those shown in Fig. 4.27.*

In summary, zymolyase did not appear to be necessary for *S. cerevisiae* protoplast preparation. Despite this finding, its use was continued.

4.3.3 *S. cerevisiae* growth assays in liquid medium

Measuring yeast growth turbidimetrically with the "Bioscreen microbiology reader" allowed for the following variations: Yeast strain, medium, medium volume, cell dilution, temperature, shaking intensity and duration, wavelength, and the total duration of growth.

Of these, the wavelength was never varied (420 - 580 nm wideband filter), and the yeast strain was chosen according to the assay. The medium composition for both ammonia and methylamine assays was varied extensively, and the most important results will be presented in the respective sections. Effects of temperature, shaking parameters, and duration of growth were not tested systematically, but they are important, and examples will be given below and in Section 4.3.4.

Yeast cell dilution

The yeast cell dilution was the subject of the first assay performed using the "Bioscreen". Its results are shown in Figure 4.45.

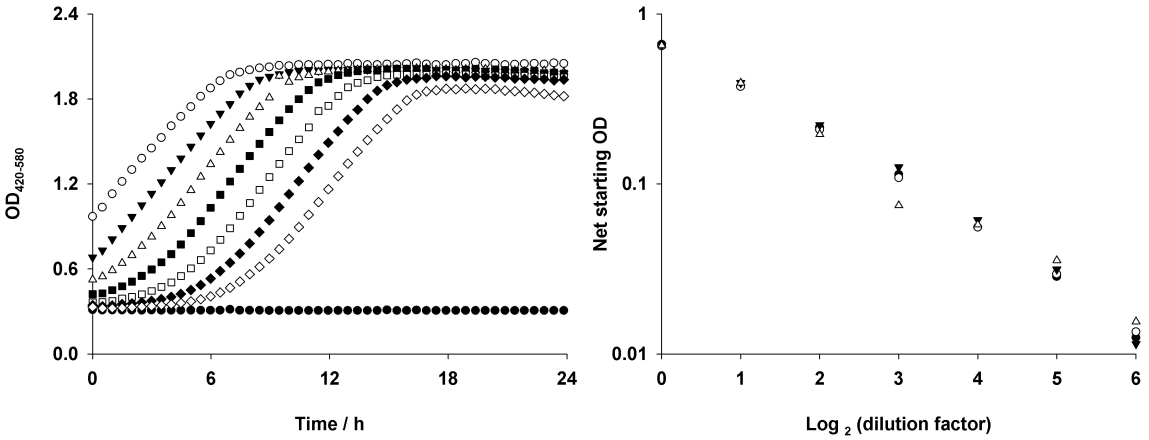

Fig 4.45: Yeast growth in liquid YPD medium at 29 °C, detected turbidimetrically ($OD_{420-580}$). *The strain was 31019b Δfps1. Twofold dilution series of the cell suspensions. The total volume per well was 390 µl.* ***Left:*** *Sample growth curves. The filled circles mark the OD of YPD medium (blank).* ***Right:*** *Net starting ODs (blank subtracted) of four sets of growth curves, plotted logarithmically against the yeast cell dilution factor exponent.*

Three things became apparent: First, each twofold dilution of inoculant cultures led to a constant delay of the onset of fastest growth (~ 2 h in this experiment). Second, the maximum OD was more or less independent of the starting OD, *i. e.* for each additional twofold dilution, the yeast cells divided once more. Third, within an OD range of about 0.01 to 0.65 (420 - 580 nm, path length ~ 9.5 mm), the logarithm of the net starting OD (OD of the medium subtracted) is inversely proportional to the logarithm of the dilution factor (2^n). The same was found in two other experiments, for water and 60 % glycerol, and path lengths of about 7.5 mm and 10 mm, with each doubling of the yeast cell number leading to an increase of OD by a factor ranging from about 1.8 to 2.2. Thus, for the apparent absorption caused by yeast cell light scattering, the linear range extends from about 0.01 to about 0.6 for a path length of close to 10 mm. Values above this range lead to an underestimation, values below to an overestimation of the yeast cell concentration.

The concentration of yeast cells for a given OD was not determined, but numerous plate assays (*e. g.* Fig. 4.2, SD KHL plate) allowed an estimate of about 10 cells per 5 µl of a suspension of nominal OD_{600} (10 mm) ≈ 0.001, or about $2 \cdot 10^6$ ml^{-1} for an OD_{600} of 1. A colleague (J. Song) found a corresponding value of $1.3 \cdot 10^6$ ml^{-1} by microscopic measurement using a counting chamber.

For the above experiment, the shortest doubling time of the yeast cells was determined to be about 4 - 5 h (t_d = ln 2 / k, for the log-linear range OD fitted to $a \cdot e^{kt}$), or about 2 - 3 h if using dilution-corrected OD values (see 5.2.1).

Volume of growth medium

The volume of medium was varied in a single experiment in which the yeast transformant 31019b Δfps1 pRS426 Fps1 was grown in ammonia assay medium (NH_4^+ 10 mM, MOPS

40 mM, pH 7.2). From 350 µl to 200 µl, the volume-adjusted AUC 48 h was found to increase linearly from about 40 h to about 60 h, and to correlate with the surface-to-volume ratio of the medium. At 175 µl and at 150 µl, AUC-values dropped to about 55 h. From 300 µl downwards, the relative standard deviation (5 wells for each volume) increased from 1 % to just over 30 %, due to the occurrence of yeast stickiness described below.
Previously, 300 µl (half the well volume) had been used in most experiments, and it seemed a good choice, particularly regarding the low relative standard deviation of yeast growth.

Yeast "stickiness"

Figure 4.46 shows a phenomenon frequently encountered when growing yeast in the "Bioscreen" wells.

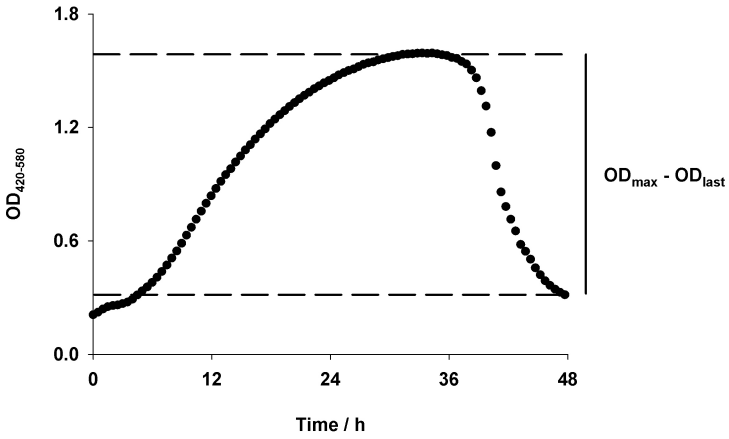

Fig 4.46: Yeast growth in liquid medium at 29 °C, detected turbidimetrically ($OD_{420-580}$). *The transformant was 31019b Δfps1 pRS426 rAQP1 H180A. Ammonia assay medium (NH_4^+ 40 mM, MOPS 40 mM, pH 7.2). The sudden drop in apparent absorption was due to yeast cells accumulating at the circular corner of the well bottom. The difference between the maximum OD and the last OD for a chosen period is a useful indicator easily determined for all wells without having to look at the growth curves.*

A look at an affected well would reveal a butterfly-shaped yeast-free zone at the bottom, with most cells sticking to the circular corner, and some cells distributed along a line perpendicular to the shaking axis.
It was found that the incidence of yeast stickiness increased with the total duration of growth (especially after more than about 2 days), and with increased stress conditions such as high pH, in particular for aquaporin-deficient yeast transformants. Another important cause was the location on the assay plate, with the edges and corners most affected, as shown in Table 4.9.

Table 4.9: Incidence of yeast stickiness for a growth period of 48 h, as measured by the difference between maximum OD and last OD of a growth curve (Fig. 4.46). *Differences larger than 0.05 are marked in grey. Plate 1: Averages from 38 experiments. Plate 2: Averages from 33 experiments. The nominal standard deviations (non-Gaussian distribution) correlated with the averages. For all experiments, the total volume per well was 300 µl. Rows 191 - 200 and 201 - 210 are situated next to each other within the incubation chamber. The numbering, starting with Well 101 rather than Well 1, is according to the data output file.*

Plate 1	100	110	120	130	140	150	160	170	180	190
1	0.04	0.05	0.05	0.01	0.08	0.01	0.09	0.02	0.05	0.08
2	0.03	0.05	0.00	0.02	0.03	0.01	0.01	0.04	0.03	0.06
3	0.02	0.00	0.00	0.01	0.02	0.04	0.02	0.02	0.06	0.06
4	0.01	0.00	0.01	0.01	0.04	0.05	0.01	0.01	0.05	0.06
5	0.01	0.01	0.01	0.01	0.01	0.06	0.05	0.02	0.01	0.06
6	0.04	0.01	0.03	0.02	0.04	0.05	0.03	0.01	0.04	0.02
7	0.05	0.03	0.04	0.02	0.03	0.01	0.01	0.02	0.05	0.03
8	0.03	0.02	0.01	0.01	0.02	0.01	0.01	0.02	0.06	0.04
9	0.06	0.03	0.01	0.01	0.02	0.01	0.03	0.01	0.06	0.05
10	0.09	0.07	0.00	0.03	0.01	0.03	0.01	0.02	0.04	0.08

Plate 2	200	210	220	230	240	250	260	270	280	290
1	0.13	0.02	0.06	0.01	0.05	0.01	0.03	0.01	0.06	0.06
2	0.07	0.01	0.01	0.00	0.04	0.01	0.01	0.01	0.01	0.07
3	0.01	0.01	0.00	0.01	0.04	0.01	0.03	0.02	0.01	0.04
4	0.01	0.01	0.00	0.00	0.04	0.01	0.03	0.01	0.02	0.06
5	0.01	0.01	0.01	0.01	0.02	0.01	0.03	0.01	0.01	0.04
6	0.01	0.01	0.01	0.01	0.01	0.01	0.03	0.01	0.01	0.04
7	0.01	0.01	0.01	0.02	0.02	0.02	0.02	0.02	0.01	0.02
8	0.01	0.01	0.02	0.00	0.01	0.01	0.01	0.01	0.01	0.02
9	0.01	0.02	0.04	0.02	0.00	0.00	0.02	0.03	0.01	0.03
10	0.04	0.04	0.04	0.03	0.01	0.04	0.01	0.03	0.01	0.09

The above table represents a crude analysis, since the only criteria were a minimum experiment duration of 48 h, and a total volume per well of 300 µl. Yeast strain and media varied, and there was a tendency for “negative control” yeast (no aquaporin) to be situated in Plate 1. Please note that the first wells in odd-numbered “columns” (*e. g.* 101 and 281) and the last wells in even-numbered ones (*e. g.* 120 and 300) are located more closely to the plate edges than are their respective counterparts (*e. g.* 290). This is due to the “honeycomb” pattern of the assay plates (Fig. 3.2).

One clue as to what might cause yeast stickiness came from a look at a plate which had been left to stand for several months: Evaporation of the liquid (which contained no microorganisms) was most pronounced at the edges, particularly in wells situated more closely to the edges and corners.

In practise, $OD_{max} - OD_{last} \geq 0.1$, or a relative value of $(OD_{max} - OD_{last}) / OD_{max} \geq 0.2$, was chosen as an approximate criterion for data rejection, with a final decision taken only after looking at the individual growth curves. If applicable, the most important samples were not placed in edge or corner wells (blanks are perfectly suited for these). If not all wells of a plate were needed, those bordering sample-containing ones were filled with a liquid such as medium or water (300 µl).

As discussed in Section 5.2.1, decreases in OD due to yeast stickiness could have been avoided by choosing no shaking. Nevertheless, their occurrence has been informative.

Temperature

In a series of four experiments, growth of yeast transformants in various media at 17 ℃, 23 ℃, 29 ℃ and 35 ℃ was tested, and was found to increase from 17 ℃ to 29 ℃, and to decrease from 29 ℃ to 35 ℃, as judged by areas under growth curves for 48 h.

Duration of growth

Most experiments with the "Bioscreen" were performed for durations of 48 h to 72 h, and in some cases up to 120 h. Evaluation of relative growth differences between yeast transformants in ammonia assays showed that at 48 h these are almost fully developed, *i. e.* longer durations were not more informative (see Figure 4.24 for an example). Nevertheless, depending on the intent of the experiment, longer durations should be considered.

4.3.4 Ammonia assay

As seen in Figure 4.25, yeast transformant growth under ammonia assay conditions depended on the pH, with yeast synthesizing presumably ammonia-permeable aquaporins more able to thrive at slightly alkaline pH than those synthesizing other or no aquaporins. In one assay, the dependence on both pH and buffer concentration was investigated, with the results shown in Figure 4.47.

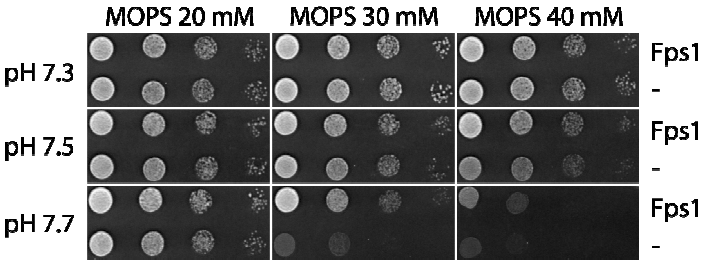

Fig. 4.47: Ammonia assay. *Yeast transformants (31019b Δfps1, pRS426 or pRS416 Fps1) were spotted in tenfold dilution series starting with an OD_{600} of 1, and grown at 29 ℃ for 3 days followed by 2 days at 4 ℃. The ammonium concentration was 4 mM, the nominal pH and the buffer concentration varied as indicated.*

The aim was to define the ammonia assay medium composition which would reproducibly allow Fps1-producing but not aquaporin-deficient yeast transformants to grow. Preparing multiple sets of assay plates was cumbersome and rather wasteful, however. In addition, autoclaving conditions were hardly reproducible with the available equipment.

The “Bioscreen” turbidometer allowed the use of liquid media which could be filtered and the pH of which was thus known more accurately. It was used extensively to test ammonia assay conditions.

In two consecutive experiments, the pH as well as the concentrations of buffer, ammonia, yeast nitrogen base and D-glucose were varied, one at a time, and L-proline was tested as a control nitrogen source (replacing ammonium ions), the standard medium composition being: Ammonium sulfate 5 mM, MOPS/NaOH 40 mM pH 7.1, yeast nitrogen base 0.17 % and D-glucose 150 mM (Fig. 4.48).

By increasing the pH from 6.6 to 7.5 (Fig. 4.48 A), growth of the aquaporin-deficient yeast was almost fully abolished, whereas growth of the Fps1-producing yeast was robust up to a pH of about 7. The AUC dependence on pH appeared to be sigmoidal, and although data beyond pH 7.5 was missing, there seemed to have been an alkaline shift of the Fps1-AUC-curve by about 0.6 pH units, corresponding to an approximate quadrupling of the hydroxide ion concentration. The experiment was not repeated, but a corresponding one had been performed previously, using the same media (fresh at the time) and several additional yeast transformants, with essentially the same result.

Varying the buffer concentration (Fig. 4.48 B) did not have any marked effect on the growth of either transformant, unlike for the plate assay shown in Figure 4.47 (this might be explained by the autoclaving necessary for the making of agar media). The experiment was repeated for a logarithmic range of the MOPS concentration (400 mM - 2 mM, and 0 mM) at pH 6.9 and 40 mM ammonium, and it was found again that MOPS had little effect up to a concentration of about 100 mM. At 400 mM it prevented growth.

Varying the ammonium ion concentration (Fig. 4.48 C) had a surprising effect: At 2 mM, there seemed to be no difference in growth, at 14 mM the difference was fully developed, the opposite of what had been expected. The experiment was repeated for a logarithmic range of ammonium concentration, as will be shown below.

With proline as the nitrogen source (Fig. 4.48 D), aquaporin-deficient yeast transformants grew slightly better than Fps1-producing ones. It appeared to be a less efficient nitrogen source than ammonium. A range of potential nitrogen sources was tested (Table 4.10).

Lowering the standard yeast nitrogen base concentration tenfold, from 0.17 % to 0.017 % (Fig. 4.48 E), did not markedly affect Fps1-transformant growth. If anything, it improved growth, with an apparent maximum at about 0.05 %. For aquaporin-deficient yeast, growth improved markedly with a similar maximum at about 0.05 %. The experiment was repeated for a logarithmic concentration range (not shown), with a different result: From 0.17 % to $0.7 \cdot 10^{-3}$ % the AUC 48 h decreased monotonously from about 30 h to about 5 h (both transformants grew equally well in that experiment). Without yeast nitrogen base, the AUC 48 h was approximately 2 h.

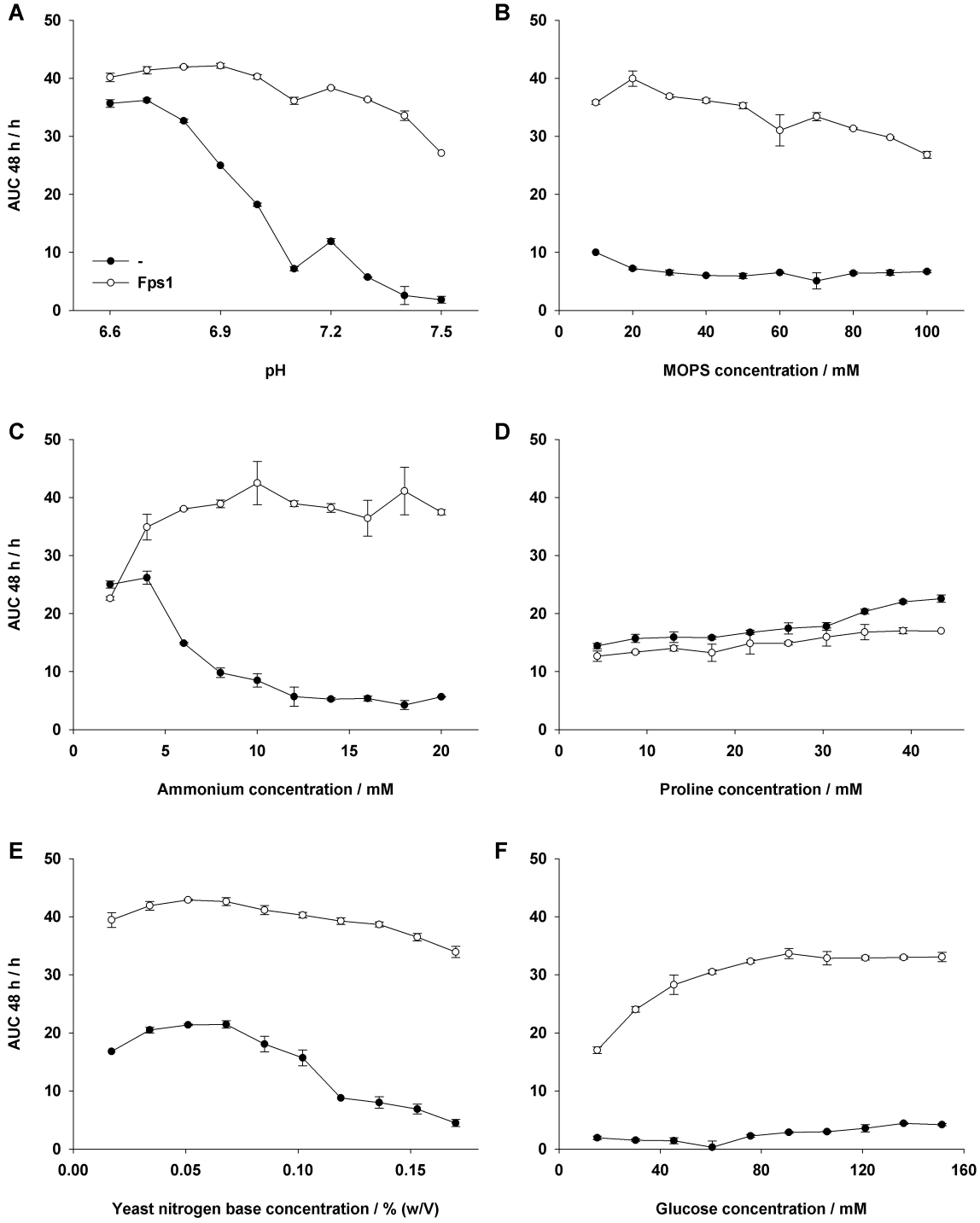

Fig. 4.48: Ammonia assay medium component concentrations varied one at a time. *Yeast transformants (31019b Δfps1, pRS426 or pRS416 Fps1) were grown in liquid media at 29 ℃. The standard medium composition was ammonium sulfate 5 mM, MOPS/NaOH 40 mM pH 7.1, yeast nitrogen base 0.17 % and D-glucose 150 mM. Growth was detected turbidimetrically ($OD_{420-580}$) and quantified by calculating areas under growth curves to 48 h (AUC 48 h). Averages of measurements of 3 wells (2 in a few cases, single measurement in one case). Error bars show standard deviations.* ***(A)*** *Variation of the pH. Media of pH 6.6. to 6.8 were buffered with 40 mM MES/NaOH. Medium of pH 7.1 was prepared one day before the assay, the other media had been prepared two months before.* ***(B)*** *Variation of the MOPS concentration.* ***(C)*** *Variation of the ammonium concentration. The pronounced AUC variability for Fps1-transformants was not due to the occurrence of yeast stickiness.* ***(D)*** *L-Proline as an alternative nitrogen source. The standard concentration was 8.7 mM (0.1 % w/V).* ***(E)*** *Variation of the yeast nitrogen base concentration.* ***(F)*** *Variation of the D-glucose concentration. The pH-, buffer- and NH_4^+-experiments (A - C) and the proline-, YNB- and glucose-experiments (D - E) were performed in groups, three days apart.*

Lowering the standard glucose concentration (~ 150 mM or 1.8 %) led to a decrease in growth of both yeast transformants, although the onset varied (Fig. 4.48 F). The individual growth curves showed a remarkable OD-ceiling effect: The curves overlapped up to a given time at which growth halted within 2 h (not shown). The higher the glucose concentration, the later the sudden stop of growth. The experiment was not repeated.

Following this first series of experiments, only the pH and the ammonium concentration were adjusted for future assays. Varying the ammonium concentration logarithmically at three different pHs gave the results shown in Figure 4.49.

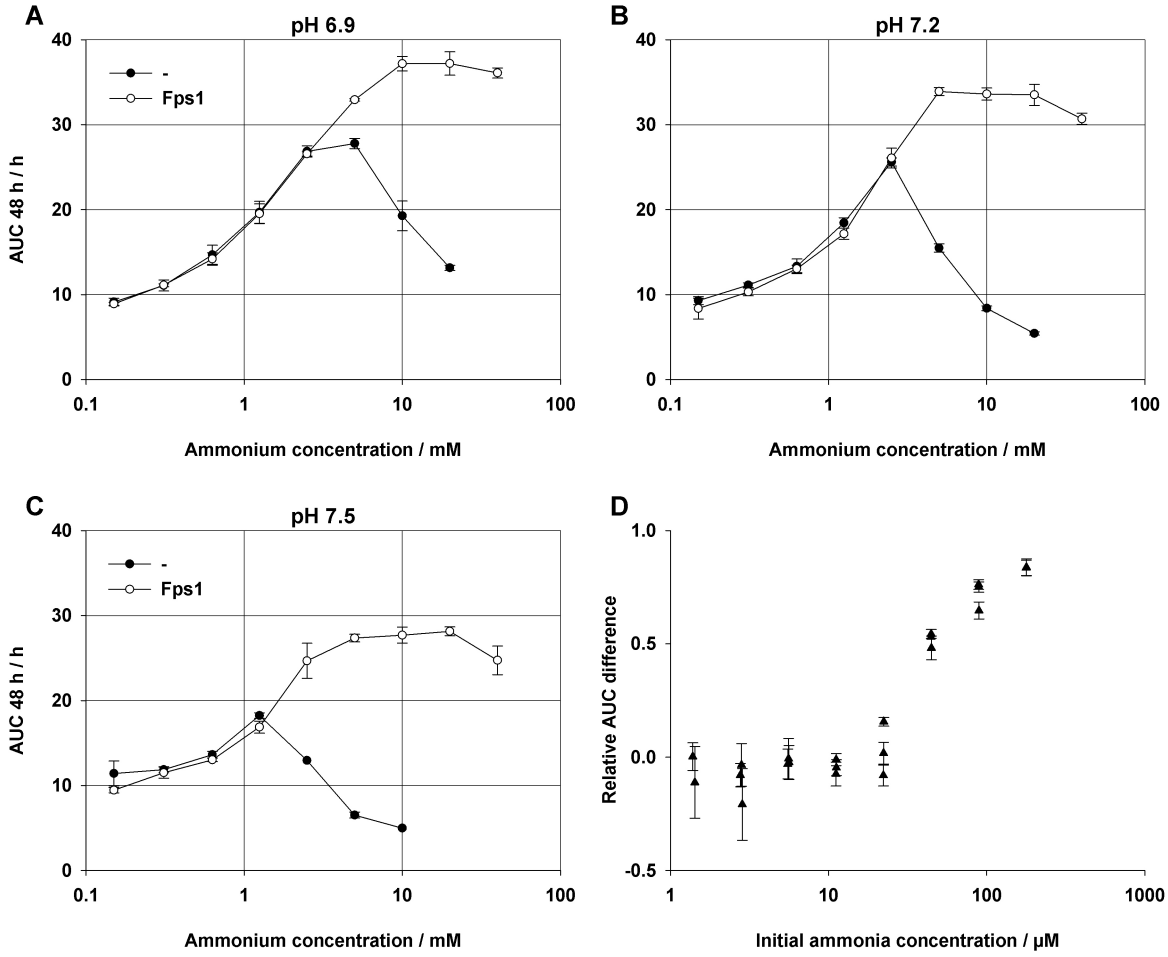

Fig. 4.49: Ammonia assays. *Yeast transformants (31019b Δfps1, pRS426 or pRS416 Fps1) were grown at 29 ℃ in liquid media of varying ammonium concentration at three different pHs. Growth was detected turbidimetrically ($OD_{420-580}$) and quantified by calculating areas under growth curves to 48 h (AUC 48 h). Averages of measurements of 3 wells (2 or 1 in a few cases). Error bars show standard deviations. Missing data are due to yeast stickiness (Fig. 4.46).* ***(A)*** *pH 6.9* ***(B)*** *pH 7.2* ***(C)*** *pH 7.5* ***(D)*** *Relative AUC difference plotted semi-logarithmically against the initial ammonia concentration as calculated by the Henderson-Hasselbalch equation. The relative AUC difference is defined as (AUC pos - AUC neg)/AUC pos, with "pos" and "neg" standing for positive control (Fps1-producing yeast) and negative control (non-producing yeast).*

The result of the previous experiment (Fig. 4.48 C) was confirmed. At pH 6.9 or 7.2, Fps1-producing and aquaporin-deficient yeast grew equally well up to an ammonium concentration of approximately 2.5 mM (~ 14 µM and 28 µM ammonia). At pH 7.5, growth was

equal for an ammonium concentration of up to about 1.5 mM (~ 34 µM ammonia). Higher concentrations of ammonium permitted Fps1-transformants to grow more, although beyond about 10 mM (~ 100 µM ammonia) they were affected as well. The maximum AUC decreased with increasing pH. Plotting the relative AUC difference ($\Delta AUC/AUC_{pos}$) against the logarithm of the calculated initial ammonia concentration revealed a seemingly sigmoidal dependence (Fig. 4.49 D).

The experiment was repeated to find out whether a non-endogenous aquaporin would have the same effect. In addition, continuous shaking was tested to find out whether it would make a difference. The results of two assays are shown in Figure 4.50.

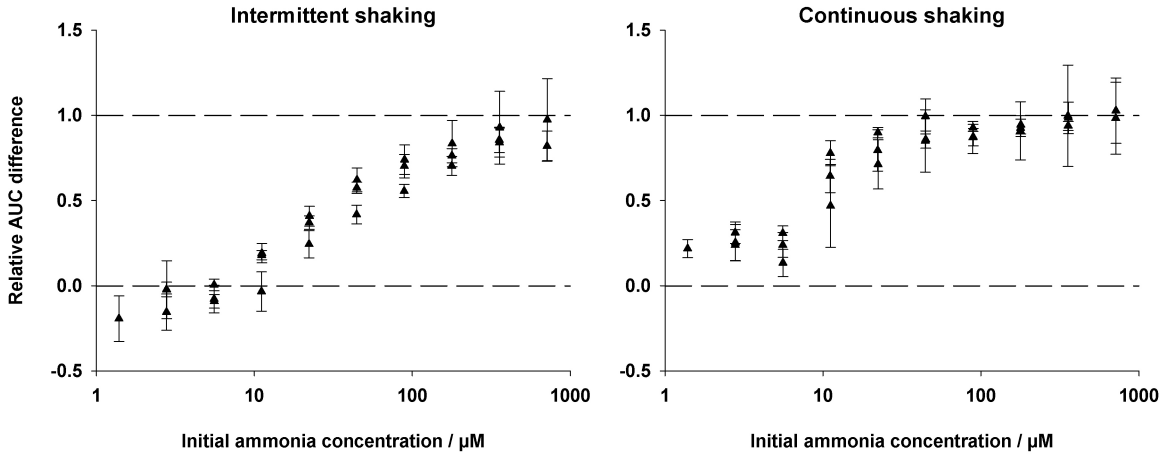

Fig. 4.50: Ammonia assays. *Yeast transformants (31019b Δfps1, pRS426) producing no AQP or rAQP1 H180A were grown at 29 °C in liquid media of varying ammonium concentration at three different pHs (6.9, 7.2, 7.5). Growth was detected turbidimetrically ($OD_{420-580}$) and quantified by calculating areas under growth curves to 48 h (AUC 48 h). Relative AUC difference plotted semilogarithmically against the initial ammonia concentration as calculated by the Henderson-Hasselbalch equation. The relative AUC difference is defined as (AUC_{pos} - AUC_{neg})/AUC_{pos}, with "pos" and "neg" standing for positive control (rAQP1 H180A-producing yeast) and negative control (aquaporin-deficient yeast). Error bars represent nominal standard deviations (n = 3).* ***Left:*** *Intermittent shaking (10 s every 30 min).* ***Right:*** *Continuous shaking. About half of AQP-deficient yeast cultures were affected by stickiness (Fig. 4.46), especially for ammonium concentrations above about 1 mM. The data was used nevertheless, which is why a relative difference of above 1 was obtained in one case. Experiment performed immediately after the first one.*

As in the previous experiment (Fig. 4.49 D), an initial ammonia concentration of more than about 100 µM was necessary to obtain a marked contrast in growth between rAQP1 H180A-producing and aquaporin-deficient yeast, the full difference developing between 10 µM and 1 mM ammonia. Continuous shaking appeared to lower the necessary ammonia concentration, possibly by preventing some kind of concentration gradient from forming. Ammonia concentrations above about 0.7 mM were not obtainable due to precipitation of an unidentified salt. Lowering the yeast nitrogen base concentration by half allowed a doubling of the ammonium sulfate concentration, or an increase of the pH by about 0.3 units, but this possibility was not applied.

In the following experiment, four media of varying pH and ammonium concentration, but of equal initial ammonia concentration, were prepared and tested by growing various yeast transformants in them (Fig. 4.52).

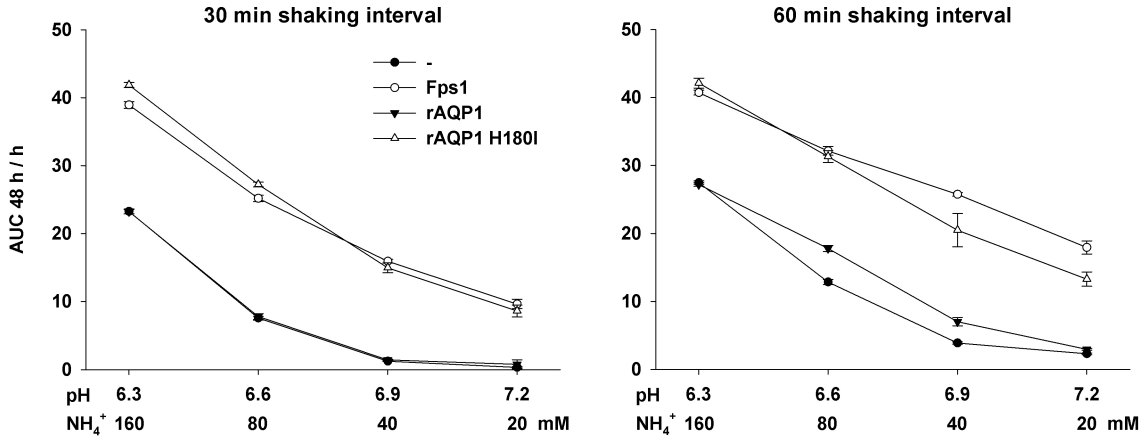

Fig. 4.51: Ammonia assays. *Yeast transformants (31019b Δfps1, pRS426, or pRS416 for Fps1) producing the indicated aquaporins were grown at 29 ℃ in liquid media of varying ammonium concentration and pH (160 mM/pH 6.3, 80 mM/pH 6.6, 40 mM/pH 6.9, 20 mM/pH 7.2), resulting in the same initial ammonia concentration of about 180 µM. Growth was detected turbidimetrically ($OD_{420-580}$) and quantified by calculating areas under growth curves to 48 h (AUC 48 h). Averages of measurements of 4 wells (3 in a few cases). Error bars show standard deviations.* ***Left:*** *30 min shaking interval.* ***Right:*** *60 min shaking interval. The experiment was performed 2 weeks after the first, using the same media.*

The difference in growth did not depend on the initial ammonia concentration alone, the pH was important as well. Thus, two conditions had to be met for liquid ammonia assay medium to be effective: The initial pH had to be close to or above 7, and the initial ammonia concentration had to be above about 100 µM. Following this experiment, and based on considerations of both absolute and relative differences in yeast transformant growth, a pH of 6.9 and an ammonium concentration of 40 mM was decided upon for future assays.

In the second experiment, the shaking interval had been set to 60 min rather than the standard 30 min. It was performed two weeks after the first, using the same media (stored at 4 ℃). Its main result was a general increase in gr owth of all yeast transformants.

The question remained as to how quickly the bulk pH changes during yeast growth under ammonia assay conditions. It was answered by performing the assay with larger volumes using Erlenmeyer flasks (3.4.3). The results of two such experiments are shown in Figure 4.52.

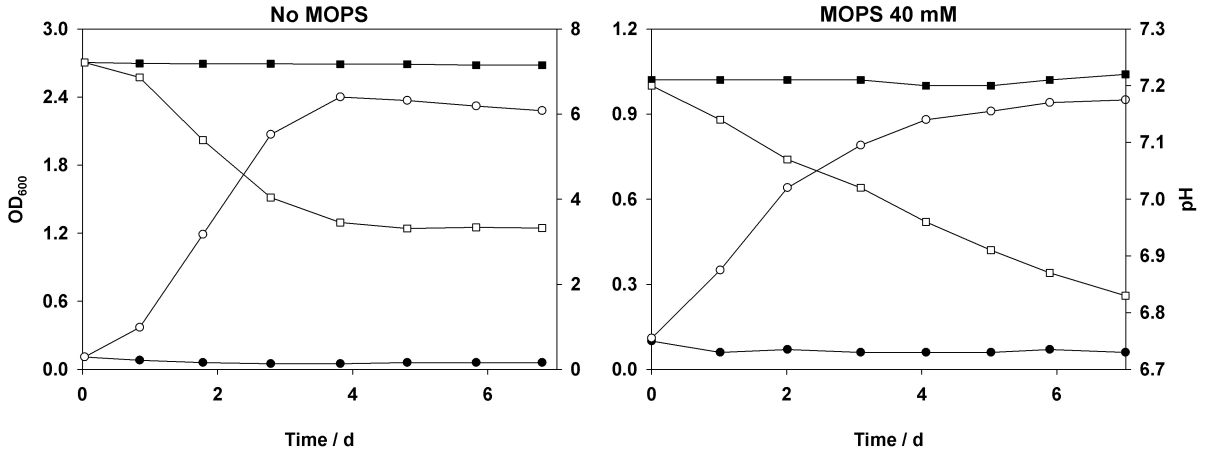

Fig. 4.52: Ammonia assay bulk medium pH changes. *Yeast transformants (31019b Δfps1, pRS426, or pRS416 for Fps1) producing no AQP (black symbols) or Fps1 (white symbols) were grown at 29 °C in liquid media (NH_4^+ 20 mM, pH 7.2) which were either additionally buffered (MOPS 40 mM) or not. The cultures in Erlenmeyer flasks were continually stirred on an orbital shaker at 180 rpm. Samples were taken to detect growth (OD_{600}, circles), and to measure the pH (squares). Please note the different ordinate scale ranges.*

Fps1-producing yeast transformants grew to an OD_{600} of about 2.4 in medium not additionnally buffered, and to an OD_{600} of about 1 in medium buffered by 40 mM MOPS. Non-producing yeast did not grow at all in either medium. Correspondingly, the pH did not decrease in the latter case, whereas in the former it did. Yet even in the absence of MOPS-buffering, the initial bulk pH change was slow, *i. e.* 0.35 units after the first day. The rate of pH change and its stabilization at a value of about 3.3 appeared to correlate with the rate of growth and the onset of the stationary phase, respectively. With MOPS-buffering, the initial rate of pH change was only about 0.07 units per day, and after seven days the yeast had barely reached stationary phase. Consequently, the difference in growth between Fps1-producing and aquaporin-deficient yeast was not due to a rapid acidification of the surrounding medium, at least not at the bulk level. Please note that standard ammonia assay medium, with its yeast nitrogen base concentration of 0.17 %, contains about 7 mM phosphate species. The buffering maximum of a 0.85 % yeast nitrogen base solution was measured and found to be situated approximately between pH 6.5 and 7. The conductivity of the media was also measured and found to change only in the case of Fps1-producing yeast growing in medium without supplementary buffering, from 51 µS/cm to 70 µS/cm after 7 days (~ 65 - 69 µS/cm with buffering), at one hundredfold dilution. Corresponding experiments were performed using ammonia assay media of pH 4.5, 5.5, 6.5 and 2 mM ammonium (a colleague's set of growth media), and SD KHL medium, with growth of Fps1-producing and aquaporin-deficient yeast nearly identical in each of these.

To find out how important the "ammonia" in the ammonia assay is, and to explore systematically which nitrogen source may best be suited for a control medium for aquaporin inhibitor assays, ammonium ions in now standard assay medium (NH_4^+ 40 mM, MOPS/NaOH 40 mM, pH 6.9) were replaced by various other nitrogen sources. The choice

of nitrogen source was based on availability, solubility, and on physiological considerations. Four pairs of aquaporin-producing and non-producing yeast transformants were tested using the “Bioscreen”. The results of three experiments, expressed as AUC values, are listed in Table 4.10.

Table 4.10: Ammonia assay nitrogen source replacement. *Yeast transformants (31019b Δfps1) producing the indicated aquaporins were grown at 29 ℃ in liquid media containing different nitrogen sources at a concentration of 40 mM each (in the case of ammonium sulfate this refers to the ammonium ion concentration). The MOPS concentration was 40 mM, the pH was 6.9. SD KHL media contained 76 mM ammonium and no MOPS. Only L-amino acids were used. Growth was detected turbidimetrically ($OD_{420-580}$) and quantified by calculating areas under growth curves to 48 h (AUC 48 h). Averages of measurements of 4 wells. Relative standard deviations were mostly below 10 %, except for yeast transformants growing poorly. The experiments were performed over a period of one month in the order shown.*

	Experiment 1		Experiment 2		Experiment 3	
	(pRS426)	Fps1	(pDR196)	PfAQP	(pRS426)	rAQP1 H180A
Nitrogen source	AUC 48 h / h					
SD KHL pH 5.6	47	45	44	42	46	44
SD KHL pH 6.9	39	49	35	44	40	47
no nitrogen	4	5	3	3	4	4
$(NH_4)_2SO_4$	4	14	2	11	4	17
NH_4Cl	4	16	3	12	5	17
NH_4CH_3COO	6	18	4	13	7	21
$(NH_4)_2CO_3$	2	10	1	9	2	10
$NaNO_3$	3	3	2	2	3	2
$NaNO_2$	3	3	2	2	3	3
urea	11	14	9	11	12	17
Gly	2	4	2	2	3	3
Ala	9	11	7	9	10	13
Val	15	21	13	18	16	21
Ile	9	9	5	6	8	9
Leu	8	9	6	6	9	10
Pro	11	12	9	9	11	11
Ser	7	8	5	6	11	9
Thr	10	18	10	13	14	17
Asn	16	22	11	20	16	24
Gln	14	19	8	15	14	21
NaAsp	14	11	13	9	16	11
NaGlu	7	6	6	4	8	6
LysHCl	1	3	2	3	2	2
ArgHCl	22	28	20	22	27	34
HisHCl	2	3	1	2	2	3

The following observations were made, keeping in mind the particular conditions of the assay:

The nominal absence of a nitrogen source nevertheless sustained significant yeast growth. The maximum concentration of residual ammonium, coming from the SD KHL medium used in precultures, is estimated to have been about 1 µM. SD KHL medium, whether at pH 5.6 or 6.9, was the best growth medium. Increasing the pH to 6.9 improved growth of the aquaporin-producing yeast and decreased that of the aquaporin-deficient ones. Urea could serve as a nitrogen source. The amino acids glycine, histidine hydrochloride, lysine

hydrochloride and the inorganic salts sodium nitrate and nitrite were not suitable as nitrogen sources, in fact they appeared to inhibit growth. Alanine and proline allowed comparable growth. Valine was a remarkably good nitrogen source, unlike isoleucine and leucine. Threonine was a better nitrogen source than serine. Asparagine was a better nitrogen source than glutamine. Curiously, sodium aspartate and sodium glutamate allowed aquaporin-deficient yeast to grow more than aquaporin-producing ones, the former allowing more growth altogether than the latter. Arginine hydrochloride was the best nitrogen source, possibly due in part to its having the highest number of nitrogen atoms per molecule.

Ammonium ions were a good nitrogen source only for the aquaporin-producing yeast. The acetate allowed the best growth but the lowest contrast, the bicarbonate the least growth but the highest contrast. The chloride and the sulfate were intermediate in growth promotion and contrast. With the exception of standard SD KHL medium, the smallest relative difference in growth was achieved with the amino acids leucine, isoleucine, serine and proline, the latter enabling better overall growth. The scrapping of proline in favour of glutamine for aquaporin inhibitor assay control media may thus have been an unfortunate choice (Fig. 4.34) based solely on the knowledge of glutamine as a common cellular nitrogen donor (biochemistry textbooks).

A fourth experiment was performed with rAQP1-producing yeast transformants which grew similarly or worse than the non-producing yeast. Due to a lack of assay media, it had to be performed with a total volume of 150 µl per well, and there was a high incidence of yeast stickiness even at 32 h. For this reason, its results are not shown in the above table.

In summary, the effectiveness of the assay depended on a near alkaline pH, and although the presence ammonium salts increased it, they were not absolutely necessary for a difference in growth between aquaporin-producing and non-producing yeast transformants to develop.

A final question remained as to how the assay media used by Jahn *et al*. (2004) could have been effective at a pH as low as 5.5, yielding growth differences convincingly dependent upon aquaporin-facilitated ammonia diffusion. Their media contained 0.7 % yeast nitrogen base (about four times the amount used in the experiments presented here) and were additionally buffered by Tris/succinate. Together with the phosphate species contained in the yeast nitrogen base, they thus had a medium which could buffer a pH range of about 4.5 to 8.5. Deciding on a pH of 5.5, an attempt was made to repeat their experiment using liquid media. Its results are presented in Fig 4.53. Jahn *et al*. had used the yeast strain 31019b which retains control over Fps1-synthesis, and so its use was tried in a second experiment.

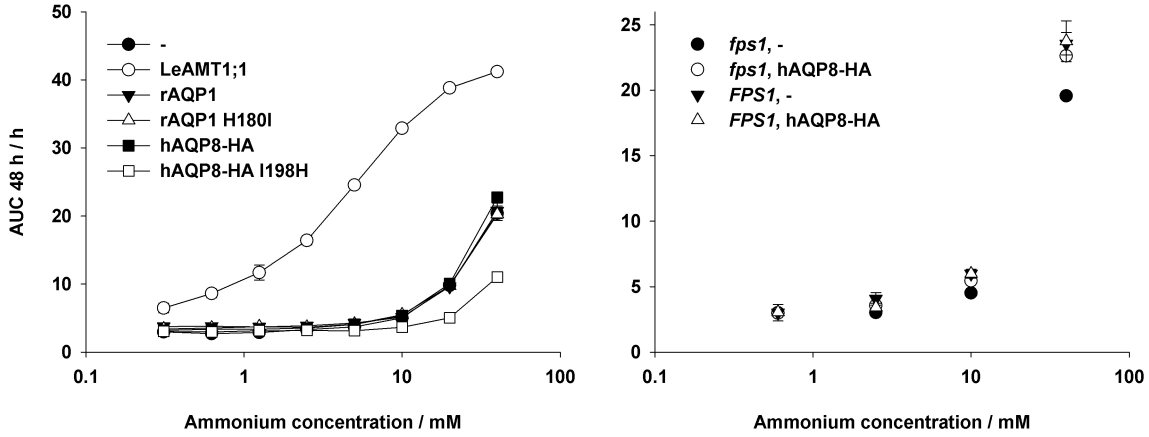

Fig. 4.53: Ammonia assays. *Yeast transformants (31019b or 31019b Δfps1, pRS426) were grown in liquid media at 29 °C. The medium composition was: yeast nitrogen base 0.70 %, D-glucose 150 mM (1.8 %), succinate/Tris 50 mM pH 5.5, with the ammonium sulfate concentration varied as indicated. Growth was detected turbidimetrically ($OD_{420-580}$), and quantified by calculation of the areas under the growth curves up to 48 h (AUC 48 h). Averages were derived from measurements of 4 wells each (3 or 2 in a few cases). Error bars represent standard deviations. They may be hidden by the data points or absent in the case of yeast stickiness (Fig. 4.46).* ***Left:*** *Experiment one. Yeast transformants expressed the indicated aquaporin or an ammonium transporter (LeAMT1;1).* ***Right:*** *Experiment two. Comparison between yeast strains 31019b Δfps1 (fps1) and 31019b (FPS1) producing no AQP or hAQP8-HA. Please note the different ordinate scales.*

The tomato ammonium transporter LeAMT1;1 improved yeast growth markedly, whereas wild-type rat Aquaporin 1 and its mutant H180I did not. Neither did HA-tagged human Aquaporin 8, and its mutant I198H appeared to decrease growth as compared to the aquaporin-deficient yeast transformant.

No marked difference in growth between hAQP8-HA-producing and non-producing transformants of either yeast strain was seen as judged by growth under ammonium limitation at pH 5.5.

Please note that galactose (2 %) served as energy and carbon source in the experiments of Jahn *et al.*, since the plasmid they used (pYES2) required it as an inductor of expression.

4.3.5 Methylamine assay

As for the ammonia assay, methylamine assay parameters could easily be varied and effects quantified by using the “Bioscreen” turbidometer. Two experiments were performed: One intended to test methylammonium concentrations at three different pH values as in the standard assay (3.4.4), the other to test the pH range around 5.5 at three different methylammonium concentrations. The first experiment yielded the results shown in Figure 4.54.

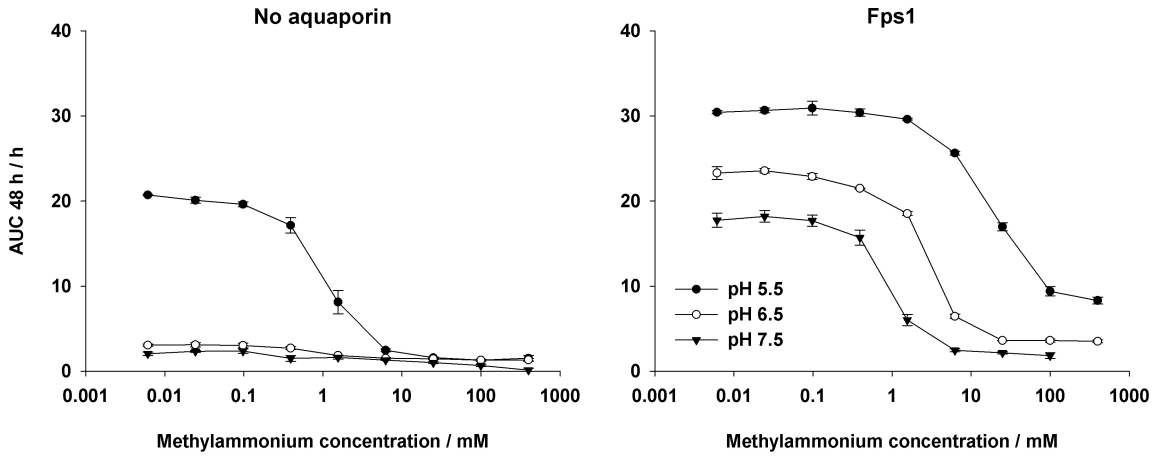

Fig. 4.54: Variation of the methylammonium concentration. *Yeast transformants (BY4742 Δfps1, pRS426 or pRS416 Fps1) were grown at 29 °C in liquid media containing various concentrations of methylammonium chloride at three different pH values. Growth was detected turbidimetrically ($OD_{420-580}$), and quantified by calculating the areas under the growth curves up to 48 h (AUC 48 h). Averages were derived from measurements of 3 wells each. Error bars represent standard deviations.* ***Left:*** *Aquaporin-deficient yeast transformants.* ***Right:*** *Fps1-producing yeast transformants.*

Aquaporin-deficient yeast transformants barely grew at pH 6.5 or 7.5, irrespective of the methylammonium concentration. A look at the growth curves revealed that this was due to an early onset of yeast stickiness (Fig. 4.46). At pH 5.5, they did grow, with an apparent IC_{50} of about 1 mM methylammonium chloride. Fps1-producing yeast transformants grew at all three pH values, with apparent IC_{50} values of about 20 mM at pH 5.5, 3 mM at pH 6.5, and 1 mM at pH 7.5. In the absence of methylammmonium, the respective AUC 48 h values were 31 h, 23 h, and 17 h, as compared to 20 h for aquaporin-deficient yeast transformants at pH 5.5. Please note that AUC values in the absence of methylammonium were all very close to those for a concentration of about 6 µM. Growth in SD KHL medium was similar. Calculating AUC differences, both absolute and relative, revealed that at pH 5.5, a methylammonium concentration of about 10 mM gave the highest contrast in growth between Fps1-producing and non-producing transformants while allowing the most robust growth of the latter. For this reason it was chosen for all subsequent methylamine assays.

In the second experiment, succinic acid was used to buffer pH values ranging from 4.6 to 6.4 at methylammonium concentrations of 100 mM, 10 mM and 0 mM (Fig. 4.55). This deviation from the standard methylamine assay conditions, in which MES serves to buffer a pH of 5.5, was justified by the low buffering capacity of MES at pH values below about 5.5. In addition, succinic acid could buffer the whole range ($pK_{a1} \approx 4.2$, $pK_{a2} \approx 5.6$), and the use of a single buffer seemed favourable for comparability.

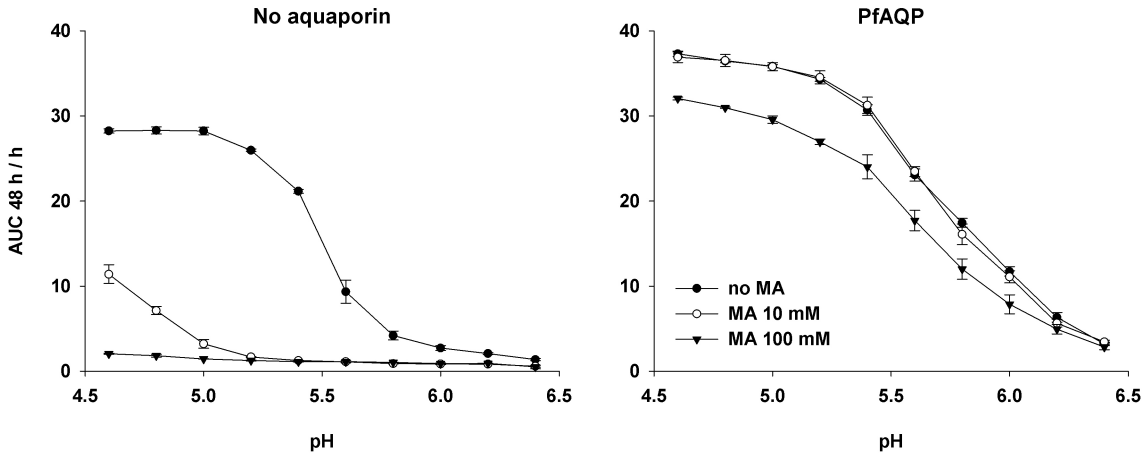

Fig. 4.55: pH variation. *Yeast transformants (BY4742 Δfps1, pDR196 or pDR196 PfAQP) were grown at 29 ℃ in liquid media of varying pH, containing three different concentrations of methylammonium chloride (MA). The buffer was succinate/NaOH 20 mM. Growth was detected turbidimetrically ($OD_{420-580}$), and quantified by calculation of the areas under the growth curves up to 48 h (AUC 48 h). Averages were derived from measurements of 3 wells each. Error bars represent standard deviations.* ***Left:*** *Aquaporin-deficient yeast transformants.* ***Right:*** *PfAQP-producing yeast transformants.*

Predictably, aquaporin-deficient yeast transformants did not grow at a methylammonium concentration of 100 mM, and only poorly at 10 mM. In the absence of methylammonium, there was a surprisingly pronounced pH-dependence of growth, with an apparent half-maximal inhibitory pH of around 5.5, and AUC 48 h values dropping from 28 h at pH 4.6 to just over 1 h at pH 6.4. PfAQP-producing yeast transformants were hardly affected by the presence of 100 mM methylammonium, but strongly so by the pH, with AUC 48 h values decreasing from around 35 h to 3 h, and an estimated half-maximal inhibitory pH of 5.6 - 5.7. Please note that the experiment had also been performed with the same yeast transformants, producing or not Fps1, as in the methylammonium concentration range test (Fig. 4.54). Its results are not shown here because aquaporin-deficient yeast were almost unaffected by 100 mM methylammonium, and because the possibility of a pipetting or labelling error could not be excluded. Nevertheless, half-maximal inhibitory pH values of about 5.5 - 5.8, were seen in that experiment as well. Since the effect may have been due to the buffering by succinic acid, with its pK_{a2} close to the apparent inhibitory pH, and since it was not investigated further, subsequent methylamine assays were performed using the standard medium composition (buffering of pH 5.5 by MES).

In summary, the pH affects the outcome of methylamine yeast growth assays in the absence of methylammonium. This result was a major reason for deciding against the use of the methylamine assay for the testing of potential aquaporin inhibitors.

5 Discussion

The presented work was pursued in order to learn about the ammonia permeability of aquaporins, in particular with regard to their aromatic/arginine constriction. In addition, the possible application of aquaporin-facilitated ammonia diffusion for the testing of potential aquaporin inhibitors by yeast growth assays in liquid medium was explored. To be able to evaluate the obtained results, the assays employed shall be considered first.

5.1 Osmotic assays

Cells from two organisms were subjected to osmotic assays for the study of aquaporin-facilitated water permeability: *Xenopus laevis* oocytes and yeast of the species *Saccharomyces cerevisiae*.

X. laevis oocyte swelling assays are the most commonly used functional assays for the characterization of heterologously expressed aquaporins, and the method originally proposed by Preston *et al.* (1992) is still in use. Little can be added here but for the impression that a tonicity decrease by two thirds (-66 %) may be too large. With the available equipment the first five to fifteen seconds of swelling were missed, leading to an underestimation of the initial rate of volume change. A smaller osmotic gradient would reduce this error without having to resort to more elaborate equipment. In addition, it would reduce the shock the oocytes are subjected to. Meinild *et al.* (1998) generated tonicity changes of about 10 % by adding or by removing 20 mM mannitol, albeit in a continuous-perfusion-chamber coupled with automated video imaging. Jung *et al.* (2012) placed oocytes in buffer of 65 % of the original tonicity (-35 %). Ideally, the gradient would be chosen so that most oocytes reach osmotic equilibrium without bursting.

S. cerevisiae transformant protoplasts proved satisfactory for the study of aquaporin-facilitated water permeation, given the availability of a stopped-flow apparatus. Due to their larger surface-to-volume ratio (~ 1 μm^{-1}) as compared to *X. laevis* oocytes (~ 0.005 μm^{-1}), they showed high rates of volume change even in the absence of aquaporins. Figures 4.18 and 4.19 provide an example of this difference. However, looking at the first 100 ms, as in Fig 4.41, and adjusting the ordinate scale, the light scattering curves obtained with yeast protoplast suspensions resemble oocyte swelling curves. The necessary one hundredfold magnification of the time scale may reflect the approximately one hundredfold difference of the surface-to-volume ratio.

One way to increase the difference in water permeability between aquaporin-producing and aquaporin-deficient yeast is to decrease the temperature. Rather than measuring at 20 °C as in most experiments presented here, a standard temperature of 10 °C or even 4 °C seems more reasonable. This would additionally shorten the temperature equilibration time following transfer of the protoplast suspension, which is kept on ice, to the stopped-flow apparatus reservoir. Measurements at 4 °C could be performed without any difficulty (Fig. 4.18).

Another option is the choice of yeast strain. In experiments not shown, BY4742 Δfps1-protoplasts producing rAQP1 or no aquaporin showed a relaxation time ratio ($\tau_{no\ AQP} / \tau_{rAQP1}$) around three times greater than the corresponding 31019b Δfps1-protoplasts. This was due both to a lower basal, and a higher aquaporin-facilitated water permeability. Nevertheless, strain 31019b Δfps1 was chosen for practical reasons, *i. e.* its frequent use in ammonia assays, and the availability of transformant glycerol stocks. By chance, the relaxation time ratio obtained for the rAQP1-mutant experiments (Table 4.8) was higher than in all previous experiments (not shown). This may have been due to the repeated partial thawing of the glycerol stocks over the course of two years, possibly leading to an unintended selection of the least water-permeable cells. The water permeability variation of *S. cerevisiae* wild-type and laboratory strains with regard to repeated washings in distilled water was investigated by Bonhivers *et al.* (1998) who found point mutations in the endogenous water-selective aquaporin AQY1 as an exemplary cause for lower basal water permeability. Will *et al.* (2010) elaborated on this in an evolutionary context and found that some freeze-thaw-sensitive *S. cerevisiae* strains have repeatedly lost and regained aquaporin function.

Concerning the determination of osmotic water permeability coefficients (P_f), light scattering measurements with yeast protoplasts yield insufficient data, unlike for the direct measurement of relative volume changes with *X. leavis* oocytes. The only way to obtain such coefficients is to measure true volume changes in yeast cells and to relate them to corresponding light scattering changes, as done by Soveral *et al.* (2007 and 2008). The equation

$$P_f = (\tau^{-1}) \cdot [V_0 / (S_0 \cdot V_w \cdot \Delta c)] \qquad \text{(or } c_\infty \text{ instead of } \Delta c\text{)}$$

used by various groups (Bertl and Kaldenhoff, 2007, Wu *et al*., 2010, Madeira *et al*., 2010), is probably wrong since it results in permeability coefficients which vary with the osmotic gradient (Δc) or the osmolarity after mixing (c_∞), because time constants (τ^{-1} or k) do not (Fig. 4.42). Its mistake seems to lie in the assumption that

$$(\tau^{-1}) = \Delta(V/V_0) / \Delta t$$

The units match, but not the meanings: The time constant (τ^{-1}) contains no information on the extent of change, whereas the relative volume change ($\Delta(V/V_0)/\Delta t$) does.

Thus, when fitting exponential curves ($A \cdot e^{-kt}$), the amplitude (A) should not be neglected. In the case of stopped-flow light scattering measurements the amplitude corresponds via the detector voltage to the change in intensity of scattered light. The amplitude alone is not enough, however: It needs to be divided by the net starting voltage in order to obtain the relative voltage change and thus the relative light scattering change (Fig. 4.39) which can then be related to the relative volume change of the yeast cells (or other vesicular structures).

The calculation of the P_f for aquaporin-deficient yeast protoplasts presented in Section 4.3.2 allowed for an estimate of its order of magnitude, assuming that yeast protoplasts behave like intact yeast cells in response to osmolarity changes: The value of 1 µm/s at 20 ℃ was close to the carefully determined one of 2 µm/s for another yeast strain (Soveral *et al.,* 2008). The corresponding value for *X. laevis* oocytes was of the order of 10 µm/s (Figs. 4.5 and 4.13), assuming their average surface area to be that of a sphere of 1.2 mm diameter (3.6). Their true surface area may be an order of magnitude larger due to the presence of folds and microvilli, impressively shown by Zampighi *et al.* (1995). The basal water permeability coefficient of the *S. cerevisiae* and *X.* laevis oocyte plasma membranes may thus be quite similar at approximately 1 µm/s. As mentioned previously, reported osmotic water permeability coefficients of artificial lipid membranes range between 2 µm/s and 70 µm/s at room temperature (Table 1.2).

To calculate corresponding water permeability coefficients for aquaporin-producing yeast protoplasts, one merely needs to multiply the P_f of the aquaporin-deficient yeast protoplasts with the ratio of rates, *e. g.* $\tau^{-1}_{AQP} / \tau^{-1}_{no\ AQP}$. The question is which rate constant to choose: τ^{-1}, k_1, k_2 or another kind? Ideally, as with the oocytes, the rate would be measured directly by determining the initial slope (light scattering signal change per time). It can be obtained by calculating the derivative of the fitted exponential function for time point 0:

$$(d/dt) \cdot (A \cdot e^{-kt}) = - k \cdot A \cdot e^{-kt}$$
$$- k \cdot A \cdot e^{-k0} = - k \cdot A \cdot 1 = - k \cdot A$$

For a double exponential function the initial slope would be

$$- k_1 \cdot A_1 - k_2 \cdot A_2$$

Indeed, when comparing estimated initial slopes with the above expression and with simple time constants (τ^{-1}, k_1, k_2) for the example given in Table 4.8, the former comes closest (not

shown). In addition, when divided by the net starting voltage (Fig. 4.39) it would yield the relative voltage change and thus the relative light scattering change per time:

$(- k_1 \cdot A_1 - k_2 \cdot A_2) / U_0$

If volume changes are proportional to light scattering changes, the coefficient of osmotic water permeability could then be calculated by

$P_f = [(- k_1 \cdot A_1 - k_2 \cdot A_2) / U_0] \cdot [V_0 / (S_0 \cdot V_w \cdot \Delta c)]$ (if $\Delta U/U_0 = \pm \Delta V/V_0$)

The proportionality between relative light scattering (detector voltage) change and relative volume change would have to be verified.

In summary, the following values must be obtained from light scattering curves (not normalized) in order to determine osmotic water permeability coefficients (Fig. 4.39): baseline voltage and starting voltage (needed to calculate the net starting voltage U_0), time constants (k_1 and possibly k_2) and amplitudes (A_1 and possibly A_2). The baseline voltage can easily be obtained prior to the experiments when rinsing the stopped-flow apparatus with the assay buffers. The correct starting voltage can be obtained even for rapidly shrinking samples (Fig. 4.41, right) if in parallel with the hyperosmotic buffer an isosmotic one is used (with a three-reservoir stopped-flow apparatus this can easily be done). For precision, the ending voltage (Fig. 4.39) should be determined as well: The voltage change should be equal or at least close to the sum of the amplitudes ($\Delta U \approx A_1 + A_2$).

Normalization of light scattering curves is not necessary but useful for their visual comparison (as in Figure 4.11), and it can be combined with the calculation of relative voltage changes ($\Delta U/U_0$) with little additional effort by using a spreadsheet like “Microsoft Excel”.

As shown in Figure 4.42, the choice of osmotic gradient had no effect on the shape of the normalized light scattering curves for a given sample of yeast transformant protoplasts. It did however affect the estimation of plateaus by shifting the onset of upward deviations frequently seen when performing yeast protoplast shrinking assays (Fig. 4.42). An optimal gradient would allow precise determination of signal plateaus (or ending voltages) while not reducing the signal-to-noise ratio too much. In addition, the tonicity change should be physiologically reasonable, *i. e.* cells should not be stressed more than necessary. Even non-living vesicles such as organelles or liposomes cannot be expected to shrink or to swell by more than a few volume percent, so they need not be subjected to large tonicity changes either. For water permeability measurements with *S. cerevisiae* protoplasts, a tonicity change of +11 % (150 mM sorbitol gradient) appeared to be a good choice. For hypertonic solute permeability measurements as shown in Figure 4.16, a tonicity change of +23 % (300 mM

solute gradient) seemed acceptable because reswelling of protoplasts counteracted excessive shrinking. Yeast protoplast swelling assays were performed initially but scrapped in favour of the shrinking assays, for reasons of conformity. In fact, the swelling of already shrivelled yeast protoplasts may be more sensible than their further shrinking: At 1.4 M external sorbitol, yeast cell volume is substantially reduced and decreases little with further increases of osmolarity, as shown by Soveral *et al.* (2008).

Regarding tonicity and osmotic gradients in the calculation of water permeability coefficients, an important consideration is the true as opposed to calculated osmotic gradient. For example, the above-mentioned calculated tonicity change of +11 % (1.48 osmol/l divided by 1.33 osmol/l) turned out to be +25 % when using osmolalities derived from measurements of freezing point depressions (2.09 osmol/kg divided by 1.67 osmol/kg). The actual osmotic pressures could not be measured with the available equipment. Which value should be used? Plotting relative signal amplitudes against varying osmolar, osmolal or pressure gradients (as in Figure 4.42) might yield a clue. With the lower osmolarity media used for *X. laevis* oocyte swelling assays, such considerations lose their importance.

Finally, the best way to compare aquaporins with regard to their water and solute permeabilities is to know exactly their plasma membrane density ratios. For *X. laevis* oocytes (and proteoliposomes) this can probably be achieved with greater ease and precision than with *S. cerevisiae* cells (Yang and Verkman, 1997). Osmotic assays with the latter are nevertheless suitable to find out whether a given aquaporin conducts water or solutes at an appreciable rate.

5.2 Yeast growth assays

5.2.1 Yeast growth in microplate liquid cultures

Before discussing the experiments on the ammonia and methylamine assays, it is worth considering yeast growth inside microplate wells.

Most experiments were performed at shaking intervals of 30 minutes, a time sufficient for all yeast cells inside a well to sink to the bottom. There, chemical and pH gradients may begin to form between them and the bulk medium, as convection is probably absent. The situation is not unlike that of yeast cells growing on agar medium. The gel is in effect an immobilized liquid, and the cells are probably not in direct contact with the air, but also immersed in liquid held to them by capillary forces. An indication of this came from observation of yeast colonies

on agar using a dissecting microscope at approximate 40-fold magnification: the surface of the colonies was reflective as a liquid surface would be. In addition, the gel pH was more acidic the closer to the colonies it was measured, as judged by inserting pH indicator paper into a scalpel-cut slit.

Thus, with intermittent shaking, yeast growth in microplate wells may be more similar to growth on agar-immobilized medium than to growth in continuously shaken Erlenmeyer cultures. At constant shaking the opposite may be true. An important difference is the possibility of gas exchange. In this regard, growth inside microplate wells resembles growth inside Erlenmeyer flasks more than growth on a gel surface. In fact, the yeast "stickiness" described in Section 4.3.3 may have to do with increased gas exchange, as evidenced by an increased rate of evaporation from wells situated at the very edges of the "Bioscreen" plates (Table 4.9). Oxygen is important in that it determines whether fermentation outweighs respiration, although some yeast, including *S. cerevisiae*, are known to produce ethanol even in the presence of sufficient oxygen, possibly for the purpose of outcompeting other micro-organisms, a phenomenon named Crabtree effect (rapid extracellular acidification, linked to glycolysis, may also contribute in this regard; Sigler *et al.*, 1981, Rozpędowska *et al.*, 2011).

The effectiveness of shaking by the "Bioscreen" incubation chamber was not investigated. However, in one instance a look at an assay plate immediately after shaking (10 s, "medium" setting) revealed that the yeast cells were still covering the well bottom rather than being suspended in the medium. Even at constant shaking, the situation is not the same as for an Erlenmeyer flask on an orbital shaker due to the axial shaking, although in both cases this depends on the amount of medium relative to the container and on the resulting surface-to-volume ratio. Smaller volumes clearly improved yeast growth (4.3.3). Hermann *et al.* (2003) studied oxygen transfer rates in standard 96-well plates and found the exceeding of a surface tension-dependent critical shaking frequency and amplitude to be necessary for an increased rate as compared to that of unshaken wells. Even so, oxygen transfer could not be increased by more than a factor of about four. Whether the maximum shaking frequency and amplitude of the "Bioscreen" incubator are sufficient to increase oxygen transfer rates would have to be verified, although it is likely. In any case, yeast grow normally in the complete absence of shaking.

Concerning the quantification of yeast growth, optical densities (OD) at a given time, as well as maximum growth rates ($\Delta OD/\Delta t$) were initially considered. A look at the growth curves shown in Figure 4.45 illustrates drawbacks of both: Optical densities require a careful choice of time, the optimum of which may differ from assay to assay, and the maximum growth rates may be identical. Skyttä and Mattila-Sandholm (1991) proposed microbial growth quantification by calculation of "area values" (areas under growth curves, AUC) for a chosen time, pointing out that these do not rely on single time point values. The approach was

immediately adopted, and a time of 48 h was chosen for yeast growth assays based on a comparison of absolute and relative AUC-differences between Fps1-producing and aquaporin-deficient yeast in a single ammonia assay, calculated for periods of 12 h to 96 h in twelve-hour-steps. The choice of 48 h was occasionally reevaluated and always found to be satisfactory.

The AUC calculated from OD values has proven to be a good measure of yeast growth, but it too has a drawback: As explained in Section 4.3.3, the linear range of a double logarithmic plot of yeast cell concentration against OD did not extend above an OD (420 - 580 nm) of about 0.6 for a path length of about 7.5 mm (300 µl medium). Above this, the OD led to an underestimation of the yeast cell concentration. In most yeast growth assays performed with the "Bioscreen", the OD reached values of up to about 1.6, leading to AUC values too low. Ideally, the AUC would be calculated from yeast cell concentrations instead of ODs. If necessary, this could be achieved by careful calibration. Alternatively, measuring the OD before and after appropriate dilution for a range of OD values is a method which has been employed by Warringer *et al.* (2003). Nevertheless, the AUC 48 h obtained by OD measurements turned out to be a surprisingly constant measure as judged by yeast growth in SD KHL medium: A value of close to 40 h was typical. Even growth of a commercial *S. cerevisiae* strain (Asmussen, Elmshorn) in SD KHL medium yielded an AUC 48 h of about 40 h.

In practise, when establishing microplate growth experiments with a microorganism, well fill volume and shaking parameters should be evaluated systematically first. For example, in the experiments presented here, yeast "stickiness" (Fig. 4.46) might have been avoided by choosing no shaking as a standard setting. In the case of microorganisms which change their colour or that of the medium during growth, the wavelength setting should be considered. Corner and edge wells should be reserved for blanks or explorative samples if possible (Fig. 4.47).

Experiments using microplate liquid cultures are particularly useful for the optimization of medium composition and for the analysis of growth curves. An instance of the latter will be given in the following section.

5.2.2 Ammonia assay

The experiments presented in Section 4.3.4 have shown that the growth of *S. cerevisiae* strain 31019b Δfps1 is decreased by the presence of more than about 10 µM unprotonated ammonia (Figs. 4.49 and 4.50), especially at neutral or mildly alkaline pH (Fig. 4.51), and that the presence of some aquaporins such as Fps1 increases this threshold to about

100 µM ammonia. This is in contrast with the experiments of Jahn *et al*. (2004) and Loqué *et al*. (2005), who found the opposite to be true (Figs. 1B and 3 of the respective publications). A major difference is their use of strain 31019b which retains control over Fps1-synthesis. Seemingly minor differences include their choice of plasmid, buffer, and potassium concentration.

The exchange of ammonium ions for a variety of amino acids or urea does not fully abolish this effect (Table 4.10), a finding that points at a neutral or alkaline pH as the ultimate cause. The literature on *S. cerevisiae* cytosolic pH (pH_c) regulation reveals that the pH_c changes with the extracellular pH (Peña *et al*., 1972), that the degree of this change depends on the growth stage of the yeast cells (Imai and Ohno, 1995, Weigert *et al*., 2009), that it increases upon addition of glucose (Orij *et al*., 2009), and that it increases upon addition of some monovalent cations, notably potassium (Calahorra *et al*., 1998) and ammonium (Peña *et al*., 1987).

The *S. cerevisiae* strain 31019b Δfps1 used in the present work lacks all three ammonium transporters, and the cells were usually added to the medium in their late log or stationary phase, following washing in deionized water. The assay media contained about 150 mM glucose, 7 mM potassium (0.17 % yeast nitrogen base), and varying ammonium concentrations. The pH was 6.9 or higher. The lack of ammonium transporters meant that ammonium ions could not enter freely. The potassium ions would have prevented ammonium ions from taking the possible alternative path through potassium channels (Hess *et al*., 2006). The bulk pH_c was not measured but may be expected to have been close to 7. Unfacilitated ammonia diffusion through the lipid bilayer portion of the plasma membrane probably contributed significantly to its entry into the cells, since the presence of aquaporins did not enhance yeast growth at low ammonia concentrations (Fig. 4.49). When transferring the washed yeast into assay medium, they were probably suffused with ammonia/ammonium before the first duplication, and this likely led to an increase in both cytosolic and vacuolar pH (Greenfield *et al*., 1987, Makarow and Nevalainen, 1987).

How did some aquaporins rescue growth of yeast cells under these conditions? All tested aquaglyceroporins, including Fps1, PfAQP, human AQP9 (Fig. 4.25, Table 4.10) and others not shown, had the required property, as did several rat AQP1 selectivity filter mutants but not the water-selective wild-type rat AQP1 (Figs. 4.7, 4.8, 4.25, Table 4.1). Thus, the rescuing property of some aquaporins probably had to do with their permeability characteristics. Beitz *et al*. (2006) have shown that synthesis of rat AQP1 H180A by *Xenopus laevis* oocytes increases their ammonia permeability, while glycerol and urea remain excluded, so the unknown permeant is probably smaller than either of these. It may be ammonia, although why its facilitated membrane permeation should improve yeast tolerance to it remains elusive. Alternatively, auqaporins such as Fps1 and rat AQP1 H180A may improve yeast

growth by facilitating the permeation of other small molecules such as carbon dioxide (Otto *et al*., 2010) or ethanol (Teixeira *et al*., 2009). Assuming that the molecule in question is ammonia, it is surprising that rAQP8 and hAQP8, both ammonia-permeable (Jahn *et al.*, 2004, Holm *et al.* 2005), were deleterious rather than growth-promoting in yeast ammonia and methylamine assays (Fig. 4.21 and Table 4.1). A possible reason may be their cellular localization: Soria *et al.* (2010) found heterologously expressed rAQP8 in the mitochondrial fraction of *S. cerevisiae* cells of strain BJ5457.

Another clue is provided by the growth curves (Fernandez-Ricaud *et al*., 2007): Increasing ammonia concentrations decreased the growth rate and especially the number of cell duplications (final OD), but did not affect the duration of the lag phase (Fig. 4.24, an exception is shown in Fig. 4.30). In experiments with toxic substances such as mercuric chloride (not shown) or methylammonium (Fig. 4.24), the lag phase was strongly affected, pointing to a different kind of growth impairment by ammonia. Replacing ammonium ions with urea or amino acids reduced the effect (Table 4.10), with almost only the number of cell duplications affected (not shown). Although the shaking parameters used (10 s shaking every 30 min) did not lead to appreciable resuspension of the yeast cells (Section 5.2.1), corresponding cultures in Erlenmeyer flasks under constant orbital shaking gave similar results (Fig. 4.52).

Serrano *et al*. (2004) have shown that the deleterious effect of alkaline pH on yeast growth is in large part due to the limited availability of copper and iron, probably due to their decreased solubility and intracellular utilization, and that supplementation of these trace elements synergistically improves growth. Incidentally, the authors mention the importance of vacuolar function for alkaline tolerance, pointing out that increased alkaline sensitivity caused by deletion of vacuolar function-related genes (*e*. *g*. genes encoding vacuolar proton-ATPase subunits) could in many cases not be alleviated by copper and iron supplementation. Taking these results into consideration, it becomes apparent that ammonia may aggravate the effects of mildly alkaline medium on yeast growth by its accumulation in acidic compartments (Marceau *et al*., 2012). In addition, its strong binding to copper(II) ions (Hathaway and Tomlinson, 1970) could conceivably hamper uptake of the metal present at approximately 0.25 µM (0.17 % yeast nitrogen base) in in the growth media. Whatever the reason for the deleterious effect of ammonium accumulation, keeping it out of the cell under slightly alkaline conditions probably requires its incorporation into other molecules such as amino acids. Hess *et al.* (2006) found that *S. cerevisiae* excrete several amino acids under high-ammonium/low-potassium conditions, in particular alanine, proline, valine, glutamate and glutamine, and that their steady-state metabolism increased with increasing ammonium concentration of the medium.

It is worth mentioning that the intracellular concentration of ammonium/ammonia was found to be about 0.7 mmol/kg of washed and centrifuged yeast (~ 1.4 mmol/l of cell water) of a commercial strain, using a diffusion/acid trap/titration method (Conway and Breen, 1945), or about 3 to 7 mmol/kg of nitrogen-starved, washed and filtered yeast (~ 6 - 14 mmol/l of cell water) of strain BY4741, using a commercial ammonium determination kit (Van Nuland *et al*., 2006). In other words, the intracellular ammonium ion concentration of *Saccharomyces cerevisiae* cells may be of the order of 1 to 10 mM, and the intracellular ammonia concentration at pH 7 correspondingly 5 to 50 µM, the concentration range of extracellular ammonia at which growth of aquaporin-deficient yeast transformants began to decrease (Fig. 4.50).

The yeast growth-rescuing properties of some aquaporins under alkaline conditions in the absence of ammonium, and in a pH gradient plate assay (Fig. 4.25), remain a mystery at present. For the time being, a simple hypothesis might be that, whatever the mechanism, aquaporins with certain permeability characteristics allow for a higher rate of metabolism which in turn allows a higher rate of detoxification of ammonium/ammonia or improved alkaline stress relief in *S. cerevisiae*. Van Aelst *et al.* (1991) have shown that overexpression of Fps1 can have such an effect.

5.2.3 Methylamine assay

The methylamine assay was studied less extensively than the ammonia assay. A few observations can be noted nevertheless:

The standard methlymmonium concentration of 50 mM (3.4.4) appears to be unnecessarily high. The poor growth of yeast transformants described in Section 4.1.1, and experienced by several colleagues as well, may have been due to this. A standard concentration of 10 mM is proposed.

Just as for the ammonia assay, the strong pH-dependence of yeast transformant growth in the absence of methylammonium (Fig. 4.54) cannot be explained at present, but it should be kept in mind when making use of this assay for the characterization of aquaporins.

It is notable that methylamine is potentially vacuolotropic as well, despite its high pK_a of about 10.7 (5.2.2).

The pattern of growth-enabling aquaporins closely resembles that obtained with the "ammonia assay" at slightly alkaline pH (Table 4.1).

The methylammonium-independent inhibitory pH of about 5.5 – 5.7 seen with succinic acid-buffering (Fig. 4.55) may have had to do with the complexation of certain metal ions by doubly charged succinate ions.

5.3 Aquaporin inhibitor assays

The use of semi-automated ammonia-dependent yeast growth assays for the testing of potential PfAQP- and hAQP9-inhibitors turned out to be dissatisfactory. Most results are not shown in the presented work, the ones that are shown were the most promising (Fig. 4.34). Frequently, growth of aquaporin-deficient yeast transformants was as good as that of the aquaporin-producing ones. In one instance they grew better than hAQP9-producing yeast transformants. While this also occurred in ammonia assays intended to compare aquaporins, it was more frequent when attempting to test inhibitors, despite equal care taken. A possible reason may have been the more frequent use of freshly transformed yeast for the inhibitor assays. The variability of yeast transformant growth was not studied systematically, but in one case several hAQP9-transformants derived from a single agar plate showed varying but clearly improved growth. In another case, several aquaporin-deficient yeast transformants derived from a single agar plate showed marked growth under ammonia assay conditions as well. This yeast colony variability should be taken into account by repeating growth assays with yeast transformants derived from different colonies and transformations, as done in the experiments shown in Table 4.1.

One and a half years of testing yielded the results presented in Section 4.2, during which time other groups managed within weeks to find PfAQP-inhibiting (G. Fischer, conference report) and murine AQP9-inhibiting substances (Jelen *et al.*, 2011), using semi-automated but unrelated assays. One of the PfAQP-blocking molecules found had also been tested using the ammonia assay and yeast protoplast glycerol permeability measurements (Figs. 4.30, 4.31). The fact that its property was missed, and that it had been predicted to bind to the intracellular part of the pore, points to a possible extrusion by the yeast cells. Kołaczkowski *et al.* (1998) have shown that *S. cerevisiae* cells are capable of extruding a large variety of drug-like molecules, and that this ability is due to several ATP-driven pumps of the ATP-binding cassette (ABC) transporter family. Performing water or glycerol permeability measurements with intracellular vesicles derived from vesicle-accumulating *S. cerevisiae* mutants (Laizé *et al.*, 1995) may have allowed the testing of intracellularly binding aquaporin-inhibitors, but at the time the experiments were performed the process of vesicle preparation as established within the laboratory was too low-yielding to be practical.

The testing of potential hAQP1-inhibitors was possible with yeast transformant protoplasts and with blood cells as shown by mercuric chloride inhibition (Figs. 4.26 and 4.28). Tetraethylammonium chloride could not be confirmed as a hAQP1-inhibitor (Detmers *et al.*, 2006) in either system. Test compounds h1-RC-1/9/10 (Table 4.4) were not found to inhibit hAQP1 in erythrocytes or when heterologously expressed in yeast. Seeliger *et al.* (2012) speculate on possible reasons for this, an important one being the conditions under which

these compounds could inhibit hAQP1-facilitated water diffusion into *X. laevis* oocytes: They only did so for low production levels of the aquaporin.

In summary, the ammonia assay may be unsuitable for the testing of potential aquaporin-inhibitors for the reasons given in Section 5.2.2, *i. e.* the growth-rescuing mechanism of aquaporins may not reflect facilitated ammonia diffusion into the cells. It is not recommended. The methylamine assay as used by Wu *et al.* (2008) may have turned out to be better suited (Fig. 4.35), but it too does not entirely reflect yeast growth improvement by aquaporin-facilitated and pH gradient-dependent methylamine efflux, as shown in Section 4.3.5. The ammonia assay as used by Jahn *et al.* (2004) may have been suitable, but it could not be reproduced in a single attempt (Fig. 4.53). In any case, it would be more suitable for the screening of ammonium transporter inhibitors.

Yeast protoplast assays may be suitable for the testing of extracellularly binding aquaporin inhibitors, given preselection of candidate molecules by virtual high-throughput screening. In this regard, human AQP 8 is particularly promising: The solving of its three-dimensional high resolution structure by electron microscopy may be imminent (Iacovache *et al.*, 2010, Agemark *et al.*, 2011), and its presence in *S. cerevisiae* protoplasts repeatedly led to the highest water permeability seen in any of the osmotic assays performed over the course of two and a half years (Fig. 4.23). A specific human AQP8-inhibitor would allow further characterization of this enigmatic aquaporin, although a murine or rat AQP8-inhibitor would be more useful for physiological studies.

5.4 Ammonia permeability of aquaporins

The ammonia permeability of aquaporins was studied by yeast growth assays. As explained in Section 5.2.2, the ammonia assay employed may reflect aquaporin-mediated permeability of a molecule other than ammonia. It is assumed for the time being that the molecule in question is ammonia, and that, similarly, the methylamine efflux assay (5.2.3) truly reflects aquaporin-mediated permeability of the ammonia analogue methylamine. As will be seen, the knowledge obtained by the presented work is not much affected by these considerations.

5.4.1 Selectivity filter mutants of Aquaporins 1 and 8

Figure 5.1 depicts the general structure of the ar/R constriction of a water-selective aquaporin.

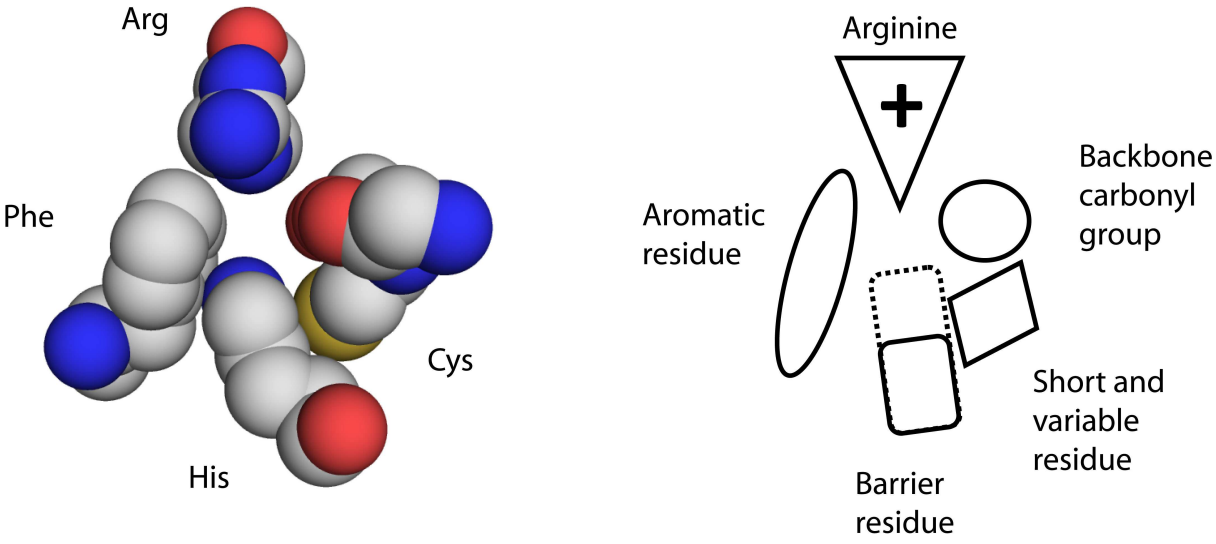

Fig. 5.1: Aquaporin aromatic/arginine constriction schematic. *View from the extracellular side through the channel.* ***Left:*** *Ar/R constriction of bovine AQP1, a water-selective aquaporin (PDB ID: 1J4N).* ***Right:*** *Corresponding schematic. Most aquaporins and some aquaglyceroporins have an ar/R constriction of this type. Other amino acid residues in close proximity to this region are not depicted but may be important (Fig. 1.8).*

The question asked at the outset was whether mutation of the ar/R constriction amino acids of rat AQP1 (identical to those shown in Figure 5.1) to ones found in AQP8 (Fig. 1.11) would increase ammonia permeability. In the following, mutations at each position and their consequences are described.

Arginine (rAQP1 Arg 195)

An arginine residue is found in the constriction region of 88 % of aquaporins listed in the MIPMod Database (Gupta *et al.*, 2012). Mutating this amino acid to valine or serine in rat AQP1, thus reducing size and eliminating a positive charge, results in an aquaporin with increased ammonia permeability as determined by electrophysiological measurements with *Xenopus* oocytes (Beitz *et al.*, 2006, Li *et al.*, 2011).

The experiment presented in Table 4.1 confirmed methylamine permeability of the rat AQP1 mutants R195V and R195S. Under ammonia assay conditions yeast transformants expressing them did not grow more than aquaporin-deficient yeast in all experiments but one (Table 4.1, Fig. 4.25 A). In another independent experiment performed by a colleague, they did not improve yeast growth either (C. Steinbronn, not shown).

Although the constriction arginine was not the subject of the presented work, these aquaporin mutants are of interest not least because their proven ammonia permeability did not lead to consistent growth improvement in the yeast ammonia assay.

Short and variable residue (rAQP1 Cys 189)

Among aquaporins listed in the MIPMod Database, the most common amino acids at this position are threonine (25 %), alanine (24 %), glycine (15 %) and cysteine (6%), excluding tyrosine (14 %) and phenylalanine (6 %) which are found in aquaglyceroporins. The constriction region of bovine AQP1 shown in Figure 5.1 illustrates the limited space available for an amino acid residue at this position in water-selective aquaporins.

Unsurprisingly, the rat AQP1 mutant C189G conducted water (Fig. 4.4). Loss of mercuric ion-sensitivity was confirmed (Fig. 4.12, Preston *et al.*, 1993). Ammonia- or methylamine permeability were absent (Figs. 4.1, 4.2, Table 4.1).

Aromatic residue (rAQP1 Phe 56)

Non-aromatic hydrophobic amino acids at this position are predicted for 9 % of aquaporins listed in the MIPMod Database, nearly all of them bearing an alkyl residue. Non-aromatic hydrophilic amino acids are predicted for the remaining 4 % of these aquaporins, chiefly serine, threonine, asparagine and glutamine. Thus, the amino acid at this position usually provides a hydrophobic residue opposite to the backbone carbonyl group (Fig. 5.1), and, in most cases, an aromatic one.

The histidine side chain found at this position in AQP8- and TIP-like aquaporins (Figs. 1.10, 1.11) is aromatic as evidenced by NMR spectroscopy of imidazole (Matuszak and Matuszak, 1976), yet it is also a versatile proton acceptor and donator found in enzymes such as proteases (Kossiakoff and Spencer, 1981). Its free nitrogen atom may be situated close to one of the arginine side chain hydrogen atoms.

Effects of a single point mutation at this position were reported by Jahn *et al.* (2004) who have shown that its mutation to phenylalanine in TaTIP2;1 reduces ammonia permeability in a yeast growth assay. Beitz *et al.* (2006) studied the rat AQP1 double mutant F56A/H180A, finding it to conduct ammonia, methylamine, urea and glycerol. They do not report effects of the single mutation F56A.

In the present study, the rat AQP1 mutant F56H was found to conduct water but neither ammonia nor methylamine (Figs. 4.1, 4.4, 4.5, 4.7, Table 4.1). The Western blot band patterns (Figs. 4.3, 4.6, 4.14 B) indicate increased retention in the endoplasmic reticulum of *Xenopus* oocytes but not in that of *S. cerevisiae*. Unlike the wild-type protein, rat AQP8 H74F did not conduct water in a single experiment with yeast protoplasts (Fig. 4.18). Its synthesis was not verified and no confident conclusions may be drawn from this experiment.

The above considerations indicate that histidine in place of phenyalanine is tolerated in rat AQP1, and that it does not improve ammonia permeability. The analogous mutation in rat AQP8 or wheat TIP2;1 may, on the other hand, be structurally deleterious since both water or ammonia permeability appear to be affected, but the paucity of evidence allows no firm conclusion.

Barrier residue (rAQP1 His 180)

Early on, experiments pointed at the shortening of the histidine residue to an isoleucine one at this position as a way of enabling ammonia and methylamine passage through rat AQP1 (4.1.1). Together with corresponding reports on the effects of substitution by alanine (Beitz *et al.*, 2006), this led to the investigation of mutants bearing residues of various length, with limits imposed by the naturally occurring proteinogenic amino acids. Figure 5.2 summarizes and illustrates the results of these experiments.

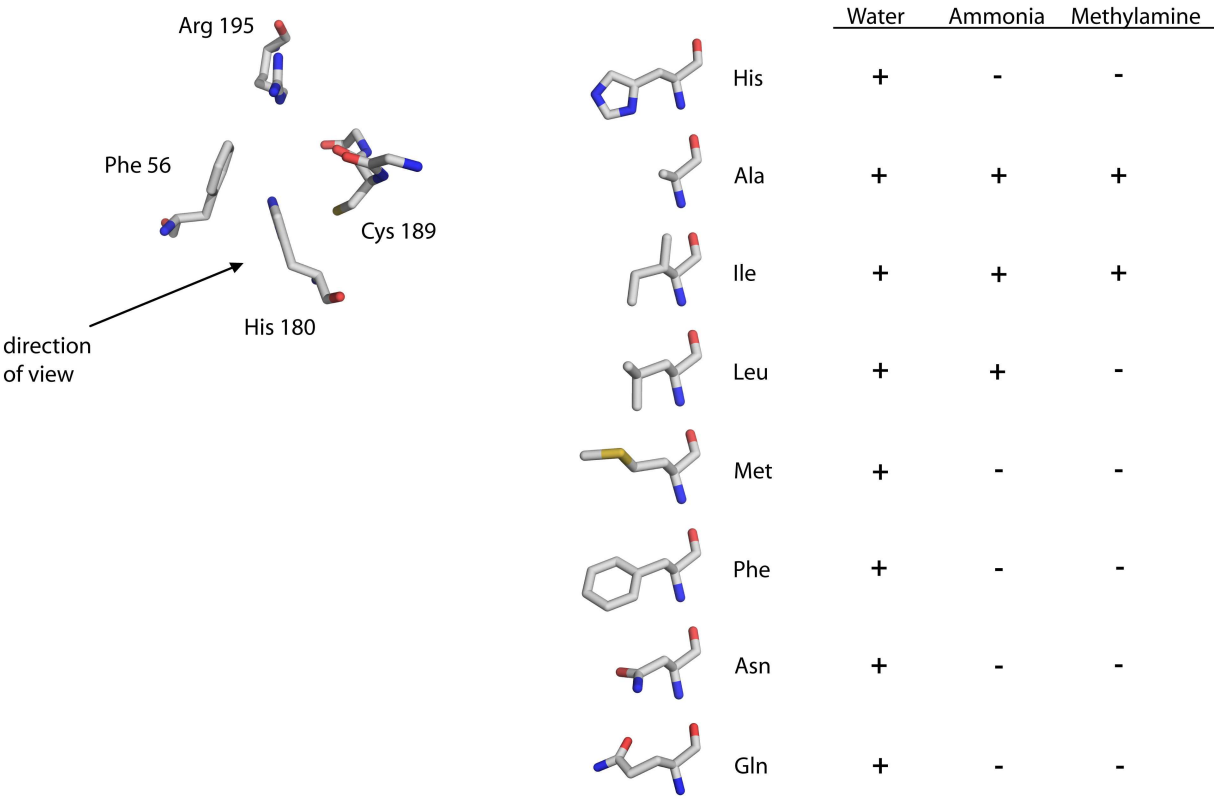

Fig. 5.2: Effects of varying the length and polarity of the amino acid residue represented by Histidine 180 in rat AQP1 on the permeability for water, ammonia and methylamine. Left: *Aromatic/arginine constriction of rat AQP1 based on the crystal structure of bovine AQP1 (PDB ID: 1J4N).* ***Right:*** *Table summarizing the qualitative permeability characteristics of Histidine 180 mutants of rat AQP1, based on osmotic assays with yeast protoplasts (water) and on yeast growth assays (ammonia and methylamine). Water permeability has been confirmed by Xenopus oocyte swelling assays in the case of isoleucine-, phenylalanine- and asparagine mutants. Methionine is shown with its side chain in the most extended conformation.*

Water permeability measurements and expression studies showed that all barrier residue mutations led to functioning channels in *S. cerevisiae* protoplasts, as well as in *Xenopus*

oocytes in the case of substitution by isoleucine, phenylalanine and asparagine (Figs. 4.3, 4.4, 4.10, 4.11, 4.13, 4.14). Even substitution of histidine by the larger and hydrophobic phenylalanine did not decrease water permeability below the detection threshold. Glutamine had been chosen partly because of its similar size compared to histidine (the DNA codons for histidine and glutamine only vary at their third position), and indeed its presence in place of histidine allows water molecules to pass. The promiscuity of ar/R-constriction amino acids with regard to water permeability has been noted before (Beitz *et al.*, 2006).

Ammonia and methylamine permeability, as judged by yeast growth assays, was only detectable for histidine substitution by the shorter alkyl residues of alanine and isoleucine. In the case of ammonia, leucine could also replace the histidine of rat AQP1, although this substitution consistently led to intermediate growth when compared to wild-type AQP1 and the H180A or H180I mutants (Figs. 4.1, 4.2, 4.7, 4.8, 4.9, 4.25, Table 4.1). The leucine side chain is branched at the γ-carbon rather than at the β-carbon atom, *i. e.* at a position expected to be closer to the ar/R-constriction pore in the mutant aquaporin. Assuming rotation of the residue, this would lead to a higher probability of collision with a passing molecule.

Asparagine is similar in size and shape to leucine, yet its presence in place of histidine did not allow detectable ammonia permeation. Amide groups are planar and represent dipoles with hydrogen bond-accepting and -donating groups. The asparagine side chain may thus be affected by dipole-dipole and hydrogen bond interactions with neighbouring residues as well as with passing molecules.

Unlike rat AQP1 H180A, human AQP1 H180A did not increase ammonia permeability, although it conducted water (Figs. 4.15, 4.16). A possible reason for this is a lower expression at the plasma membrane, as indicated by consistently lower water permeability of human AQP1-producing yeast protoplasts compared to rat AQP1-producing ones (not shown). Studies by a colleague (A. Almasalmeh) on hydrogen peroxide permeability of these aquaporins yield corresponding results, a finding that points at a threshold effect as illustrated in Figure 1.9.

The rat AQP8 mutant I200H retained water permeability (Figs. 4.18, 4.19), as did the human AQP8 mutant I198H (Figs. 4.22, 4.23), findings that agree with the water permeability of the wheat TIP2;1 mutant I184H/G193C (Holm *et al.*, 2005). It is possible that human AQP8 I198H has reduced ammonia permeability compared to the wild-type protein (Fig. 4.21). This would agree with the reduced ammonia permeability of wheat TIP2;1 I184H/G193C (Holm *et al.*, 2005).

Multiple mutations

Multiple rat AQP1 mutants, such as F56H/H180I/C189G which has an ar/R constriction resembling that of human AQP8, were ammonia-permeable only if Histidine 180 was replaced by isoleucine or leucine (Figs. 4.1, 4.2, 4.7, 4.8, Table 4.1). Water permeability was retained in the case of the triple mutant, as judged by two experiments using the same yeast protoplast preparation (Figs. 4.4, 4.12).

Other residues lining the aromatic/arginine constriction (hAQP8 Cys 53, Phe 145)

Cysteine 53 of human AQP8 is predicted by amino acid sequence alignment to correspond to Isoleucine 29 of human AQP1 and to Leucine 29 of human AQP5, both located at the C-terminal end of Helix 1 (Figs 1.2, 1.3). According to the crystal structures of the latter two, this amino acid residue lies close to the guanidinium group of the arginine residue, on the same side as the aromatic amino acid of the ar/R constriction. Its mutation to serine (hAQP8 C53S) did not affect water permeability (Fig. 4.23). The thiol group of Cysteine 53 probably does not react with the guanidinium group of Arginine 213.

Phenylalanine 145 of human AQP8 is predicted to be located approximately at the midsection of Loop C (Fig. 1.2). Its side chain may thus be located close to the ar/R constriction (Fig. 1.8). Mutation to alanine (hAQP8 F145A) markedly diminished water permeability despite undiminished synthesis of the mutant aquaporin (Figs. 4.22, 4.23). Thus, the phenylalanine residue is essential, although it is not clear whether mutation to alanine affects channel function or plasma membrane localization. Phenylalanine is not conserved at the corresponding position, or those surrounding it along Loop C, in tonoplast intrinsic proteins.

5.4.2 Potential permeants other than ammonia

In Section 5.2.2 the possibility was mentioned that the yeast “ammonia” assay used to qualitatively determine ammonia permeability of heterologously expressed aquaporins may, in fact, indicate permeability of another molecule. Which other molecules may be expected to pass? Since urea is not conducted by rat AQP1 H180A (Beitz *et al.*, 2006), the aquaporin mutant with the widest ar/R constriction studied here (Fig. 5.2), candidate molecules are likely to be triatomic (not counting hydrogen atoms) or smaller. The number of such molecules is not large when considering carbon, oxygen, and nitrogen atoms only. In addition, “homoatomic” molecules (again not counting hydrogen) such as ethane, dinitrogen and ozone are unlikely with the exception of hydrogen peroxide, as are carbon-nitrogen compounds. Among carbon-oxygen compounds, dimethylether, formic acid, and the two aldehydes can be excluded due to their metabolic insignificance, charge, or reactivity. Other

molecules such as carbon monoxide or nitrogen monoxide are also unlikely. Thus, going through a list of about 70 molecules, one is left with a few that fulfil the criteria of being small, stable, uncharged and likely to be found in meaningful concentrations: Other than ammonia, these are hydrogen peroxide, carbon dioxide, and ethanol. Hydrogen peroxide is kinetically stable, but its decomposition is accelerated by catalase. Carbon dioxide and ethanol are bulk metabolites, but much of the former is rapidly converted to hydrogen carbonate under cellular conditions, whereas ethanol is triatomic, saturated, angular and thus somewhat large. The major reasons against ammonia being the permeant are the lack of aquaporin-facilitated yeast growth at low concentrations of this nitrogen source (Figs. 4.49, 4.53), and the aquaporin-dependent growth on alkaline media in the absence of ammonium (Fig. 4.25).
Incidentally, nature has provided an aquaporin with an ar/R constriction similar to that of the rat AQP1 mutant H180I, one that has been studied both structurally and functionally. Figure 5.3 compares the two.

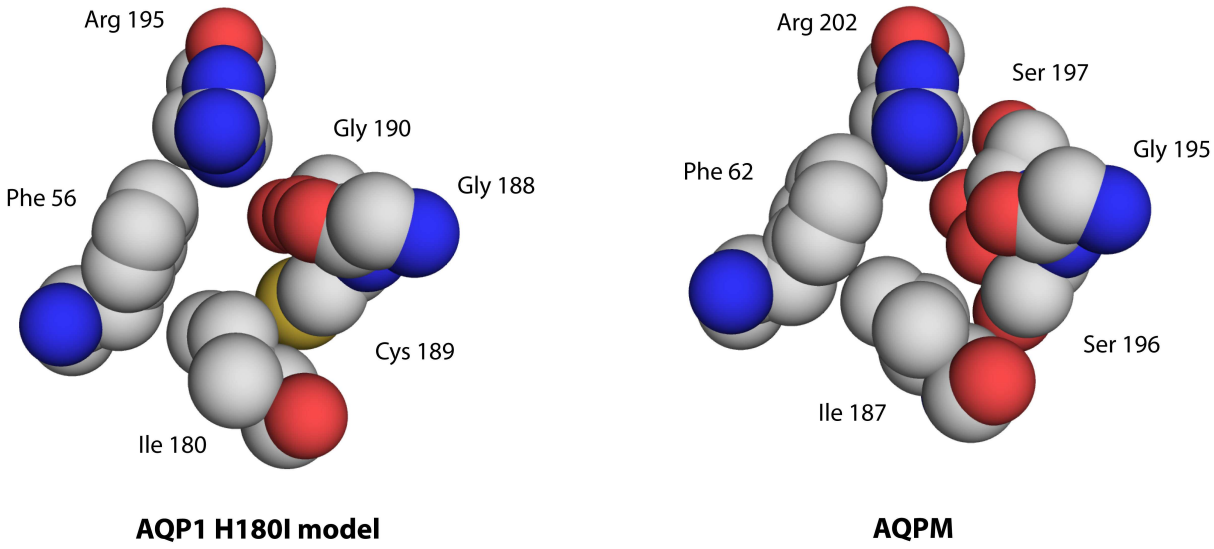

Fig. 5.3: Aromatic/arginine constrictions of the rat AQP1 mutant H180I, and the naturally occurring aquaporin of an archaeon. *The model of rAQP1 H180I is based on the crystal structure of bovine AQP1 (PDB ID: 1J4N). AQPM is the only aquaporin of the archaeon Methanothermobacter marburgensis (PDB ID: 2F2B).*

M. marburgensis is a lithoautotrophic thermophilic archaeon that requires anaerobic conditions for growth and which generates energy by converting carbon dioxide and dihydrogen to methane (Smith *et al.*, 1997). Its single aquaporin, AQPM (Ding and Kozono, 2001), has been found to conduct water and glycerol (Kozono *et al.*, 2003). The authors admit that glycerol conductivity (absent in rAQP1 H180I) is unlikely to be biologically relevant, and point out that carbon dioxide may be a more likely substrate in addition to water. In another report they mention the possibility of dihydrogen sulfide as a permeant waste product (Lee *et al.*, 2005), although subsequent studies on dihydrogen sulfide permeation of the related aquaporin of another anaerobic archaeon, *A. fulgidus* (Table 1.1), with an identical ar/R

constriction, do not support this (Mathai *et al.*, 2009). *M. marburgensis* uses ammonium as a nitrogen source, but it is likely to have ammonium transporters since *A. fulgidus* certainly does (Smith *et al.*, 1997, Andrade *et al.*, 2005). As so often, the biological function of an aquaporin remains elusive.

5.4.3 Conclusion

Jahn and colleagues (2004) say: “A more hydrophobic environment at the constriction region may therefore allow the transport of NH_3 and the slightly larger size of the ammonia molecule may require a larger pore diameter”. Beitz and colleagues (2006) say: “…it appears that hydrophobic niches at the entry site are needed to permit NH_3 passage”.
The presented work has merely and literally narrowed the size requirements for ammonia passage through an aquaporin, if truly ammonia permeability was studied by the yeast growth assays. If the actual permeant was carbon dioxide, ethanol, or another molecule, then one would conclude that the larger and more hydrophobic carbon dioxide, ethanol, or other molecule, requires a wider and more hydrophobic ar/R constriction, and that this is partly due to the facilitated replacement of water by a more hydrophobic permeant (Hub and de Groot, 2008). It is hard to think of a biologically relevant, stable and uncharged molecule smaller and more hydrophilic than water.
Varying the length of the ar/R constriction histidine residue of water-selective aquaporins appears to be the easiest way of achieving differential selectivity for uncharged solutes smaller than urea, and nature may have chosen isoleucine and valine over leucine and alanine (see 9.1) for a reason.

5.5 Outlook

The presented work is incomplete in several ways, especially so in that it lacks more direct measurements of aquaporin-mediated ammonia permeability, for example by electrophysiological measurements with *Xenopus laevis* oocytes. Thus, if it was to be pursued, the main task would lie in such measurements. A colleague’s efforts (A. Almasalmeh) at reproducing a published method, based on yeast cell loading with a pH-sensitive fluorescent dye, have not been met with success. An alternative might be the measurement of extracellular bulk acidification rates of yeast transformant suspensions subjected to the sudden presence of a

weakly buffered ammonium salt solution. Direct measurements of ammonia accumulation in yeast cells are also feasible with commercial kits.

Water permeability measurements of the aquaporin mutants have been repeated by a colleague (J. Song) who used the yeast strain BY4742 Δfps1. They agree with the measurements presented here, with one notable exception: rat AQP1 H180F barely increased water permeability of the yeast protoplasts.

Another set of experiments would serve to identify the solute responsible for the improved growth under “ammonia" assay conditions of yeast synthesizing particular aquaporins, if it is not ammonia itself. An ethanol sensitivity assay is easily conceivable, a pH- and hydrogen carbonate concentration-dependent yeast growth assay less so but still worth a try.

A preliminary experiment has shown that the cupric ammine complex hypothesis (5.2.2) is false, that is, an increased cupric ion concentration does increase growth of aquaporin-deficient yeast, and synergistically so if ferrous/ferric ion concentration is increased concomitantly, but not to a level comparable with growth of aquaporin-producing yeast. Another preliminary experiment has shown that replacing ammonium with other amines (methyl-, pentyl-, adamantylammonium, and chloroquine) in the presence of proline as nitrogen source, abolishes the aquaporin-dependent growth difference produced by ammonia at mildly alkaline pH.

The presence of isoleucine instead of histidine in the aromatic/arginine constriction of Aquaporin 8 and tonoplast intrinsic proteins may be explained by a requirement for (or tolerance of) the passage of solutes larger than water. The reason for its conserved combination with histidine, instead of phenylalanine, as the aromatic amino acid (1.2) remains obscure. Whether the histidine residue is needed at this position for its acid-base properties may be found out by replacing it with an artificial amino acid bearing an isoelectronic but less basic oxazole residue (Oδ and Nε, or vice versa).

6 Summary

Ammonia is a molecule similar in size and polarity to water, yet its rate of permeation through water-selective aquaporins (AQP) is comparatively low.

The amino acids lining the narrowest region of the water-selective rat AQP1, the so-called aromatic/arginine (ar/R) constriction, were altered by site-directed mutagenesis so as to resemble the corresponding region in the water- and ammonia-permeable human AQP8.

The resulting AQP1 mutants were tested for water permeability by osmotic assays with *Xenopus laevis* oocytes and with protoplasts of the yeast *Saccharomyces cerevisiae*. Permeability for ammonia and its analogue methylamine were tested with yeast growth assays.

All AQP1 mutants retained water permeability to some degree, even the H180F mutant which is expected to have an ar/R constriction narrower than that of the wild-type channel.

Ammonia- and methylamine permeability was found in those AQP1 mutants which had an alanine or isoleucine in place of Histidine 180, the latter being the corresponding amino acid in AQP8. In the case of ammonia, leucine was also permissible.

Human and rat AQP8 mutants with histidine in place of Isoleucine 198 and 200, respectively, retained water permeability. Their ammonia and methylamine permeability could not be studied by yeast growth assays.

The ammonia influx assay makes use of a yeast strain lacking its ammonium transporters Mep1-3 as well as its ammonia-permeable aquaglyceroporin Fps1. It was found to indicate elevated ammonia tolerance at neutral or mildly alkaline pH, rather than facilitated influx of ammonia as nitrogen source. In addition, replacing ammonium ions by amino acids such as glutamine did not completely abolish this pH-dependent effect.

The methylamine efflux assay makes use of a yeast strain lacking its aquaglyceroporin Fps1 which would otherwise allow accumulated toxic methylamine to escape from the cell. It was found to indicate increased tolerance of yeast to pH 6.5 and 7.5, even in the absence of methylammonium in the growth medium.

Yeast growth assays and osmotic assays with yeast protoplasts and human erythrocytes were employed for the study of potential inhibitors of human AQP1, AQP9, and of *Plasmodium falciparum* AQP. The substances had been discovered by collaborators using *in silico* high-throughput screening. No test compound was found to be active. Inhibition of human AQP1 by mercuric chloride, and of human AQP9 by mercuric chloride and phloretin, was confirmed.

7 Zusammenfassung

Das Ammoniakmolekül ähnelt dem Wassermolekül hinsichtlich seiner Größe und seiner Polarität. Trotzdem ist seine Permeationsrate durch wasserselektive Aquaporine (AQP) verhältnismäßig gering.

Die aromatische/Arginin (ar/R)-Konstriktion des wasserselektiven AQP1 der Ratte, wurde durch einzelne sowie durch mehrfache gezielte Punktmutationen von Aminosäuren so geändert, dass sie der ar/R-Konstriktion des Wasser und Ammoniak leitenden AQP8 ähnelte.

Die erhaltenen AQP1-Mutanten wurden in osmotischen Tests mit *Xenopus laevis* Oozyten und Protoplasten der Bäckerhefe *Saccharomyces cerevisiae* auf ihre Wasserleitfähigkeit hin untersucht. Ammoniak- und Methylaminleitfähigkeit wurden in Hefewachstumstests geprüft.

Alle AQP1-Mutanten wiesen Wasserleitfähigkeit auf, sogar AQP1 H180F, dessen ar/R-Konstriktion wahrscheinlich schmaler ist als die des Wildtypkanals.

Ammoniak- und Methylaminleitfähigkeit wurden festgestellt für AQP1-Mutanten in denen Histidin 180 durch Alanin oder Isoleucin ausgetauscht worden ist. Bezüglich der Ammoniakleitfähigkeit war Leucin an dieser Stelle ebenfalls einsetzbar.

Die Wasserleitfähigkeit des AQP8 des Menschen und der Ratte blieb nach Austausch von Isoleucin 198 bzw. Isoleucin 200 durch Histidin bestehen. Ihre Ammoniak- und Methylaminleitfähigkeit konnte mittels Hefewachstumstests nicht überprüft werden.

Der Ammoniakinfluxtest bedient sich eines Hefestammes welchem die Ammoniumtransporter Mep1-3 und das Ammoniak leitende Aquaglyceroporin Fps1 fehlen. Er zeigte eine durch heterologe AQP erhöhte Ammoniaktoleranz bei neutralem oder leicht alkalischem pH an, nicht jedoch den erleichterten Einstrom von Ammoniak als Stickstoffquelle. Außerdem konnte der Austausch von Ammoniumionen durch Aminosäuren, z. B. Glutamin, diesen pH-abhängigen Effekt nicht vollständig eliminieren.

Der Methylamineffluxtest bedient sich eines Hefestammes dem das Aquaglyceroporin Fps1 fehlt, welches ansonsten den Ausstrom von aufgenommenem, toxischem, Methylamin ermöglichen würde. Er zeigte eine zusätzliche methylaminunabhängige AQP-vermittelte Toleranz der Hefe gegenüber pH Werten von 6,5 und 7,5 an.

Hefewachstumstests und osmotische Tests mit Hefeprotoplasten und humanen Erythrocyten wurden zur Untersuchung von potentiellen Inhibitoren der humanen Aquaporine AQP1 und AQP9, sowie des *Plasmodium falciparum* AQP, verwendet. Die Testsubstanzen waren von Kooperationspartnern mittels *in silico* Hochdurchsatz-*Screening* gefunden worden. Keine der Substanzen zeigte Aktivität. Die Blockierung von menschlichem AQP1 durch Quecksilber(II)chlorid, sowie von menschlichem AQP9 durch Quecksilber(II)chlorid und Phloretin, konnte bestätigt werden.

8 Literature

Adeva MM, Souto G, Blanco N, Donapetry C.
Ammonium metabolism in humans.
Metabolism. 2012 Nov;61(11): 1495-511.

Agemark M, Kowal J, Kukulski W, Nordén K, Gustavsson N, Johanson U, Engel A, Kjellbom P.
Reconstitution of water channel function and 2D-crystallization of human aquaporin 8.
Biochim Biophys Acta. 2012 Mar;1818(3): 839-50.

Aguilera J, Van Dijken JP, De Winde JH, Pronk JT.
Carbonic anhydrase (Nce103p): an essential biosynthetic enzyme for growth of Saccharomyces cerevisiae at atmospheric carbon dioxide pressure.
Biochem J. 2005 Oct 15;391(Pt 2):311-6.

Andrade SL, Dickmanns A, Ficner R, Einsle O.
Crystal structure of the archaeal ammonium transporter Amt-1 from Archaeoglobus fulgidus.
Proc Natl Acad Sci U S A. 2005 Oct 18;102(42):14994-9.

Aponte-Santamaría C, Hub JS, de Groot BL.
Dynamics and energetics of solute permeation through the Plasmodium falciparum aquaglyceroporin.
Phys Chem Chem Phys. 2010 Sep 21;12(35):10246-54.

Atkins P, de Paula J.
Physical chemistry for the life sciences.
Oxford University Press. 2006.

Baker N, Glover L, Munday JC, Aguinaga Andrés D, Barrett MP, de Koning HP, Horn D.
Aquaglyceroporin 2 controls susceptibility to melarsoprol and pentamidine in African trypanosomes.
Proc Natl Acad Sci U S A. 2012 Jul 3;109(27):10996-1001.

Beitz E, Pavlovic-Djuranovic S, Yasui M, Agre P, Schultz JE.
Molecular dissection of water and glycerol permeability of the aquaglyceroporin from Plasmodium falciparum by mutational analysis.
Proc Natl Acad Sci U S A. 2004 Feb 3;101(5):1153-8.

Beitz E, Wu B, Holm LM, Schultz JE, Zeuthen T.
Point mutations in the aromatic/arginine region in aquaporin 1 allow passage of urea, glycerol, ammonia, and protons.
Proc Natl Acad Sci U S A. 2006 Jan 10;103(2):269-74.

Beitz E, Liu K, Ikeda M, Guggino WB, Agre P, Yasui M.
Determinants of AQP6 trafficking to intracellular sites versus the plasma membrane in transfected mammalian cells.
Biol Cell. 2006 Feb;98(2):101-9.

Benga G, Popescu O, Pop VI, Holmes RP.
p-(Chloromercuri)benzenesulfonate binding by membrane proteins and the inhibition of water transport in human erythrocytes.
Biochemistry. 1986 Apr 8;25(7):1535-8.

Berg JM, Tymoczko JL, Stryer L.
Biochemistry.
WH Freeman and Co., New York. 2002.

Berry V, Francis P, Kaushal S, Moore A, Bhattacharya S.
Missense mutations in MIP underlie autosomal dominant 'polymorphic' and lamellar cataracts linked to 12q.
Nat Genet. 2000 May;25(1):15-7.

Bertl A, Kaldenhoff R.
Function of a separate NH3-pore in Aquaporin TIP2;2 from wheat.
FEBS Lett. 2007 Nov 27;581(28):5413-7.

Bienert GP, Schjoerring JK, Jahn TP.
Membrane transport of hydrogen peroxide.
Biochim Biophys Acta. 2006 Aug;1758(8):994-1003.

Bienert GP, Møller AL, Kristiansen KA, Schulz A, Møller IM, Schjoerring JK, Jahn TP.
Specific aquaporins facilitate the diffusion of hydrogen peroxide across membranes.
J Biol Chem. 2007 Jan 12;282(2):1183-92.

Binder DK, Oshio K, Ma T, Verkman AS, Manley GT.
Increased seizure threshold in mice lacking aquaporin-4 water channels.
Neuroreport. 2004 Feb 9;15(2):259-62.

Bok D, Dockstader J, Horwitz J.
Immunocytochemical localization of the lens main intrinsic polypeptide (MIP26) in communicating junctions.
J Cell Biol. 1982 Jan;92(1):213-20.

Bonhivers M, Carbrey JM, Gould SJ, Agre P.
Aquaporins in Saccharomyces. Genetic and functional distinctions between laboratory and wild-type strains.
J Biol Chem. 1998 Oct 16;273(42):27565-72.

Borgnia MJ, Agre P.
Reconstitution and functional comparison of purified GlpF and AqpZ, the glycerol and water channels from Escherichia coli.
Proc Natl Acad Sci U S A. 2001 Feb 27;98(5):2888-93.

Brachmann CB, Davies A, Cost GJ, Caputo E, Li J, Hieter P, Boeke JD.
Designer deletion strains derived from Saccharomyces cerevisiae S288C: a useful set of strains and plasmids for PCR-mediated gene disruption and other applications.
Yeast. 1998 Jan 30;14(2):115-32.

Bradford MM.
A rapid and sensitive method for the quantitation of microgram quantities of protein utilizing the principle of protein-dye binding.
Anal Biochem. 1976 May 7;72:248-54.

Brändén M, Tabaei SR, Fischer G, Neutze R, Höök F.
Refractive-index-based screening of membrane-protein-mediated transfer across biological membranes.
Biophys J. 2010 Jul 7;99(1):124-33.

Bruge F, Bernasconi M, Parrinello M.
Ab initio simulation of rotational dynamics of solvated ammonium ion in water.
J Am Chem Soc. 1999;121:10883-88.

Calahorra M, Martínez GA, Hernández-Cruz A, Peña A.
Influence of monovalent cations on yeast cytoplasmic and vacuolar pH.
Yeast. 1998 Apr 30;14(6):501-15.

Calamita G, Bishai WR, Preston GM, Guggino WB, Agre P.
Molecular cloning and characterization of AqpZ, a water channel from Escherichia coli.
J Biol Chem. 1995 Dec 8;270(49):29063-6.

Calamita G, Mazzone A, Cho YS, Valenti G, Svelto M.
Expression and localization of the aquaporin-8 water channel in rat testis.
Biol Reprod. 2001 Jun;64(6):1660-6.

Calamita G, Mazzone A, Bizzoca A, Cavalier A, Cassano G, Thomas D, Svelto M.
Expression and immunolocalization of the aquaporin-8 water channel in rat gastrointestinal tract.
Eur J Cell Biol. 2001 Nov;80(11):711-9.

Calamita G, Ferri D, Gena P, Liquori GE, Cavalier A, Thomas D, Svelto M.
The inner mitochondrial membrane has aquaporin-8 water channels and is highly permeable to water.
J Biol Chem. 2005 Apr 29;280(17):17149-53.

Calamita G, Ferri D, Bazzini C, Mazzone A, Bottà G, Liquori GE, Paulmichl M, Portincasa P, Meyer G, Svelto M.
Expression and subcellular localization of the AQP8 and AQP1 water channels in the mouse gall-bladder epithelium.
Biol Cell. 2005 Jun;97(6):415-23.

Carbrey JM, Bonhivers M, Boeke JD, Agre P.
Aquaporins in Saccharomyces: Characterization of a second functional water channel protein.
Proc Natl Acad Sci U S A. 2001 Jan 30;98(3):1000-5.

Carbrey JM, Gorelick-Feldman DA, Kozono D, Praetorius J, Nielsen S, Agre P.
Aquaglyceroporin AQP9: solute permeation and metabolic control of expression in liver.
Proc Natl Acad Sci U S A. 2003 Mar 4;100(5):2945-50.

Carlsen A, Wieth JO.
Glycerol transport in human red cells.
Acta Physiol Scand. 1976 Aug;97(4):501-13.

Chang A, Hammond TG, Sun TT, Zeidel ML.
Permeability properties of the mammalian bladder apical membrane.
Am J Physiol. 1994 Nov;267(5 Pt 1):C1483-92.

Chepelinsky AB.
Structural function of MIP/aquaporin 0 in the eye lens; genetic defects lead to congenital inherited cataracts.
Handb Exp Pharmacol. 2009;(190):265-97.

Cho SJ, Sattar AK, Jeong EH, Satchi M, Cho JA, Dash S, Mayes MS, Stromer MH, Jena BP.
Aquaporin 1 regulates GTP-induced rapid gating of water in secretory vesicles.
Proc Natl Acad Sci U S A. 2002 Apr 2;99(7): 4720-4.

Chou CL, Ma T, Yang B, Knepper MA, Verkman AS.
Fourfold reduction of water permeability in inner medullary collecting duct of aquaporin-4 knockout mice.
Am J Physiol. 1998 Feb;274(2 Pt 1):C549-54.

Chung CT, Niemela SL, Miller RH.
One-step preparation of competent Escherichia coli: transformation and storage of bacterial cells in the same solution.
Proc Natl Acad Sci U S A. 1989 Apr;86(7):2172-5.

Cohen SN, Chang AC, Hsu L.
Nonchromosomal antibiotic resistance in bacteria: genetic transformation of Escherichia coli by R-factor DNA.
Proc Natl Acad Sci U S A. 1972 Aug;69(8):2110-4.

Collingro A, Toenshoff ER, Taylor MW, Fritsche TR, Wagner M, Horn M.
'Candidatus Protochlamydia amoebophila', an endosymbiont of Acanthamoeba spp.
Int J Syst Evol Microbiol. 2005 Sep;55(Pt 5):1863-6.

Conway EJ, Breen J.
An ammonia-yeast and some of its properties.
Biochem J. 1945;39(4):368-71.

Cooper GJ, Boron WF.
Effect of PCMBS on CO2 permeability of Xenopus oocytes expressing aquaporin 1 or its C189S mutant.
Am J Physiol. 1998 Dec;275(6 Pt 1):C1481-6.

de Groot BL, Engel A, Grubmüller H.
A refined structure of human aquaporin-1.
FEBS Lett. 2001 Aug 31;504(3): 206-11.

de Groot BL, Grubmüller H.
Water permeation across biological membranes: mechanism and dynamics of aquaporin-1 and GlpF.
Science. 2001 Dec 14;294(5550):2353-7.

de Groot BL, Frigato T, Helms V, Grubmüller H.
The mechanism of proton exclusion in the aquaporin-1 water channel.
J Mol Biol. 2003 Oct 17;333(2):279-93.

de Groot BL, Hub JS.
A decade of debate: significance of CO2 permeation through membrane channels still controversial.
Chemphyschem. 2011 Apr 4;12(5):1021-2.

Deen PM, Verdijk MA, Knoers NV, Wieringa B, Monnens LA, van Os CH, van Oost BA.
Requirement of human renal water channel aquaporin-2 for vasopressin-dependent concentration of urine.
Science. 1994 Apr 1;264(5155):92-5.

Denker BM, Smith BL, Kuhajda FP, Agre P.
Identification, purification, and partial characterization of a novel Mr 28,000 integral membrane protein from erythrocytes and renal tubules.
J Biol Chem. 1988 Oct 25;263(30):15634-42.

Detmers FJ, de Groot BL, Müller EM, Hinton A, Konings IB, Sze M, Flitsch SL, Grubmüller H, Deen PM.
Quaternary ammonium compounds as water channel blockers. Specificity, potency, and site of action.
J Biol Chem. 2006 May 19;281(20):14207-14.

Diem K, Lentner C, Ed.
Documenta Geigy, Wissenschaftliche Tabellen.
J. R. Geigy A. G., Pharma, Basel. 1969.

Ding X, Kitagawa Y.
Rapid amplification of a water channel-like gene and its flanking sequences from the Methanothermobacter marburgensis genome using a single primer PCR strategy.
J Biosci Bioeng. 2001;92(5): 488-91.

Doerge FD, Gisvold O, Wilson CO, Ed.
Textbook of organic medicinal and pharmaceutical chemistry.
J. B. Lippincot Company. 1971.

Dynowski M, Mayer M, Moran O, Ludewig U.
Molecular determinants of ammonia and urea conductance in plant aquaporin homologs.
FEBS Lett. 2008 Jul 9;582(16):2458-62.

Ecelbarger CA, Terris J, Frindt G, Echevarria M, Marples D, Nielsen S, Knepper MA.
Aquaporin-3 water channel localization and regulation in rat kidney.
Am J Physiol. 1995 Nov;269(5 Pt 2):F663-72.

Farmer RE, Macey RI.
Perturbation of red cell volume: rectification of osmotic flow.
Biochim Biophys Acta. 1970 Jan 6;196(1):53-65.

Fast D.
Sporulation synchrony of Saccharomyces cerevisiae grown in various carbon sources.
J Bacteriol. 1973 Nov;116(2):925-30.

Fernandez-Ricaud L, Warringer J, Ericson E, Glaab K, Davidsson P, Nilsson F, Kemp GJ, Nerman O, Blomberg A.
PROPHECY--a yeast phenome database, update 2006.
Nucleic Acids Res. 2007 Jan;35(Database issue):D463-7.

Fischer G, Kosinska-Eriksson U, Aponte-Santamaría C, Palmgren M, Geijer C, Hedfalk K, Hohmann S, de Groot BL, Neutze R, Lindkvist-Petersson K.
Crystal structure of a yeast aquaporin at 1.15 angstrom reveals a novel gating mechanism.
PLoS Biol. 2009 Jun;7(6):e1000130.

Fu D, Libson A, Miercke LJ, Weitzman C, Nollert P, Krucinski J, Stroud RM.
Structure of a glycerol-conducting channel and the basis for its selectivity.
Science. 2000 Oct 20;290(5491):481-6.

Fushimi K, Uchida S, Hara Y, Hirata Y, Marumo F, Sasaki S.
Cloning and expression of apical membrane water channel of rat kidney collecting tubule.
Nature. 1993 Feb 11;361(6412):549-52.

Gattolin S, Sorieul M, Frigerio L.
Mapping of tonoplast intrinsic proteins in maturing and germinating Arabidopsis seeds reveals dual localization of embryonic TIPs to the tonoplast and plasma membrane.
Mol Plant. 2011 Jan;4(1):180-9.

Gietz RD, Schiestl RH, Willems AR, Woods RA.
Studies on the transformation of intact yeast cells by the LiAc/SS-DNA/PEG procedure.
Yeast. 1995 Apr 15;11(4):355-60.

Golchini K, Kurtz I.
NH3 permeation through the apical membrane of MDCK cells is via a lipid pathway.
Am J Physiol. 1988 Jul;255(1 Pt 2):F135-41.

Gonen T, Cheng Y, Kistler J, Walz T.
Aquaporin-0 membrane junctions form upon proteolytic cleavage.
J Mol Biol. 2004 Sep 24;342(4):1337-45.

Gourbal B, Sonuc N, Bhattacharjee H, Legare D, Sundar S, Ouellette M, Rosen BP, Mukhopadhyay R.
Drug uptake and modulation of drug resistance in Leishmania by an aquaglyceroporin.
J Biol Chem. 2004 Jul 23;279(30):31010-7.

Gradilone SA, Tietz PS, Splinter PL, Marinelli RA, LaRusso NF.
Expression and subcellular localization of aquaporin water channels in the polarized hepatocyte cell line, WIF-B.
BMC Physiol. 2005 Aug 18;5:13.

Greenfield NJ, Hussain M, Lenard J.
Effects of growth state and amines on cytoplasmic and vacuolar pH, phosphate and polyphosphate levels in Saccharomyces cerevisiae: a 31P-nuclear magnetic resonance study.
Biochim Biophys Acta. 1987 Dec 7;926(3):205-14.

Gruswitz F, Chaudhary S, Ho JD, Schlessinger A, Pezeshki B, Ho CM, Sali A, Westhoff CM, Stroud RM.
Function of human Rh based on structure of RhCG at 2.1 A.
Proc Natl Acad Sci U S A. 2010 May 25;107(21):9638-43.

Guan XG, Su WH, Yi F, Zhang D, Hao F, Zhang HG, Liu YJ, Feng XC, Ma TH.
NPA motifs play a key role in plasma membrane targeting of aquaporin-4.
IUBMB Life. 2010 Mar;62(3):222-6.

Gupta AB, Verma RK, Agarwal V, Vajpai M, Bansal V, Sankararamakrishnan R.
MIPModDB: a central resource for the superfamily of major intrinsic proteins.
Nucleic Acids Res. 2012 Jan;40(Database issue):D362-9.

Hamm LL, Trigg D, Martin D, Gillespie C, Buerkert J.
Transport of ammonia in the rabbit cortical collecting tubule.
J Clin Invest. 1985 Feb;75(2):478-85.

Hansen M, Kun JF, Schultz JE, Beitz E.
A single, bi-functional aquaglyceroporin in blood-stage Plasmodium falciparum malaria parasites.
J Biol Chem. 2002 Feb 15;277(7):4874-82.

Hara M, Verkman AS.
Glycerol replacement corrects defective skin hydration, elasticity, and barrier function in aquaporin-3-deficient mice.
Proc Natl Acad Sci U S A. 2003 Jun 10;100(12):7360-5.

Hara-Chikuma M, Sohara E, Rai T, Ikawa M, Okabe M, Sasaki S, Uchida S, Verkman AS.
Progressive adipocyte hypertrophy in aquaporin-7-deficient mice: adipocyte glycerol permeability as a novel regulator of fat accumulation.
J Biol Chem. 2005 Apr 22;280(16):15493-6.

Hathaway BJ, Tomlinson AAG.
Copper(II) ammonia complexes.
Coordination Chemistry Reviews. 1970;5:1-43.

Hermann R, Lehmann M, Büchs J.
Characterization of gas-liquid mass transfer phenomena in microtiter plates.
Biotechnol Bioeng. 2003 Jan 20;81(2):178-86.

Herrera M, Garvin JL.
Novel role of AQP-1 in NO-dependent vasorelaxation.
Am J Physiol Renal Physiol. 2007 May;292(5):F1443-51.

Hess DC, Lu W, Rabinowitz JD, Botstein D.
Ammonium toxicity and potassium limitation in yeast.
PLoS Biol. 2006 Oct;4(11):e351.

Hill WG, Zeidel ML.
Reconstituting the barrier properties of a water-tight epithelial membrane by design of leaflet-specific liposomes.
J Biol Chem. 2000 Sep 29;275(39):30176-85.

Hiroaki Y, Tani K, Kamegawa A, Gyobu N, Nishikawa K, Suzuki H, Walz T, Sasaki S, Mitsuoka K, Kimura K, Mizoguchi A, Fujiyoshi Y.
Implications of the aquaporin-4 structure on array formation and cell adhesion.
J Mol Biol. 2006 Jan 27;355(4):628-39.

Holm LM, Klaerke DA, Zeuthen T.
Aquaporin 6 is permeable to glycerol and urea.
Pflugers Arch. 2004 May;448 (2):181-6.

Holm LM, Jahn TP, Møller AL, Schjoerring JK, Ferri D, Klaerke DA, Zeuthen T.
NH3 and NH4+ permeability in aquaporin-expressing Xenopus oocytes.
Pflugers Arch. 2005 Sep;450(6):415-28.

Huang CG, Lamitina T, Agre P, Strange K.
Functional analysis of the aquaporin gene family in Caenorhabditis elegans.
Am J Physiol Cell Physiol. 2007 May;292(5):C1867-73.

Hub JS, de Groot BL.
Mechanism of selectivity in aquaporins and aquaglyceroporins.
Proc Natl Acad Sci U S A. 2008 Jan 29;105(4):1198-203.

Hwang JH, Ellingson SR, Roberts DM.
Ammonia permeability of the soybean nodulin 26 channel.
FEBS Lett. 2010 Oct 22;584(20):4339-43.

Iacovache I, Biasini M, Kowal J, Kukulski W, Chami M, van der Goot FG, Engel A, Rémigy HW.
The 2DX robot: a membrane protein 2D crystallization Swiss Army knife.
J Struct Biol. 2010 Mar;169(3):370-8.

Ikeda M, Beitz E, Kozono D, Guggino WB, Agre P, Yasui M.
Characterization of aquaporin-6 as a nitrate channel in mammalian cells. Requirement of pore-lining residue threonine 63.
J Biol Chem. 2002 Oct 18;277(42):39873-9.

Imai T, Ohno T.
Measurement of yeast intracellular pH by image processing and the change it undergoes during growth phase.
J Biotechnol. 1995 Jan 15;38(2):165-72.

Irwin JJ, Shoichet BK.
ZINC--a free database of commercially available compounds for virtual screening.
J Chem Inf Model. 2005 Jan-Feb;45(1):177-82.

Ishibashi K, Sasaki S, Fushimi K, Uchida S, Kuwahara M, Saito H, Furukawa T, Nakajima K, Yamaguchi Y, Gojobori T, et al.
Molecular cloning and expression of a member of the aquaporin family with permeability to glycerol and urea in addition to water expressed at the basolateral membrane of kidney collecting duct cells.
Proc Natl Acad Sci U S A. 1994 Jul 5;91(14):6269-73.

Ishibashi K, Sasaki S, Saito F, Ikeuchi T, Marumo F.
Structure and chromosomal localization of a human water channel (AQP3) gene.
Genomics. 1995 May 20;27(2):352-4.

Ishibashi K, Kuwahara M, Kageyama Y, Tohsaka A, Marumo F, Sasaki S.
Cloning and functional expression of a second new aquaporin abundantly expressed in testis.
Biochem Biophys Res Commun. 1997 Aug 28;237(3):714-8.

Ishibashi K, Yamauchi K, Kageyama Y, Saito-Ohara F, Ikeuchi T, Marumo F, Sasaki S.
Molecular characterization of human Aquaporin-7 gene and its chromosomal mapping.
Biochim Biophys Acta. 1998 Jul 30;1399(1):62-6.

Itoh T, Rai T, Kuwahara M, Ko SB, Uchida S, Sasaki S, Ishibashi K.
Identification of a novel aquaporin, AQP12, expressed in pancreatic acinar cells.
Biochem Biophys Res Commun. 2005 May 13;330(3):832-8.

Jahn TP, Møller AL, Zeuthen T, Holm LM, Klaerke DA, Mohsin B, Kühlbrandt W, Schjoerring JK.
Aquaporin homologues in plants and mammals transport ammonia.
FEBS Lett. 2004 Sep 10;574(1-3):31-6.

Jelen S, Wacker S, Aponte-Santamaría C, Skott M, Rojek A, Johanson U, Kjellbom P, Nielsen S, de Groot BL, Rützler M.
Aquaporin-9 protein is the primary route of hepatocyte glycerol uptake for glycerol gluconeogenesis in mice.
J Biol Chem. 2011 Dec 30;286(52):44319-25.

Jensen MØ, Mouritsen OG.
Single-channel water permeabilities of Escherichia coli aquaporins AqpZ and GlpF.
Biophys J. 2006 Apr 1;90(7):2270-84.

Jeremic A, Cho WJ, Jena BP.
Involvement of water channels in synaptic vesicle swelling.
Exp Biol Med (Maywood). 2005 Oct;230(9):674-80.

Jung D, MacIver B, Jackson BP, Barnaby R, Sato JD, Zeidel ML, Shaw JR, Stanton BA.
A novel aquaporin 3 in killifish (Fundulus heteroclitus) is not an arsenic channel.
Toxicol Sci. 2012 May;127(1):101-9.

Khademi S, Stroud RM.
The Amt/MEP/Rh family: structure of AmtB and the mechanism of ammonia gas conduction.
Physiology (Bethesda). 2006 Dec;21:419-29.

Khoo KH, Culberson CH, Bates RG.
Thermodynamics of the dissociation of ammonium ion in seawater from 5 to 40℃.
Journal of Solution Chemistry. 1977; 6:281-90.

King N, Westbrook MJ, Young SL, Kuo A, Abedin M, Chapman J, Fairclough S, Hellsten U, Isogai Y, Letunic I, Marr M, Pincus D, Putnam N, Rokas A, Wright KJ, Zuzow R, Dirks W, Good M, Goodstein D, Lemons D, Li W, Lyons JB, Morris A, Nichols S, Richter DJ, Salamov A, Sequencing JG, Bork P, Lim WA, Manning G, Miller WT, McGinnis W, Shapiro H, Tjian R, Grigoriev IV, Rokhsar D.
The genome of the choanoflagellate Monosiga brevicollis and the origin of metazoans.
Nature. 2008 Feb 14;451(7180):783-8.

Klebl F, Wolf M, Sauer N.
A defect in the yeast plasma membrane urea transporter Dur3p is complemented by CpNIP1, a Nod26-like protein from zucchini (Cucurbita pepo L.), and by Arabidopsis thaliana delta-TIP or gamma-TIP.
FEBS Lett. 2003 Jul 17;547(1-3):69-74.

Klocke RA, Andersson KK, Rotman HH, Forster RE.
Permeability of human erythrocytes to ammonia and weak acids.
Am J Physiol. 1972 Apr;222(4):1004-13.

Kołaczkowski M, Kołaczowska A, Luczynski J, Witek S, Goffeau A.
In vivo characterization of the drug resistance profile of the major ABC transporters and other components of the yeast pleiotropic drug resistance network.
Microb Drug Resist. 1998 Fall;4(3):143-58.

Kossiakoff AA, Spencer SA.
Direct determination of the protonation states of aspartic acid-102 and histidine-57 in the tetrahedral intermediate of the serine proteases: neutron structure of trypsin.
Biochemistry. 1981 Oct 27;20(22):6462-74.

Koyama Y, Yamamoto T, Kondo D, Funaki H, Yaoita E, Kawasaki K, Sato N, Hatakeyama K, Kihara I.
Molecular cloning of a new aquaporin from rat pancreas and liver.
J Biol Chem. 1997 Nov 28;272(48):30329-33.

Koyama N, Ishibashi K, Kuwahara M, Inase N, Ichioka M, Sasaki S, Marumo F.
Cloning and functional expression of human aquaporin8 cDNA and analysis of its gene.
Genomics. 1998 Nov 15;54(1):169-72.

Koyama Y, Yamamoto T, Tani T, Nihei K, Kondo D, Funaki H, Yaoita E, Kawasaki K, Sato N, Hatakeyama K, Kihara I.
Expression and localization of aquaporins in rat gastrointestinal tract.
Am J Physiol. 1999 Mar;276(3 Pt 1):C621-7.

Kozono D, Ding X, Iwasaki I, Meng X, Kamagata Y, Agre P, Kitagawa Y.
Functional expression and characterization of an archaeal aquaporin. AqpM from methanothermobacter marburgensis.
J Biol Chem. 2003 Mar 21;278(12):10649-56.

Kwon TH, Nielsen J, Møller HB, Fenton RA, Nielsen S, Frøkiaer J.
Aquaporins in the kidney.
Handb Exp Pharmacol. 2009;(190):95-132.

Labotka RJ, Lundberg P, Kuchel PW.
Ammonia permeability of erythrocyte membrane studied by 14N and 15N saturation transfer NMR spectroscopy.
Am J Physiol. 1995 Mar;268(3 Pt 1):C686-99.

Laforenza U, Cova E, Gastaldi G, Tritto S, Grazioli M, LaRusso NF, Splinter PL, D'Adamo P, Tosco M, Ventura U.
Aquaporin-8 is involved in water transport in isolated superficial colonocytes from rat proximal colon.
J Nutr. 2005 Oct;135(10):2329-36.

Laizé V, Rousselet G, Verbavatz JM, Berthonaud V, Gobin R, Roudier N, Abrami L, Ripoche P, Tacnet F.
Functional expression of the human CHIP28 water channel in a yeast secretory mutant.
FEBS Lett. 1995 Oct 16;373(3):269-74.

Lamoureux G, Javelle A, Baday S, Wang S, Bernèche S.
Transport mechanisms in the ammonium transporter family.
Transfus Clin Biol. 2010 Sep;17(3):168-75.

Lande MB, Donovan JM, Zeidel ML.
The relationship between membrane fluidity and permeabilities to water, solutes, ammonia, and protons.
J Gen Physiol. 1995 Jul;106(1):67-84.

Lee JK, Kozono D, Remis J, Kitagawa Y, Agre P, Stroud RM.
Structural basis for conductance by the archaeal aquaporin AqpM at 1.68 A.
Proc Natl Acad Sci U S A. 2005 Dec 27;102(52):18932-7.

Lee JS, Cho WJ, Shin L, Jena BP.
Involvement of cholesterol in synaptic vesicle swelling.
Exp Biol Med (Maywood). 2010 Apr;235(4):470-7.

Lee WK, Bork U, Gholamrezaei F, Thévenod F.
Cd(2+)-induced cytochrome c release in apoptotic proximal tubule cells: role of mitochondrial permeability transition pore and Ca(2+) uniporter.
Am J Physiol Renal Physiol. 2005 Jan;288(1):F27-39.

LeFevre PG.
Evidence of active transfer of certain non-electrolytes across the human red cell membrane.
J Gen Physiol. 1948 Jul 20;31(6):505-27.

LeFevre PG.
Molecular structural factors in competitive inhibition of sugar transport.
Science. 1959 Jul 10;130 (3367):104-5.

Lehmann GL, Larocca MC, Soria LR, Marinelli RA.
Aquaporins: their role in cholestatic liver disease.
World J Gastroenterol. 2008 Dec 14;14(46):7059-67.

Li H, Chen H, Steinbronn C, Wu B, Beitz E, Zeuthen T, Voth GA.
Enhancement of proton conductance by mutations of the selectivity filter of aquaporin-1.
J Mol Biol. 2011 Apr 8;407(4):607-20.

Li L, Li Z, Wang C, Xu D, Mariano PS, Guo H, Dunaway-Mariano D.
The electrostatic driving force for nucleophilic catalysis in L-arginine deiminase: a combined experimental and theoretical study.
Biochemistry. 2008 Apr 22;47(16):4721-32.

Liu K, Kozono D, Kato Y, Agre P, Hazama A, Yasui M.
Conversion of aquaporin 6 from an anion channel to a water-selective channel by a single amino acid substitution.
Proc Natl Acad Sci U S A. 2005 Feb 8;102(6):2192-7.

Liu K, Nagase H, Huang CG, Calamita G, Agre P.
Purification and functional characterization of aquaporin-8.
Biol Cell. 2006 Mar;98(3):153-61.

Liu Y, Promeneur D, Rojek A, Kumar N, Frøkiaer J, Nielsen S, King LS, Agre P, Carbrey JM.
Aquaporin 9 is the major pathway for glycerol uptake by mouse erythrocytes, with implications for malarial virulence.
Proc Natl Acad Sci U S A. 2007 Jul 24;104(30):12560-4.

Loqué D, Ludewig U, Yuan L, von Wirén N.
Tonoplast intrinsic proteins AtTIP2;1 and AtTIP2;3 facilitate NH3 transport into the vacuole.
Plant Physiol. 2005 Feb;137(2):671-80.

Ma JF, Tamai K, Yamaji N, Mitani N, Konishi S, Katsuhara M, Ishiguro M, Murata Y, Yano M.
A silicon transporter in rice.
Nature. 2006 Mar 30;440(7084):688-91.

Ma T, Yang B, Verkman AS.
Cloning of a novel water and urea-permeable aquaporin from mouse expressed strongly in colon, placenta, liver, and heart.
Biochem Biophys Res Commun. 1997 Nov 17;240(2):324-8.

Ma T, Yang B, Gillespie A, Carlson EJ, Epstein CJ, Verkman AS.
Severely impaired urinary concentrating ability in transgenic mice lacking aquaporin-1 water channels.
J Biol Chem. 1998 Feb 20;273(8):4296-9.

Ma T, Song Y, Yang B, Gillespie A, Carlson EJ, Epstein CJ, Verkman AS.
Nephrogenic diabetes insipidus in mice lacking aquaporin-3 water channels.
Proc Natl Acad Sci U S A. 2000 Apr 11;97(8):4386-91.

Macey RI, Farmer RE.
Inhibition of water and solute permeability in human red cells.
Biochim Biophys Acta. 1970 Jul 7;211(1):104-6.

Madeira A, Leitão L, Soveral G, Dias P, Prista C, Moura T, Loureiro-Dias MC.
Effect of ethanol on fluxes of water and protons across the plasma membrane of Saccharomyces cerevisiae.
FEMS Yeast Res. 2010 May;10(3):252-8.

Makarow M, Nevalainen LT.
Transport of a fluorescent macromolecule via endosomes to the vacuole in Saccharomyces cerevisiae.
J Cell Biol. 1987 Jan;104(1):67-75.

Marceau F, Bawolak MT, Lodge R, Bouthillier J, Gagné-Henley A, Gaudreault RC, Morissette G.
Cation trapping by cellular acidic compartments: beyond the concept of lysosomotropic drugs.
Toxicol Appl Pharmacol. 2012 Feb 15;259(1):1-12.

Marchissio MJ, Francés DE, Carnovale CE, Marinelli RA.
Mitochondrial aquaporin-8 knockdown in human hepatoma HepG2 cells causes ROS-induced mitochondrial depolarization and loss of viability.
Toxicol Appl Pharmacol. 2012 Oct 15;264(2):246-54.

Maresova L, Sychrova H.
Physiological characterization of Saccharomyces cerevisiae kha1 deletion mutants.
Mol Microbiol. 2005 Jan;55(2):588-600.

Marini AM, Soussi-Boudekou S, Vissers S, Andre B.
A family of ammonium transporters in Saccharomyces cerevisiae.
Mol Cell Biol. 1997 Aug;17(8):4282-93.

Mathai JC, Mori S, Smith BL, Preston GM, Mohandas N, Collins M, van Zijl PC, Zeidel ML, Agre P.
Functional analysis of aquaporin-1 deficient red cells. The Colton-null phenotype.
J Biol Chem. 1996 Jan 19;271(3):1309-13.

Mathai JC, Missner A, Kügler P, Saparov SM, Zeidel ML, Lee JK, Pohl P.
No facilitator required for membrane transport of hydrogen sulfide.
Proc Natl Acad Sci U S A. 2009 Sep 29;106(39):16633-8.

Maurel C, Reizer J, Schroeder JI, Chrispeels MJ, Saier MH Jr.
Functional characterization of the Escherichia coli glycerol facilitator, GlpF, in Xenopus oocytes.
J Biol Chem. 1994 Apr 22;269(16):11869-72.

Maurel C, Reizer J, Schroeder JI, Chrispeels MJ.
The vacuolar membrane protein gamma-TIP creates water specific channels in Xenopus oocytes.
EMBO J. 1993 Jun;12(6):2241-7.

Matuszak CA, Matuszak AJ.
Imidazole - Versatile today, prominent tomorrow.
J. Chem. Educ. 1976 May;53(5): 280-4.

McConnell NA, Yunus RS, Gross SA, Bost KL, Clemens MG, Hughes FM Jr.
Water permeability of an ovarian antral follicle is predominantly transcellular and mediated by aquaporins.
Endocrinology. 2002 Aug;143(8):2905-12.

Meinild AK, Klaerke DA, Zeuthen T.
Bidirectional water fluxes and specificity for small hydrophilic molecules in aquaporins 0-5.
J Biol Chem. 1998 Dec 4;273(49):32446-51.

Meyrial V, Laizé V, Gobin R, Ripoche P, Hohmann S, Tacnet F.
Existence of a tightly regulated water channel in Saccharomyces cerevisiae.
Eur J Biochem. 2001 Jan;268(2):334-43.

Miller EW, Dickinson BC, Chang CJ.
Aquaporin-3 mediates hydrogen peroxide uptake to regulate downstream intracellular signaling.
Proc Natl Acad Sci U S A. 2010 Sep 7;107(36):15681-6.

Mobasheri A, Marples D, Young IS, Floyd RV, Moskaluk CA, Frigeri A.
Distribution of the AQP4 water channel in normal human tissues: protein and tissue microarrays reveal expression in several new anatomical locations, including the prostate gland and seminal vesicles.
Channels (Austin). 2007 Jan-Feb;1(1):29-38.

Molinas SM, Trumper L, Marinelli RA.
Mitochondrial aquaporin-8 in renal proximal tubule cells: evidence for a role in the response to metabolic acidosis.
Am J Physiol Renal Physiol. 2012 Aug;303(3):F458-66.

Monzani E, Bazzotti R, Perego C, La Porta CA.
AQP1 is not only a water channel: it contributes to cell migration through Lin7/beta-catenin.
PLoS One. 2009 Jul 8;4(7):e6167.

Morishita Y, Matsuzaki T, Hara-chikuma M, Andoo A, Shimono M, Matsuki A, Kobayashi K, Ikeda M, Yamamoto T, Verkman A, Kusano E, Ookawara S, Takata K, Sasaki S, Ishibashi K.
Disruption of aquaporin-11 produces polycystic kidneys following vacuolization of the proximal tubule.
Mol Cell Biol. 2005 Sep;25(17):7770-9.

Mouro-Chanteloup I, Cochet S, Chami M, Genetet S, Zidi-Yahiaoui N, Engel A, Colin Y, Bertrand O, Ripoche P.
Functional reconstitution into liposomes of purified human RhCG ammonia channel.
PLoS One. 2010 Jan 28;5(1):e8921.

Moustafa A, Reyes-Prieto A, Bhattacharya D.
Chlamydiae has contributed at least 55 genes to Plantae with predominantly plastid functions.
PLoS One. 2008 May 21;3(5):e2205.

Mulders SM, Preston GM, Deen PM, Guggino WB, van Os CH, Agre P.
Water channel properties of major intrinsic protein of lens.
J Biol Chem. 1995 Apr 14;270(15):9010-16.

Mumberg D, Müller R, Funk M.
Regulatable promoters of Saccharomyces cerevisiae: comparison of transcriptional activity and their use for heterologous expression.
Nucleic Acids Res. 1994 Dec 25;22(25):5767-8.

Murata K, Mitsuoka K, Hirai T, Walz T, Agre P, Heymann JB, Engel A, Fujiyoshi Y.
Structural determinants of water permeation through aquaporin-1.
Nature. 2000 Oct 5;407(6804):599-605.

Musa-Aziz R, Jiang L, Chen LM, Behar KL, Boron WF.
Concentration-dependent effects on intracellular and surface pH of exposing Xenopus oocytes to solutions containing NH3/NH4(+).
J Membr Biol. 2009 Mar;228(1):15-31.

Musa-Aziz R, Chen LM, Pelletier MF, Boron WF.
Relative CO2/NH3 selectivities of AQP1, AQP4, AQP5, AmtB, and RhAG.
Proc Natl Acad Sci U S A. 2009 Mar 31;106(13):5406-11.

Nakhoul NL, Hering-Smith KS, Abdulnour-Nakhoul SM, Hamm LL.
Transport of NH3/NH4+ in oocytes expressing aquaporin-1.
Am J Physiol Renal Physiol. 2001 Aug;281(2):F255-63.

Nelson DD Jr, Fraser GT, Klemperer W.
Does ammonia hydrogen bond?
Science. 1987 Dec 18;238(4834):1670-4.

Newby ZE, O'Connell J 3rd, Robles-Colmenares Y, Khademi S, Miercke LJ, Stroud RM.
Crystal structure of the aquaglyceroporin PfAQP from the malarial parasite Plasmodium falciparum.
Nat Struct Mol Biol. 2008 Jun;15(6):619-25.

Nielsen S, Smith BL, Christensen EI, Agre P.
Distribution of the aquaporin CHIP in secretory and resorptive epithelia and capillary endothelia.
Proc Natl Acad Sci U S A. 1993 Aug 1;90(15):7275-9.

Niemietz CM, Tyerman SD.
Channel-mediated permeation of ammonia gas through the peribacteroid membrane of soybean nodules.
FEBS Lett. 2000 Jan 14;465(2-3):110-4.

Niemietz CM, Tyerman SD.
New potent inhibitors of aquaporins: silver and gold compounds inhibit aquaporins of plant and human origin.
FEBS Lett. 2002 Nov 20;531(3):443-7.

Niethammer P, Grabher C, Look AT, Mitchison TJ.
A tissue-scale gradient of hydrogen peroxide mediates rapid wound detection in zebrafish.
Nature. 2009 Jun 18;459(7249):996-9.

Orij R, Postmus J, Ter Beek A, Brul S, Smits GJ.
In vivo measurement of cytosolic and mitochondrial pH using a pH-sensitive GFP derivative in Saccharomyces cerevisiae reveals a relation between intracellular pH and growth.
Microbiology. 2009 Jan;155(Pt 1):268-78.

Oshio K, Binder DK, Yang B, Schecter S, Verkman AS, Manley GT.
Expression of aquaporin water channels in mouse spinal cord.
Neuroscience. 2004;127(3):685-93.

Otto B, Uehlein N, Sdorra S, Fischer M, Ayaz M, Belastegui-Macadam X, Heckwolf M, Lachnit M, Pede N, Priem N, Reinhard A, Siegfart S, Urban M, Kaldenhoff R.
Aquaporin tetramer composition modifies the function of tobacco aquaporins.
J Biol Chem. 2010 Oct 8;285(41):31253-60.

Paganelli CV, Solomon AK.
The rate of exchange of tritiated water across the human red cell membrane.
J Gen Physiol. 1957 Nov 20;41(2):259-77.

Papadopoulos MC, Saadoun S, Verkman AS.
quaporins and cell migration.
Pflugers Arch. 2008 Jul;456(4):693-700.

Peña A, Cinco G, Gómez-Puyou A, Tuena M.
Effect of the pH of the incubation medium on glycolysis and respiration in Saccharomyces cerevisiae.
Arch Biochem Biophys. 1972 Dec;153(2):413-25.

Peña A, Pardo JP, Ramírez J.
Early metabolic effects and mechanism of ammonium transport in yeast.
Arch *Biochem Biophys*. 1987 Mar;253(2):431-8.

Pettersson N, Hagström J, Bill RM, Hohmann S.
Expression of heterologous aquaporins for functional analysis in Saccharomyces cerevisiae.
Curr Genet. 2006 Oct;50(4):247-55.

Poater J, Fradera X, Sola M, Duran M, Simon S.
On the electron-pair nature of the hydrogen bond in the framework of the atoms in molecules theory.
Chemical Physics Letters. 2003; 369:248–55.

Pocock G, Richards CD.
Human physiology, the basis of medicine.
Oxford University Press. 2004.

Preston GM, Agre P.
Isolation of the cDNA for erythrocyte integral membrane protein of 28 kilodaltons: member of an ancient channel family.
Proc Natl Acad Sci U S A. 1991 Dec 15;88(24):11110-4.

Preston GM, Carroll TP, Guggino WB, Agre P.
Appearance of water channels in Xenopus oocytes expressing red cell CHIP28 protein.
Science. 1992 Apr 17;256(5055):385-7.

Preston GM, Jung JS, Guggino WB, Agre P.
The mercury-sensitive residue at cysteine 189 in the CHIP28 water channel.
J Biol Chem. 1993 Jan 5;268(1):17-20.

Preston GM, Jung JS, Guggino WB, Agre P. Membrane topology of aquaporin CHIP.
Analysis of functional epitope-scanning mutants by vectorial proteolysis.
J Biol Chem. 1994 Jan 21;269(3):1668-73.

Priver NA, Rabon EC, Zeidel ML.
Apical membrane of the gastric parietal cell: water, proton, and nonelectrolyte permeabilities.
Biochemistry. 1993 Mar 16;32(10):2459-68.

Quigley F, Rosenberg JM, Shachar-Hill Y, Bohnert HJ.
From genome to function: the Arabidopsis aquaporins.
Genome Biol. 2002;3(1):RESEARCH0001.

Quigley R, Gupta N, Lisec A, Baum M.
Maturational changes in rabbit renal basolateral membrane vesicle osmotic water permeability.
J Membr Biol. 2000 Mar 1;174(1):53-8.

Rabaud NE, Song L, Wang Y, Agre P, Yasui M, Carbrey JM.
Aquaporin 6 binds calmodulin in a calcium-dependent manner.
Biochem Biophys Res Commun. 2009 May 22;383(1):54-7.

Richardson JS, Richardson DC.
Amino acid preferences for specific locations at the ends of alpha helices.
Science. 1988 Jun 17;240(4859):1648-52.

Richey DP, Lin EC.
Importance of facilitated diffusion for effective utilization of glycerol by Escherichia coli.
J Bacteriol. 1972 Nov;112(2):784-90.

Ripoche P, Bertrand O, Gane P, Birkenmeier C, Colin Y, Cartron JP.
Human Rhesus-associated glycoprotein mediates facilitated transport of NH(3) into red blood cells.
Proc Natl Acad Sci U S A. 2004 Dec 7;101(49):17222-7.

Ritchie RJ, Gibson J.
Permeability of ammonia, methylamine and ethylamine in the cyanobacterium, Synecho-coccus R-2 (Anacystis nidulans) PCC 7942.
J Membr Biol. 1987;95:131-42.

Ritchie RJ, Gibson J.
Permeability of ammonia and amines in Rhodobacter sphaeroides and Bacillus firmus.
Arch *Biochem Biophys*. 1987 Nov 1;258(2):332-41.

Rivers RL, Dean RM, Chandy G, Hall JE, Roberts DM, Zeidel ML.
Functional analysis of nodulin 26, an aquaporin in soybean root nodule symbiosomes.
J Biol Chem. 1997 Jun 27;272(26):16256-61.

Robinson JR.
The effect of sodium and chloride ions upon swelling of rat kidney slices treated with a mercurial diuretic.
J Physiol. 1956 Oct 29;134(1):216-28.

Rojek AM, Skowronski MT, Füchtbauer EM, Füchtbauer AC, Fenton RA, Agre P, Frøkiaer J, Nielsen S.
Defective glycerol metabolism in aquaporin 9 (AQP9) knockout mice.
Proc Natl Acad Sci U S A. 2007 Feb 27;104(9):3609-14.

Roudier N, Verbavatz JM, Maurel C, Ripoche P, Tacnet F.
Evidence for the presence of aquaporin-3 in human red blood cells.
J Biol Chem. 1998 Apr 3;273(14):8407-12.

Rozpędowska E, Hellborg L, Ishchuk OP, Orhan F, Galafassi S, Merico A, Woolfit M, Compagno C, Piskur J.
Parallel evolution of the make-accumulate-consume strategy in Saccharomyces and Dekkera yeasts.
Nat Commun. 2011;2:302.

Saadoun S, Papadopoulos MC, Hara-Chikuma M, Verkman AS.
Impairment of angiogenesis and cell migration by targeted aquaporin-1 gene disruption.
Nature. 2005 Apr 7;434(7034):786-92.

Saadoun S, Papadopoulos MC, Watanabe H, Yan D, Manley GT, Verkman AS.
Involvement of aquaporin-4 in astroglial cell migration and glial scar formation.
J Cell Sci. 2005 Dec 15;118(Pt 24):5691-8.

Sanno Y, Wilson TH, Lin EC.
Control of permeation to glycerol in cells of Escherichia coli.
Biochem Biophys Res Commun. 1968 Jul 26;32(2):344-9.

Saparov SM, Liu K, Agre P, Pohl P.
Fast and selective ammonia transport by aquaporin-8.
J Biol Chem. 2007 Feb 23;282(8):5296-301.

Sasaki S, Fushimi K, Saito H, Saito F, Uchida S, Ishibashi K, Kuwahara M, Ikeuchi T, Inui K, Nakajima K, et al.
Cloning, characterization, and chromosomal mapping of human aquaporin of collecting duct.
J Clin Invest. 1994 Mar;93(3):1250-6.

Savage DF, Egea PF, Robles-Colmenares Y, O'Connell JD 3rd, Stroud RM.
Architecture and selectivity in aquaporins: 2.5 a X-ray structure of aquaporin Z.
PLoS Biol. 2003 Dec;1(3):E72.

Savage DF, O'Connell JD 3rd, Miercke LJ, Finer-Moore J, Stroud RM.
Structural context shapes the aquaporin selectivity filter.
Proc Natl Acad Sci U S A. 2010 Oct 5;107(40):17164-9.

Schüssler MD, Alexandersson E, Bienert GP, Kichey T, Laursen KH, Johanson U, Kjellbom P, Schjoerring JK, Jahn TP.
The effects of the loss of TIP1;1 and TIP1;2 aquaporins in Arabidopsis thaliana.
Plant J. 2008 Dec;56(5):756-67.

Schwab A.
Function and spatial distribution of ion channels and transporters in cell migration.
Am J Physiol Renal Physiol. 2001 May;280(5):F739-47.

Seeliger D, Zapater C, Krenc D, Haddoub R, Flitsch S, Beitz E, Cerda J, de Groot BL.
Discovery of novel human aquaporin-1 blockers.
ACS Chem Biol. 2012; in press.

Serrano R, Bernal D, Simón E, Ariño J.
Copper and iron are the limiting factors for growth of the yeast Saccharomyces cerevisiae in an alkaline environment.
J Biol Chem. 2004 May 7;279(19):19698-704.

Shiels A, Bassnett S, Varadaraj K, Mathias R, Al-Ghoul K, Kuszak J, Donoviel D, Lilleberg S, Friedrich G, Zambrowicz B.
Optical dysfunction of the crystalline lens in aquaporin-0-deficient mice.
Physiol Genomics. 2001 Dec 21;7(2):179-86.

Sidoux-Walter F, Pettersson N, Hohmann S.
The Saccharomyces cerevisiae aquaporin Aqy1 is involved in sporulation.
Proc Natl Acad Sci U S A. 2004 Dec 14;101(50):17422-7.

Sigler K, Knotková A, Kotyk A.
Factors governing substrate-induced generation and extrusion of protons in the yeast Saccharomyces cerevisiae.

Biochim Biophys Acta. 1981 May 20;643(3):572-82.

Sikorski RS, Hieter P.
A system of shuttle vectors and yeast host strains designed for efficient manipulation of DNA in Saccharomyces cerevisiae.
Genetics. 1989 May;122(1):19-27.

Skyttä E, Mattila-Sandholm T.
A quantitative method for assessing bacteriocins and other food antimicrobials by automated turbidometry.
J Microbiol Methods. 1991; 14:77-88.

Smith BL, Agre P.
Erythrocyte Mr 28,000 transmembrane protein exists as a multisubunit oligomer similar to channel proteins.
J Biol Chem. 1991 Apr 5;266(10):6407-15.

Smith CP.
Mammalian urea transporters.
Exp Physiol. 2009 Feb;94(2):180-5.

Smith DR, Doucette-Stamm LA, Deloughery C, Lee H, Dubois J, Aldredge T, Bashirzadeh R, Blakely D, Cook R, Gilbert K, Harrison D, Hoang L, Keagle P, Lumm W, Pothier B, Qiu D, Spadafora R, Vicaire R, Wang Y, Wierzbowski J, Gibson R, Jiwani N, Caruso A, Bush D, Reeve JN, et al.
Complete genome sequence of Methanobacterium thermoautotrophicum deltaH: functional analysis and comparative genomics.
J Bacteriol. 1997 Nov;179(22):7135-55.

Sohara E, Rai T, Miyazaki J, Verkman AS, Sasaki S, Uchida S.
Defective water and glycerol transport in the proximal tubules of AQP7 knockout mice.
Am J Physiol Renal Physiol. 2005 Dec;289(6):F1195-200.

Song J, Almasalmeh A, Krenc D, Beitz E.
Molar concentrations of sorbitol and polyethylene glycol inhibit the Plasmodium aquaglyceroporin but not that of E. coli: Involvement of the channel vestibules.
Biochim Biophys Acta. 2012 May;1818(5):1218-24.

Soria LR, Fanelli E, Altamura N, Svelto M, Marinelli RA, Calamita G.
Aquaporin-8-facilitated mitochondrial ammonia transport.
Biochem Biophys Res Commun. 2010 Mar 5;393(2):217-21.

Soveral G, Madeira A, Loureiro-Dias MC, Moura TF.
Water transport in intact yeast cells as assessed by fluorescence self-quenching.
Appl Environ Microbiol. 2007 Apr;73(7):2341-3.

Soveral G, Madeira A, Loureiro-Dias MC, Moura TF.
Membrane tension regulates water transport in yeast.
Biochim Biophys Acta. 2008 Nov;1778(11):2573-9.

Steinfeld S, Cogan E, King LS, Agre P, Kiss R, Delporte C.
Abnormal distribution of aquaporin-5 water channel protein in salivary glands from Sjögren's syndrome patients.
Lab Invest. 2001 Feb;81(2):143-8.

Su W, Qiao Y, Yi F, Guan X, Zhang D, Zhang S, Hao F, Xiao Y, Zhang H, Guo L, Yang L, Feng X, Ma T.
Increased female fertility in aquaporin 8-deficient mice.
IUBMB Life. 2010 Nov;62(11):852-7.

Sui H, Han BG, Lee JK, Walian P, Jap BK.
Structural basis of water-specific transport through the AQP1 water channel.
Nature. 2001 Dec 20-27;414(6866):872-8.

Tamás MJ, Luyten K, Sutherland FC, Hernandez A, Albertyn J, Valadi H, Li H, Prior BA, Kilian SG, Ramos J, Gustafsson L, Thevelein JM, Hohmann S.
Fps1p controls the accumulation and release of the compatible solute glycerol in yeast osmoregulation.
Mol Microbiol. 1999 Feb;31(4):1087-104.

Tanghe A, Van Dijck P, Dumortier F, Teunissen A, Hohmann S, Thevelein JM.
Aquaporin expression correlates with freeze tolerance in baker's yeast, and overexpression improves freeze tolerance in industrial strains.

Appl Environ Microbiol. 2002 Dec;68(12):5981-9.

Tanghe A, Van Dijck P, Thevelein JM.
Why do microorganisms have aquaporins?
Trends Microbiol. 2006 Feb;14(2):78-85.

Tani T, Koyama Y, Nihei K, Hatakeyama S, Ohshiro K, Yoshida Y, Yaoita E, Sakai Y, Hatakeyama K, Yamamoto T.
Immunolocalization of aquaporin-8 in rat digestive organs and testis.
Arch Histol Cytol. 2001 May;64(2):159-68.

Teixeira MC, Raposo LR, Mira NP, Lourenço AB, Sá-Correia I.
Genome-wide identification of Saccharomyces cerevisiae genes required for maximal tolerance to ethanol. *Appl Environ Microbiol*. 2009 Sep;75(18):5761-72.

Thrane AS, Rappold PM, Fujita T, Torres A, Bekar LK, Takano T, Peng W, Wang F, Thrane VR, Enger R, Haj-Yasein NN, Skare Ø, Holen T, Klungland A, Ottersen OP, Nedergaard M, Nagelhus EA.
Critical role of aquaporin-4 (AQP4) in astrocytic Ca2+ signaling events elicited by cerebral edema.
Proc Natl Acad Sci U S A. 2011 Jan 11;108(2):846-51.

Tingaud-Sequeira A, Calusinska M, Finn RN, Chauvigné F, Lozano J, Cerdà J.
The zebrafish genome encodes the largest vertebrate repertoire of functional aquaporins with dual paralogy and substrate specificities similar to mammals.
BMC Evol Biol. 2010 Feb 11;10:38.

Törnroth-Horsefield S, Wang Y, Hedfalk K, Johanson U, Karlsson M, Tajkhorshid E, Neutze R, Kjellbom P.
Structural mechanism of plant aquaporin gating.
Nature. 2006 Feb 9;439(7077):688-94.

Tsubota K, Hirai S, King LS, Agre P, Ishida N.
Defective cellular trafficking of lacrimal gland aquaporin-5 in Sjögren's syndrome.
Lancet. 2001 Mar 3;357(9257):688-9.

Tsukaguchi H, Weremowicz S, Morton CC, Hediger MA.
Functional and molecular characterization of the human neutral solute channel aquaporin-9.
Am J Physiol. 1999 Nov;277(5 Pt 2):F685-96.

Tsunoda SP, Wiesner B, Lorenz D, Rosenthal W, Pohl P.
Aquaporin-1, nothing but a water channel.
J Biol Chem. 2004 Mar 19;279(12):11364-7.

Uehlein N, Lovisolo C, Siefritz F, Kaldenhoff R.
The tobacco aquaporin NtAQP1 is a membrane CO2 pore with physiological functions.
Nature. 2003 Oct 16;425(6959):734-7.

Van Aelst L, Hohmann S, Zimmermann FK, Jans AW, Thevelein JM.
A yeast homologue of the bovine lens fibre MIP gene family complements the growth defect of a Saccharomyces cerevisiae mutant on fermentable sugars but not its defect in glucose-induced RAS-mediated cAMP signalling.
EMBO J. 1991 Aug;10(8):2095-104.

van Hoek AN, Hom ML, Luthjens LH, de Jong MD, Dempster JA, van Os CH.
Functional unit of 30 kDa for proximal tubule water channels as revealed by radiation inactivation.
J Biol Chem. 1991 Sep 5;266(25):16633-5.

Van Nuland A, Vandormael P, Donaton M, Alenquer M, Lourenço A, Quintino E, Versele M, Thevelein JM.
Ammonium permease-based sensing mechanism for rapid ammonium activation of the protein kinase A pathway in yeast.
Mol Microbiol. 2006 Mar;59(5):1485-505.

Vander AJ, Malvin RL, Wilde WS, Sullivan LP.
Localization of the site of action of mercurial diuretics by stop flow analysis.
Am J Physiol. 1958 Dec;195(3):558-62.

Verbalis JG.
AVP receptor antagonists as aquaretics: review and assessment of clinical data.
Cleve Clin J Med. 2006 Sep;73 Suppl 3:S24-33.

Verkman AS.
More than just water channels: unexpected cellular roles of aquaporins.
J Cell Sci. 2005 Aug 1;118(Pt 15):3225-32.

von Bülow J, Müller-Lucks A, Kai L, Bernhard F, Beitz E.
Functional characterization of a novel aquaporin from Dictyostelium discoideum amoebae implies a unique gating mechanism.
J Biol Chem. 2012 Mar 2;287(10):7487-94.

Walter A, Gutknecht J.
Permeability of small nonelectrolytes through lipid bilayer membranes.
J Membr Biol. 1986;90(3):207-17.

Walz T, Smith BL, Agre P, Engel A.
The three-dimensional structure of human erythrocyte aquaporin CHIP.
EMBO J. 1994 Jul 1;13(13):2985-93.

Wang Y, Schulten K, Tajkhorshid E.
What makes an aquaporin a glycerol channel? A comparative study of AqpZ and GlpF.
Structure. 2005 Aug;13(8):1107-18.

Warringer J, Blomberg A.
Automated screening in environmental arrays allows analysis of quantitative phenotypic profiles in Saccharomyces cerevisiae.
Yeast. 2003 Jan 15;20(1):53-67.

Weast RC, Ed.
Handbook of Chemistry and Physics.
CRC Press, Cleveland. 1977.

Weigert C, Steffler F, Kurz T, Shellhammer TH, Methner FJ.
Application of a short intracellular pH method to flow cytometry for determining Saccharomyces cerevisiae vitality.
Appl Environ Microbiol. 2009 Sep;75(17):5615-20.

Weiner ID, Verlander JW.
Role of NH3 and NH4+ transporters in renal acid-base transport.
Am J Physiol Renal Physiol. 2011 Jan;300(1):F11-23.

Wellner RB, Hoque AT, Goldsmith CM, Baum BJ.
Evidence that aquaporin-8 is located in the basolateral membrane of rat submandibular gland acinar cells.
Pflugers Arch. 2000 Nov;441(1):49-56.

Wellner RB, Cotrim AP, Hong S, Swaim WD, Baum BJ.
Localization of AQP5/AQP8 chimeras in MDCK-II cells: exchange of the N- and C-termini.
Biochem Biophys Res Commun. 2005 Apr 29;330(1):172-7.

Wiberg N.
Lehrbuch der anorganischen Chemie.
1995;101:645-659.

Will JL, Kim HS, Clarke J, Painter JC, Fay JC, Gasch AP.
Incipient balancing selection through adaptive loss of aquaporins in natural Saccharomyces cerevisiae populations.
PLoS Genet. 2010 Apr 1;6(4):e1000893.

Wipf D, Benjdia M, Rikirsch E, Zimmermann S, Tegeder M, Frommer WB.
An expression cDNA library for suppression cloning in yeast mutants, complementation of a yeast his4 mutant, and EST analysis from the symbiotic basidiomycete Hebeloma cylindrosporum.
Genome. 2003 Apr;46(2):177-81.

Witte CP.
Urea metabolism in plants.
Plant Sci. 2011 Mar;180(3):431-8.

Wree D, Wu B, Zeuthen T, Beitz E.
Requirement for asparagine in the aquaporin NPA sequence signature motifs for cation exclusion.
FEBS J. 2011 Mar;278(5):740-8.

Wu B, Altmann K, Barzel I, Krehan S, Beitz E.

A yeast-based phenotypic screen for aquaporin inhibitors.
Pflugers Arch. 2008 Jul;456(4):717-20.

Wu B, Steinbronn C, Alsterfjord M, Zeuthen T, Beitz E.
Concerted action of two cation filters in the aquaporin water channel.
EMBO J. 2009 Aug 5;28(15):2188-94.

Wu B, Song J, Beitz E.
Novel channel enzyme fusion proteins confer arsenate resistance.
J Biol Chem. 2010 Dec 17;285(51):40081-7.

Yakata K, Tani K, Fujiyoshi Y.
Water permeability and characterization of aquaporin-11.
J Struct Biol. 2011 May;174(2):315-20.

Yamamura Y, Nakamura S, Itoh S, Hirano T, Onogawa T, Yamashita T, Yamada Y, Tsujimae K, Aoyama M, Kotosai K, Ogawa H, Yamashita H, Kondo K, Tominaga M, Tsujimoto G, Mori T.
OPC-41061, a highly potent human vasopressin V2-receptor antagonist: pharmacological profile and aquaretic effect by single and multiple oral dosing in rats.
J Pharmacol Exp Ther. 1998 Dec;287(3):860-7.

Yang B, Verkman AS.
Water and glycerol permeabilities of aquaporins 1-5 and MIP determined quantitatively by expression of epitope-tagged constructs in Xenopus oocytes.
J Biol Chem. 1997 Jun 27;272(26):16140-6.

Yang B, Song Y, Zhao D, Verkman AS.
Phenotype analysis of aquaporin-8 null mice.
Am J Physiol Cell Physiol. 2005 May;288(5):C1161-70.

Yang B, Zhao D, Verkman AS.
Evidence against functionally significant aquaporin expression in mitochondria.
J Biol Chem. 2006 Jun 16;281(24):16202-6.

Yang B, Zhao D, Solenov E, Verkman AS.
Evidence from knockout mice against physiologically significant aquaporin 8-facilitated ammonia transport.
Am J Physiol Cell Physiol. 2006 Sep;291(3):C417-23.

Yang B, Kim JK, Verkman AS.
Comparative efficacy of HgCl2 with candidate aquaporin-1 inhibitors DMSO, gold, TEA+ and acetazolamide.
FEBS Lett. 2006 Dec 11;580(28-29):6679-84.

Yasui M, Hazama A, Kwon TH, Nielsen S, Guggino WB, Agre P.
Rapid gating and anion permeability of an intracellular aquaporin.
Nature. 1999 Nov 11;402(6758):184-7.

Yeung CH.
Aquaporins in spermatozoa and testicular germ cells: identification and potential role.
Asian J Androl. 2010 Jul;12(4):490-9.

Yool AJ, Campbell EM.
Structure, function and translational relevance of aquaporin dual water and ion channels.
Mol Aspects Med. 2012 Oct;33(5-6):553-61.

Yukutake Y, Hirano Y, Suematsu M, Yasui M.
Rapid and reversible inhibition of aquaporin-4 by zinc.
Biochemistry. 2009 Dec 29;48(51):12059-61.

Zampighi GA, Kreman M, Boorer KJ, Loo DD, Bezanilla F, Chandy G, Hall JE, Wright EM.
A method for determining the unitary functional capacity of cloned channels and transporters expressed in Xenopus laevis oocytes.
J Membr Biol. 1995 Nov;148(1):65-78.

Zardoya R.
Phylogeny and evolution of the major intrinsic protein family.
Biol Cell. 2005 Jun;97(6):397-414.

Zeidel ML, Nielsen S, Smith BL, Ambudkar SV, Maunsbach AB, Agre P.

Ultrastructure, pharmacologic inhibition, and transport selectivity of aquaporin channel-forming integral protein in proteoliposomes.
Biochemistry. 1994 Feb 15;33(6):1606-15.

Zeuthen T, Klaerke DA.
Transport of water and glycerol in aquaporin 3 is gated by H(+).
J Biol Chem. 1999 Jul 30;274(31):21631-6.

Zeuthen T, Wu B, Pavlovic-Djuranovic S, Holm LM, Uzcategui NL, Duszenko M, Kun JF, Schultz JE, Beitz E.
Ammonia permeability of the aquaglyceroporins from Plasmodium falciparum, Toxoplasma gondii and Trypansoma brucei.
Mol Microbiol. 2006 Sep;61(6):1598-608.

Zhang H, Verkman AS.
Evidence against involvement of aquaporin-4 in cell-cell adhesion.
J Mol Biol. 2008 Oct 24;382(5):1136-43.

Zhu T, Yang W.
Structure of the ammonia dimer studied by density functional theory.
International Journal of Quantum Chemistry. 1994;49:613-23.

9 Appendix

9.1 Ar/R constriction statistics

The following percentages of occurence of amino acids at the four major positions lining the aromatic/arginine constriction of aquaporins (Fig. 1.6) are based on predictions by the MIP Mod Database (Gupta *et al.*, 2012). At the time of writing, data for 1008 aquaporins from 340 organisms is included. ‘H2’, ‘H5’, ‘HE’, ‘LE1’ denote the respective helices or loop (Figs. 1.2, 1.6). Numbers are rounded to the nearest integer, absence is indicated by a minus sign.

	occurence (%)			
Amino acid	**H2**	**H5**	**LE1**	**HE**
Gly	1	22	15	0
Ala	2	3	24	1
Val	1	9	1	6
Ile	2	15	1	1
Leu	2	1	1	2
Phe	48	0	6	0
Tyr	2	1	14	-
Trp	24	-	1	-
Pro	0	-	3	-
Cys	0	0	6	-
Met	0	1	0	-
Ser	1	4	2	0
Thr	1	1	25	-
Asn	1	1	-	1
Gln	1	0	-	-
Asp	-	0	-	-
Glu	0	4	-	-
His	12	37	-	-
Lys	-	0	-	0
Arg	-	0	-	88
sum	99.0	99.6	99.3	98.7

Incomplete sums are due to errors made during visual evaluation.

Please keep in mind the possible biases due to the choice of sequenced genomes with regard to the organism (*e. g.* mammals rather than marsupials), and to the number of aquaporin isoforms encoded by those genomes (*e. g.*, many in plants, few in microorganisms).

9.2 DNA sequences

Rat AQP1

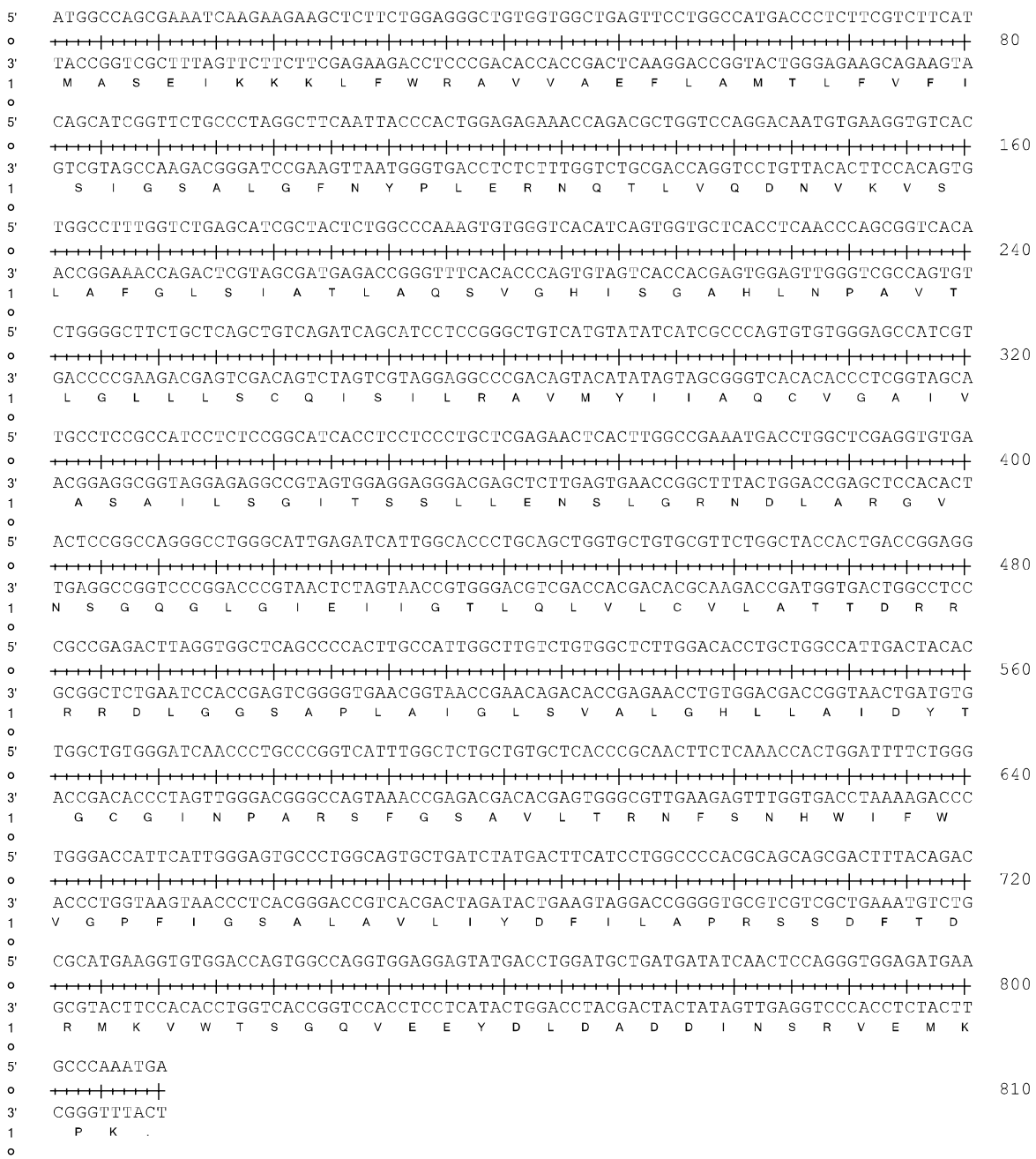

Rat AQP8 ΔQ5 S31P

Lower case letters indicate differences as compared to reference sequences. Three of them are located in the third codon position and are without consequence with regard to the encoded amino acid, one leads to the mutation S31P.

```
5'   ATGTCTGGGGAGACGCCGATGTGTAGTATGGACCTACGTGAGATCAAGGGGAAGGAGACCAACATGGCTGACAGTTACCA
o    +----+----+----+----+----+----+----+----+----+----+----+----+----+----+----+----+  80
3'   TACAGACCCCTCTGCGGCTACACATCATACCTGGATGCACTCTAGTTCCCCTTCCTCTGGTTGTACCGACTGTCAATGGT
1     M  S  G  E  T  P  M  C  S  M  D  L  R  E  I  K  G  K  E  T  N  M  A  D  S  Y  H
o
5'   TGGCATGcCCTGGTATGAGCAGTACATACAACCGTGTGTGGTGGAACTTTTGGGCTCCGCTCTCTTCATCTTCATTGGGT
o    +----+----+----+----+----+----+----+----+----+----+----+----+----+----+----+----+ 160
3'   ACCGTACgGGACCATACTCGTCATGTATGTTGGCACACACCACCTTGAAAACCCGAGGCGAGAGAAGTAGAAGTAACCCA
1       G  M  P  W  Y  E  Q  Y  I  Q  P  C  V  V  E  L  L  G  S  A  L  F  I  F  I  G
o
5'   GTCTATCGGTCATCGAGAACAGTCCgAATACTGGGCTCCTGCAGCCTGCCCTGGCTCATGGGCTGGCCTTGGGGCTCATC
o    +----+----+----+----+----+----+----+----+----+----+----+----+----+----+----+----+ 240
3'   CAGATAGCCAGTAGCTCTTGTCAGGcTTATGACCCGAGGACGTCGGACGGGACCGAGTACCCGACCGGAACCCCGAGTAG
1    C  L  S  V  I  E  N  S  P  N  T  G  L  L  Q  P  A  L  A  H  G  L  A  L  G  L  I
o
5'   ATTGCTACCTTGGGGAACATCAGCGGTGGACACTTCAACCCTGCTGTGTCGCTGGCAGTCACACTGGTTGGAGGCCTcAA
o    +----+----+----+----+----+----+----+----+----+----+----+----+----+----+----+----+ 320
3'   TAACGATGGAACCCCTTGTAGTCGCCACCTGTGAAGTTGGGACGACACAGCGACCGTCAGTGTGACCAACCTCCGGAgTT
1     I  A  T  L  G  N  I  S  G  G  H  F  N  P  A  V  S  L  A  V  T  L  V  G  G  L  K
o
5'   GACCATGCTGCTAATTCCCTACTGGGTCTCCCAGCTGTTTGGGGGAATGATCGGAGCTGCCCTGGCTAAGGTGGTGAGTC
o    +----+----+----+----+----+----+----+----+----+----+----+----+----+----+----+----+ 400
3'   CTGGTACGACGATTAAGGGATGACCCAGAGGGTCGACAAACCCCCTTACTAGCCTCGACGGGACCGATTCCACCACTCAG
1       T  M  L  L  I  P  Y  W  V  S  Q  L  F  G  G  M  I  G  A  A  L  A  K  V  V  S
o
5'   CAGAGGAAAGGTTCTGGAATGCGTCTGGGGCAGCCTTTGCCATAGTCCAGGAGCAGGAGCAGGTGGCAGAAGCCCTGGGG
o    +----+----+----+----+----+----+----+----+----+----+----+----+----+----+----+----+ 480
3'   GTCTCCTTTCCAAGACCTTACGCAGACCCCGTCGGAAACGGTATCAGGTCCTCGTCCTCGTCCACCGTCTTCGGGACCCC
1    P  E  E  R  F  W  N  A  S  G  A  A  F  A  I  V  Q  E  Q  E  Q  V  A  E  A  L  G
o
5'   GTAGAGATCGTTATGACGATGCTGTTGGTATTGGCTGTaTGTATGGGTGCCGTCAATGAGAAGACAATGGGTCCCCTAGC
o    +----+----+----+----+----+----+----+----+----+----+----+----+----+----+----+----+ 560
3'   CATCTCTAGCAATACTGCTACGACAACCATAACCGACAtACATACCCACGGCAGTTACTCTTCTGTTACCCAGGGGATCG
1     V  E  I  V  M  T  M  L  L  V  L  A  V  C  M  G  A  V  N  E  K  T  M  G  P  L  A
o
5'   CCCATTCTCCATTGGTTTCTCTGTCATTGTGGATATCCTGGCAGGTGGTGGGATCTCTGGAGCCTGCATGAACCCTGCTC
o    +----+----+----+----+----+----+----+----+----+----+----+----+----+----+----+----+ 640
3'   GGGTAAGAGGTAACCAAAGAGACAGTAACACCTATAGGACCGTCCACCACCCTAGAGACCTCGGACGTACTTGGGACGAG
1       P  F  S  I  G  F  S  V  I  V  D  I  L  A  G  G  G  I  S  G  A  C  M  N  P  A
o
5'   GTGCCTTTGGACCTGCTGTGATGGCTGGCTACTGGGACTTCCATTGGATCTACTGGCTGGGCCCACTCCTGGCTGGCCTC
o    +----+----+----+----+----+----+----+----+----+----+----+----+----+----+----+----+ 720
3'   CACGGAAACCTGGACGACACTACCGACCGATGACCCTGAAGGTAACCTAGATGACCGACCCGGGTGAGGACCGACCGGAG
1    R  A  F  G  P  A  V  M  A  G  Y  W  D  F  H  W  I  Y  W  L  G  P  L  L  A  G  L
o
5'   TTTGTGGGACTGCTCATTAGGCTCTTCATTGGAGATGAGAAAACCCGCCTGATTCTAAAGTCGAGGTGA
o    +----+----+----+----+----+----+----+----+----+----+----+----+----+----+  789
3'   AAACACCCTGACGAGTAATCCGAGAAGTAACCTCTACTCTTTTGGGCGGACTAAGATTTCAGCTCCACT
1     F  V  G  L  L  I  R  L  F  I  G  D  E  K  T  R  L  I  L  K  S  R  .
o
```

Human AQP8-HA

The first 48 nucleotides encode the N-terminal human influenza hemagglutinin tag. Lower case letters indicate differences as compared to reference sequences. All but one are synonymous: Valine is encoded in place of Alanine 130 in one reference sequence, in another it is also alanine.

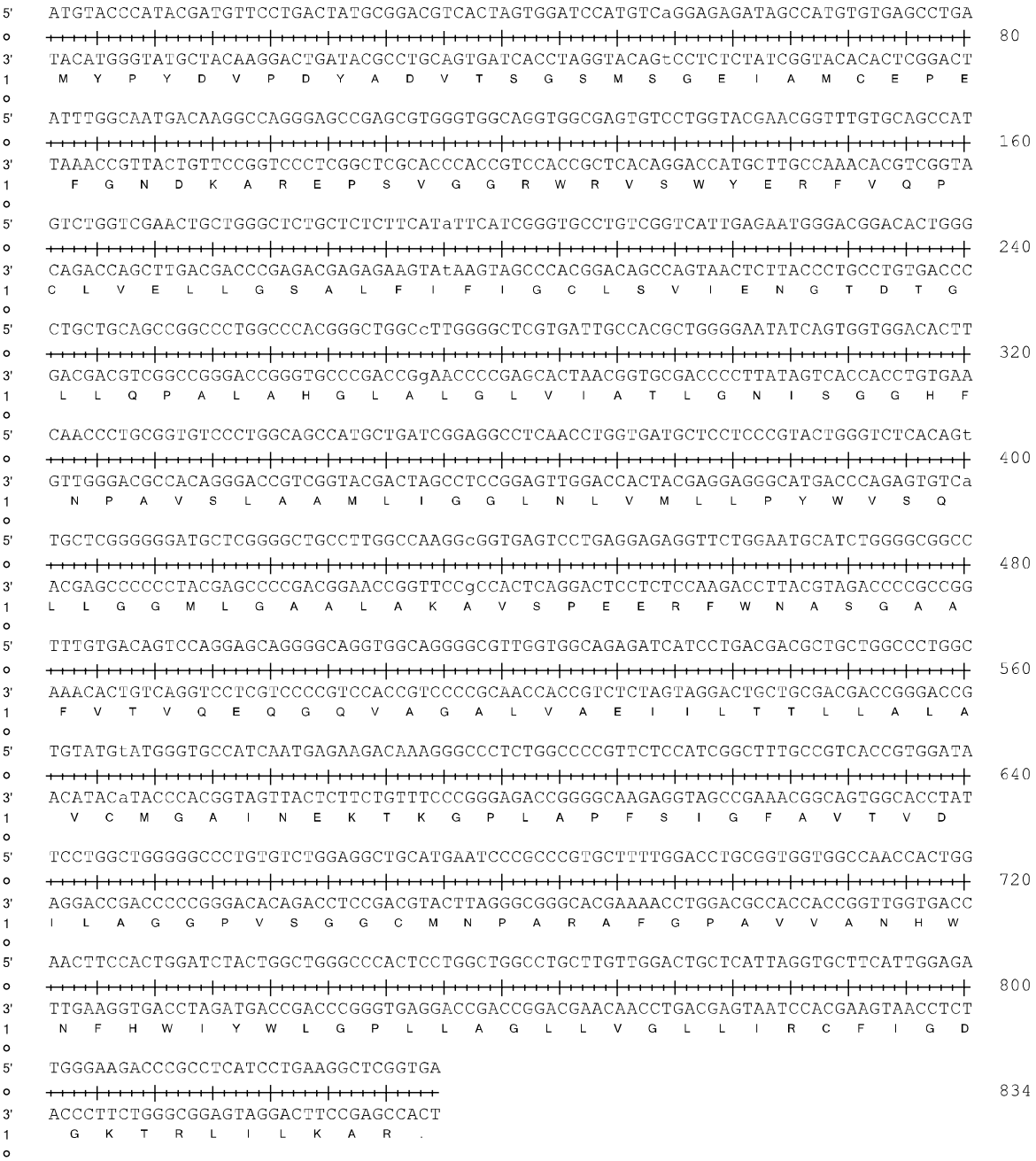

Publications

Beitz E, Becker D, von Bülow J, Conrad C, Fricke N, Geadkaew A, Krenc D, Song J, Wree D, Wu B.
In vitro analysis and modification of aquaporin pore selectivity.
Handb Exp Pharmacol. 2009;(190):77-92.

Song J, Almasalmeh A, Krenc D, Beitz E.
Molar concentrations of sorbitol and polyethylene glycol inhibit the Plasmodium aquaglyceroporin but not that of E. coli: Involvement of the channel vestibules.
Biochim Biophys Acta. 2012 May;1818(5):1218-24.

Krenc D, Wu B, Beitz E.
Specific aquaporins increase the ammonia tolerance of a Saccharomyces cerevisiae mep1-3 fps1 deletion strain.
Mol Membr Biol. 2012; in press.

Seeliger D, Zapater C, Krenc D, Haddoub R, Flitsch S, Beitz E, Cerda J, de Groot BL.
Discovery of novel human aquaporin-1 blockers.
ACS Chem Biol. 2012; in press.

von Bülow J, Song J, Krenc D, Wu B, Beitz E.
Zelluläre Wasser- und Glycerinkanäle.
Naturwissenschaftliche Rundschau. 2012 Nov;65(11):561-566.

Erklärung

Diese Abhandlung ist, abgesehen von der Beratung durch meinen Betreuer, nach Inhalt und Form meine eigene Arbeit. Sie hat bisher an keiner anderen Stelle im Rahmen eines Prüfungsverfahrens vorgelegen.
Die Arbeit ist unter Einhaltung der Regeln guter wissenschaftlicher Praxis der Deutschen Forschungsgemeinschaft entstanden.

Kiel, im November 2012

Dawid Krenc

Acknowledgements

This piece of work was 16 months in the making, a gestation period similar to that of the sperm whale, *Physeter macrocephalus*. The experiments preceding it took me about 40 months, including many weekends, and the outcome hardly justifies the effort. Yet I would not have been able to do it without the help of many people: Those who taught me, those who did things I could not do, and those whose encouragement kept my mind in working condition.

First of all I would like to thank my advisor Eric for giving me a problem that I liked immediately, however little I contributed to its solving. And for being patient with me: Some of his advice I understood very late. He also provided me with a substantial extra period of funding.

Bert was similarly patient, and I thank him for coming to my thesis defence. Funding by EDICT I owe to him.

Mrs. Ihlow did great to calm me down whenever I felt I was drowning in documents, and Mrs. Voß has a very friendly way of greeting.

Julia would often peek into the lab and talk to me briefly before going home in the evenings. This really helped during the first few months, a time when I was not feeling so good. Not least, she operated on those poor frogs so I could do experiments with their oocytes (which were helpful I am glad to say).

Britta is a “real scientist” and a remarkable person, her encouragement I appreciate very much.

Jie joined the lab two months after me and left a month before me, I feel lucky that our time here overlapped so closely.

Binghua was always ready to answer questions and sometimes came up with something helpful when I did not expect it.

My project students Anika and Meike knew how to tease me in a friendly way, I felt very comfortable working with them.

Haixia bounced into and out of our lab, and somehow we get along to this day.

Meeting my Spanish friend Nacho after so many years, thanks to a sponsored conference trip, was wonderful. He is not a scientist, but his encouragement helped my “science” in many ways.

Björn could always be counted on, and his calm manner was soothing.

Susan took her time to show me the HPLC equipment and to explain the subtleties of her Karl-Fischer-titrations. We did not work much together, but I enjoyed it.

Gerhard took good care of me in Göteborg.

Katie was quick at providing me with test compounds - if only I had been able to reciprocate.

Sören was always friendly to me, even when my experiments failed to help him.

Dr. Girreser was particularly apt at instilling a sense of guilt in me, I will remember him whenever and wherever standards are to be set or met.

Prof. Heber was a most friendly host, his “Teerunde” I always looked forward to, and I shall never forget the joyful expression on his face when I threw apples down for him to catch during the autumnal apple picking. His wife, Dr. Brunschweiger, was equally friendly and forgiving, and she saved me from being late at my thesis defence. Their son Roland did his best to walk and to manipulate doors quietly after 10 pm: I appreciate that, and I can imagine how hard it must have been for a musician whose activity peaks at night.

Patrizia, with students Damiana and Daniele, showed me around in her lab in Bari, and provided me with two substances that confirmed the suitability of at least some of my experiments. This would never have happened if Prof. Calamita had not invited us to the conference in Bari, perhaps the most pleasant that I attended.

Prof. Bleich took his time to read my thesis, he greeted me whenever our paths crossed at the canteen, and I could move freely in his lab. Kerstin showed me her experiments, trying to measure the membrane properties of tiny algal cells, and she helped Christina and me when we had trouble with the capillary puller.

Christina could be soothingly joyful. She often made me feel more at ease in our lab.

Dorothea helped me with the stopped-flow measurements when I had very little experience, and she eventually warmed up to me which made me feel better.

Nadine was a remarkably good teacher, though I had only one occasion to enjoy that because our work hardly overlapped.

Prof. Blaschek took a lot of anxiety from me before my thesis defence, simply by being friendly.

Some of my breaks I spent at the botanical garden where Carsten, Henning and Steffi took their time to answer my questions. It is a pity I discovered that place so late.

The IT guys, Arne and Detlef, were always quick to help, and patient when I looked at the material in their office asking questions about this and that.

Dr. Furkert had complete trust in me when it came to spending time alone at the clean room for osmolality measurements. Sven showed me how to use the equipment, and he always greeted me.

Our electrician Kalle is a hero, we all know that. I would like to thank him in addition for showing me around in his nice workshop, and for helping me make my first battery.

Mr. Boehme and Mr. Selig were quick to provide any repairs and non-standard equipment, and Mr. Selig even regularly asked me about my progress.

Some of the “Clementines” were understandably hesitant towards me, yet they always helped when necessary.

Many project students helped me with my labwork. Admittedly, I was not a good instructor for some. In particular, I would like to thank Kristin, Heinke and Alina, whom I could trust to work independently.

Annika was a pleasant labmate, and she introduced me to the soul-soothing PhD comics of Jorge Cham. Her holiday souvenir, a piece of sulfur from the Stromboli area, was a nice and unexpected gift.

Nasser is one of the friendliest and calmest people I know, and he did his best to help me by patiently attempting to establish an experimental technique.

My “juniors”, Ellen, Sinja, Janis and Sonja, quickly caught up and are now more experienced than me in many ways. I thank them for their friendliness towards me.

Mrs. Koberg at the PhD office must have calmed hundreds of anxious PhD candidates before me, I am no less grateful for it.

Dorte taught me many things unrelated to science, and she helped me feel a little better about what I have achieved.

Lena and her parents are like a second family, full of subtle and not-so-subtle encouragement.

Kemi taught me the language I am writing in, and a lot more.

Kwang was patient with me, and her advice precious, and some things I cannot express in words.

My parents allowed me to study as much as I liked, and to spend the time necessary to complete my thesis in the way I felt I should. Staying with them, and with our family in Poland, was the best way to “recharge my batteries”.

Lebenslauf

Persönliche Daten

Name	Dawid Michał Krenc
Geburtsdatum	7. März 1980
Geburtsort	Wrocław, Polen
Staatsangehörigkeit	deutsch

Schulbildung

1986 - 1990	Albert-Schweitzer-Schule, Velbert
1990 - 1992	Nikolaus-Ehlen-Gymnasium, Velbert
1992 - 1996	Maria-Wächtler-Gymnasium, Essen
1996 - 1997	Lycée Ombrosa, Lyon, Frankreich
1997 - 1998	Suiran Highschool, Yokohama, Japan
1998 - 2000	Maria-Wächtler-Gymnasium, Essen

Studium und Ausbildung

10/2001 - 09/2005	Pharmaziestudium an der Goethe Universität Frankfurt am Main
09/2005 - 10/2006	King's College London (praktisches Jahr)
11/2006 - 04/2007	Kaiser-Wilhelm-Apotheke Essen (praktisches Jahr)
05/2007	Approbation als Apotheker

Promotion und Weiterbildung

10/2007 - 12/2012	Wissenschaftlicher Angestellter am Institut für pharmazeutische Chemie der Christian-Albrechts-Universität zu Kiel und Anfertigung der Dissertation unter Leitung von Prof. Dr. E. Beitz
01/2011	Fachapotheker für pharmazeutische Analytik